# Examination of the roles of the AP-1 transcription factors, JunB and c-Jun, in the pathobiology of Anaplastic Lymphoma Kinase-positive, Anaplastic Large Cell Lymphoma (ALK+ ALCL)

by

Zuoqiao Wu

A thesis submitted in partial fulfillment of the requirements for the degree of

Doctor of Philosophy

In

Immunology

Department of Medical Microbiology and Immunology
University of Alberta

## Abstract

Anaplastic lymphoma kinase-positive, anaplastic large cell lymphoma (ALK+ ALCL) is an aggressive T cell lymphoma that is characterized by chromosomal translocations involving the gene encoding for the *ALK* tyrosine kinase. The ALK fusion proteins generated through these translocations initiate downstream signalling pathways and contribute to the pathobiology of ALK+ ALCL. Signalling by NPM-ALK, the most common ALK fusion protein, elevates the expression and/or constitutively activates the activator protein-1 (AP-1) transcription factors, JunB and c-Jun. In this thesis, I investigated the role that JunB and c-Jun play in the pathobiology of ALK+ ALCL.

To examine the role of JunB and c-Jun in ALK+ ALCL, the expression of the two AP-1 proteins was knocked-down stably in ALK+ ALCL cell lines with short-hairpin RNAs (shRNA)s. I found that knock-down of JunB resulted in a reduced growth rate characterized by defect in $G_0/G_1$ cell cycle progression in the majority of the cell lines examined. In contrast, knock-down of c-Jun in multiple cell lines resulted in no observable effect on proliferation.

To further investigate the function of JunB in the pathobiology of ALK+ ALCL, microarray experiments were performed to compare the gene expression between control shRNA-expressing and JunB shRNA-expressing Karpas 299 cells, an ALK+ ALCL cell line. When JunB was knocked-down in Karpas 299 cells, expression of 678 genes (549 up-regulated and 132 down-regulated) were altered by a greater than 2-fold change. KEGG pathway annotation analysis revealed that “natural killer cell mediated cytotoxicity” as the most statistically significant category amongst the functional pathways that showed up in the analysis. Within this functional category, I confirmed that

several ligands for NK activating receptors were up-regulated at the mRNA and protein levels in JunB knock-down cells. My data further suggested that the up-regulation of these ligands could be partially due to epigenetic changes. More importantly, my data suggested that the up-regulation of these ligands made one ALK+ ALCL cell line more susceptible to NK-mediated killing.

To further identify the transcriptional targets of JunB and c-Jun, ChIP-seq was performed in Karpas 299 cells with anti-JunB and anti-c-Jun antibodies. I found a large number of genes were associated with JunB or/and c-Jun intervals, which was consistent with the fact that AP-1 sites are abundant in the genome. More genes were associated with JunB intervals alone or both JunB and c-Jun intervals, and a small number of genes were associated with c-Jun intervals alone. This suggested that JunB and c-Jun could regulate common genes, but JunB may regulate many more genes than c-Jun. FAM129B was identified as a potential direct transcriptional target of JunB and c-Jun because it was associated with JunB and c-Jun intervals at the putative promoter based on the ChIP-seq data. Knock-down of FAM129B resulted in a growth defect and increased sub-$G_0/G_1$ populations in ALK+ ALCL cell lines. Moreover, FAM129B electrophoretic mobility was dependent on NPM-ALK activity, suggesting that NPM-ALK may promote the phosphorylation of FAM129B.

In summary, I showed that JunB played a critical role in promoting proliferation in ALK+ ALCL, but this function was not shared with the related transcription factor, c-Jun. Secondly, I addressed the potential role for JunB in protecting ALK+ALCL tumour cells from immune surveillance. Thirdly, I identified a novel potential JunB and c-Jun transcriptional target that could contribute to growth and survival of ALK+ ALCL cells.

***Stay hungry. Stay foolish.***

***------- Whole Earth Catalog***

**Acknowledgements**

First of all, I would like to thank Dr. Robert Ingham for taking me as a PhD student in his lab from 2012 to 2018. Dr. Ingham showed great support and patience during the past six years. The feedback he provided was very informative and constructive that helped me grow into an independent researcher throughout the years. Dr. Ingham also provided me with great opportunities to attend conferences, where I got exposed to the academia and thought about the scientific questions deeper. I was provided with opportunities to train undergraduate students during my PhD program, and I could understand the training process in difference perspectives.

I would like to thank Dr. Hanne Ostergaard and Dr. Deborah Burshtyn for their advice and help on my research projects as committee members. I would like to thank Dr. Judy Gnarpe for being my mentor for Graduate Teaching and Learning program and I learnt a lot from the teaching experience and guidance she provided. I would like to thank Dr. James Lim and Dr. Kristi Baker for taking time to be my thesis examiners.

I would like to thank the Ingham lab members, both past and present. When I first came here, Dr. Joel Pearson and Mr. Jason Lee had set up a welcoming lab environment and taught me all the key techniques I would apply in my research. I would like to thank Mr. Patrick Paszkowski, who joined the lab in 2016 and maintained the lab in a very organized condition since then on.

I would like to thank Drs. Amanda Scott, Samuel Cheung and Shugang Yao from Dr. Ostergaard's lab for sharing the nucleofector and reagents with me. I would like to thank Mr. Kang Yu, Dr. Heather Eaton, and Ms. Bara'ah Azaizeh from Dr. Burshtyn's lab for providing me with the primary NK cells and related reagents. I would like to

thank our former neighbours Dr. Adil Mohamed, Mr. Wan Kong Yip and Mr. Kevin James from Dr. Shmulevitz's lab for sharing the reagents and equipment with me. I would like to our current neighbours, Mr. Brendan Todd, Dr. Egor Tchesnokov from the Dr. Gotte's lab, for their help and suggestions. I would like to thank Dr. Marchant's lab, Dr. Foley's lab and Dr. Evans' lab for sharing the equipment with me. I would like to thank the MMI office for their administrative support during the past 6 years.

At last, I would like to thank my family for their endless understanding, support, and encouragement during the past years and the years to come.

## Table of contents

**List of figures**

**List of tables**

**List of abbreviations**

| | |
|---|---|
| 2B4 | CD 244, Cluster of Differentiation 244 |
| 7-AAD | 7-amino-actinomycin D |
| ADCC | antibody-dependent cell-mediated cytotoxicity |
| ALCL | anaplastic larger cell lymphoma |
| ALK+ ALCL | Anaplastic lymphoma kinase positive, anaplastic larger cell lymphoma |
| ANOVA | Analysis of Variance |
| ANXA1 | Annexin A1 |
| AP-1 | activator protein-1 |
| aRNA | amplified RNA |
| ATCC | American Type Culture Collection |
| ATF | activating transcription factor |
| BCA | bicinchoninic acid |
| BrdU | Bromodeoxyuridine |
| BSA | bovine serum albumin |
| bZIP | basic leucine zipper |
| CCLE | Cancer Cell Line Encyclopedia |
| CD48 | Cluster of Differentiation 48 |
| CDK | cyclin dependent kinases |
| ChIP | chromatin immunoprecipitation |
| cHL | classic Hodgkin lymphoma |
| CHOP | cyclophosphamide, hydroxydaunorubicin (doxorubicin), oncovin, and prednisone |
| CML | chronic myeloid leukemia |
| CRE | cyclin AMP responsive element |
| CXCL12 | C-X-C Motif Chemokine Ligand 12 |
| Cyp40 | Cyclophilin 40 |
| DAC | 5-aza-2′-deoxycytidine |
| DAPI | 4',6-diamidino-2-phenylindole |
| DAVID | Database for Annotation, Visualization, and Integrated Discovery |
| DDX | DEAD/DEAH box helicases |
| DLBCL | diffuse large B-cell lymphoma |
| DMEM | Dulbecco's Modified Eagle's Medium |
| DNA | deoxyribonucleic acid |
| DNMT | DNA methyltransferase |
| dNTP | deoxynucleotide triphosphate |
| Doxo | doxorubicin |
| E. coli | Escherichia coli |
| EGFP | Enhanced green fluorescent protein |
| EMSA | Electrophoretic mobility shift assay |
| FAM129B | Family with sequence similarity 129 member B |
| FBS | fetal bovine serum |
| FDA | Food and Drug Administration |

| | |
|---|---|
| FJX1 | Four Jointed Box 1 |
| GBP1 | Guanylate Binding Protein-1 |
| GzB | Granzyme B |
| GZMA | Granzyme A |
| HDAC | histone deacetylases |
| HEK-293 | Human embryonic kidney cells 293 |
| hMTIIA | human metallothionein |
| HRP | horseradish-peroxidase |
| IL | interleukin |
| IMT | inflammatory myofibroblastic tumour |
| ITK | IL2 inducible T Cell Kinase |
| JAK | Janus kinase |
| JNK | c-Jun N-terminal kinase |
| KIR | Killer-cell immunoglobulin-like receptor |
| KEGG | Kyoto Encyclopedia of Genes and Genomes |
| LB | Luria-Bertani |
| MEK | ERK kinase |
| MICA | MHC class I related chain A |
| mTOR | mammalian target of rapamycin |
| MXD1 | MAX Dimerization Protein 1 |
| NK cell | natural kill cell |
| NPM | nucleophosmin |
| NSCLC | non-small cell lung carcinoma |
| $p21^{Cip1}$ | cyclin dependent kinase inhibitor |
| P2A | self-cleaving 2A peptide |
| PBMC | peripheral blood mononuclear cell |
| PBS | phosphate-buffered saline |
| PCR | polymerase chain reaction |
| PD-L1 | Programmed death-ligand 1 |
| PDGFR-β | Beta-type platelet-derived growth factor receptor |
| PDK1 | protein 3-phosphoinositide-dependent protein kinase 1 |
| PI3K | phosphatidylinositide 3-kinase |
| PIC | protease inhibitor cocktail |
| PMSF | phenylmethyl sulfonyl fluoride |
| POU2AF1 | POU domain class 2-associating factor 1 |
| PRKA2B | Protein Kinase cAMP-dependent Type II Regulatory Subunit Beta |
| PTPN22 | Protein Tyrosine Phosphatase, Non-Receptor Type 22 |
| qRT-PCR | quantitative real-time polymerase chain reaction |
| RCC | renal cell carcinoma |
| RNA | ribonucleic acid |
| RPMI | Roswell Park Memorial Institute |
| SCC | squamous cell carcinoma |
| SDS-PAGE | sodium dodecyl sulphate-polyacrylamide gel electrophoresis |

| | |
|---|---|
| SGN-35 | Brentuximab vedotin |
| shRNA | short hairpin RNA |
| siRNA | small interfering RNA |
| SLAMF7 | SLAM family member 7 |
| STAT | signal transducer and activator of transcription |
| STS | staurosporine |
| TBE buffer | Tris/borate/EDTA buffer |
| TBL1X | Transducin (beta)-like 1X-linked |
| TBS | Tris-buffered saline |
| TBST | Tris-buffered saline containing Tween-20 |
| TCF | T cell factor |
| TCR | T cell receptor |
| TNF | Tumor necrosis factor |
| TRE | TPA responsive |
| TSS | transcription start site |
| TUNEL | Terminal deoxynucleotidyl transferase (TdT) dUTP Nick-End Labeling assay |
| ULBP3 | UL16 binding protein 3 |
| WHO | World Health Organization |
| WNT-7B | Wnt family member 7B |
| ZEB2 | Zinc Finger E-Box Binding Homeobox 2 |

# Chapter 1: Introduction

## 1.1 ALK+ ALCL

### 1.1.1 Identification and epidemiology

Anaplastic lymphoma kinase positive, anaplastic large cell lymphoma (ALK+ ALCL) is an aggressive CD30+ positive T cell lymphoma and it is under the category of anaplastic large cell lymphoma (ALCL), which was first described in 1985 by H. Stein. *et al* as a unique lymphoma type with large pleomorphic cells expressing CD30 (Ki-1) [1]. The hallmark cells in ALCL are large neoplastic cells with horseshoe shaped nuclei and abundant cytoplasm [2, 3] and multiple morphological patterns can be recognized in ALCL [4]. Depending on whether the ALCL cells possess the chromosomal translocations involving the *ALK* gene that generate the ALK fusion proteins, ALCL is further divided into ALK+ ALCL and ALK− ALCL [5-7]. ALK fusion proteins contribute to the pathogenesis of the disease by initiating a series of signalling pathways [8]. In general, ALK+ ALCL accounts for about 3% [9] of adult non-Hodgkin lymphomas (NHL) and 10-20% of the childhood non-Hodgkin lymphomas [10-12] and ALK+ ALCL is commonly seen in children and young adults with a median age of ~11 years old [10, 13, 14].

### 1.1.2 Disease presentation and prognosis

In general, ALK+ ALCL is an aggressive lymphoma in children and young adult. About 65% of the patients with ALK+ ALCL have advanced stage disease at presentation and 75% of the patients experienced systemic symptoms, especially high fever [10, 13, 15]. This disease mostly impacts lymph nodes (90%), and extranodal involvement is

commonly found in skin (25%), bone (17%), lung (10%) and liver (8%) [13, 16]; central nervous system is rarely impacted by ALK+ ALCL [17].

The prognosis of ALK+ ALCL patients is favorable compared to those of other T cell lymphomas [18]. Approximately 90% of the ALK+ ALCL patients achieve complete remission with chemotherapy; among them, 30 % of the patients relapsed in 2 years and 60% of patients remained relapse free for 5 years [13, 19]. After relapse, some patients can be cured with chemotherapy and some can be cured with intense salvage therapy like hematopoietic stem cell bone marrow transplantation [19-21]. Specifically in ALK+ ALCL, involvement of liver, spleen, lung and skin increases the risk of progression and relapse of the disease [15]. In addition, the serum soluble CD30 level has been reported as a negative prognostic indicator for ALK+ ALCL [22].

### 1.1.3 Treatment

The current first line treatment approach for ALK+ ALCL is based on doxorubicin-containing combination chemotherapy regimens such as CHOP (cyclophosphamide, doxorubicin, vincristine, prednisolone), which is associated with an overall response rate of 90% and 5-year overall survival rate of 65-80% [13, 16, 23]. However, relapse and resistance happen in ~30 % of the cases [19, 23]. More intense chemotherapy strategies have been used, but did not decrease the failure rate [24]. The overall survival rate for the relapsed cases can reach 50-60% recently, and the treatment for recurrent or refractory disease varies for ALK+ ALCL, including single agent chemotherapy, hematopoietic stem cells transplant, and different combinations of the two [19-21, 25-27]. Although some of the recurrent cases are chemo-sensitive and respond to the chemotherapy, the

patients who are refractory to the initial chemotherapy have a poorer overall survival [28].

Targeted therapies have been also developed for patients with high-risk and relapses, although ALK+ ALCL is a rare disease and could be treated with favorable overall survival rate through conventional chemotherapy. Based on the unique phenotype and molecular features of ALK+ ALCL, novel therapies targeting CD30 and ALK fusion proteins are available in the treatment of ALK+ ALCL. A CD30-specific antibody conjugated with an anti-mitotic agent, called Brentuximab vedotin (SGN-35), was approved by FDA in August 2011 to treat relapsed ALCL after failure of chemotherapy regimen [29], and 80%-90% of the patients demonstrated overall response and tumour reduction [30]. The combination of conventional chemotherapy and SGN-35 holds promise as the first-line treatment for ALK+ ALCL in future [24, 31-34]. On the other hand, Crizotinib was the first ALK inhibitor to be tested and used in clinical practice. It is primarily used to treat ALK+ non-small cell lung carcinoma (NSCLC) [35] and it also shows efficacy to treat refractory ALK+ ALCL [36, 37]. Crizotinib has also demonstrated effective as a bridge therapy for hematopoietic stem cell transplantation in ALK+ ALCL refractory to chemotherapy [38]. Thus, Crizotinib may also impact the frontline treatment in the future, given the promising positive effect of it.

### 1.1.4 Cellular Origin of ALK+ ALCL

It is currently accepted that ALK+ ALCL is derived from T cells, as the T cell receptor (TCR) β chain rearrangements could be detected by PCR in 60-90% of the cases [39, 40], although several pan T cell antigens are lost [41]. Several mechanisms could account for

the failure of expression TCRs in ALK+ ALCL cells although the TCRβ rearrangements are present. Mutations in the coding regions or regulatory regions of the gene may contribute to the lack of TCR expression; the TCR-specific transcription factor may be deficient in ALK+ ALCL cells and contribute to the absence of TCR expression [41-43]. In addition, post-transcriptional mechanisms affecting RNA processing and protein stability may also contribute to the deficient TCR expression [41, 44]. CD3 is negative in most cases, while TCR signalling molecules ZAP70, LAT, and SLP76 are negative in more than 75% cases [41]. NPM-ALK/STAT3 dependent epigenetic mechanisms may account for the silencing through methylating the CpG islands in the promoter regions of these genes [45]. CD2, CD4, and CD5 are positive in about 70% cases, but CD8 is negative [46]. Most patient samples are positive for cytotoxic associated-antigens TIA1, granzyme B and perforin [47], thus cytotoxic T lymphocytes is thought to be one possible healthy counterpart of ALK+ALCL cells. Molecules associated with TH17 phenotypes, including IL-17A and IL-17F, were recently detected in some ALK+ ALCL cases, and it suggests that some ALK+ ALCL may originate from TH17 cells [48]. It was recently demonstrated that ALK+ ALCL express genes associated with a set of early thymic progenitors, suggesting ALK+ ALCL might originate from primitive thymic T cell progenitor cells [49, 50]. In addition, NPM-ALK was shown to mimic the TCR-induced signalling thus contributing to the tumourigenesis of ALK+ ALCL [40].

### 1.1.5 Molecular features

#### 1.1.5.1 CD30

ALK+ ALCL is immunophenotypically characterized by the expression of CD30 (also known as TNFRSF8) that is a member of tumor necrosis factor receptor (TNFR). CD30 is expressed by T cells when both TCR ligation and CD28 costimulation happen together; CD30 signalling promotes the cell proliferation and regulates survival of T cells [51]. Other than ALK+ ALCL, CD30 positive lymphomas include classical Hodgkin lymphoma (cHL), cutaneous anaplastic large cell lymphoma (cALCL), CD30-expressing mycosis fungoides (MF) and a subset of diffuse large B-cell lymphoma (DLBCL) [52].

In ALK+ ALCL, CD30 is up-regulated by ALK fusion protein initiated signalling through ERK1/2-JunB and STAT3 pathways [53, 54]. Although CD30 and CD30 ligand (CD30L) interaction or CD30 self-aggregation leads to recruitment of TNFR-associated factor (TRAF) proteins to CD30 cytoplasmic tail and the activation of NF-κB signalling in cHL [55, 56], CD30 signalling does not activate NF-κB signalling in ALK+ ALCL because NPM-ALK blocks the interaction of TRAF with CD30 cytoplasmic tail [57]. Thus, the pro-proliferation pathway NF-κB is not activated by CD30 in ALK+ ALCL, and different roles of CD30 were observed. It was demonstrated that CD30 stimulation causes cell cycle arrest and induces apoptosis in ALK+ ALCL [55, 58, 59]. Watanabe *et al*. showed that siRNA-mediated CD30 knock-down did not result in slower proliferation of Karpas 299 cells, a ALK+ ALCL cell line [60], while Atsaves *et al*. observed reduced proliferation when CD30 was knocked-down with siRNA in SU-DHL1 cells, another ALK+ ALCL cell line [61] On the other hand, CD30 signalling activates the MAPK-ERK1/2 pathway and induces the expression of AP-1 transcription factor JunB in ALK+

ALCL as well as cHL [54, 62]. JunB binds the promoter of CD30 and promote the transcription of CD30 in these lymphomas [54].

#### 1.1.5.2 ALK fusion proteins

The characteristic molecular feature of ALK+ ALCL are chromosomal translocations involving the *ALK* gene, of which *NPM-ALK* was identified in 1994 [63]. Later on, ALK+ ALCL was recognized as a distinct clinicopathological entity in World Health Organization (WHO) classification system [3]. *NPM-ALK* is also the most common ALK translocation, which is generated by fusing the nucleophosmin (*NPM*) gene on 5q35 to the *ALK* gene on 2p23 (**Figure 1.1**) [63, 64]. Several other chromosomal translocations involving the *ALK* gene have been also identified in ALK+ ALCL, generating ALK fusion proteins, and are listed in **Table 1.1**. Moreover, genetic alterations (either translocations or inversions) involving the *ALK* gene have been observed in other malignancies as well, including lung cancer, renal cell carcinoma and inflammatory breast cancer (**Table 1.1**). One example worth mentioning is EML4-ALK, which is found in some cases of non-small cell lung cancer (NSCLC) [65].

**Figure 1.1**

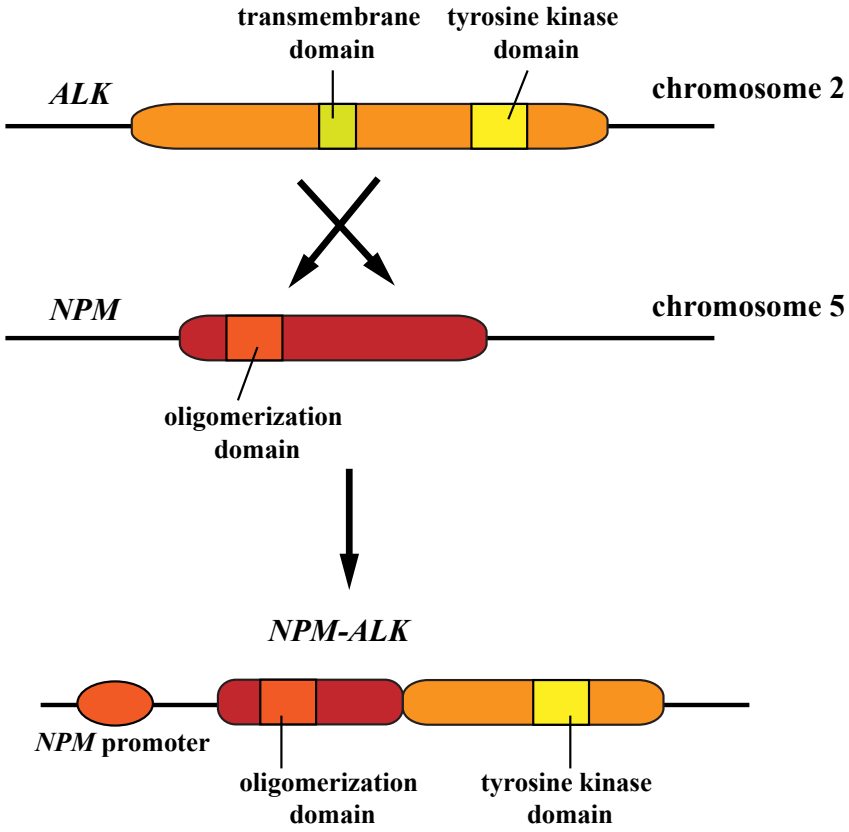


**Figure 1.1 – Chromosomal translocations generating *NPM-ALK***

Schematic diagram showing translocation between the *ALK* gene and the *NPM* gene. The ALK gene is on chromosome 2 and the NPM gene is on chromosome 5. The 5' region of NPM, which has the oligomerization domain, is fused with 3' region of ALK, which has the tyrosine kinase domain. The transcription of NPM-ALK is under the control of *NPM* promoter.

**Table 1.1 ALK fusion proteins**

ALCL: anaplastic large cell lymphoma; DLBCL: diffuse large B-cell lymphoma; IMT: inflammatory myofibroblastic tumour; NSCLC: non-small cell lung carcinoma; RCC: renal cell carcinoma; SCC: squamous cell carcinoma. This table is adapted from tables in the following references [8, 66].

| Fusion protein | Tumour types | References |
|---|---|---|
| NPM-ALK | ALCL, DLBCL | [63, 64, 67] |
| MSN-ALK | ALCL | [68] |
| ALO17-ALK | ALCL | [69] |
| MYH9-ALC | ALCL | [70] |
| TPM3-ALK | ALCL, IMT, RCC | [65, 71-73] |
| TPM4-ALK | ALCL, IMT, SCC | [73-76] |
| TFG-ALK | ALCL, NSCLC | [77, 78] |
| ATIC-ALK | ALCL, IMT | [79-82] |
| CLTC-ALK | ALCL, DLBCL, IMT, extramedullary plasmacytoma | [83-86] |
| CARS-ALK | IMT | [69] |
| RANBP2-ALK | IMT | [87] |
| SEC31L1-ALK | IMT, DLBCL | [88-90] |
| PPFIBP1-ALK | IMT | [91] |
| SQSTM1-ALK | DLBCL | [92] |
| EML4-ALK | NSCLC, breast, colorectal, RCC | [65, 78, 93, 94] |
| KIF5B-ALK | NSCLC | [95] |
| KLC1-ALK | NSCLC | [96] |
| C2orf44-ALK | Colorectal | [97] |
| VCL-ALK | RCC | [98, 99] |

#### 1.1.5.3 ALK signalling

As a transmembrane receptor tyrosine kinase of the insulin receptor superfamily, ALK is expressed only in cells of neural origin under normal physiological condition and contributes to the development of nervous system [100, 101]. It possesses an extracellular ligand-binding domain, a transmembrane-spanning region, and an intracellular tyrosine kinase domain. The ligand for ALK had been an intriguing and debated question, and ALKALs (also known as FAM150) was recently recognized as the physiological ligand for ALK [102-104]. Upon the binding of ALKALs to ALK, ALK can be activated and initiates downstream pathways to promote the growth of the nervous cells [102, 104]. In general, in the model animals including *C. elegans* and *Drosophila*, the deletion of *ALK* resulted in defects in mid gut development, neuronal wiring and plasticity [105]. The loss of *ALK* gene had no overly abnormalities in adult mice [105-107], but the lack of ALK seemed to enhance the cognitive performance and increase alcohol consumption in mice [106-108]. The expression of ALK was increased in neurons to facilitate the regeneration of myelinated axons post-neuronal injuries [109]

While in ALK+ ALCL, chromosomal translocations involving *ALK* gene leads to the abnormal expression and constitutive activation of ALK, the uncontrolled ALK signaling promotes the malignancy formation [110]. Specifically, most of the partners to which the *ALK* gene fuses provides an oligomerization domain, and the dimerization/oligomerization of ALK fusion proteins leads to activation of the ALK tyrosine kinase domain by allowing the fusion proteins to transphosphorylate themselves [111]. NPM-ALK could form oligomers and it can also form dimers with NPM protein, which could shuttle between the cytoplasm and the nucleus [111]. MSN (moesin)-ALK

does not possess an oligomerization domain and it is activated possibly through colocalization of the fusion proteins to cellular membranes [112].

Since 80% of the chromosomal translocations involve the *NPM* gene and *ALK* gene in ALK+ ALCL, I will use NPM-ALK as the example to discuss how ALK fusion proteins play an oncogenic role in ALK+ALCL. NPM-ALK has been proven to be oncogenic in both cell lines and transgenic mouse models [49, 111, 113-118], and this is probably mediated through a variety of downstream pathways that NPM-ALK could activate. The most relevant and well-characterized pathways are the JAK3-STAT3 pathway, RAS-ERK pathway, and PI3K-AKT pathway and these pathways contribute to the cell growth, survival and migration of ALK+ ALCL cells (**Figure 1.2**).

The JAK3-STAT3 pathway contributes to cell proliferation and resistance to apoptosis of ALK+ ALCL cells. STAT3 is a member of the signal transducer and activator of transcription (STAT) family of transcription factors and the phosphorylation of STAT3 facilitates the dimerization and translocation of STAT3 to nucleus and further regulates down-stream targets [119]. NPM-ALK directly phosphorylates STAT3 or activates STAT3 through Janus kinase 3 (JAK3) phosphorylation in ALK+ ALCL [120-122]. STAT3 is activated in ALK+ ALCL patients and ALK+ ALCL cell lines [120, 123, 124], and STAT3 has been demonstrated to promote the tumourigenesis in ALK+ ALCL. Inhibition of STAT3 either by siRNA [125] or a dominant negative STAT3 construct [126] resulted in increased proliferation and apoptosis in ALK+ ALCL. In addition, the survival of NPM-ALK expressed in murine T cells required STAT3 expression [125]. Specially, STAT3 can up-regulate Cyclin D1, Cyclin D3, c-Myc, C/EBP $\beta$ and ICOS to promote the proliferation of ALK+ ALCL cells [125-129]; STAT3 can also promote the

survival of the ALK+ ALCL cells by up-regulating anti-apoptotic molecules including BCL-X [120], survivin and MCL-1 [130-132].

NPM-ALK also binds to and activates phosphatidylinositol 3-kinase (PI3K) through the p85 regulator subunit of PI3K and the p110 catalytic subunit further leads to the downstream AKT activation [133]. NPM-ALK/PI3K/AKT signalling promotes cell proliferation and survival in ALK+ ALCL, as inhibition of PI3K impairs proliferation, induces apoptosis in ALK+ ALCL cell lines [133, 134]. PI3K/AKT pathway leads to down-regulation of Bim and $p27^{Kip1}$, which together promote the cell survival and cell cycle progression of ALK+ ALCL [135]. mTOR is also activated through PI3K/AKT signalling in ALK+ ALCL, and contribute to the translation process in general [136, 137].

The RAS-ERK pathway is also activated in ALK+ ALCL cells and mainly contributes to the increasing proliferation and suppressing apoptosis of the ALK+ ALCL cells [138, 139]. mTOR is one important downstream molecule regulated by ERK signalling [140], and inhibition of mTOR by rapamycin or siRNA impairs cell growth and induce apoptosis in ALK+ ALCL [140], possibly through decreased level of $p27^{Kip1}$, $p21^{Cip1}$ and increased levels of Bcl2, MCL-1 and cFLIP [141]. Another important target of RAS-ERK signalling is JunB, which is promoted through the ETS-1 transcription factor [60]. JunB has been demonstrated to promote cell proliferation in ALK+ ALCL and a more detailed discussion of this protein will be addressed in Section **1.3**.

In addition, NPM-ALK is important for the phosphorylation of JUN N-terminal kinase (JNK) and downstream signalling of JNK further promote cell proliferation by up-regulating cyclin D3 and down-regulating $p21^{Cip1}$ [142]. NPM-ALK signaling can also

modulate the cytoskeleton to increase the migration and invasion. The expression of ALK fusion proteins increases the cell migration rate of fibroblasts and ALK+ ALCL cells, and the change is associated with the changes in cell shape [143-145]. ALK or ALK-fusions have been shown to induce actin filament depolymerization and loss of cell cell-matrix adhesion through a Rho family GTPase [131, 143, 144, 146, 147], thus may contribute to the migration and dissemination of the tumour cells.

**Figure 1.2**

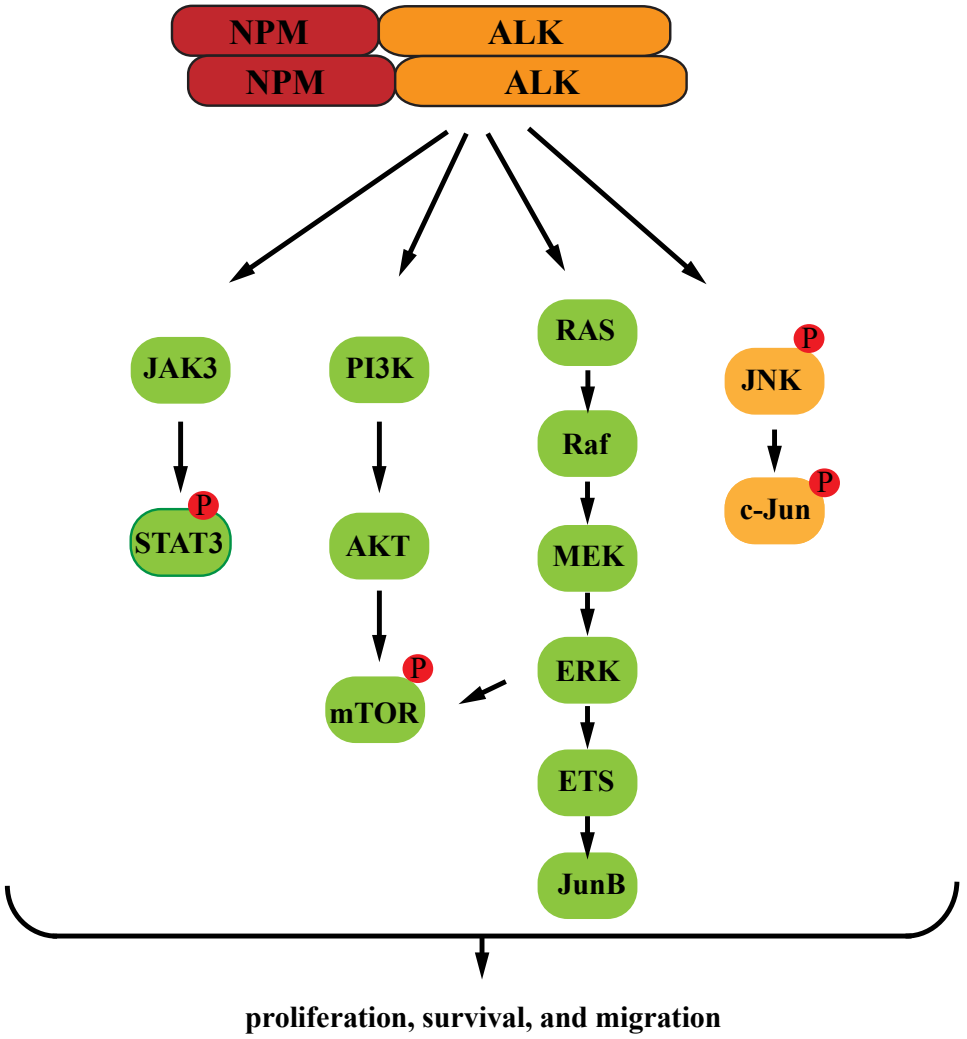


**Figure 1.2 - Downstream pathways activated by NPM-ALK.**

Schematic cartoon showing that constitutively active NPM-ALK activates JAK3/STAT3, PI3K/AKT, MER/ERK, and JNK/c-Jun signalling pathways to promote proliferation, survival and migration of ALK+ ALCL cells.

## 1.2 AP-1 transcription factors

As mentioned above, constitutively active NPM-ALK signalling activates a number of downstream pathways and among them we were intrigued by the AP-1 transcription factors, JunB and c-Jun [54, 60, 142]. Here in this section, I will briefly introduce the AP-1 transcription factors and talk about the function of JunB and c-Jun in normal cell development and tumourigenesis.

### 1.2.1 AP-1 proteins: history and biochemistry

AP-1 proteins are a group of transcription factors that possess a basic leucine zipper domain (**Figure 1.3**). The gene *v-fos* was first identified and isolated from FBJ murine osteogenic sarcoma virus as cell-transforming gene in 1982 [148, 149], and AP-1 transcription factor was first designated as a novel group of transcription factor interacting the human metallothionein (hMTIIA) promoter in 1987 [150]. c-Jun was the first member of AP-1 protein that was described to bind to the TPA-inducible element [151-154], and it was later shown to trans-activate the expression of genes [155]. Then it was demonstrated that c-Fos was not able to form homo-dimers and only have trans-activation capability when forming dimers with other proteins like, c-Jun [156, 157]. Afterwards, more members of AP-1 transcription factor family were identified. Specifically, Jun, Fos, ATF and Maf subfamily members belong to the AP-1 transcription factor family listed in **Figure 1.3A** [158-160]. The AP-1 proteins all possess a bZIP domain which is comprised of a basic DNA binding region and a leucine zipper region, and the structures of Jun subfamily is shown in **Figure 1.3B.** AP-1 proteins form a large variety of dimers through the leucine zipper motif, thus bind to the promoters of genes with different affinities through DNA binding motifs [161]. In general,

the Fos family members cannot form homodimers but form stable heterodimers with Jun family members; Jun family members can form both homo- and heterodimers [156]. Specially, JunB and c-Jun can form dimers with other Jun family members, and JunB and c-Jun can also form dimers with several members from Fos, ATF and Maf families [160]. The Jun-Fos heterodimers preferentially bind to the TPA responsive element (TRE) (5' -TGA (C/G) TCA-3') sites. Jun-ATF and Fos-ATF dimers preferentially bind to another consensus sequence called cyclic AMP responsive element (CRE) (5'-TGA(CG/GC)TCA-3') [160]. Maf family members can form homodimers or heterodimers within the group, and bind to sites consisting of TGCtgaC half-sites [162]. Similarly, Fos-Maf and Jun-Maf dimers preferentially interact with recognition sites composed of AP-1 (TGAC) and Maf (TGCtgaC) half-sites [163]. The sequence that AP-1 binds to may not always be the same. Other transcription factors, like NFAT, ETS-1 and Smad, can bind to regulatory elements adjacent to AP-1 sites and interfere with the interaction of AP-1 dimers and the binding sequences [160].

**Figure 1.3**

**A**

| AP-1 family members | |
|---|---|
| **JUN** | c-Jun, JunB, JunD |
| **FOS** | c-Fos, FosB, Fra-1, Fra-2 |
| **ATF** | ATF-2, ATF-3, ATF-4, ATF-5, ATF-6, ATF-6B ATF-7, BATF, BATF-2, BATF-3, JDP2 |
| **MAF** | c-Maf, MafA, MafB, MafF, MafG, MafK |

**B**

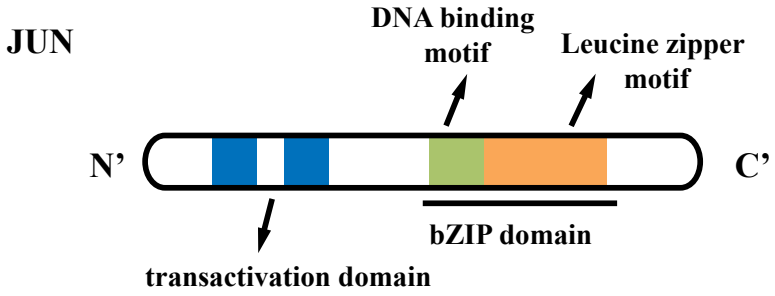


**Figure 1.3 – AP-1 family members and structure of Jun subfamily**

**A.** Table showing the members of AP-1 proteins in different subfamilies. Adapted from review by Garces de Los Fayos Alonso, *et al.* [164]. **B.** Schematic diagram showing the structure of Jun subfamily. Jun family members all possess a transactivation domain and a bZIP domain that consists of a DNA binding motif and a leucine zipper motif for dimerization.

### 1.2.2 JunB and c-Jun regulate many functions in normal cells.

Growth factors control the expression of JunB and c-Jun in cells, and JunB and c-Jun regulate many processes, including the development of skin, bone and immune systems [165] and cellular functions like proliferation and apoptosis [166]. The function of JunB and c-Jun in development was examined in genetic knock-out mice [166]. c-Jun homozygous knock-out and JunB homozygous knock-out in mice were both embryonic lethal [167-169]: c-Jun knock-out mainly impacted liver and heart development [167, 170], while JunB knock-out impacted extra-placenta tissues [169]. The analysis of c-Jun homozygous mutant embryonic stem cells in RAG2 deficient mice revealed that c-Jun could contribute to lymphocyte development [171]. Specifically, the lack of c-Jun impacted the restoration of lymphocytes in bone marrow chimeric mice primary through regulating the T cell receptor induced lymphocyte apoptosis [172]. Likely, JunB appeared to be important for hematopoietic development [173], as mice specifically lacking JunB in the myeloid linage developed myeloid leukemia [173]. In addition, JunB overexpression in T cells affected the T helper cell differentiation, with increased expression of Th2 cytokine, including IL4, which positive regulated Th2 differentiation [174]. This suggested that JunB could contribute to converting naïve T cell into effector populations.

### 1.2.3 JunB and c-Jun function as oncogene and suppressor in tumour cells.

It was long believed that c-Jun generally function as a positive cell cycle regulator as c-Jun could repress the transcription of p53, $p21^{Cip1}$ and $p16^{Ink4a}$ and induce the transcription of cyclin D1 in mouse fibroblasts [175-177]. While JunB was believed to act as negative cell cycle regulator as JunB could down-regulate cyclin D 1 and up-regulate $p16^{Ink4a}$ in mouse

fibroblasts [178]. However, as more investigations were done in other cell types and tumour cells, both c-Jun and JunB have been show to conduct different roles dependent on cell context. I will focus on the role of c-Jun and JunB in tumourigenesis in the following paragraphs.

#### 1.2.3.1 The role of c-Jun in tumourigenesis

**Pro-tumour function**

Here I will provide some clinical evidence showing that c-Jun functions as a pro-tumour gene. In DLBCL, c-Jun was highly activated and activation of c-Jun correlated with the expression of cyclin A [179]. In addition, the expression of c-Jun was associated with poor prognosis in ovarian cancer [180] as well as with chemo-resistance in brain tumours and lung cancer [181]. c-Jun, cooperating with STAT3, repressed the transcription of Fas death receptor directly and increases the resistance of melanomas to UV light [182-184]; it also protected chemically induced hepatocellular carcinomas from undergoing TNF-α-induced p53-dependent apoptosis [185]. c-Jun also promoted the transformation of adipogenic cells into sarcoma, by interrupting the C/EBPβ adipogenic transcription factor, thus preventing the cells undergoing adipogenic differentiation [186]. In the intestinal neoplastic transgenic mouse model where the one *adenomatous polyposis coli (APC)* gene allele was mutated, the inactivation of c-Jun reduced the numbers and sizes of the intestinal tumours [187]. Specifically, JNK phosphorylated c-Jun could interact with T cell factor 4 (TCF4) and form a complex containing c-Jun, β-catenin, TCF4 and nuclear Dvl [187, 188]. Then the complex could further increase the transcription of c-Jun and other β-catenin targets to promote the tumourigenesis [189, 190].

As the new hallmarks of cancer have emerged [191], studies have revealed the role of c-Jun in other aspects of tumour biology. In prostate cancer, c-Jun was up-regulated [192] and promotes angiogenesis through VEGFA-induced signal cascade [193]. In invasive breast cancer cases, c-Jun was expressed at the invasive front and was associated with proliferation and angiogenesis [194]. Specifically, c-Jun/Fra1 together promote the transcription of Zinc Finger E-Box Binding Homeobox 2 (ZEB2) [194, 195], which in turn repressed the expression of E-cadherin by binding to the E2 boxes of E-cadherin promoter [196]. The decrease of E-cadherin could further contribute to the invasion of triple negative breast cancer cells [195]. In addition, TGF-β induced the up-regulation of c-Jun and ATF3; the c-Jun/ATF3 dimers further bound to the AP-1 site in the promoter of MMP13, which may also contribute to the invasion human breast cancer cell line [197]. In DLBCL, c-Jun could promote tumour dissemination through up-regulating *ITGAV*, *FoxC1*, and *CXSCR1* [198].

**Anti-tumour function**

Although most of the reports support c-Jun functioning as a pro-tumour gene, c-Jun has also been demonstrated to possess anti-tumour functions in several tumours. Several studies suggest that low c-Jun levels were linked with transformed cells and low-grade differentiation cells. For example in epithelial cells, c-Jun regulated differentiation-associated genes and it was decreased in esophageal squamous cell carcinoma [199]. In breast cancer, *c-Jun* mRNA level was lower than the surrounding tissues suggesting a negative correlation between c-Jun and breast tumour cells [200]. In addition, c-Jun and JunB were shown to up-regulate the expression of the tumour suppressor cyclin D-interacting Myb-like protein 1 (Dmp-1), which in turn up-regulated the cyclin-dependent kinase inhibitors $p19^{Arf}$ in mouse

(known as $p14^{Arf}$ in human,) to in mouse embryonic fibroblasts [201].

### 1.2.3.2 The role of JunB in tumourigenesis

**Pro-tumour function**

In contrast to the long believed growth-inhibiting role of JunB [159, 202], it was found to promote neoplastic transformation in certain tissues. It was shown that JunB promoted the transcription of cyclin A in fibroblasts [203] and inhibited apoptosis in insulin-producing cell lines [204] or in nigral neurons [205]. In general, JunB was required for cells to re-enter the cell cycle after quiescence in mouse fibroblasts [206] and cooperated with c-Jun to in the development of fibrosarcoma [207]. Moreover, JunB was also suggested to substitute for c-Jun in improving the survival of c-Jun-deficient embryos [208].

The overexpression of JunB was observed in multiple hematopoietic malignancies. Specifically, the overexpression of JunB was observed in CD30-positive lymphomas, cHL and ALK+ ALCL, and lymphomatoid papulosis and cutaneous lymphomas patients [209-212]. JunB, together with c-Jun, JunD and c-Fos were found to be up-regulated in splenic marginal zone B cell lymphoma patients as well [213]. In DLBCL, JunB was also highly expressed and positively correlated with proliferation markers, including cyclin A, cyclin B1 and cyclin E [179]. In multiple myeloma cells co-cultured with bone marrow stromal cells JunB was highly induced and is essential for cell proliferation, survival and drug resistance [214]. Other than hematopoietic tumours, JunB was demonstrated to be important in solid tumours. In breast cancer, TGF-β-mediated up-regulation of JunB induced the expression of WNT7A/B, thus contributing to tumour invasion [215]. JunB was also induced after breast cancer cells were treated with kinase inhibitors and this contributed to treatment resistance

[216]. In addition, JunB was up-regulated in gallbladder cancer through protein 3-phosphoinositide-dependent protein kinase 1 (PDK1) signalling, and associated with expression of N-cadherin and E-cadherin which contribute to tumour invasion [217]. Collectively, JunB can promote proliferation and cooperate with c-Jun to transform tumour cells, especially lymphomas.

**Anti-tumour function**

JunB has been long believed to act as a negative regulator of proliferation: it down-regulated cyclin D expression and up-regulated the $p16^{Ink4a}$ expression in mouse fibroblasts [176]. JunB also promoted apoptosis by inhibiting autophagy in starved HeLa cells [218]. Evidence from clinical studies also supported that JunB functions as a tumour suppressor. JunB expression was negatively correlated with the grade of prostate cancer, and loss of JunB led to the increased proliferation and decreased senescence through inhibiting $p16^{Ink4a}$ and $p21^{Cip1}$ in prostate epithelial cells [219].

JunB has also been shown to act as a tumour suppressor in transgenic mouse models. Specifically, the B-lymphoid cells of JunB transgenic mice (Ubi-JunB mice), where JunB was constitutively overexpressed from a human ubiquitin C promoter [220], responded poorly to mitogenic stimuli and were less susceptible to the transforming oncogene [221]. Lack of JunB in transgenic mice ($JunB^{-/-}$Ubi-JunB mice) resulted in increased proliferation of myeloid progenitor cells, which resembled the human chronic myeloid leukemia (CML); ectopic expression of JunB reverted the hyper-proliferative phenotype of JunB-deficient myeloid cells [173]. Consistently, methylation-induced silencing of JunB was observed in human CML patients [222]. Other than CML, JunB was also down-regulated in AML

patients; JunB was a direct target of PU.1 and repression of PU.1 led to low level of JunB and further develop into myeloid leukemic cells in mice [223]. In T-cell acute lymphoblastic leukemia, miRNA-149 repressed the expression of JunB, and thus promoted tumour cells proliferation by up-regulating cyclin D1 and down-regulating $p21^{Cip1}$ and inhibited apoptosis [224].

Taken together, c-Jun and JunB regulate many functions in tumourigenesis and whether they function as oncogenes or tumour suppressors is dependent on the cell context. In the next section I will focus on c-Jun and JunB in ALK+ ALCL and address how they contribute to the pathogenesis of this disease.

## 1.3 JunB and c-Jun are up-regulated and activated in ALK+ ALCL

### 1.3.1 Mechanisms for JunB/c-Jun up-regulation and activation

In ALK+ ALCL, multiple mechanisms accounts for the up-regulation of JunB (**Figure 1.4**). First of all, *JunB* gene amplification was observed in ALK+ ALCL patient samples, but there was no correlation with the increased JunB level and gene amplification [61]. In addition, CD30 and NPM-ALK both activated MEK-ERK1/2-ETS-1 pathway [54, 136], and ETS-1 transcription factor bound to the promoter of *JunB* to increased the transcription of JunB [60]. Moreover, NPM-ALK also activated PI3K-AKT-mTOR signalling, and mTOR directed JunB mRNA to ribosome-rich polysomes thus increased the translation of JunB [136]. In addition, the activated AKT inhibited GSK-β activity and further protected JunB from degradation in ALK+ ALCL [225]. Specifically, the GSK-β was necessary for the phosphorylation of JunB on serine 251 and threonine 255 sites; the $SCF_{FBXW7}$ ubiquitin ligase is recruited to JunB that is phosphorylated at serine 251 and threonine 255, which mediates the ubiquitylation and

degradation of JunB [225]. As for c-Jun, the activity of c-Jun was regulated by JNK that was activated through NPM-ALK signalling (**Figure 1.4**). Phosphorylation of c-Jun N-terminal domain at residues S63/S73 by JNK facilitated the interaction with co-activators thus promoting the transcription of target genes [226, 227]. Given the fact that an AP-1 site was located in c-Jun promoter, the activated c-Jun bound to its own promoter to increase the transcription of itself in ALK+ ALCL [142].

**Figure 1.4**

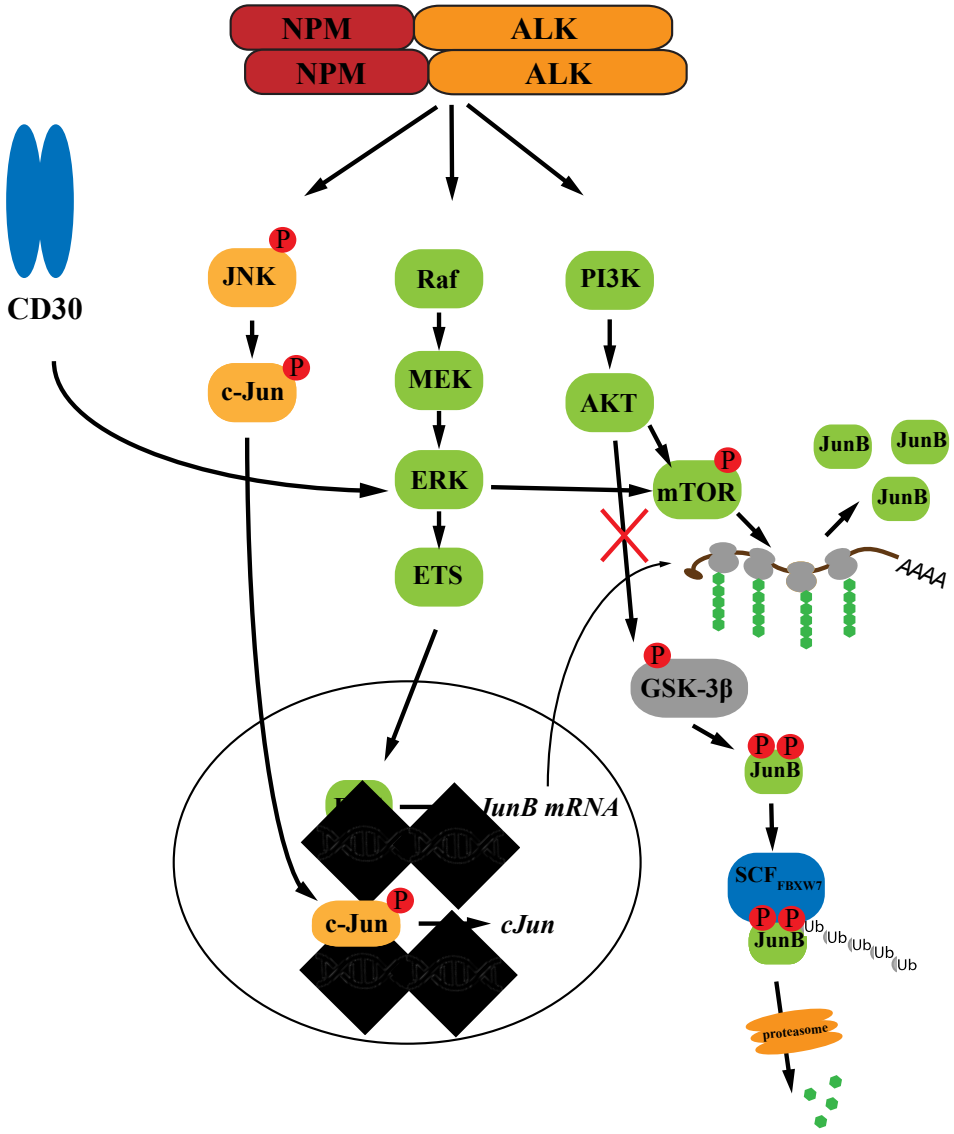


**Figure 1.4 - JunB and c-Jun are highly up-regulated or activated in ALK+ ALCL through multiple mechanisms**

Schematic graph showing how the transcription of JunB could be up-regulated through MEK/ERK/ETS-1 pathway and CD30 signalling. PI3K/AKT/mTOR pathway elevates the translation of JunB by directing JunB mRNA to ribosome-rich polysomes, and represses the GSK-3β-mediated degradation of JunB. c-Jun is activated through JNK signalling and promotes the transcription of itself in ALK+ ALCL.

### 1.3.2 Function of JunB and c-Jun in ALK+ ALCL

In terms of the function of JunB, Staber *et.al* demonstrated that siRNA-mediated JunB knock-down impaired cell growth with increased percentage of cells in $G_0/G_1$ phase and decreased percentage of cells in $G_2$/M phase [136]. Atsaves *et.al* demonstrated that siRNA targeting of JunB resulted in more cells in $G_0/G_1$ phase, but a lower percentage of cells in S phase; JunB knock-down resulted in modest change in colony formation of Karpas 299 cells in methylcellulose culture although the change did nor reach statistical significance [61]. In addition, BATF was shown to dimerize with JunB and knock-down of BATF resulted in reduced proliferation in ALK+ ALCL cell lines. This also suggested that JunB played important role in promoting cell proliferation [228]. Moreover, several targets of JunB have been identified by researchers during the past decades. EMSA experiments revealed that JunB bound to the AP-1 site in the promoter of *CD30* and luciferase assay demonstrated that JunB could activate the AP-1 site in the *CD30* promoter [54]. Thus a positive feedback loop was formed where CD30 signalling also increased the transcription of JunB through MEK-ERK-ETS-1 pathway [54, 60].

JunB also bound to the promoter of *PDGFR-β* and promoted the transcription of *PDGFR-β*, which was highly expressed on the surface of ALK+ ALCL cell lines and patient samples and promoted the proliferation of ALK+ ALCL cells [229]. *GzB* and *Cyp40* were also shown as potentially direct transcriptional targets of JunB by the Ingham lab, as the EMSA experiments demonstrated that AP-1 sites in the promoter region of *GzB* and *Cyp40* could be bound by JunB. [230, 231]. Stable *GzB* knock-down sensitized the ALK+ALCL cell lines to drug-induced apoptosis, thus the high expression level of GzB may be a reason why ALK+ ALCL patients were generally responsive to first line chemotherapies [231]. Cyp40

could promote the survival of ALK+ALCL cells, as siRNA-mediated knock-down of Cyp40 impaired the growth of ALK+ ALCL cell lines [230]. EMSA experiments also revealed that JunB also bound to AP-1 sites in the promoter of *AKT-1* and two other isoforms *AKT-2* and *AKT-3*; JunB synergized with STAT3 to control the transcription of *AKT-1* in ALK+ALCL cell lines, and further promoted cell proliferation[232]. *DDX11*, a DNA helicase, was claimed as a JunB target as well. Specifically, DDX11 levels were negatively correlated with JunB levels, and JunB was shown to bind to the promoter of this gene, suggesting JunB could repress the transcription of *DDX11* gene [225]. The repression of DDX11 may contribute to chromosomal instability in ALK+ ALCL [225].

Regarding the function of c-Jun in ALK+ALCL, discrepancies exist in the literature. Staber *et.al* showed that siRNA-mediated c-Jun knock-down did not affect Karpas 299 cell growth [136]; while Atsaves *et.al* showed c-Jun siRNA transfection resulted in decreased colony formation ability in methylcellulose matrix [61]. Furthermore, Leventaki *et.al* showed inhibition of JNK kinase by SP600125 resulted in slower growth of SUDHL1 cell, an ALK+ ALCL cell line. In addition, siRNA-mediated knock-down of c-Jun reduced the cell viability and cell growth with increased level of $p21^{Cip1}$ and decreased level of cyclin D3 [142].

JunB and c-Jun have also been suggested to overlap in function in ALK+ ALCL tumour/ colony formation. Specifically, the expression of NPM-ALK under control of the CD4 promoter resulted in T cell tumours in transgenic mice [229]. When either JunB or c-Jun was deleted in the NPM-ALK transgenic CD4+ T cells, tumour size did not change; however, when JunB and c-Jun were both deleted, the formation of tumour was impaired and mice lived longer [229]. This data suggest JunB and c-Jun may have overlapping functions in tumour formation in NPM-ALK expressed murine T cells. Atsaves *et.al* also demonstrated

that knocking down both JunB and c-Jun with siRNA resulted in a more dramatic reduction in the colony formation ability in Karpas 299 cells, suggesting overlapping role of c-Jun and JunB in cell growth and migration in ALK+ ALCL cells [61]. c-Jun was shown to bind to the promoters of *PDGFR- β* and *AKT-1*/2/3 as well, but with lower affinity compared to JunB; luciferase reporter assays also demonstrated that c-Jun synergized with JunB to promote the transcription of *PDGFR- β* and *AKT-1/2/3* [229, 232]. Collectively, JunB and c-Jun could function together to regulate the tumourigensis of ALK+ ALCL.

**Figure 1.5**

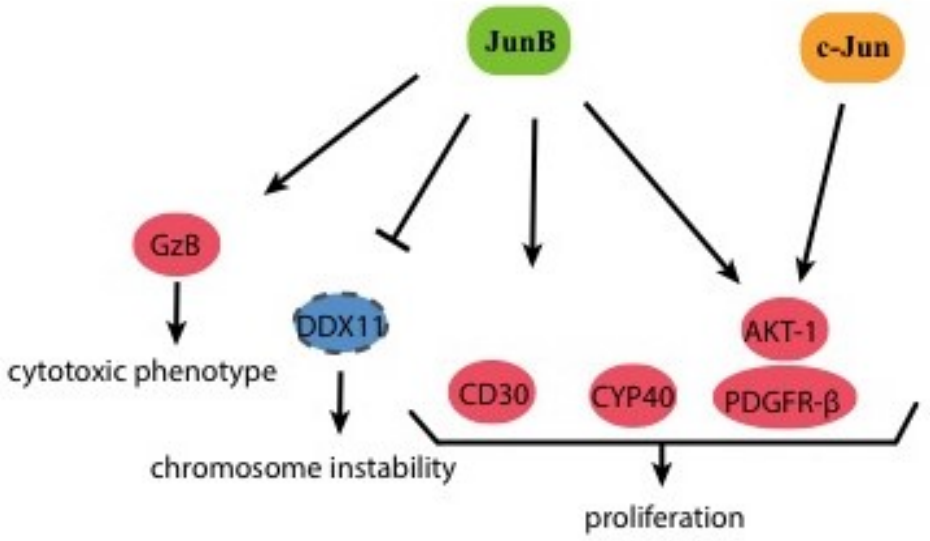


**Figure 1.5 – Targets of JunB and c-Jun in ALK+ ALCL**

The described transcriptional targets of JunB and c-Jun in ALK+ ALCL are shown in the schematic. GzB is up-regulated by JunB to contribute to the cytotoxic phenotype and could be a reason why ALK+ ALCL is sensitive to chemotherapy. DDX11 is claimed to be down-regulated by JunB and contributes to the chromosome instability. CD30 and CYP40 are up-regulated by JunB to promote proliferation and survival of ALK+ ALCL cells. JunB and c-Jun together up-regulate AKT-1 and PDGFR- β to promote ALK+ ALCL cell proliferation. Red colour indicates up-regulated targets; blue colour indicates down-regulated targets.

### 1.4 Research questions

JunB has been demonstrated to promote tumour cell proliferation, as knock-down JunB with siRNA resulted in slower growth of ALK+ ALCL cells lines [61, 136], but no work has been done to examine the outcome of stably knocking down JunB for a longer period of time. In addition, discrepancies exist as to whether c-Jun is important to promote cell proliferation in ALK+ALCL as mentioned above. Thus, further investigation is needed to address whether c-Jun promotes the proliferation of ALK+ ALCL cells. Moreover, JunB and c-Jun have been demonstrated to overlap in function in murine model. Therefore, a more thorough and systematic work was needed to further elucidate and compare the role of JunB and c-Jun in ALK+ ALCL. Although several targets of JunB and c-Jun had been identified, such as *CD30, GzB, Cyp40, AKT-1/2/3* and *DDX11*, I believed additional targets of these AP-1 proteins remained to be identified. **The overall goal of my thesis was to examine how JunB and c-Jun contribute to the pathogenesis of ALK+ALCL, and ultimately I want to identify novel downstream targets of the two AP-1 proteins and elucidate what role the targets play in ALK+ ALCL.** To achieve the goal of my research, I had three specific aims.

**Aim 1**: Examine the role of JunB and c-Jun in ALK+ ALCL cell growth by stably reducing JunB or c-Jun expression. (Chapter 3)

**Aim 2**: Identify the genes with changed expression when JunB is stably knocked-down with microarray, and characterize the genes in the pathobiology of ALK+ ALCL (Chapter 4)

**Aim 3**: Identify the binding sites of JunB and c-Jun in ALK+ ALCL with ChIP-seq and characterize the genes as potential targets of JunB and c-Jun. (Chapter 5)

# Chapter 2: Materials and Methods

Some of the methods in Chapter 2 were adapted from protocols in Dr. Ingham's lab.

## 2.1 Cell culture

### 2.1.1 Cell lines

ALK+ ALCL cell lines (Karpas 299, SUP-M2, and SUDHL-1) were obtained from the Leibniz Institute DSMZ-German Collection of Microorganisms and Cell Cultures (Braunschweig, Germany). The ALK+ ALCL cell line, SR, was obtained from the American Type Culture Collection (ATCC, Manassas, VA). The UCONN-L2 ALK+ ALCL cell line was obtained from Dr. Raymond Lai (University of Alberta, Edmonton, AB). The Burkitt's lymphoma cell line BJAB was from Dr. Tony Pawson (University of Toronto, Toronto, ON); the Burkitt lymphoma cell line, Ramos, was from Dr. Michael Gold (University of British Columbia, Vancouver, BC); DG-75 were obtained from the ATCC. The classic Hodgkin lymphoma cell lines L-540, L-428, KM-H2, and HDMY-Z were obtained from the Leibniz Institute DSMZ. T cell leukemia cell line, Jurkat was obtained from Dr. Tony Pawson (University of Toronto). All the mentioned hematopoietic cell lines were grown in Roswell Park Memorial Institute (RPMI) 1640 media supplemented with 10% fetal bovine serum (FBS), 2 mM L-glutamine (Gibco; Burlington, ON, Canada), 1 mM sodium pyruvate (Sigma-Aldrich; St Louis, MO), and 50 μM 2-mercaptoethanol (BioShop; Burlington, ON, Canada), except that KM-H2 and L-540 cell lines were supplemented with 20% heat-inactivated FBS. HEK-293T cells and HeLa cells were obtained from the ATCC and were cultured in DMEM supplemented with 10% FBS, 1 mM sodium pyruvate and 2 mM L-glutamine. Tet-on HEK-293 cells carrying pTRE-TIGHT/NPM-ALK were obtained from Dr. Raymond Lai (University of Alberta) and maintained in DMEM supplemented with 10% Tet-System Approved FBS (Clontech, Moutain View, CA), 100 μg/ml G418 (Sigma) and 50 μg/ml hyrogomycin B (Clontech) [233]. Tetracycline was added to the culture to induce the

expression of NPM-ALK and the lysates were collected by Dr. Joel Pearson, a former PhD student in Dr. Ingham's lab. All cells were maintained at 37°C in a 5% $CO_2$ atmosphere.

The human NK cell lines, NK-92, NKL and YTS were generously provided by Dr. Deborah Burshtyn (University of Alberta, Edmonton, AB). NK-92 cells were cultured in αMEM medium supplemented with 12.5% heat inactivated HyClone characterized FBS, 12.5% horse serum, 0.2 mM Inositol, 0.02 mM folic acid, 100 μM 2-ME, 2 mM L-glutamine and 1,000 U/ml human recombinant IL-2 (TECIN, obtained from the Biological Resources Branch, DCTC, NCI-Frederick Cancer Research and Development Center). NKL cell line was maintained in Iscove's modified Dulbecco's medium supplemented with 10% HyClone characterized FBS with 2mM L-glutamine 2,000 U/ml recombinant human interleukin (IL)-2 (Sigma-Aldrich). YTS cells maintained in Iscove's modified Dulbecco's medium supplemented with 15% HyClone characterized FBS, 50 μM 2- ME / 2mM L-glutamine. 721.221 (221) cells, an EBV transformed B cell line, were obtained from the Burshtyn lab and were cultured in Iscove's Modified Dulbecco's Medium (Invitrogen Gibco) supplemented with 10% HI FBS, 2 mM L-glutamine (Invitrogen Gibco).

Primary NK cells were isolated and maintained in Dr. Burshtyn's lab. Studies performed with primary NK cells were approved by the University of Alberta Health Research Board (Protocol No. Pro00000920; Dr. Deborah Burshtyn) and blood was collected with consent from normal healthy donors. Briefly, the NK cells were purified from total peripheral blood mononuclear cell (PBMC) using the StemSep Human NK Cell Enrichment Kit (StemCell Technologies, Vancouver, BC). Isolated NK cells were plated on irradiated 221 cells in Iscove's medium supplemented with 10% HI human serum (Life Technologies, Invitrogen), 500 mM Gentamicin (Invitrogen Gibco) and 1000 U/mL IL-2 (TECIN). Cells

were fed every 2-3 days with new media and IL-2 for 7 days and then split 1:2 every 2-3 days. Primary NK cells were used between 8 and 20 days following isolation. All cells were maintained at 37°C in a 5% $CO_2$ atmosphere.

### 2.1.2 Generating stable cell lines with lentiviral particles

#### 2.1.2.1 Generating lentiviral particles

Lentiviral particles were generated using the MISSION short hairpin RNA (shRNA) lentiviral system (Sigma-Aldrich) in HEK-293T cells. Specifically, HEK-293T cells were seeded at 40% confluence in a six-well plate one day before transfection; media was removed and replaced with 1 ml fresh media on the day of transfection. The transfection cocktail contains 1.13 μg of shRNA plasmid and 10 μl of lentiviral packaging mix (SHP001; Sigma-Aldrich), 79 μl of serum free DMEM and 7 μl FuGene HD (Promega; Madison, WI). Then the transfection cocktail was incubated for 10 min at room temperature, then added to each well of HEK-293T cells. The cells were incubated at 37°C overnight and the media was discarded and replaced with 3ml fresh media16 hours post-transfection. The virus-containing media was collected 48 hours post-transfection and 3 ml fresh media was added back into the wells; the virus-containing media was collected again at 72 hours post-transfection. The collected virus-containing media was passed through a 0.45 μm low protein-binding syringe filter (EMD Millipore; Billerica, Massachusetts) to get rid off the HEK-293T cells and other debris. The virus supernatants were aliquoted into 1 ml per tube and stored at -80°C for use. The shRNA plasmids used to generate lentiviral particles are listed in **Table 2.1**.

#### 2.1.2.2 Titration of the lentiviral particles

To make sure every infection was done with similar multiplicity of infection (MOI), the viral supernatants were tittered as following. Each lentiviral supernatant was diluted into 1, 1/3, 1/9 and 1/27 dilutions with RPMI media and then the diluted supernatants were used to infect HEK-293T cells with 8 μg/ml polybrene present in the culture. 24 hours post infection, the virus supernatant was washed off with PBS and fresh media was added onto the HEK-293T cells. 48 hours post infection, 1 μg/ml puromycin was added to each well and cells were incubated at 37°C for another two to three days. After selection with puromycin, cells were examined under the microscope to determine the optimal dilution of viral supernatants and the lowest dilution achieved the highest viability was used in subsequent infections.

#### 2.1.2.3 Infecting cells with lentiviral particles

ALK+ ALCL cell lines were counted and resuspended to $5x10^5$ cells/ml before infection and 1 ml of the cell culture was transferred to one well of 6 well plate. 1 ml of lentiviral supernatants at proper dilution was added to each well of cells and 8 μg/ml polybrene (Sigma-Aldrich) was added to the infection mixture. Cells were incubated at 37°C for 24 hours. Then cells were washed twice with 10 ml RPMI media and resuspended in 5 ml fresh RPMI media. After another 24 hours incubation at 37°C hours, puromycin (Sigma-Aldrich) was added to a final concentration of 0.5 μg/ml to select the successfully infected cells.

### 2.1.3 Nucleofection

Nucleofection was performed using an Amaxa$^{TM}$ cell line Nucleofector$^{TM}$ Kit V using an AMAXA nucleofector (Lonza AG; Basel Switzerland). Briefly, $5\times10^{6}$ cells were resuspended into 100 µl with the nucleofection reagent, which contains 90 µl of the cell line specific Nucleofection$^{TM}$ solution V and 10 µl of the supplement solution from the kit (Lonza AG). 5 µg of the plasmid was added into the transfection mixture, pulsed using Program A30, and then incubated at room temperature for 10 min. The nucleofected cells was resuspended into 5 ml of fresh media and incubated at 37 °C. Cells were collected at different time points post nucleofection for western blotting or flow cytometry analysis.

**Table 2.1. shRNAs used in lentiviral particle generation**

Puro: puromycin resistance. shRNA sequence is listed with targeting sequences bolded.

| Name | Catalogue ID | Vector | shRNA sequence |
|---|---|---|---|
| **Ctrl shRNA (Non targeting)** | SHC216 | pLKO.5-puro | CCG G**GC GCG ATA GCG CTA ATA ATT T**CT CGA G**AA ATT ATT AGC GCT ATC GCG C**TT TTT |
| **Ctrl shRNA (Non-mammalian shRNA Control)** | SHC002 | pLKO.1-puro | CCG G**CA ACA AGA TGA AGA GCA CCA A**CT CGA G**TT GGT GCT CTT CAT CTT GTT G**TT TTT |
| **JunB shRNA#1** | TRCN0000014943 | pLKO.1-puro | CCG G**CA GAC TCG ATT CAT ATT GAA T**CT CGA G**AT TCA ATA TGA ATC GAG TCT G**TT TTT |
| **JunB shRNA#6** | TRCN0000232087 | pLKO.5-puro | CCG G**GG AAA CAG ACT CGA TTC ATA T**CT CGA G**AT ATG AAT CGA GTC TGT TTC C**TT TTT G |
| **c-Jun shRNA#1** | TRCN0000010366 | pLKO.1-puro | CCG G**TA GTA CTC CTT AAG AAC ACA A**CT CGA G**TT GTG TTC TTA AGG AGT ACT A**TT TTT G |
| **c-Jun shRNA#5** | TRCN0000039591 | pLKO.1-puro | CCG G**AC TCA TGC TAA CGC AGC AGT T**CT CGA **GAA CTG CTG CGT TAG CAT GAG T**TT TTTG |
| **FAM129B shRNA#A2** | TRCN0000140763 | pLKO.1-puro | CCG G**GA GCT GAT CTT CGA GGA CTT T**CT CGA G**AA AGT CCT CGA AGA TCA GCT CT**T TTT TG |
| **FAM129B shRNA#A3** | TRCN0000122833 | pLKO.1-puro | CCG G**GC AGA GCT GCT ATG AGA AGA T**CT CGA G**AT CTT CTC ATA GCA GCT CTG CT**T TTT TG |

## 2.2 DNA methods

### 2.2.1 Polymerase chain reaction (PCR) for cloning

PCR was performed with *Pfu* polymerase system. In a 50 $\mu$l reaction system, 0.8mM deoxynucleotide triphosphate (dNTP) mix (Fermentas), 4 mM $MgSO_4$, 0.3 μM forward and reverse primers, 1 μl DMSO and 2.5 U of *Pfu* polymerase (Fermentas) were added. PCR reactions were performed on a Biometra T-gradient thermal cycler (Biometra; Goettingen Germany) and the PCR cycling steps started with an initial denaturing step at 95°C for 3 min, followed by 35 cycles of denaturing at 95°C for 30 sec, annealing at 52-60°C for 30 sec, and extension at 72°C for 1-2 min, and then a final extension step at 72°C for 5 min. The sizes of the PCR products were determined on a 1% (w/v) agarose gel prepared in 1× Tris-acetate-EDTA (TAE) buffer (40 mM Tris, 20 mM acetic acid, 1 mM EDTA) containing 1:10,000 SYBR Safe DNA gel stain (Invitrogen). PCR products were then purified using the QIAquick PCR Purification kit (Qiagen) as described in manufacturer's instructions.

### 2.2.2 Restriction endonuclease digestions

In a 20 μl reaction system, 0.5-2 μg of purified PCR product or plasmid DNA was incubated with 0.5-1.0 μl of the desired restriction enzyme(s) in 1× FastDigest buffer (Fermentas) at 37°C for 1-3 hours. Then the DNA was purified using the QIAquick PCR Purification kit (Qiagen) as described in the manufacturer's protocol.

### 2.2.3 DNA ligations

Ligations were performed with 50 ng of digested vector and the appropriate amount of insert to give an insert to vector molar ratio of 3/1 or 6/1. The ligation was done in 20 μl reaction

volumes using 1 U of T4 DNA ligase (Fermentas) in the supplied T4 DNA ligase buffer (Fermentas) and incubated overnight at room temperature.

### 2.2.4 Bacterial transformation

Half of the ligation products/plasmid DNA was transformed into chemically competent *Escherichia coli* (*E. coli*). Specifically, the competent *E. coli* were incubated with DNA on ice for 30 min, and heat shocked at 42°C for 2 min. Cells were then incubated for 5 min on ice and plated on Luria- Bertani (LB) agar plates (1% (w/v) tryptone, 0.5% (w/v) yeast extract, 1% (w/v) NaCl, 1.5% (w/v) agar, pH 7.4) containing 100 μg/ml ampicillin (Sigma-Aldrich). LB plates were then incubated at 37°C for 16-20 hours. For lentiviral system plasmids, the STBL3 strain was used; for regular cloning, DH5α was used.

### 2.2.5 Isolation and purification of plasmid DNA

Plasmid DNA was isolated from *E. coli* with Qiagen Qiaprep Spin Miniprep kit (QIAGEN). Briefly, the 2 ml overnight culture of bacteria was harvested by centrifugation. Bacterial cells were then lysed and the DNA bound to columns. Following several washes, the DNA was eluted from the column, and the DNA concentration quantified using a NanoDrop ND-1000 spectrophotometer (Thermo Scientific). For nucleofection experiments, the large amount of plasmid was purified with Qiagen Plasmid Maxi (QIAGEN, Germany) from a 125 ml culture of bacteria.

### 2.2.6 DNA sequencing and analysis

The constructed plasmids were sequenced at The Applied Genomics Centre (TAGC) (University of Alberta) using the T7-forward and SP6 sequencing primers supplied by TAGC. The reference DNA sequences for EGFP and JunB were obtained from National Center for biotechnology Information (NCBI). The comparison and sequence chromatograms were analyzed using SnapGene (GSL Biotech, IL).

### 2.2.7 Cloning strategies for pcDNA3-EGFP-P2A-FLAG-JunB

EGFP-P2A fragments was synthesized by Integrated DNA Technologies (IDT Inc, IL), and cloned into pcDNA3 plasmid (Invitrogen) after *HindIII* (FastDigest$^{TM}$ ThermoScientific) and *NotI* (FastDigest$^{TM}$ Thermo Scientific) endonuclease digestion. Flag-tagged JunB cDNA was amplified from pcDNA3-Myc-JunB by PCR, which was constructed by a former PhD student, Joel Pearson. Then the Flag-tagged JunB cDNA was further cloned into pcDNA3-EGFP-P2A construct after digestion with *NotI* and *XbaI*. To make the plasmids smaller, both pcDNA3-EGFP-P2A and pcDNA3-EGFP-P2A-Flag-JunB were digested with *PsiI* (FastDigest$^{TM}$ ThermoScientific) to remove a fragment of 1.5 kb and then ligated together with T4 ligase (Thermo Scientific).

### 2.2.8 Cloning strategy for pLKO.1-puro-CMV-CD48 plasmid

CD48 cDNA was amplified from pBABE-CD48 plasmid, which was provided by Dr. Karsten Watzl (Leibnez Research Centre for Working Environment and Human Factors; Dortmund, Germany) Then the Turbo-GFP fragment in pLKO.1-puro-CMV-TurboGFP was

replaced with the CD48 cDNA after digestion with NheI (FastDigest$^{TM}$ Thermo Scientific) and PstI (FastDigest$^{TM}$ Thermo Scientific) endonucleases. Thus, CD48 cDNA was cloned into the pLKO.1-puro-CMV plasmid that used for lentiviral particle generation and stable CD48 overexpression. The pLKO.1-puro-CMV-CD48 plasmid cloning process was done by Patrick Paszkowski.

**Table 2.2 primers used for PCR**

F: forward primers; R: reverse primers. The primers are from 5' to 3'.

| Genes | Sequence | Notes |
|---|---|---|
| | | |
| **Flag-JunB** | **R**: TTT TTT TCT AGA TCA GAA GGC GTG TCC CTT GAC CCC AAG CAG CAG CTG ACA GCC GTT GCT GAC GTG GG<br>**F:** TTT TTT GCG GCC GCG ATG GAC TAC AAA GAC GAT GAC GAC AAG GGA GGA AGC GGA GGA GGA TGC ACT AAA ATG GAA CAG CCC TT | **pcDNA3-EGFP-P2A-FLAG-JunB construct** |
| **CD48** | **F:** CGA TCA CTG CTA GCC TCT AGC CAG GCT CTC AAC TG<br>**R:** CTA GCT GAC TGC AGT GAG GAG CAT GAT CAC | **pLKO.1-puro-CMV-CD48 plasmid** |

## 2.3 RNA methods

### 2.3.1 Extraction

$5\times10^6$ cells ALK+ ALCL cells were collected for RNA extraction with the RNeasy® mini kit (QIAGEN, Germany). Cells were spun down at 688 ×g for 5 min, washed with PBS and lysed in 350 µl RLT buffer for 5 min on ice to allow for complete lysis. An equal volume of 70% ethanol was added to lysis mixture. The entire sample was transferred to a RNeasy spin column and incubated at room temperature for 2 min before centrifugation as described in the manufacturer's protocol. RNA bound to the column was washed with RW1 and RPE buffers and eluted in RNase/DNase-free $H_2O$. The concentration and purity of RNA was determined by NanoDrop ND-1000 spectrometer (Thermo Scientific).

### 2.3.2 DNA digestion

Genomic DNA was removed by DNA digestion before reverse transcription. Two µg of RNA was added to a PCR tube for DNA digestion and reverse transcription: 1 µl 10X DNase reaction buffer, 1 µl DNase I amplification grade (Invitrogen) and UtraPureTM DNase/RNase-free dd$H_2O$ (Invitrogen) were added for a total volume of 10 µl. DNA digestion was performed at room temperature for 15 min, then 1 µl of 25 mM EDTA was added to the mixture and incubated at 65°C for 10 min to terminate the digestion. The reaction mixture was then cooled down on ice for 2 min.

### 2.3.3 Reverse transcription

To the cooled-down digestion reaction containing 2 µg RNA, 1 µl of 10 mM dNTPs (Thermo Scientific) and 1 µl (1 µg) random primers (Invitrogen) was added. The mixture was heated at

65°C for 5 min and cooled down on ice for 2 min. Then, 4 µl of 5× First strand buffer (Invitrogen), 1 µl the 0.1 m DTT, 1 µl 40 U/µl RNaseOUT ribonuclease inhibitor (Invitrogen) and 1 µl 200 U/µl Superscript II reverse transcriptase (Invitrogen) were added to the mixture with RNA/dNTP/random pirmer. The reaction was carried out as following: 25°C for 5 min, 50°C for 1 hour and 70°C for 15 min. cDNA was diluted with dd$H_2O$ to 1/4 for polymerase chain reaction (PCR) analysis and 1/64 for quantitative real time polymerase chain reaction (qRT-PCR).

### 2.3.4 qRT-PCR

The 1/64 diluted cDNA samples were used for qRT-PCR using PerfeCTa SYBR Green FastMix (Quanta Biosciences; Gaithersburg, MD). 2.5 µl of 1/64 cDNA samples, 2.5 µl of 1.2 µM forward and reverse primer mix and 5 µl of 2× PerfeCTa SYBR Green FastMix were plated in 96-well real time PCR plate (VWR, ON) in triplicate. Water was used to replace the cDNA as the negative control. Reactions were run on a Bio-Rad CFX96 Real-Time PCR Detection System (Bio-Rad, CA) with following steps: initial denaturing step at 95°C for 2 min, then 40 cycles of denaturing at 95°C for 15 sec, annealing at 50-53°C depending on the primers for 20 sec and extension at 68°C for 30 sec. A melting curve was also recorded and used to exclude any impure product or faulty readings. The relative expression level was determined using ΔΔ-CT [234] and expression level of the gene of interest was normalized to β-actin/GAPDH and averaged within the triplicates. The primers used for qRT-PCR were listed in **Table 2.3**.

**Table 2.3 primers used for qRT-PCR**

F: forward primers; R: reverse primers. The primers are from 5' to 3'.

| Gene | Sequence | Annealing Temperature(°C) |
|---|---|---|
| JunB | **F:** TGGCTTCTCTCTACACGACTA | 50 |
| | **R:** TGACCAGAAAAGTAGCTGCCG | |
| c-Jun | **F:** GCATCATCTGTAGATACTAGC | 50 |
| | **R:** ATAACCTGACCATAGCATCA | |
| P27 | **F:** GACAAACAGCGGAAAATCTAC | 50 |
| | **R:** CTGGGCTGCCTTGAGTC | |
| GZMA | **F:** CAT CTG TGC TGG GGC TTT GA | 50 |
| | **R:** GAG GCT TCC AGC ACA AAC CA | |
| GBP-1 | **F:** GCC CAC AGA AAC GTA AG | 53 |
| | **R:** ATA AAT TCC CGC CTT CAC TTC TT | |
| ANXA1 | **F:** GCA GGC CTG GTT TAT TGA AA | 50 |
| | **R:** GCT GTG CAT TGT TTC GCT TA | |
| MXD1 | **F:** GAAGCTGGGCATTGAGAGGAT | 50 |
| | **R:** CTTGATGCTGGTGCTGGAATAG | |
| PTPN22 | **F:** TTCTCCCCCACCTCCTC | 50 |
| | **R:** GTGGGCAAGAATTACAGATACTC | |
| FJX1 | **F:** GCTCGCGATAGGACAAAG | 50 |
| | **R:** TGCGAGAGGGAGGAAGA | |
| PRKA2B | **F:** GAACGCCTGAAAGTAGTAGATGT | 50 |
| | **R:** AGCTGCTCGAGGTTTGTTAG | |
| ITK | **F:** AAGGCAAAATCCCGTATGA | 50 |
| | **R:** CTGGCCGATCTTCTGGTC | |
| CXCL12 | **F:** CCTGGGGATGTGTAATGGTC | 47 |
| | **R:** GAGGGGGTAGTGGCAAGATG | |
| CD48 | **F:** TGCGTTGCTGGGAAGTT | 50 |
| | **R:** TCTCAGGCAGGCTCTCAG | |

| | | |
|---|---|---|
| SLAMF7 | **F:** CACTGTGGAAATACCGAAAAA | 48 |
| | **R:** GTGGATGGAATTATGAACTCTTA | |
| ULBP3 | **F:** CAGGCGGATGAAAGAGAAG | 50 |
| | **R:** ATGCCAGGGAGGATGAAG | |
| CLEC2B | **F:** CACTCAACATGCCGACCTAACTA | 50 |
| | **R:** TCCCTCTCATGCCAAACGAT | |
| TBLX1 | **F:** GAACGCCCGAGGAGACA | 50 |
| | **R:** TGCGGCCAGAGACGAGT | |
| POU2AF1 | **F:** GGTGGGAGGATGTGATGACG | 50 |
| | **R:** CGGACGCCCTGGTATGG | |
| MICA | **F:** GCTGCTGCTATTTTTGTTATTA | 50 |
| | **R:** CCGCCTGGCTGTAGAGT | |
| MICB | **F:** CAGGATTCGCCAAGGAG | 50 |
| | **R:** CTGCCGCTGATGTTTTCT | |
| SH2D1A | **F:** GCAGTAGCAGCGGCATCTCC | 53 |
| | **R:** CTGGCACGCTCTCGCTGTC | |
| SH2D1B | **F:** GTGGATGGCAACTTTCTTTT | 48 |
| | **R:** TCCCCTGATTTGGTTTTTC | |
| β-actin | **F:** AGAAAATCTGGCACCACACC | 48-53 |
| | **R:** TAGCACAGCCTGGATAGCAA | |
| GAPDH | **F:** GAC AGT CAG CCG CAT CTT CT | 48-53 |
| | **R:** TTA AAA GCA GCC CTG GTG AC | |

## 2.4 Protein methods

### 2.4.1 Lysing cells

Cells were collected at the density of about 3-5×$10^5$ cells/ml by centrifuging at 688 ×g for 5 min, washed once with PBS, lysed in 1% NP-40 lysis buffer for 10 min on ice and then centrifuged at 20,817 ×g at 4°C for 10 min. The supernatants were the lysates used for further experiments. The lysis buffer contains 1% NP-40, 10% glycerol, 150 mM NaCl, 2 mM EDTA, 50 mM Tris pH 7.4, 1 mM sodium orthovanadate (Sigma-Aldrich), 1 mM phenylmethyl sulfonyl fluoride (PMSF; BioShop, Burlington, ON), and 1:100 dilution of protease inhibitor cocktail (PIC; Sigma-Aldrich).

### 2.4.2 Bicinchoninic acid (BCA) assay

The concentrations of protein for the lysates were determined with the Pierce BCA protein assay kit (Thermo Scientific, Illinois). Ten µl of lysates were diluted 1/4 with 30 µl dd$H_2O$; 10 µl of diluted lysates or lysis buffer alone (blank) were loaded in triplicate into a 96 well plate. The BCA standards with a range of known protein concentrations was loaded the same way into the 96-well plate. BCA Reagent A was mixed with Reagent B at 1:50 ratio and then 90 µl of BCA reagent mixture was added to the sample and standards. After incubation at 37°C for 30 min, the absorbance was measured at 562 nm wavelength in a FLUOstar OPTIMA microplate reader (BMG Labtech; Ortenberg, Germany). Absorbance of the blanks was subtracted from the readings for all the samples and standard curve was generated based on the BSA standards. The protein concentrations of the samples were calculated from the standard curve and normalized to an equal concentration with lysis buffer. Samples were then stored in 1× Sodium Dodecyl Sulfate-Polyacrylamide Gel Electrophoresis (SDS-PAGE)

sample buffer by adding ¼ of the samples volume of the 5× sample buffer (312.5 mM Tris pH 6.8, 10% glycerol, 11.5% SDS, 500 mM DTT, 0.1% bromophenol blue, pH 6.8).

### 2.4.3 Western blotting

Protein samples were analyzed by SDS-PAGE and the samples in sample buffer were denatured for 5 min on a heating block before loading onto SDS-PAGE gels. Protein samples and pre-stained protein ladders (Thermo Scientific) were run on SDS-PAGE gels at the constant current of 25 mA for each gel with maximum voltage of 200 V for 1.5-2 hours in running buffer (25 mM Tris, 192 mM glycine, 0.1% SDS). Afterwards, proteins were transferred onto nitrocellulose membranes (Bio-Rad) in transfer buffer (25 mM Tris pH 8.5, 20% methanol, 192 mM glycine) on a Bio-Rad Trans-Blot SD Semi- Dry transfer cell at a constant voltage of 15 V for 30-60 min. The membranes were blocked in 5% milk in 1 × TBS (50 mM Tris-Cl, pH 7.5, 150 mM NaCl) for 30 min at room temperature and then washed with 0.05% TBST (TBS, 0.1% Tween 20) 3 times for 10 min. The membranes were incubated with primary antibodies for 30 min to 1 hour at room temperature or 4°C overnight. Afterwards, blots were washed with 0.05% or 0.1% TBST 3 times for 10min. Membranes were then incubated in horseradish-peroxidase (HRP)-conjugated goat anti-mouse or goat anti-rabbit IgG (H+L) secondary antibodies (Jackson ImmunoResearch Laboratories) at 1:10,000 dilution for 30-60 min at room temperature, washed with 0.05% or 0.1% TBST 3 times for 10min. Images were visualized on a ImageQuant LAS 4000 imager (GE Life Sciences) after addition of Pierce™ ECL Plus Western Blotting Substrate (Thermo Scientific) for 2 min. For some of the blots in Chapter 3, bands were visualized with film (Clonex; Markham, ON, Canada) after addition of Enhanced SuperSignal® West Pico

Chemiluminescent solution (Thermo Scientific). Films were developed on an M35A X-OMAT (Kodak; Rochester, NY) or AGFA CP1000 (AGFA Healthcare; Greenville, SC) film processor. After images were recorded, membranes were stripped with stripping solution (0.1% TBST, pH 2) 3 times for 10 min for, washed and re-probed with different antibodies as described above. The primary antibodies used for western blotting are listed in **Table 2.4.**

**Table 2.4 Antibodies used for western blotting**

| Name | Dilution from stock | Species | Company |
|---|---|---|---|
| JunB (C-11) | 1/200 from 0.2 mg/ml stock | mouse | Santa Cruz |
| c-Jun (60A8) | 1/1000 | rabbit | Cell Signaling |
| α-tubulin (DM1A) | 1/5000 from 0.2 mg/ml stock | mouse | Santa Cruz |
| CDK2 (78B2) | 1/1000 | rabbit | Cell Signaling |
| $p18^{Ink4C}$(DCS118) | 1/1000 | mouse | Cell Signaling |
| $p27^{Kip1}$ (D660C12) | 1/1000 | rabbit | Cell Signaling |
| Cyclin E (E4) | 1/1000 | mouse | Cell Signaling |
| CDK4 (D9G3E) | 1/1000 | rabbit | Cell Signaling |
| Cyclin D3 (DCS22) | 1/1000 | rabbit | Cell Signaling |
| β-actin (AC15) | 1/5000 from 0.1 mg/ml stock | mouse | Santa Cruz |
| ANAX1 (EH17a) | 1/200 from 0.2 mg/ml stock | mouse | Santa Cruz |
| GBP-1(1B1) | 1/500 from 0.2 mg/ml stock | rat | Santa Cruz |
| GZMA(#4928) | 1/1000 | rabbit | Cell Signaling |
| Alk (ALK1) | 1/1000 from 0.053 mg/ml stock | mouse | Darko |
| p-ALK(#3983) | 1/1000 | rabbit | Cell Signaling |
| FAM129B | 1/1000 | rabbit | Cell Signaling |

### 2.4.4 Analysis of the expression of NK ligands on the cell surface by flow cytometry

Cells were collected by centrifuging at 688 ×g for 5 min, washed with PBS and blocked with 2% Bovine Serum Albumin (BSA) (Sigma) in PBS for 30 min at room temperature. Then, cells were incubated with primary antibodies at proper dilution for 1 hour at room temperature and washed twice again with PBS. Afterwards, cells were incubated with Fluorescein isothiocyanate (FITC)-conjugated secondary antibody at 1/500 dilution (Life Technologies) for 30 min at room temperature in the dark and washed twice. The samples are analyzed on a BD LSR Fortessa (BD Biosciences; San Jose, CA). Antibodies used for surface staining are listed in **Table 2.5**.

**Table 2.5 Antibodies used flow cytometry surface staining**

| Name | Dilution from stock | Species | Company |
|---|---|---|---|
| MICA/B (6D4) | 1/100 from 0.5 mg/ml stock | mouse | Biolegend |
| SLAMF7 (CRACC) | 1/100 from 0.5 mg/ml stock | mouse | Biolegend |
| ULBP3 (2F9) | 1/20 from 0.2 mg/ml stock | mouse | Santa Cruz |
| CLEC2B (ab175106) | 1/20 from 0.5 mg/ml stock | rabbit | Abcam |
| 2B4 (C1.7) | 1/100 from 0.5 mg/ml stock | mouse | Biolegend |
| NKG2D (1D11) | 1/100 from 1 mg/ml stock | mouse | Biolegend |
| CD48 (MEM-102) | 1/20 from 0.1 mg/ml stock | mouse | Santa Cruz |

## 2.5 Cell based assays

### 2.5.1 Growth curves

Cells were counted and resuspended to $5\times10^4$ cells/ml in 5 ml fresh media. Every 24 hours, cells were mixed with Trypan blue (Gibco) at a 1:1 ratio to exclude the dead cells and then viable cells were counted with hemocytometer (VWR) for 5 or 6 days.

### 2.5.2 Cell cycle analysis

The cell cycle analysis was performed by Bromodeoxyuridine (BrdU) and 7-amino-actinomycin D (7-AAD) double staining using the BD Pharmingen$^{TM}$ FITC-BrdU Flow kit (BD Biosciences, San Jose, CA). Specifically, cells were cultured at $3\text{-}5\times10^5$ cells/ml and incubated with 10 μM BrdU for 30 min. The BrdU-labeled cells were collected and washed with PBS. Then, cells were fixed with BD Cytofix/Cytoperm buffer for 15 min on ice and washed once. Cells were then permeabilized with BD Cytoperm Permeabilization Buffer Plus for 10 min on ice and washed once; the cells were fixed again with BD Cytofix/Cytoperm Buffer for 5 min on ice and washed once. Cells were then treated with DNase (300 μg/ml in PBS) at 37°C for 1 hour, and then stained with anti-BrdU antibody (1/50 dilution) for 20 min at room temperature in the dark. Total DNA was stained with 10 μl of 50 μg/ml 7-AAD solution for 5 min at room temperature in dark. In the end, the cells were then washed and resuspended in FACS buffer (Dulbecco's PBS containing 1% FBS, 0.02% $NaN_3$) for cell cycle analysis on a BD LSR Fortessa flow cytometer (BD Biosciences). Washing was performed by centrifuging at 6800 ×g for 5 min at 4°C with 1× Perm/Wash buffer. Compensation controls were prepared as described in the manufacturer's protocol. All data were analyzed using FlowJo software (Ashland, OR).

### 2.5.3 Reintroduction of JunB cDNA into JunB knock-down cells and measuring BrdU-labelling.

$5\times10^6$ Karpas 299 cells were transfected with 5 μg of plasmid DNA (pcDNA3-EGFP-P2A or pcDNA3-EGFP-P2A-FLAG-JunB) as described in the nucleofection section. The latter plasmid expresses a fusion protein between EGFP and JunB linked by the self-cleaving P2A peptide [235]. Seventy-two hours post-transfection, cells were labelled with BrdU for 1 h, followed by LIVE/DEAD$^{TM}$ Fixable Dead Cell Stain (Invitrogen; Carlsbad, CA) for 30 min on ice in the dark. Cells were then stained with an anti-GFP (AB290, Abcam) antibody followed by a FITC-conjugated anti-rabbit F(ab)' fragment (eBiocience) to enable us to specifically examine BrdU incorporation in transfected cells. Flow cytometry data was collected on BD LSR Fortessa flow cytometer (BD Biosciences). All data were analyzed using FlowJo software (Ashland, OR).

### 2.5.4 Ki-67

Cells were labelled with BrdU, processed and stained with 7-AAD as described in the BrdU/7-AAD labeling section. After DNase treatment, cells were stained with an anti-Ki-67-PE (SolA15, eBioscience) conjugated antibody at 1/50 dilution together with anti-BrdU antibody for 30 min at room temperature. Flow cytometry data was collected analysis on BD LSR Fortessa flow cytometer (BD Biosciences). All data were analyzed using FlowJo software (Ashland, OR).

### 2.5.5 TUNEL

Apoptosis was analyzed by terminal deoxynucleotidyl transferase dUTP nick end labelling (TUNEL) using the In Situ Cell Death Detection Kit, Fluorescein (Roche Applied Science; Laval, QC, Canada). The cells were cultured at 3-5×$10^5$ cells/ml, and 2×$10^7$ cells were collected, and washed three times in PBS. Cells were fixed in 2% Paraformaldehyde (Sigma) for 1 hour shaking at room temperature, and washed twice with PBS. Cells were then permeabilized with permeabilization solution (0.1% Triton X-100 in 0.1% sodium citrate) for 2 min on ice and washed twice with PBS. 50 µl TUNEL reaction mixture (1/10 enzyme solution in label solution) was added into each sample and incubated at 37°C for 1 hour in dark. In the end, the cells were washed with PBS and resuspended in FACS buffer for analysis on a BD LSR Fortessa flow cytometer (BD Biosciences). Positive controls were cells treated with DNase (300 µg/ml in PBS; BD Pharmingen$^{TM}$, BD Biosciences, CA) for 10 min at room temperature and then stained with TUNEL reaction mixture; negative controls were cells incubated in label solution without enzyme solution. All washing steps were performed by centrifuging cells at 1500 ×g for 5 min at room temperature.

## 2.6 Calculation of doubling times and time spent in each phase of cell cycle

Doubling times were calculated from growth curves by exponential curve fitting in Excel (Microsoft, Washington). The formula generated from curve fitting could be converted into $Y=a\times2^{X/b}$, where "Y" refers to cell density, "X" refers to time (day), "a" refers to initial cell density, and "b" refers doubling time (day). This method was adapted from Korzynska et al [236]. The doubling time $T_{2\times}=24\times b$ (hours). The time for the cells to progress through each stage of the cell cycle was calculated using the formula T ($G_N$) (hours) = $T_{2\times}$ × % ($G_N$),

where T ($G_N$) refers to the time duration in each specific stage of cell cycle [237], $T_{2\times}$ refers to doubling time and % ($G_N$) refers to the percentage of cells in that particular stage of the cell cycle determined by cell cycle analysis in section **2.5.2**.

### 2.7 Calcein-AM based NK cell-mediated killing assays

Target cells were resuspended in RPMI 1640 media at a final concentration of $1\times10^6$ cells/ml and incubated with 5 μg/ml Calcein-AM (Thermo Scientific), for 30 min at 37°C with shaking every 10 min. After two washes in RPMI 1640 media, cells were to $1\times10^4$/ml. The NK cells were washed with RPMI 1640 media and diluted to the appropriate concentration in the RPMI 1640 media. The killing assay was performed in V bottom 96-well microtiter plates (Nunc), with effector to target ratios (E:T ratios) ranging from 50:1 to 1:1, in triplicate. Spontaneous release was target cells alone in complete medium and maximum release was target cells alone in medium plus 2% Triton X-100. After incubation at 37°C in 5% $CO_2$ for 4 h, the plate was centrifuge at 9 ×g for 5 min and 100 μl of each supernatant was transferred into 96-well black assay plates (Nunc). Samples were measured using a FLUOstar OPTIMA microplate reader (BMG Labtech; Ortenberg, Germany) at 520 nm wavelength. The percentage of killing was calculated as the formula: lysis% = (Calcein-AM release of sample - Calcein-AM spontaneous release) / (Calcein-AM release of maximum – Calcein-AM spontaneous release) ×100%. For antibody blocking experiments, the target or effector cells were incubated with antibodies at room temperature for 30 min prior to adding to the killing system on a V-bottom 96 well plate. Specifically, target cells were incubated with anti-CD48 (4H9, Santa Cruz) antibody at 10 μg/ml or the effector cells were incubated with anti-NKG2D (1D11, Biolegend) antibody at 10 μg/ml. Mouse anti-human $IgG_1$ Isotype antibodies

(MOPC-21, Sigma) controls were used as negative controls for the antibody blocking killing assays. 221 cells were used as positive controls for the killing assays [238].

## 2.8 Drug treatments

### 2.8.1 Crizotinib treatment of cells

Cells were treated with ALK inhibitor Crizotinib (BioVision, CA) for 72 hours and then analyzed for NK ligands expression on the cell surface as described in the surface staining of NK ligands section **2.4.4**. Specifically, Karpas 299 cells were treated with 75 nM Crizotinib and SUP-M2 cells were treated with 150 nM. For western blot experiments checking the bandshifts of FAM129B, Karpas 299 cells were collected at 24, 48, 72 hours post Crizotinib treatment.

### 2.8.2 DAC treatment of cells

Karpas 299 and SUP-M2 cells were treated with 1μM DNA methyltransferase inhibitor (DNMT) inhibitor, 5-aza-2′-deoxycytidine (DAC) (Sigma-Aldrich) for 96 hours and then analyzed for NK ligand expression on the cell surface as described in the surface staining of NK ligands section **2.4.4**.

### 2.8.3 HDAC treatment of cells

Karpas 299 and SUP-M2 cells were treated with 1mM, 2mM, and 3 mM HDAC inhibitor MGCD0103 (Selleckchem) for 24 hour or 48 hours respectively and then analyzed for NK ligands expression on the cell surface as described in the surface staining of NK ligands section **2.4.4**.

### 2.8.4 Staurosporine and Doxorubicin experiments

Karpas 299 cells expressing JunB shRNA or control shRNA were treated with 0.1, 0.3, and 0.5 μM staurosporine (STS) (Enzo Life Sciences, NY) for 6 hours or treated with 1 mM, 3 mM, 5 mM doxorubicin (Doxo) (Sigma-Aldrich) for 12 hours, and then the percentage of apoptotic cells was analyzed by TUNEL assay as described previously in section **2.5.5**.

## 2.9 Microarray Experiments

Three sets of RNA were collected from c-Jun, JunB, or control shRNA-expressing Karpas 299 cells with RNeasy® mini kit (QIAGEN, Germany) and sent to the Alberta Transplant Applied Genomics Centre (University of Alberta, Edmonton, AB, Canada). The mRNAs were converted into amplified RNAs (aRNAs) as described in the GeneChip® 3' IVT Express Protocol (Cat # 901229) (Affymetrix, Santa Clara, CA). aRNAs were then probed on GeneChip® PrimeView™ human gene expression arrays (Affymetrix), which contains 59,000 probes for 28,000 human genes. Data were analyzed by Dr. Konrad Famulski (University of Alberta) using GeneSpring GX software (Agilent Technologies, Mississauga, ON) and the expression values from the c-Jun/JunB shRNA-expressing cells were normalized to control shRNA-expressing cells. Dr. Ingham has the raw data that will be submitted into a repository when this data is published.

## 2.10 Chromatin immunoprecipitation (ChIP)-sequencing (seq)

ChIP-seq was performed in Karpas 299 cells with anti-JunB antibody (Cell Signaling Technology, Catalog ID: 3753) and anti-c-Jun antibody (Santa Cruz, Catalog ID: SC-1694).

Specifically, frozen pellets of Karpas 299 cells were sent for experiments by Active Motif (Carlsbad, CA). The cell pellets were fixed and immuno-precipitate with anti-JunB, anti-c-Jun or control antibodies; the DNA fragments that were associated with JunB/c-Jun were purified and sequenced by Illumina sequencing.

The data was analyzed by Active Motif as well. Specifically based on the service report from Active Motif, sequences were mapped to the genome and peaks were called using either the MACS or SICER algorithms in R [239, 240]. The consensus motifs were identified with the findMotifsGenome program of the HOMER package using default parameters and input sequences comprising +/- 200 bp from the center of the top 1000 peaks [241].

The UCSC Genome Brower (http://genome.ucsc.edu) was used to visualize the peaks and intervals throughout the genome. BED and bigWig files were uploaded as custom tracks. The track files contain the locations and names of all Intervals (shown as orange bars) and Active Regions (green). The files also contain the location and values of the Interval summits (purple) and show peak shapes in the form of a signal histogram. Screenshots were taken for the selected genes to show the peak regions and intensities. Dr. Ingham has the raw data that will be submitted into a repository when this data is published.

### 2.11 KEGG annotation

Gene lists were analyzed using Database for Annotation, Visualization, and Integrated Discovery (DAVID) bioinformatics resources 6.7 (http://david.abcc.ncifcrf.gov) for functional annotation [242]. Specifically, we chose Kyoto Encyclopedia of Genes and Genomes (KEGG) to perform the functional annotation. The p values were adjusted using the

Benjamini-Hochberg (BH) method to determine whether the functional group reached significance or not.

### 2.12 Hierarchical heat map

The hierarchy heat map was generate with the microarray data for the probes with fold change greater than or equal to two, using the online tool called "Expression Heat Map" (http://www1.heatmapper.ca/expression/). Parameters were as follows: "Complete Linkage" was chosen for "Clustering method", "Euclidean" was chosen for "Distance Measurement Method", and the Clustering were applied to "Rows".

### 2.13 Statistical analysis

Statistical analyses comparing two groups were performed with two-tailed independent t tests as indicated in the figure legends. Statistical analysis comparing more than two groups were performed with ANOVA with TUKEY *post-hoc* test as indicated in the figure legends.

# Chapter 3: JunB, but not c-Jun, promotes cell proliferation by facilitating cells transiting through $G_1$ phase in ALK+ ALCL

All experiments were performed by Zuoqiao Wu. Part of this chapter was published: "The c-Jun and JunB transcription factors facilitate the transit of classical Hodgkin lymphoma tumour cells through $G_1$" in *Scientific Reports* [243]. This manuscript was written by myself, JingXi (Cathy) Zhang, and Dr. Ingham. I am the co-first author of this publication.

## 3.1 Introduction

JunB has been demonstrated to promote tumour cell proliferation in ALK+ ALCL, as knocking down JunB with siRNA resulted in slower growth of ALK+ ALCL cells lines [61, 136, 142], but no work had been done to study the outcome of stably knocking down JunB, which allowed us to knock-down JunB more efficiently and look at the effect of loss of JunB on cell growth for a longer period. As well, discrepancies existed as to whether c-Jun was important for promoting proliferation in ALK+ ALCL [61, 136, 142]. Staber *et al.* showed that siRNA-mediated c-Jun knock-down did affect Karpas 299 cell growth [136]; while Atsaves *et al.* showed c-Jun siRNA transfection resulted in decreased colony formation ability of Karpas 299 cells in methylcellulose matrix [61]. Leventaki *et al.* showed inhibition of JNK kinase resulted in slower growth of SU-DHL1 cells [142]. Thus, further investigation was needed to address whether c-Jun promotes the proliferation of ALK+ ALCL cells. Moreover, we wanted to compare the role of JunB and c-Jun between ALK+ ALCL and a related lymphoma, classic Hodgkin lymphoma where JunB and c-Jun are also highly expressed [54, 60, 209] using shRNA-mediated stable knock-down. Thus, to further elucidate the role of JunB and c-Jun in ALK+ ALCL, I examined the effect of stably reducing JunB or c-Jun expression and investigated their role in tumour cell proliferation.

## 3.2 Results

### 3.2.1 Stable knock-down of JunB and c-Jun using shRNA

To examine the outcome of reducing JunB and c-Jun expression in ALK+ ALCL, I generated stable knock-downs of JunB or c-Jun with shRNA. Specifically, I infected the Karpas 299, SUP-M2, and UCONN-L2 cell lines with the lentiviral particles that contain JunB shRNA, c-

Jun shRNA, or control shRNA. After being selected in puromycin for five days, mRNA was collected for quantitative RT-PCR and lysates were collected for western blotting to evaluate the efficacy of JunB/c-Jun knock-down. As shown in **Figure 3.1A,** JunB shRNA-expressing Karpas 299 cells have a 73% reduction in JunB mRNA levels compared to control shRNA-expressing cells; c-Jun shRNA-expressing cells had a 53% reduction in c-Jun mRNA levels compared to control cells. Western blotting demonstrated that of JunB/c-Jun protein levels were also significantly decreased in JunB/c-Jun shRNA-expressing cells compared to control shRNA-expressing cells (**Figures 3.1 B-G**). Thus, the treatment of ALK+ ALCL cell lines with c-Jun/JunB shRNAs resulted in a reduction in c-Jun and JunB mRNA and protein levels in all three ALK+ ALCL cell lines examined.

### 3.2.2 Stable knock-down of JunB, but not c-Jun, results in a reduced growth rate in ALK+ALCL

To examine the consequence of stable knock-down of JunB or c-Jun on cell growth of ALK+ ALCL cells, I performed growth curves on JunB shRNA-expressing cells, c-Jun shRNA-expressing cells and control shRNA-expressing cells. Karpas 299 cells (**Figure 3.2A**) and SUP-M2 cells (**Figure 3.2B**) had a reduced growth rate when JunB was knocked-down, suggesting JunB is important for the growth of Karpas 299 and SUP-M2 cells. In contrast to Karpas 299 and SUP-M2 cells, no growth defect was observed in UCONN-L2 cells when JunB was knock-down (**Figure 3.2C**). Thus the role of JunB in cell growth varies among ALK+ALCL cell lines. Unfortunately, I could not identify a second shRNA that significantly reduced JunB expression, so I tried to reintroduce JunB cDNA into JunB shRNA-expressing cells to see if I could rescue the growth defect, which will be discussed in Section 3. In

contrast, c-Jun knock-down cells grew at a similar rate as control cells in all three ALK+ALCL cell lines.

**Figure 3.1**

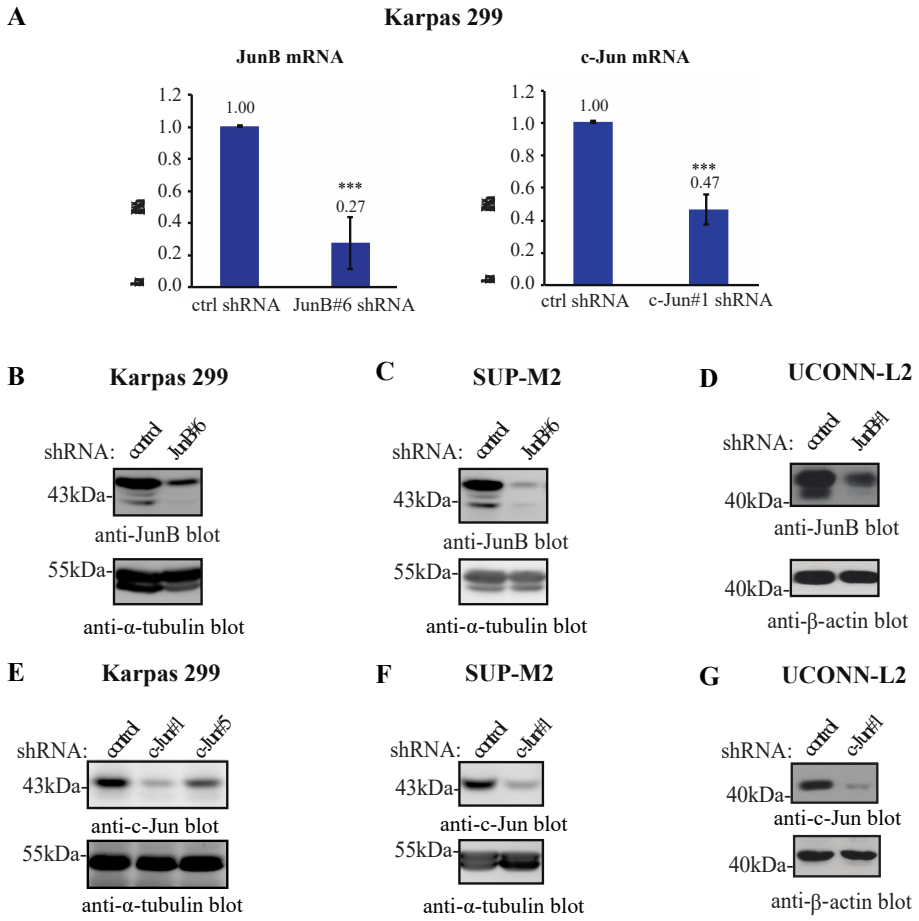


**Figure 3.1 - shRNA-mediated knock-down of JunB or c-Jun in ALK+ ALCL cell lines.**

**A.** mRNA levels of JunB and c-Jun in JunB shRNA-expressing and c-Jun shRNA-expressing Karpas 299 cells. The results represent the averages and standard deviations of three independent experiments. **B-D.** Western blots showing levels of JunB in JunB shRNA-expressing Karpas 299 cells **(B)**, SUP-M2 cells **(C)**, or UCONN-L2 **(D)** cells. **E-F.** Western blots showing levels of c-Jun in c-Jun shRNA-expressing **(E)**, SUP-M2 cells **(F)**, or UCONN-L2 **(G)** cells. p values represent independent, two-tailed t tests.* $p<0.05$, ** $p<0.01$, *** $p<0.001$. Molecular mass markers (in kDa) are indicated to the left of western blots.

**Figure 3.2**

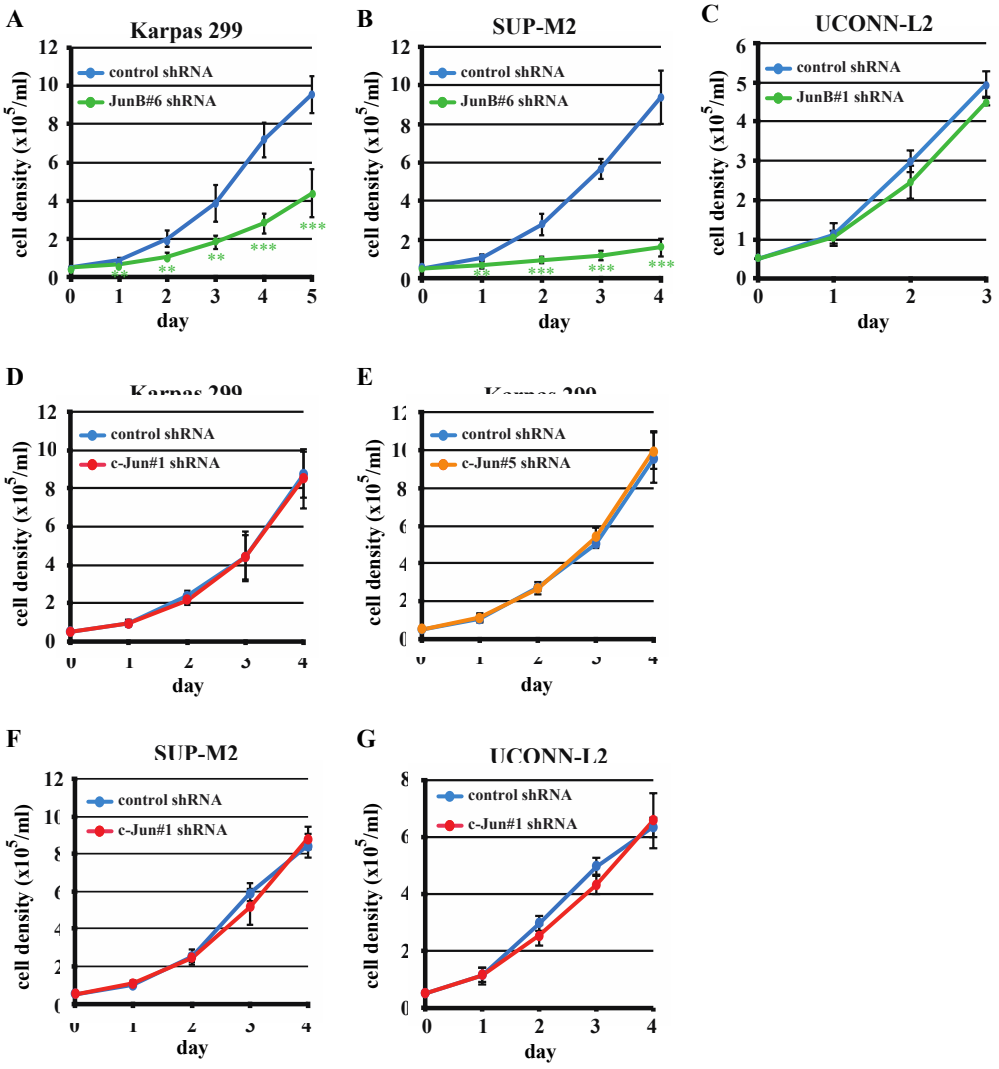


**Figure 3.2 - Knock-down of JunB, but not c-Jun results in a reduced growth rate in ALK+ALCL**

**A-C.** Growth curves associated with JunB shRNA-expressing Karpas 299 cells **(A)**, SUP-M2 cells **(B)**, and UCONN-L2 cells **(C)**. Growth curves represent the average and standard deviation of five experiments from three infections **(A)**, five experiments from five infections **(B)**, and three experiments from one infection **(C)**. **D-G.** Growth curves associated with c-Jun shRNA-expressing Karpas 299 cells **(D, E)**, SUP-M2 cells **(F)**, and UCONN-L2 cells **(G)**. Growth curves represent the average and standard deviation of four experiments from four infections **(D)** and five experiments from three experiments **(E)**, three experiments from three infections **(F)**, and three experiments from one infection **(G)**. p values represent independent, two-tailed t tests.* $p<0.05$, ** $p<0.01$, *** $p<0.001$.

(**Figure 3.2D-G**). In addition, two distinct c-Jun shRNAs were utilized in Karpas 299 cells to verify that this phenotype was not due to that the shRNA off-targeting other genes other than *c-Jun* (**Figures 3.2D and E**). Therefore, I found that knocking down JunB results in a growth defect in two out of the three ALK+ ALCL cell lines examined, but knocking down c-Jun had no effect on cell growth in all the three ALK+ ALCL cells lines examined. This argues that JunB, but not c-Jun, plays a role in promoting cell growth in ALK+ ALCL cells.

### 3.2.3 Stable knock-down of JunB does not result in increased spontaneous apoptosis

The slower growth rate observed in JunB knock-down Karpas 299 and SUP-M2 cells could be caused by either increased apoptosis, decreased proliferation rate, or both these processes. To investigate the reason for the growth defect in JunB shRNA-expressing cells, I first examined whether JunB knock-down resulted in any spontaneous apoptosis in ALK+ ALCL by Terminal deoxynucleotidyl transferase (TdT) dUTP Nick-End Labeling (TUNEL) assay. The TUNEL assay specifically detects the DNA fragmentation during apoptosis process [244], and I used DNase-treated cells as a positive control group and no nick-end labeling antibody treated cells as a negative control. The flow cytometry histograms of JunB knock-down cells and control shRNA-expressing cells were largely similar to the negative control group (**Figure 3.3**), showing no evidence of spontaneous apoptosis when JunB was knocked-down in either Karpas 299 (**Figure 3.3A**) or SUP-M2 (**Figure 3.3B**) cells. In all, reducing JunB does not result in increased spontaneous apoptosis in ALK+ ALCL cells; the decreased growth rate observed in JunB knock-down cells is not due to increased apoptosis.

**Figure 3.3**

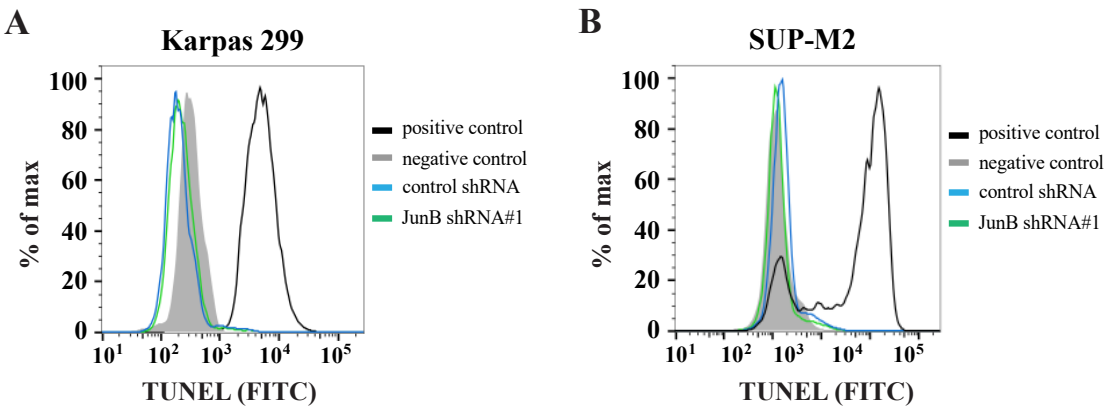


**Figure 3.3 - Knock-down of JunB does not result in increased spontaneous apoptosis**

**A-B**. Overlaid histograms of TUNEL assay of Karpas 299 cells **(A)** and SUP-M2 cells **(B)** expressing either control or JunB shRNA. Shown is a representative result of three independent experiments. Positive controls are cells treated with DNase and the negative controls are cells treated with labeling solution only.

### 3.2.4 Stable knock-down of JunB results in a decreased percentage of cells in S phase and an increased percentage of cells in $G_0/G_1$ phase

To further investigate the reason for the slower growth rate in JunB knock-down cells, I checked the cell cycle distribution in JunB shRNA-expressing cells. I stained the cells with BrdU and 7-AAD and then analyzed by flow cytometry to distinguish the different stages of cell cycle. For both Karpas 299 and SUP-M2 cell lines, I observed a decreased percentage of cells in S phase and an increased percentage of cells in $G_0/G_1$ phase in JunB knock-down cells compared to control shRNA-expressing cells. Specifically in Karpas 299 cells, there were ~50% of cells in S phase, ~40% cells in $G_0/G_1$ phase and ~5% in $G_2$/M phase for control shRNA-expressing cells; there were ~30 % (~1.7 fold decease) of cells in S phase, ~60 % (~1.5 fold increase) in $G_0/G_1$ phase and expressing cells, and ~6 % in $G_2$/M phase for JunB shRNA-expressing cells (**Figures 3.4A and B**). In SUP-M2 cells, the change was even more dramatic, which was consistent with the more severe growth defect observed in the growth curves (**Figure 3.2B**). The percentage of cells in S phase decreased from ~50 % in control cells to ~25 % (~2.1 fold decrease) in JunB knock-down cells. The percentage of cells in $G_0/G_1$ phage went up from ~35% in control cells to ~65% (~1.8 fold increase) in JunB knock-down cells. The percentage of cells in $G_2$/M phase was similar in JunB knock-down cells compared to control shRNA-expressing cells (**Figures 3.4C and D**). Therefore, knocking down JunB resulted in decreased percentage of cells in S phase and increased percentage of cells in $G_0/G_1$ phase in both Karpas 299 and SUP-M2 cells, suggesting JunB could contribute to cell cycle progression through $G_0/G_1$ phase to S phase in ALK+ ALCL.

To see whether the cell cycle distribution was changed in c-Jun knock-down cells, I also performed BrdU and 7-AAD staining in c-Jun shRNA-expressing cells. As shown in

**Figures 3.4E and F**, the percentages of cells in the S, $G_0/G_1$, and $G_2/M$ in c-Jun knock-down cells were similar as those for control shRNA-expressing cells. Thus, knocking down c-Jun did not result in an alteration in the cell cycle, which is consistent with what I observed in my growth curve experiments (**Figures 3.1D-G)**, arguing c-Jun is not critical for cell proliferation in ALK+ ALCL.

I also checked whether JunB or c-Jun knock-down resulted in altered cell cycle distribution in UCONN-L2 cells (**Appendix 1**). No differences were observed in the percentages of cells in each phase of cell cycle when comparing JunB shRNA/c-Jun shRNA-expressing cells to control shRNA-expressing cells. Therefore, JunB and c-Jun did not have an effect on cell cycle progression in UCONN-L2 cells.

**Figure 3.4**

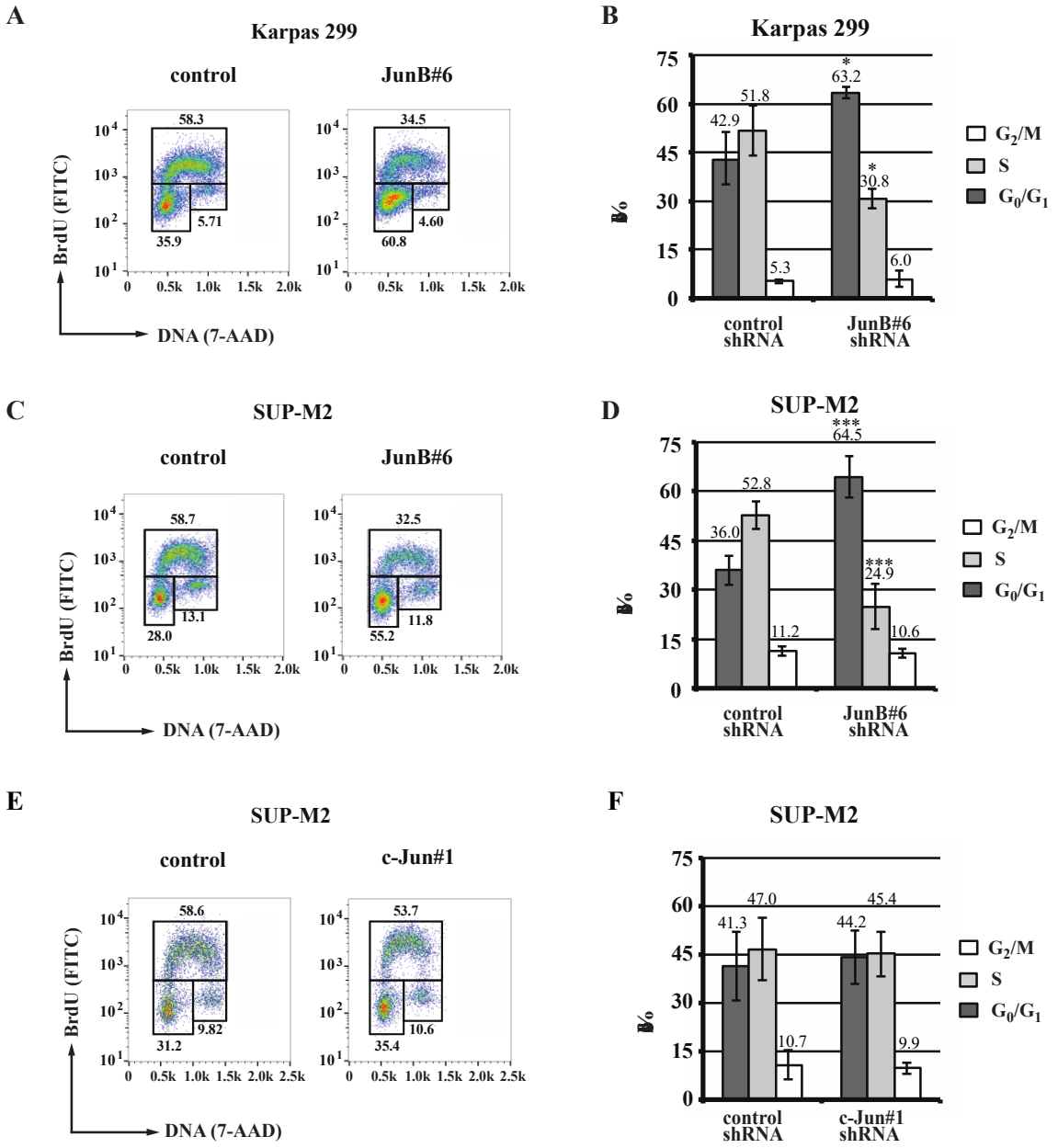


**Figure 3.4 – Knock-down JunB, but not c-Jun, results in decreased percentage of cells in S phase and an increased percentage of cells in $G_0/G_1$ phase**

**A-B.** Representative BrdU/7-AAD plots (**A**) and summary (**B**) for cell cycle analysis in JunB shRNA or control shRNA-expressing Karpas 299. **C-D.** Representative BrdU/7AAD plots (**C**) and summary (**D**) of cell cycle analysis in JunB shRNA or control shRNA-expressing SUP-M2 cells. D-E. Representative BrdU/7AAD plots (**D**) and summary (**E**) for c-Jun shRNA or control shRNA-expressing SUP-M2 cells. Results represent the average and standard deviation of three independent experiments from three infections in B, and eight independent experiments from six infections for **D**, and three experiments from three infections for **F**. p values represent independent, two-tailed t tests. * $p<0.05$, ** $p<0.01$, *** $p<0.001$.

### 3.2.5 Restoration of JunB expression in JunB knock-down Karpas 299 cells

Since we could not identify a second shRNA that reduced JunB to the extent of JunB#6 shRNA, I tried to restore the expression of JunB in JunB shRNA-expressing cells. The fact that the JunB #6 shRNA targets the 3' untranslated region of the *JunB* mRNA makes it possible to express a JunB cDNA in JunB shRNA-expressing cells. First of all, I constructed the EGFP-P2A-FLAG-JunB plasmid in the pcDNA3 backbone. EGFP allowed me identify the cells successfully transfected with the plasmid; P2A is a self-cleaving peptide [235], and FLAG-JunB will be released from EGFP-P2A.

Secondly, I nucleofected the plasmid into Karpas 299 cells with an Amaxa nucleofector. I tested different amounts of plasmid and different time points after transfection to identify the best conditions for generating EGFP-positive cells. I started with the 2 μg plasmid and 5 million Karpas 299 cells and then checked EGFP expression at 48 hours and 72 hours post-transfection. I observed 38% and 28% EGFP-positive cells respectively in the live populations (**Figures 3.5A and B**). Then, I increased the amount of plasmid to 5 μg/5 million cells and checked EGFP expression at 48, 72, and 96 hours post-transfection. I observed 65%, 55% and 33% EGFP-positive cells in the live populations, respectively (**Figures 3.5C-E**). Thus, with 5 μg of plasmid and 5 million cells, I achieved a greater percentage of EGFP-positive cells and about half of the cells were alive post-transfection, which gave me enough EGFP positive cells for further experimentation. I chose 72 hours post-transfection as time point to perform functional assay, because the cells still retained the reasonable expression of EGFP and would give me better chance to see the effect of expression of JunB at 72 hours post-transfection.

I tried to make the plasmid smaller as it may enter the cells with higher efficiency. Specifically, I cut the 1.5 kb eukaryotic marker fragment out of the plasmids and transfected Karpas 299 cells with the eukaryotic marker deletion plasmids and the intact plasmids. I found that with the smaller plasmid the percentage and intensity of EGFP-positive cells both increased (**Figure 3.6A**). So I went with 5 μg eukaryotic marker deletion plasmid and 5 million Karpas 299 cell at 72 hours post-transfection and examine whether the expression of JunB would rescue the growth defect in JunB knock-down cells.

**Figure 3.5**

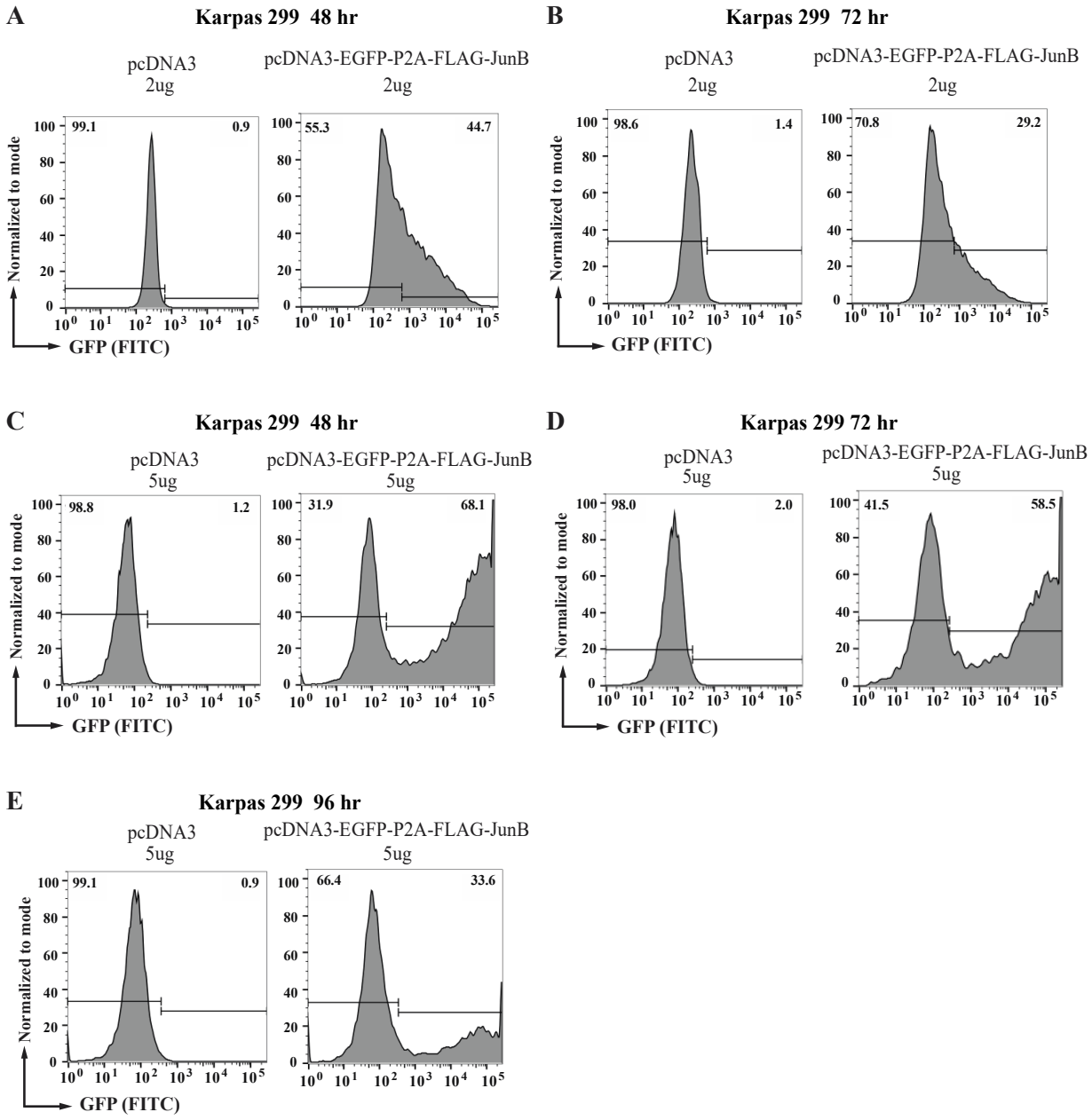


**Figure 3.5 – Transfection Karpas 299 with pcDNA3-EGFP-P2A-FLAG-JunB plasmid**

**A-B.** Histograms of EGFP+ cells at 48 hours **(A)** and 72 hours **(B)** after Karpas 299 transfected with 2 µg pcDNA3-GFP-P2A-FLAG-JunB plasmid or pcDNA3 plasmid. **C-E.** Histograms of GFP+ cells at 48 hours **(C)**, 72 hours **(D)**, and 96 hours **(E)** after Karpas 299 transfected with 5 µg pcDNA3-GFP-P2A-FLAG-JunB plasmid or pcDNA3 plasmid. The histograms represent one experiment for each transfection with different amount of plasmid.

**Figure 3.6**

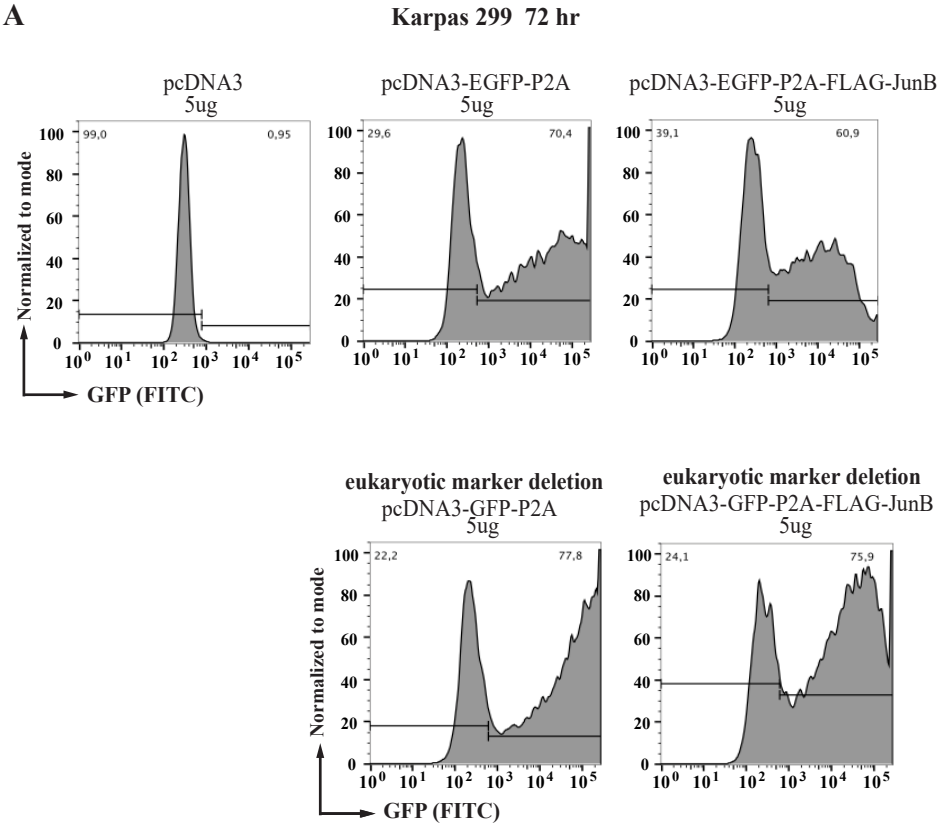


**Figure 3.6 – Transfection Karpas 299 with smaller version of pcDNA3-EGFP-P2A-FLAG-JunB plasmid**

**A.** Histograms of EGFP+ cells at 72 hours after Karpas 299 transfected with pDNA3-EGFP-P2A or pcDNA3-EGFP-P2A-FLAG-JunB or the cut versions of them. The histograms represent one experiment for each transfection.

### 3.2.6 The proliferation defect is restored when JunB is reintroduced in JunB knock-down cells

To examine whether the growth defect observed in JunB knock-down cells was due to the lack of JunB protein, I reintroduced a JunB cDNA into the JunB shRNA-expressing cells and measured cell proliferation by BrdU labelling. Specifically, I transfected the control shRNA-expressing cells with pcDNA3-EGFP-P2A plasmid, and JunB shRNA-expressing cells with pcDNA3-EGFP-P2A plasmid or pcDNA3-EGFP-P2A-FLAG-JunB plasmid. At 72 hours post-transfection, cells were collected for western blot and labeled with BrdU (**Figure 3.7A**). As shown in **Figure 3.7C**, JunB levels were decreased in JunB shRNA-expressing cells and FLAG-JunB was successfully expressed in the pcDNA3-EGFP-P2A-FLAG-JunB transfected JunB shRNA-expressing cells. After labelling the cells with BrdU, I measured the percentage of BrdU-positive cells within the EGFP-positive population by flow cytometry. EGFP-positive populations are indicated by the boxes in **Figure 3.7i**; the percentage of BrdU-positive cells within the EGFP-positive populations are illustrated by the histograms in **Figure 3.7Bii**. The percentage of BrdU-positive cells was 35.8% in pcDNA3-EGFP-P2A-transfected control cells and 15.1% in pcDNA3-EGFP-P2A transfected JunB knock-down cells. The percentage of BrdU-positive cells increased to 26.8% when pcDNA3-EGFP-P2A-FLAG-JunB was transfected into JunB knock-down cells (**Figure 3.7 D**). Thus, the JunB shRNA-expressing cells grew faster after JunB was reintroduced into them, arguing that the proliferation defect in these cells is due to decreased JunB expression and not the shRNA targeting some other gene(s).

**Figure 3.7**

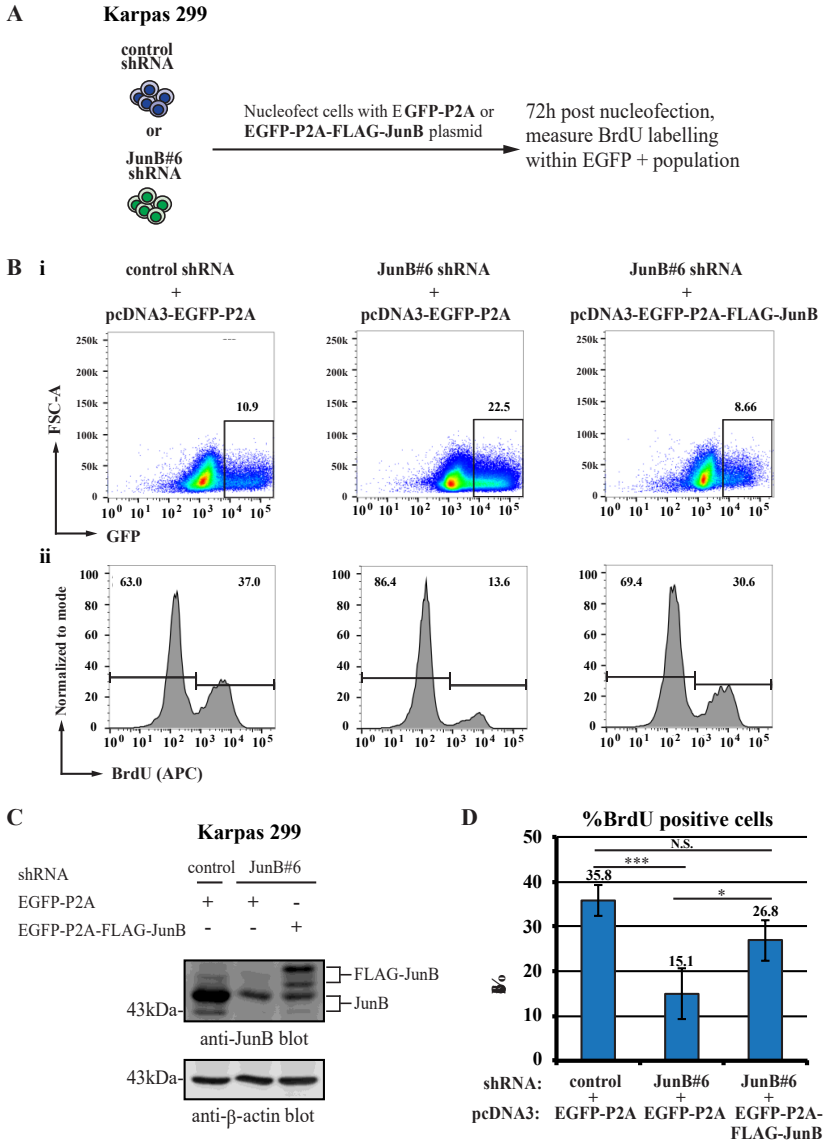


**Figure 3.7 – Introduction of a JunB cDNA into JunB shRNA–expressing Karpas 299 cells**

**A.** Diagram showing the process for reintroduction of JunB into JunB shRNA–expressing Karpas 299 cells. **B. i.** Representative flow plots illustrating the EGFP–positive population in Karpas 299 cells expressing control or JunB shRNA, and transfected with the indicated plasmids. **ii.** Histogram plots showing BrdU staining within the EGFP–positive population shown in **i**. **C.** Western blots showing the expression of FLAG-JunB introduced into JunB shRNA–expressing Karpas 299 cells. **D.** Bar graph showing the percentage of cells in S phase (% BrdU positive cells) observed when control shRNA or JunB shRNA–expressing Karpas 299 cells were transfected with plasmids expressing EGFP-P2A or EGFP-P2A-FLAG-JunB. The results represent the average and standard deviation of four independent experiments. Molecular mass markers (in kDa) are indicated to the left of western blots. p values represent ANOVA test with TUKEY *post-hoc* test.* $p<0.05$, ** $p<0.01$, *** $p<0.001$, N.S. not significant.

### 3.2.7 Stable knock-down of JunB results in an extended $G_0/G_1$ phase

To better understand the kinetics of cell cycle progression in JunB shRNA-expressing cells, I calculated the doubling time and the time spent in each phase. The doubling time was calculated by curve fitting the growth curves to the formula shown in **Figure 3.8A** [236], and time spent in each phase was further calculated based on doubling time and cell cycle distribution results [237]. For Karpas 299 cells, the doubling time for control shRNA-expressing cells was 25 hours, and for JunB shRNA-expressing cells it was increased to 37 hours. JunB knock-down cells spent 23.4 hours in $G_0/G_1$ phase, while control shRNA-expressing cells spent 10.5 hours in $G_0/G_1$ phase. The time spent in S phase and $G_2$/M phase did not change significantly in JunB shRNA-expressing cell compared to control shRNA-expressing Karpas 299 cells (**Figure 3.8B**). Similarly for SUP-M2 cells, JunB knock-down cells had a much longer doubling time (58 hours) compared to 22 hours for control shRNA-expressing cells. Control shRNA-expressing cells spent 7.9 hours in $G_0/G_1$ phase, whereas JunB knock-down cells spent 37.4 hours (4.7 fold increase) in $G_0/G_1$ phase. The time spent in S phase did not change significantly in JunB shRNA-expressing cells compared to control shRNA-expressing SUP-M2 cells. The time spent in $G_2$/M increased to 6.1 hours for JunB shRNA-expressing SUP-M2 cells compared to 2.5 hours for control shRNA-expressing cells, but the major growth defect was in $G_0/G_1$ phase for SUP-M2 cells as well (**Figure 3.8C**). Thus, in both ALK+ ALCL cell lines, JunB shRNA-expressing cells spent much longer time in $G_0/G_1$ phase compared to control shRNA–expressing cells, suggesting a $G_0/G_1$ cell cycle delay or arrest in JunB knock-down cells.

**Figure 3.8**

**A**

$$y = a \cdot 2^{\frac{x}{b}}$$

y: cell density
x: time
*a*: initial cell density
*b*: doubling time (day)

**B**

**Karpas 299**

| | control shRNA | JunB#6 shRNA |
|---|---|---|
| **Doubling time (h)** | 25 | 37 |
| **$G_0/G_1$ (h)** | 10.5 +/- 2.1 | 23.4 +/- 0.2 *** |
| **S (h)** | 12.7 +/- 1.9 | 11.4 +/- 1.1 ns |
| **$G_2$/M (h)** | 1.3 +/- 0.2 | 2.2 +/- 0.9 ns |

**C**

**SUP-M2**

| | control shRNA | JunB#6 shRNA |
|---|---|---|
| **Doubling time (h)** | 22 | 58 |
| **$G_0/G_1$ (h)** | 7.9 +/- 1.0 | 37.4 +/- 3.7 *** |
| **S (h)** | 11.6 +/- 0.9 | 14.4 +/- 4.0 ns |
| **$G_2$/M (h)** | 2.5 +/- 0.3 | 6.13 +/- 0.7 *** |

**Figure 3.8 - Doubling time and time spent in each phase of the cell cycle**

**A.** Formula used to calculate the doubling time [236]. Use data from **Figure 3.2A and B** to calculate the doubling time. **B.** Approximate doubling times and time spent in each stage of the cell cycle was determined for Karpas 299 cells expressing control or JunB shRNA. **C.** Approximate doubling times and time spent in each stage of the cell cycle was determined for SUP-M2 cells expressing control or JunB shRNA. Results represent the average and standard deviation of three independent experiments for Karpas 299 cells, and eight independent experiments for SUP-M2 cells. p values were obtained by performing independent, two-tailed *t* tests comparing the JunB knock-down to control shRNA-expressing cells.

### 3.2.8 Stable knock-down of JunB results in $G_0$-like cells

Since JunB knock-down cells spent a longer time in $G_0/G_1$ phase, and BrdU/7AAD staining could not separate $G_0$ from $G_1$ phase apart, I examined whether the JunB shRNA-expressing cells were delayed in the $G_0$ phase by Ki-67 staining and Pyronin-Y/DAPI staining [245]. Pyronin-Y stained RNA content [246] and DAPI-stained DNA content in the cells [247]. Ki-67 is expressed in cycling cells but absent in $G_0$ cells or reduced in those that have recently left cell cycle [248, 249]. Thus, I did Ki-67 staining on the $G_0/G_1$ phase population to distinguish cells in $G_0$ and $G_1$ (**Figure 3.9A**). In SUP-M2 cells, a population of cells with lower Ki-67 levels was observed when JunB was knocked down (**Figures 3.9B and C**), suggesting that some JunB knock-down cells were leaving cell cycle. In addition, I also stained the cells with Pyronin-Y and DAPI to identify the cells that left cell cycle [245]. Because Pyronin-Y stained RNA content [246] and DAPI-stained DNA content in the cells [247], $G_0$ cells would be separated with low Pyronin-Y staining and medium DAPI staining (**Figure 3.9 D**) [245]. For SUP-M2 cells, there was a greater population with low Pyronin-Y in JunB shRNA-expressing cells compared to control shRNA-expressing cells, suggesting JunB knock-down cells were leaving cell cycle. Taken together, my data using two methods demonstrate that knocking down JunB results in a population of cells that phenotypically resemble cells that have left the cell cycle, arguing JunB could contribute to the progression of the cell cycle through $G_0/G_1$ phase.

**Figure 3.9**

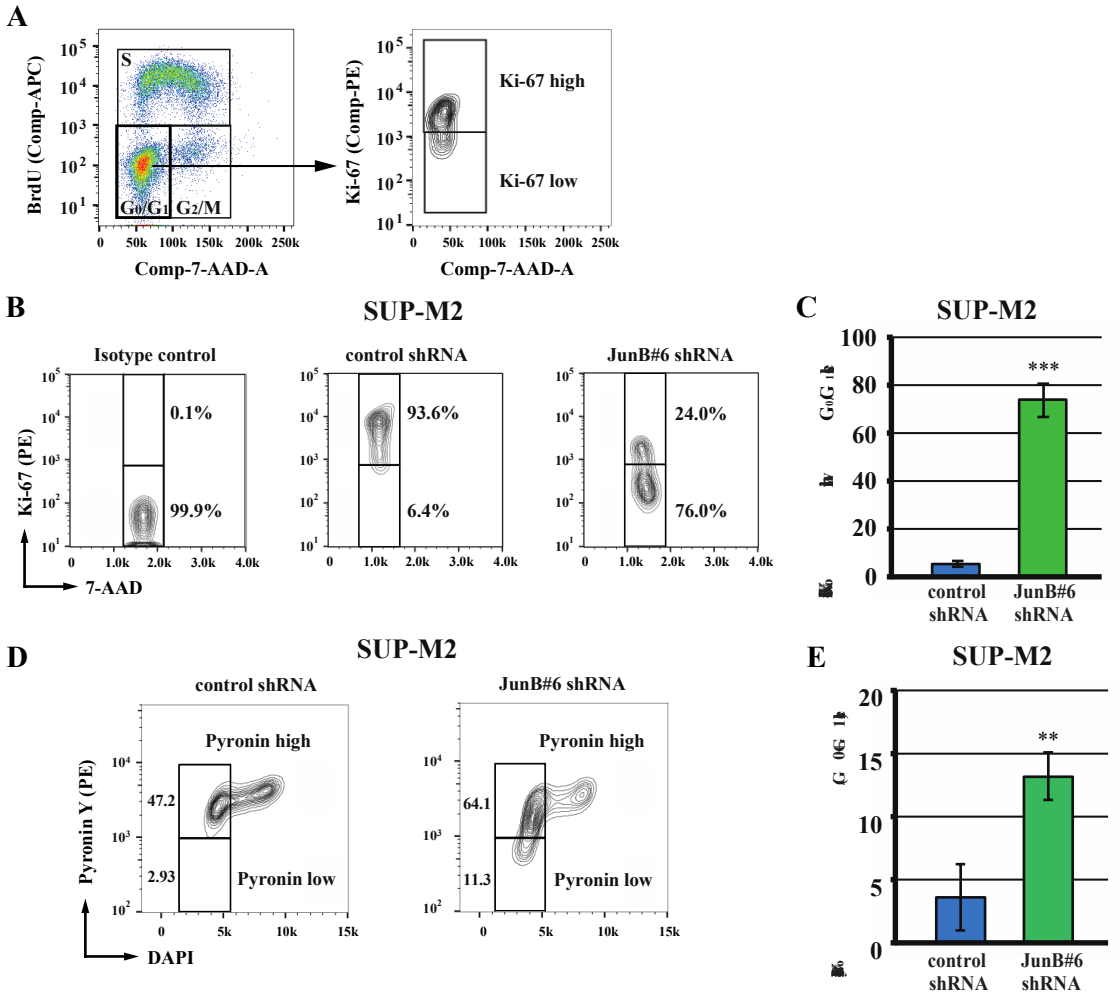


**Figure 3.9 – Knocking down JunB results in cells phenotypically resembling the cells leaving cell cycle**

**A.** Gating strategies for Ki-67 staining in $G_0/G_1$ population. **B-C.** Representative flow cytometry data (**B**) and summary (**C**) of Ki-67 expression within the $G_0/G_1$ population of SUP-M2 cells expressing control or JunB shRNA. **D-E.** Representative flow cytometry data (**D**) and summary (**E**) of Pyronin-Y and DAPI staining of SUP-M2 cells expressing control or JunB shRNA. The summary represents the average and standard deviation of three independent experiments from two separate infections. p values were obtained by performing independent, two-tailed *t* tests comparing the JunB knock-down to control shRNA–expressing cells.

### 3.2.9 Stable knock-down of JunB results in altered expression of $G_1$ phase cell cycle regulators.

After showing reduction in JunB results in a population of cells phenotypically resembling cells leaving cell cycle, I further examined whether JunB knock-down affect $G_0/G_1$ progression in this section. To examine whether the $G_0/G_1$ progression was interrupted or not, I checked the expression of cell cycle regulators participating in $G_1$ including cyclins, cyclin-dependent kinases (CDKs), and CDK inhibitors in control cells and JunB knock-down cells by western blot. I observed increased expression of $p27^{Kip}$ (*CDKNIB*) and $p18^{Ink4C}$ (*CDKN2C*), and modestly decreased expression of CDK2 when JunB was knocked down in Karpas 299 cells (**Figure 3.10A**). Similarly for SUP-M2, $p27^{Kip1}$ was up-regulated, and CDK2 and cyclin E were down-regulated in JunB shRNA-expressing cells; the change in $p27^{Kip1}$ and CDK2 was very prominent (**Figure 3.10B**). Additional $G_1$ regulators that were unchanged between control and JunB shRNA-expressing cells are shown in **Figure 3.10C**. Then I further performed qPCR to examine whether $p27^{Kip1}$and CDK2 were changed at the mRNA level in JunB knock-down Karpas 299 and SUP-M2 cells. The mRNA levels of $p27^{Kip1}$ were not significantly changed when JunB was knocked-down in Karpas 299 and SUP-M2 cells (**Figure 3.10D**). Thus, JunB knock-down leads to the increased expression of CDK inhibitors and the decreased expression of cyclins participating in $G_1$ phase progression, arguing that JunB promotes cells transiting through $G_1$ phase to promote cell proliferation.

**Figure 3.10**

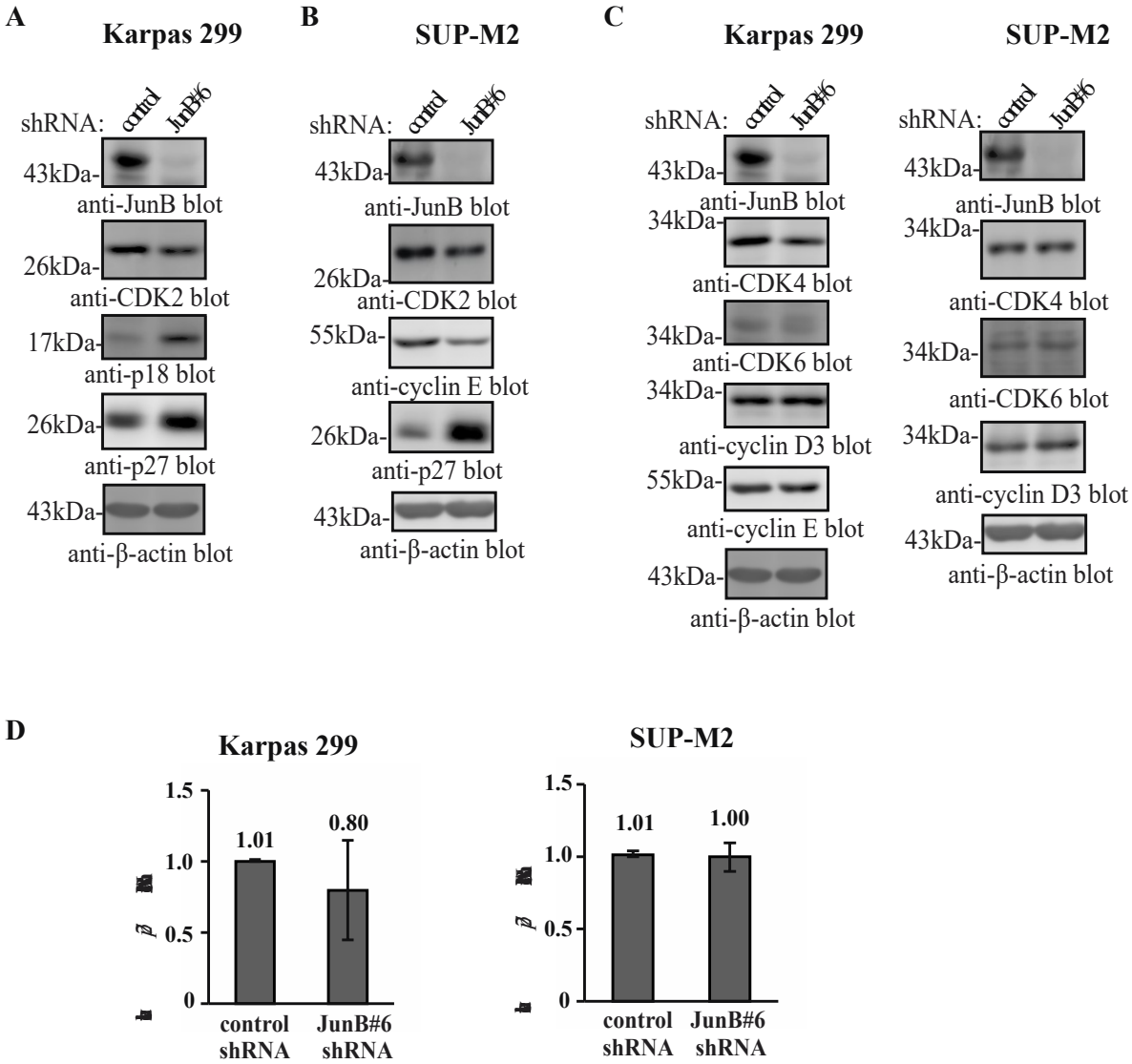


**Figure 3.10 – Knocking down JunB results in altered expression of $G_1$ phase cell cycle regulators.**

**A-B.** Western blots comparing the expression of the indicated cell cycle regulators with altered expression in control and JunB shRNA–expressing Karpas 299 cells (**A**) and SUP-M2 cells (**B**). **C.** Western blots comparing the expression of the indicated cell cycle regulators with unchanged expression between control and JunB shRNA–expressing Karpas 299 cells and SUP-M2 cells. Molecular mass markers (in kDa) are indicated to the left of western blots. **D**. Bar graph showing the mRNA levels of $p27^{Kip1}$ in JunB shRNA-expressing Karpas 299 cells and SUP-M2 cells. The results represent the averages and standard deviations from at least three independent experiments from two infections. Independent, two-tailed t tests were performed to compare the mRNA levels in control shRNA-expressing cells to that in JunB shRNA-expressing cells.

### 3.3 Discussion

In Chapter 3, I examined the role of JunB and c-Jun in cell growth in ALK+ ALCL by stabling knocking the expression of these genes down with shRNAs (**Figure 3.1**). I found that knocking down JunB, but not c-Jun, resulted in a significantly slower growth rate with a prolonged $G_0/G_1$ phase compared to control shRNA-expressing cells in two of three ALK+ ALCL cell lines examined (**Figures 3.2, 3.4, and 3.8**); knocking down JunB did not trigger spontaneous apoptosis (**Figure 3.3**). This suggests the differences in growth rate in JunB knock-down Karpas 299 and SUP-M2 cells is due to decreased proliferation ALK+ ALCL (**Figures 3.2, 3.4, and 3.8**). Proliferation was restored when JunB was reintroduced into JunB knock-down cells (**Figure 3.7**), ruling out the possibility that the proliferation defect was caused by the shRNA targeting other genes. Furthermore, there was a large population of $G_0$-like cells, with lower Ki-67 levels and low RNA content (**Figure 3.9**), in JunB knock-down cells, suggesting that reducing JunB leads to cells leaving cell cycle entering $G_0$ phase. The expression levels of cell cycle regulators were also altered in JunB knock-down cells: $p27^{Kip1}$ was up-regulated and CDK2 down-regulated in Karpas 299 and SUP-M2 cells when JunB was reduced (**Figure 3.10**). All the results together argue that JunB promotes cell proliferation in ALK+ ALCL by facilitating cells transiting through $G_0/G_1$ phase.

Although the expression of $p27^{Kip1}$ increased consistently when JunB was knocked down in Karpas 299 and SUP-M2 cells, the mRNA levels of $p27^{Kip1}$ were not significantly changed in Karpas 299 and SUP-M2 cells (**Figure 3.10**). This suggests $p27^{Kip1}$ was possibly regulated through post-transcriptional mechanism in ALK+ ALCL, and $p27^{Kip1}$ has been shown to be regulated through multiple post-transcriptional mechanisms [250]. For example, $P27^{Kip1}$ could be targeted by microRNA 221 and microRNA 222 at the 3' UTR thus to inhibit

the translation of the $p27^{Kip1}$ protein [251]; these microRNA are overexpressed in multiple cancers [250, 252-255]. In addition, the phosphorylation of $p27^{Kip1}$ at Tyr187 recruits the E3 ubiquitin ligase and leads to the degradation of $p27^{Kip1}$ [256, 257], and the proteolysis of $p27^{Kip1}$ could be promoted by oncogenic pathways in hematopoietic malignancies [258, 259]. The stable overexpression of $p27^{Kip1}$ in ALK+ ALCL cell line SUDHL-1 and Karpas 299 resulted in increased percentage of cells in $G_0/G_1$ phase and decreased percentage of cells in S phase [260, 261], which is consistent with what I observed in JunB knock-down ALK+ ALCL cells. While overexpression of $p27^{Kip}$ with adenovirus in Karpas 299 resulted in slight change of the cell cycle distribution and the $p27^{Kip}$ expression was less prominent than SUDHL-1 cells [262]. This is also consistent with our observation that the JunB knock-down in different ALK+ ALCL cell lines resulted in a different extent of changes in cell cycle distribution and levels of cell cycle regulators.

The cell cycle progresses to $G_1$ phase then to S and $G_2$/M phase, and the cell could leave the cell cycle, which is called $G_0$ phase **(Figure 3.11A)**. In this process, CDK2 and cyclin E form complexes to mediate cell cycle progression; $p27^{Kip1}$ could form stable complexes with CDK2/cyclin E, thus to inhibit the activity of CDK/cyclin E to repress proliferation [263, 264]. I observed the altered expression of all three components (CDK2/ cyclin E/ $p27^{Kip1}$) in SUP-M2 cells (**Figure 3.10B**), which is consistent with the dramatic growth defect with more cells resembling cells leaving cell cycle in SUP-M2 cells. Consistent with this, $p27^{Kip1}$ expression has been suggested to contribute to $G_0/G_1$ arrest [265-267]. In Karpas 299 cells, I observed increased $p18^{Ink4C}$ and changes in CDK2 and $p27^{Kip1}$ protein expression were less dramatic (**Figure 3.10A**), which may explain why I observed that the proliferation defect was less dramatic. $p18^{Ink4C}$ which inhibits the CDK4/cyclin D1

complex could also result in cell cycle arrest [268]. Other than the cell cycle regulators mentioned above, it is possible that other cell cycle regulators that I did not examine may also contribute to the changed cell cycle distribution.

Although, the levels of cell cycle regulators were changed when JunB was knocked-down in Karpas 299 and SUP-M2 cells, I postulate JunB does not directly regulate the those cell cycle regulators but possibly does so through other signalling molecules. One possibility is CD30. JunB directly regulates the transcription of *CD30* and CD30 can promote cell proliferation of ALK+ ALCL cells [54, 61]. Another possibility is AKT-1. AKT-1 was shown to be a target of JunB in ALK+ ALCL cell lines [232], and $p27^{Kip1}$ was demonstrated to be up-regulated when PI3K/AKT signalling was inhibited in NPM-ALK transformed murine lymphocytes [269].

The question we did not answer in this study is whether knocking down JunB could result in spontaneous apoptosis at the very early stages of knock-down. The approach I used selected the cells in puromycin for 3-5 days after infection, and before I performed the experiments. It is possible that some cells had undergone apoptosis because of the reduction of JunB during the 3-5 days and I did not catch the phenotype. To address this question, a transient knock-down of JunB without selection would provide the opportunity to examine whether there is apoptosis at very early stages.

For the role of c-Jun in ALK+ ALCL, some discrepancies have been described. Staber *et al.* showed that siRNA-mediated c-Jun knock-down in Karpas 299 cells had no effect on cell growth [136]. While Atsaves *et al*. demonstrated that siRNA-mediated c-Jun silencing in Karpas 299 cells resulted in slower colony formation [61]; Leventaki *et al.* demonstrated reducing c-Jun levels with siRNA or inactivating p-cJun with the JNK inhibitor, SP600126,

both leads to slower cell growth and increased apoptosis[142]. I showed shRNA-mediated stable c-Jun knock-down in multiple ALK+ ALCL cell lines neither affected cell growth and nor altered the cell cycle distribution. Thus, my data is consistent with the observation made by Staber *et al.* that reducing c-Jun levels did not result in slower proliferation in ALK+ ALCL cell lines [136]. In addition, I also used two c-Jun shRNA in Karpas 299 cells to rule out the possibility of off-targeting. It is not clear why different groups observed different phenotypes, but my results clearly demonstrate that stable knock-down of c-Jun with shRNA does not result in growth defect in ALK+ ALCL cells.

Collectively in this chapter, I clearly demonstrated that JunB promoted ALK+ ALCL cell proliferation, a major aspect of tumour biology, by promoting the cell cycle transition through $G_0/G_1$ phase in the cell cycle in the majority of the cell lines examined. In contrast, our results suggest that c-Jun does not have any effect on cell proliferation (**Figure 3.11B**). These results argue that these AP-1 proteins play different roles in cell proliferation in ALK+ ALCL, which is a major aspect of tumour biology.

**Figure 3.11**

**A**

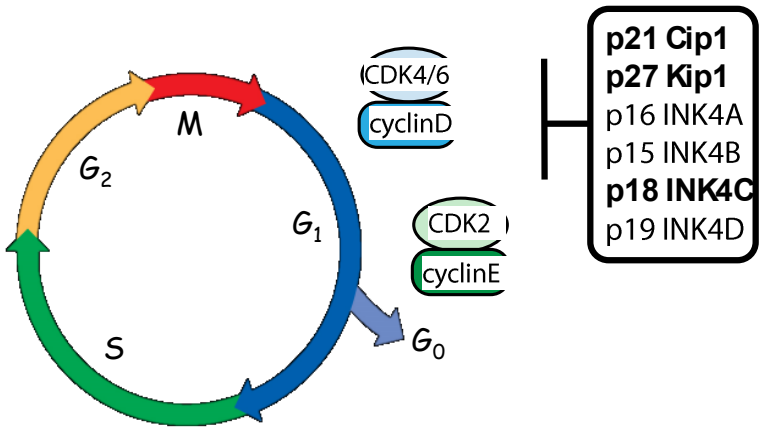


**B**

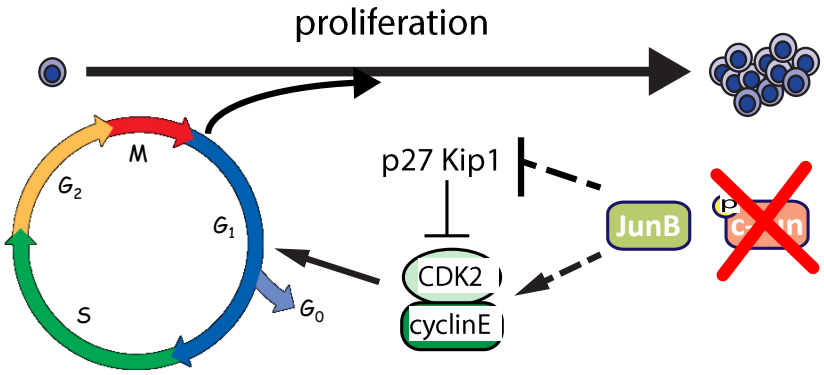


**Figure 3.11 – JunB, but not c-Jun promotes cell cycle progression through $G_0/G_1$ phase in ALK+ ALCL.**

**A.** The schematic diagram showing the cell cycle progression process. Cyclins, CDKs and CDK inhibitor that involve in G1 phase progression are indicated. The highlighted CDK inhibitors are the ones examined in **Figure 3.10. B.** Diagram showing the potential model for **Chapter 3**. JunB, but not c-Jun could contribute to the cell proliferation through promoting cell transition through $G_0/G_1$ phase in ALK+ ALCL by directly or indirectly down-regulating $p27^{Kip}$ and up-regulating CDK2.

# Chapter 4: Identifying and characterizing genes regulated by JunB in ALK+ ALCL

All experiments were performed by Zuoqiao Wu. The CD48 expression cDNA was constructed by Patrick Paszkowski. The primary NK cells were obtained from and cultured with the help of Dr. Burshtyn lab. Part of the chapter is from a draft manuscript written by Dr. Ingham and myself.

## 4.1 Introduction

In Chapter 3, I examined the role of JunB and c-Jun in cell growth in ALK+ ALCL, and I demonstrated that JunB, but not c-Jun, promoted ALK+ ALCL cell proliferation by facilitating cell cycle transition through the $G_0/G_1$ phase. The next question I wanted to address was what genes JunB regulated in ALK+ ALCL and how they contributed to the pathogenesis of ALK+ ALCL.

During the past decade, several targets of JunB have been identified in ALK+ ALCL. JunB has been shown to promote the transcription of *CD30* directly, and signalling through CD30 also promotes *JunB* transcription generating an autocrine loop that ensures that JunB and CD30 levels are high in ALK+ ALCL and other CD30-positive lymphomas [54, 60]. We showed JunB also promotes the transcription of the serine/protease Granzyme B (*GzB*) in ALK+ ALCL, which is associated with the cytotoxic phenotype of this lymphoma [270]. The expression of GzB was also demonstrated to sensitize ALK+ ALCL cells to drug-induced apoptosis and may be one reason why these tumour cells are susceptible to chemotherapeutic drugs [270]. We also showed that JunB promoted the expression of the co-chaperone protein, *Cyclophilin 40*, and knock-down of this co-chaperone protein reduced the viability of ALK+ ALCL cell lines [230]. JunB, as well as c-Jun, bind to the promoter of *PDGFR-β* and promotes the transcription of *PDGFR-β* [229]. *DDX11*, a DNA helicase, was suggested as a JunB target as well, since *DDX11* levels were negatively correlated with JunB levels and JunB was shown to bind to the promoter of this gene [225].

Given the fact that JunB regulates important functions and genes in ALK+ ALCL and many AP-1 sites are present in the genome, I postulated that many additional critical genes and functions that JunB regulates in ALK+ ALCL remained to be determined. In addition,

JunB transcriptional targets, such as *CD30* and *PDGFR-β*, have been shown to be viable drug targets in the treatment of ALK+ ALCL in the clinic [34, 271, 272], so identifying additional JunB targets may provide novel ways to treat this lymphoma.

Thus, I wanted to comprehensively identify genes and cellular activities, directly or indirectly, regulated by JunB in ALK+ ALCL in this Chapter. Specifically, I performed microarray experiments comparing gene expression in the Karpas 299 ALK+ ALCL cell line expressing control shRNA with Karpas 299 cells expressing JunB shRNA. Furthermore, I examined the role of some of these genes in the pathobiology of ALK+ ALCL.

## 4.2 Results

### 4.2.1 Performing microarray experiments on Karpas 299 cells expressing JunB or control shRNA

To comprehensively identify genes, directly or indirectly regulated by JunB, in ALK+ ALCL, microarray experiments were performed to compare the mRNA expression profiles of three sets of mRNA isolated from control or JunB shRNA–expressing Karpas 299 cells **(Figures 4.1A and B**). A total of 8,993 probes corresponding to 5,090 genes were significantly altered ($p<0.05$) in Karpas 299 cells when JunB was knocked-down **(Figure 4.1C)**. The top 20 probes with decreased or increased expression in JunB knock-down cells are shown in **Figure 4.1E**. We found that the fold changes for up-regulated genes were greater compared to the fold changes observed for down-regulated genes. 3,224 probes were altered by 1.5-fold or greater in JunB knock-down cells; these probes corresponded to 1,856 genes: 1,268 (68.3%) were up-regulated, and 588 (31.7%) were down-regulated **(Figure 4.1D)**. I found 1,116 probes were altered 2-fold or greater change in the JunB knock-down cells **(Figure 4.1**

**D)**. These probes corresponded to 678 genes whose expression changed >2-fold: 546 (90.0%) were up-regulated, and 132 (10.0%) were down-regulated **(Figure 4.1 D)**. Thus, knocking down JunB in Karpas 299 resulted in altered expression of a large number of genes. The changes associated with up-regulated genes were much more dramatic than down-regulated genes. Moreover, the large majority of the genes with altered expression were up-regulated, and a small portion were down-regulated.

## Figure 4.1

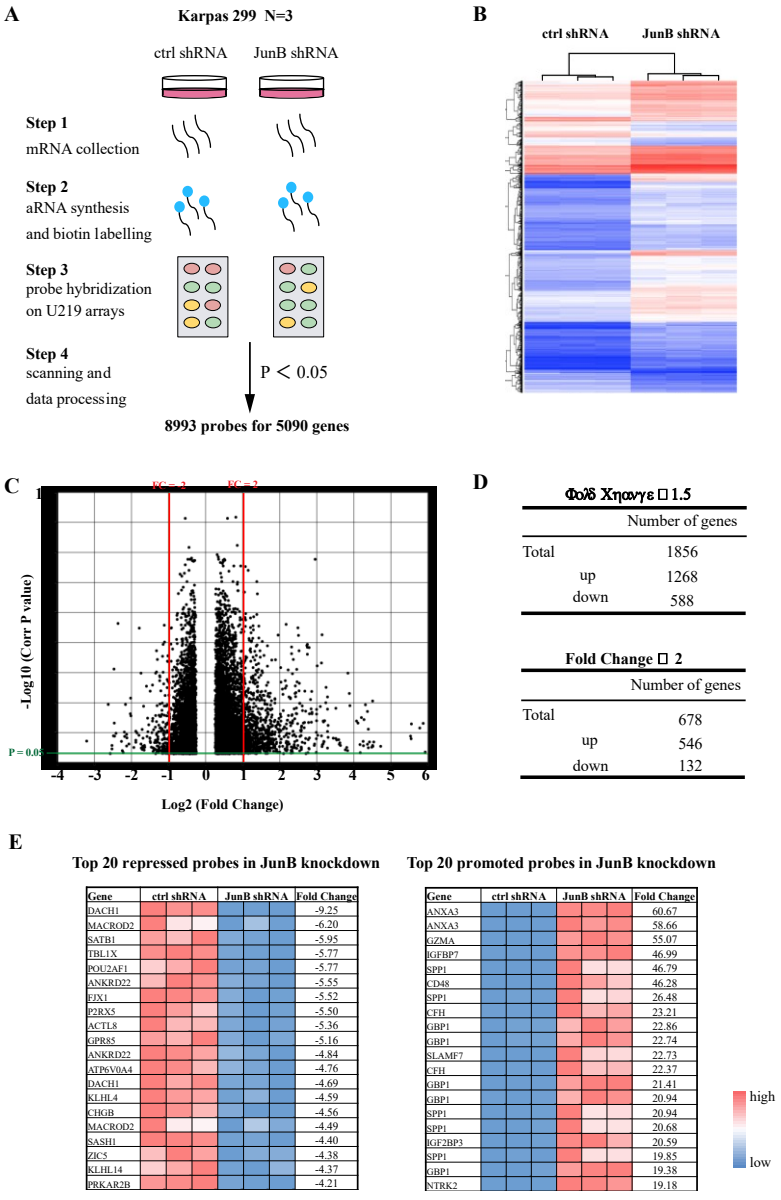


| Gene | ctrl shRNA | JunB shRNA | Fold Change |
|---|---|---|---|
| DACH1 | | | -9.25 |
| MACROD2 | | | -6.20 |
| SATB1 | | | -5.95 |
| TBL1X | | | -5.77 |
| POU2AF1 | | | -5.77 |
| ANKRD22 | | | -5.55 |
| FJX1 | | | -5.52 |
| P2RX5 | | | -5.50 |
| ACTL8 | | | -5.36 |
| GPR85 | | | -5.16 |
| ANKRD22 | | | -4.84 |
| ATP6V0A4 | | | -4.76 |
| DACH1 | | | -4.69 |
| KLHL4 | | | -4.59 |
| CHGB | | | -4.56 |
| MACROD2 | | | -4.49 |
| SASH1 | | | -4.40 |
| ZIC5 | | | -4.38 |
| KLHL14 | | | -4.37 |
| PRKAR2B | | | -4.21 |

| Gene | ctrl shRNA | JunB shRNA | Fold Change |
|---|---|---|---|
| ANXA3 | | | 60.67 |
| ANXA3 | | | 58.66 |
| GZMA | | | 55.07 |
| IGFBP7 | | | 46.99 |
| SPP1 | | | 46.79 |
| CD48 | | | 46.28 |
| SPP1 | | | 26.48 |
| CFH | | | 23.21 |
| GBP1 | | | 22.86 |
| GBP1 | | | 22.74 |
| SLAMF7 | | | 22.73 |
| CFH | | | 22.37 |
| GBP1 | | | 21.41 |
| GBP1 | | | 20.94 |
| SPP1 | | | 20.94 |
| SPP1 | | | 20.68 |
| IGF2BP3 | | | 20.59 |
| SPP1 | | | 19.85 |
| GBP1 | | | 19.38 |
| NTRK2 | | | 19.18 |

**Figure 4.1 - Identifying genes with altered expression by microarray when JunB was knocked-down in Karpas 299 cells.**

**A.** Schematic diagram showing the microarray procedure. **B.** Hierarchical clustering heat map showing the three independent experiments with probes of average of fold-change greater than 2. **C.** Volcano plots showing all the significantly changed probes with $p<0.05$. The two red lines indicate the fold change of +/-2. **D.** Number of genes with fold change ≥ 2 and 1.5. **E.** The top 20 probes either up-regulated (left) or down-regulated (right) in JunB knock-down Karpas 299 cells. Each box represents the value from a single microarray experiment. Fold change represents the average of the three independent microarray experiments.

### 4.2.2 Verification of microarray data

qRT-PCR was performed on a select number of the identified genes to verify our microarray findings and examine whether knock-down of the related AP-1 transcription factor, c-Jun, in Karpas 299 cells also affected the expression of these genes. Consistent with the microarray results, the mRNA levels of *GZMA* (Granzyme A), *GBP1* (Guanylate Binding Protein-1), *ANXA1* (Annexin A1), *MXD1* (MAX Dimerization Protein 1), and *PTPN22* (Protein Tyrosine Phosphatase, Non-Receptor Type 22) were found to be up-regulated in qRT-PCR experiments **(Figure 4.2A**). Likewise, down-regulated genes identified in the microarray experiments, such as *FJX1* (Four Jointed Box 1), *PRKA2B* (Protein Kinase cAMP-dependent Type II Regulatory Subunit Beta), *ITK* (IL2 inducible T Cell Kinase), and *CXCL12* (C-X-C Motif Chemokine Ligand 12) were also determined to be down-regulated by qRT-PCR **(Figure 4.2B**). While knocking-down c-Jun in Karpas 299 cells also resulted in statistically significant changes in gene expression that trended in the same direction as JunB knock-down for most genes, the magnitude of these changes were not as great as was observed in JunB knock-down cells **(Figures 4.2A and B**). We further examined whether these changes in mRNA expression also resulted in changes in protein expression. **Figure 4.2C** shows that GZMA and GBP1 protein levels were elevated when JunB was knocked-down in Karpas 299 cells, and ANXA1 was elevated in both c-Jun and JunB shRNA shRNA-expressing Karpas 299 cells, which correlated with what we observed in the qRT-PCR experiments. Thus, several of the genes identified by microarray were verified to be changed at the mRNA level when JunB was knocked down in Karpas 299 cells; some of them were also verified to change at the protein level in JunB shRNA-expressing Karpas 299 cells.

## Figure 4.2

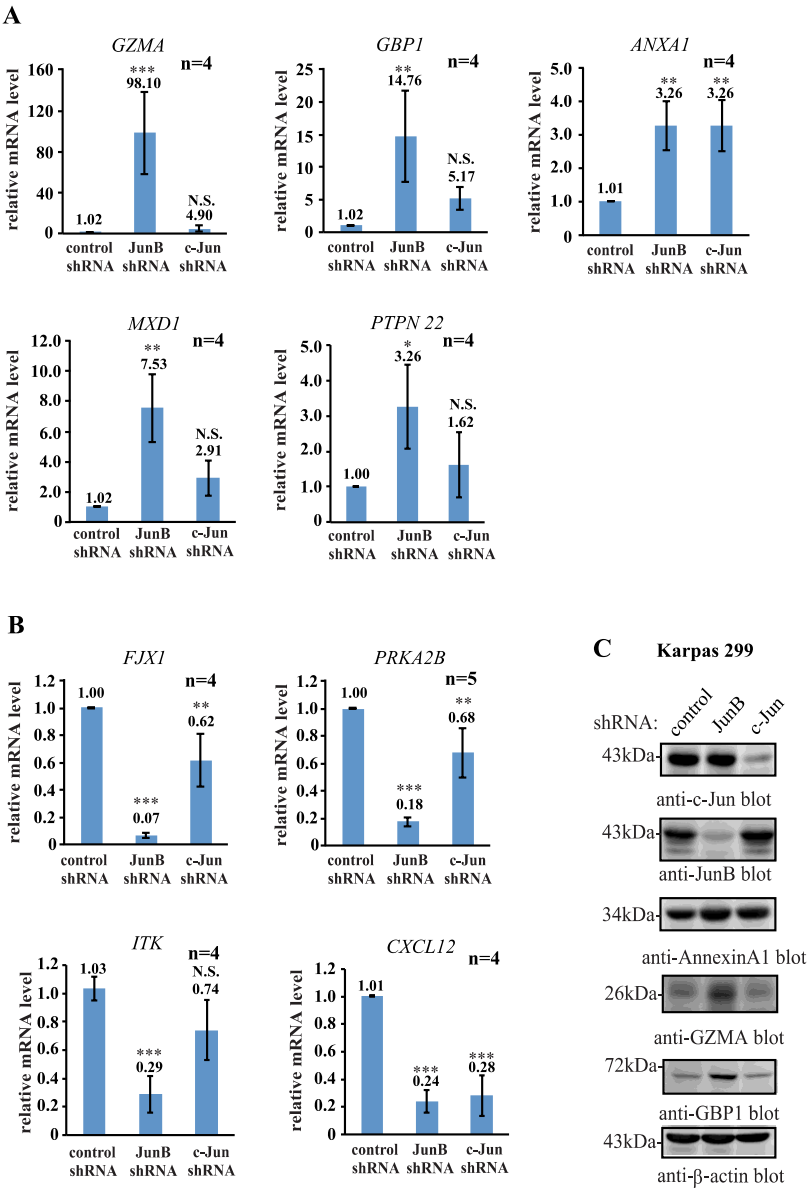


**Figure 4.2 – PCR verification of microarray results**

**A-B.** qRT-PCR checking the mRNA level of genes that were identified as up-regulated (**A)** or down-regulated (**B**) in JunB knock-down Karpas 299 cells from the microarray data. The results represent the average and standard deviation of four/five independent experiments. p values represent ANOVA test with TUKEY *post-hoc* test comparing the JunB/c-Jun shRNA-expressing cells to control shRNA-expressing cells.* $p<0.05$, ** $p<0.01$, *** $p<0.001$, N.S. not significant. **C.** Western blots showing the expression of genes in JunB/c-Jun shRNA-expressing Karpas 299 cells. The western blots represent more than three independent experiments. Molecular mass markers (in kDa) are indicated to the left of western blots.

### 4.2.3 Functional annotation of genes identified by microarray

I next performed an analysis using the Kyoto Encyclopedia of Genes and Genomes (KEGG) database to determine whether the dysregulated genes in JunB knock-down cells could be grouped into common cellular pathways or biological processes. This analysis revealed that genes with altered expression in JunB knock-down cells were enriched in many pathways that would be predicted to be important in the pathobiology of ALK+ ALCL, including "cytokine-cytokine receptor signaling", "p53 signaling pathway", "pathways in cancer", "proteoglycans in cancer", "chemokine signaling pathway", and "MAPK signaling pathway" **(Figure 4.3A)**. Complete KEGG pathway list is included in **Appendix 2**; genes from top 10 categories are included in **Appendix 3**.

Among the functional categories, I was intrigued by the most statistically significant category that was "natural killer cell mediated cytotoxicity". This functional category included receptors expressed on NK cells **(Figures 4.3B and D)**, signalling molecules expressed in NK cells **(Figures 4.3B and E)**, and ligands targeted by NK cells for killing **(Figures 4.3B and C)**. As shown in **Figure 4.3B**, JunB knock-down in Karpas 299 cells resulted in altered expression of ligands for NK receptors, NK receptors and signalling molecules. The probes for genes within each subgroup of the "natural killer cell mediated cytotoxicity" category are shown in the heat maps with data from all three sets of samples indicated **(Figures 4.3C, D and E)**. Moreover, the majority of the genes in this category were up-regulated when JunB was knocked-down; this group included some of the most prominently up-regulated genes (like *CD48*, *SLAMF7*, and *SH2D1A*) identified in the microarray experiments.

We were particularly struck by the number of the ligands mediating NK killing that were up-regulated in the JunB knock-down cells, and we identified several other ligands that were up-regulated when we lowered our cut-off threshold (**Figure 4.3C**). The interaction of these ligands with corresponding activating receptors on NK cells results in the killing of target cells through the release of granzymes and perforin [273], therefore the down-regulation of these ligands may protect the ALK+ ALCL cells form NK mediated killing. I focused on the ligands for NK activating receptors for further investigation. Specifically, CD48 is recognized by the 2B4 (CD244) receptor on NK cells [274, 275], whereas SLAMF7 is recognized by SLAMF7 on the NK cells [276]. MICA, MICB, and ULBP3 bind to the NKG2D receptor on NK cells [277]. CLEC2B interacts with the NK receptor NKp80 [278]. Thus, if these ligands are confirmed to be increased in JunB knock-down ALK+ ALCL cells, which is examined in the following section, then I hypothesized that the elevated expression of these ligands may trigger the killing by NK cells.

## Figure 4.3

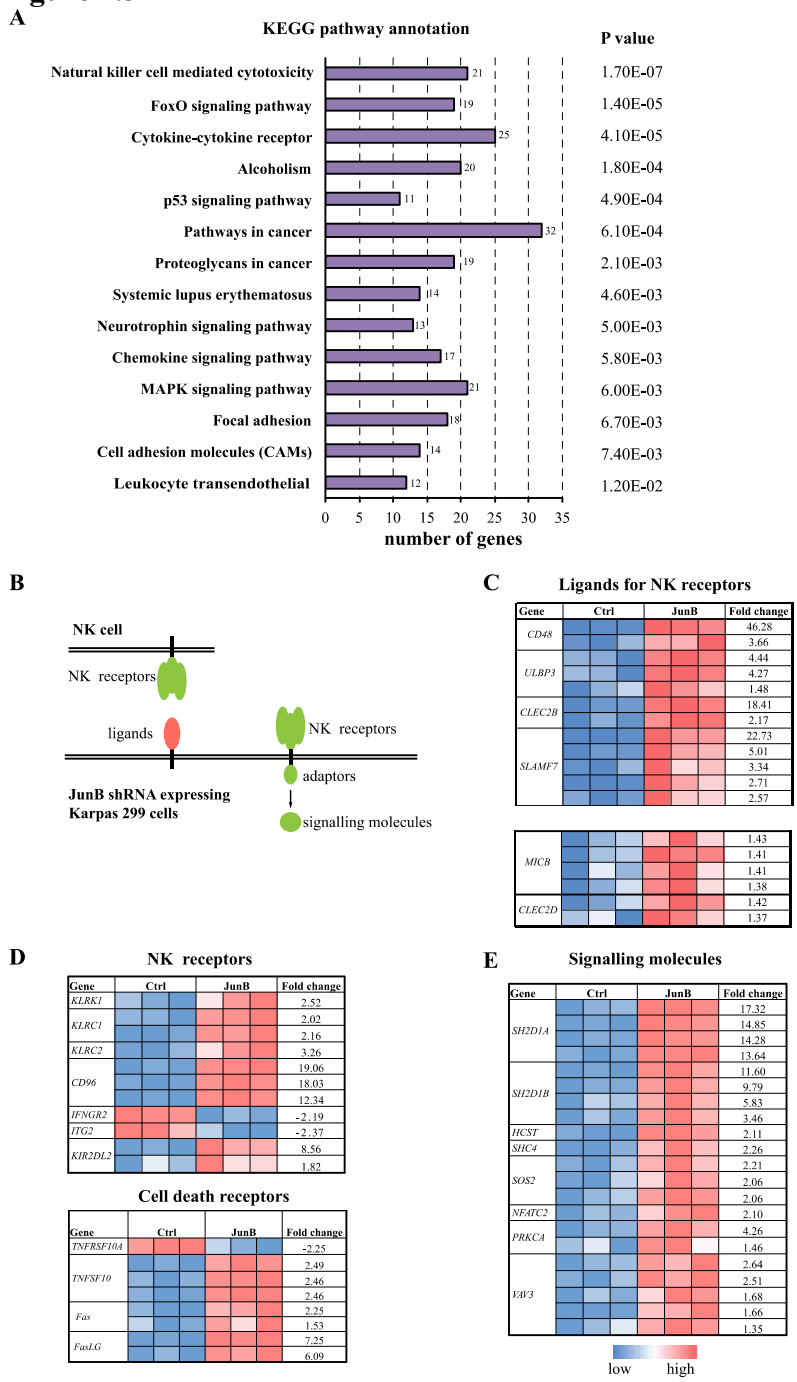


**Figure 4.3 - Functional annotation of genes identified by microarray**

**A.** Chart showing the top 14 most statistically significant functional categories from KEGG pathway annotation. **B.** Schematic diagram showing the different subgroups in the "natural killer cell mediated cytotoxicity" category that were altered in JunB shRNA-expressing Karpas 299 cells. **C-E.** Heat maps showing the genes in different subgroups. Each coloured box indicates the change in one independent experiment. The fold change was calculated by comparing the JunB shRNA-expressing cells to control shRNA-expressing cells. Fold change represents the average of the three independent microarray experiments.

### 4.2.4 JunB knock-down in Karpas 299 cells resultes in the dysregulation of genes associated with NK cells

To confirm the up-regulation of the genes in the category of "natural killer cell mediated cytotoxicity", qRT-PCR experiments were performed to compare the mRNA levels of those genes in JunB and control shRNA-expressing cells (**Figure 4.4A)**. *CD48* and *SLAMF7* mRNA levels were considerably increased, whereas *ULBP3* and *CLEC2B* mRNA were only modestly augmented in JunB knock-down cells. I also examined the expression of *MICB* and the closely related gene, *MICA,* in JunB shRNA-expressing cells, and I found that both *MICA* and *MICB* were increased at mRNA level when JunB was knocked down in Karpas 299 cells **(Figure 4.4A)**. The two signalling molecules known to be expressed in NK cells *SH2D1A* and *SH2D1B* [279] were also up-regulated at mRNA level in JunB shRNA-expressing Karpas 299 cells, consistent with our microarray results **(Figure 4.3C)**. I further examined whether the mRNAs for these ligands were also up-regulated in another ALK+ ALCL cell line, SUP-M2 **(Figure 4.4B)**. *CD48, SLAMF7, CLEC2B, SH2D1A* and *SH2D1B* mRNAs were also increased when JunB was knocked down in SUP-M2 cells, while the levels of *MICA, MICB, and ULBP3* did not change significantly in JunB knock-down SUP-M2 cells (**Figure 4.4B)**. Thus, I confirmed the genes in the category of "natural killer cell mediated cytotoxicity" were up-regulated at mRNA level when JunB was knocked down and the up-regulation of most genes in this category were observed in two ALK+ ALCL cell lines.

## Figure 4.4

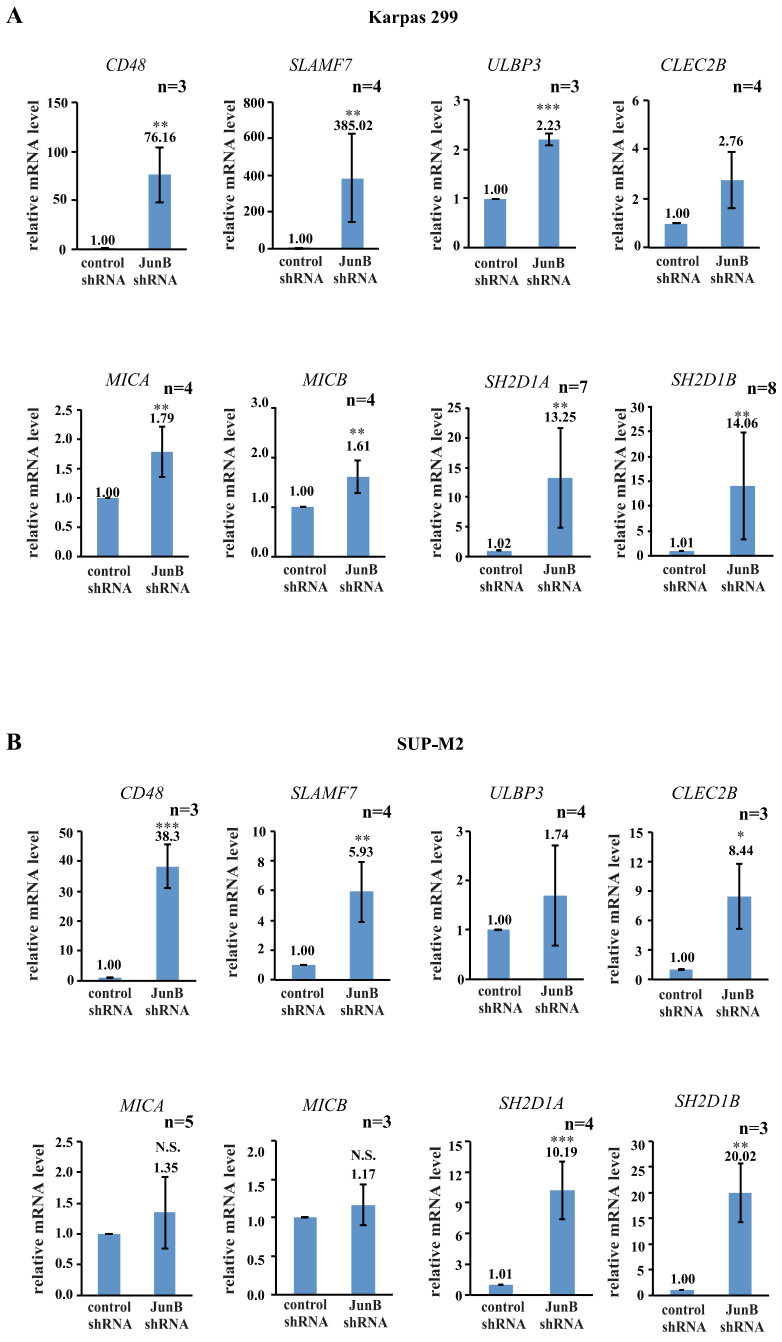


**Figure 4.4 - JunB knock-down in Karpas 299 and SUP-M2 cells resulted in the dysregulation of genes associated with NK cells and NK cell–mediated killing**

**A-B.** qRT-PCR examining the levels of indicated genes in JunB and control shRNA-expressing Karpas 299 cells (**A**) and SUP-M2 cells (**B**). The results represent the average and standard deviation of three or four independent experiments. p values represent independent, two-tailed t tests.* $p<0.05$, ** $p<0.01$, *** $p<0.001$, N.S. not significant.

### 4.2.5 JunB knock-down results in increased surface expression of NK ligands on ALK+ ALCL cells

I next focused on the genes in the "NK ligands subgroup", and examined whether the surface expression of these NK ligands was increased in the JunB knock-down cells. Although I could not identify a second shRNA that reduced JunB to the same extent as JunB#1 shRNA, I did find a second shRNA that slightly reduced JunB levels (**Figures 4.5A and B**) and I examined whether NK ligands were up-regulated in cells expressing the second shRNA as well. Flow cytometry revealed that CD48 and MICA/B surface expression were significantly increased in JunB shRNA–expressing Karpas 299 cells (**Figure 4.5C**). SLAMF7 expression was comparable between control and JunB shRNA–expressing Karpas 299 cells; albeit a tail of cells with high SLAMF7 expression was observed when JunB was knocked-down (**Figure 4.5C**). Raji cells were used as the positive control for SLAMF7 staining[280]. Prominent SLAMF7 signal was observed in Raji cells, demonstrating the antibody was functional. The changes of CD48, MICA/B, and SLAMF7 were also examined in a second JunB shRNA-expressing cells. As the silencing of JunB was not as efficient as in JunB#1 shRNA-expressing cells, only very moderate change of the ligands was observed in the second shRNA-expressing cells (**Figure 4.5C**). Expression of ULBP3 and CLEC2B did not change in Karpas 299 cells when JunB was knocked-down (**Figures 4.5E and F**). We also examined whether these ligands were up-regulated in SUP-M2 cells expressing JunB shRNAs. Similar to Karpas 299 cells, CD48 and MICA/B were increased in surface expression in SUP-M2 cells when JunB was knocked-down, although the up-regulation of CD48 was not as dramatic as what was observed in Karpas 299 cells (**Figure 4.5D**). SLAMF7 expression was also increased in JunB shRNA-expressing SUP-M2 cells (**Figure 4.5 D**). Thus, the results above

showed that reducing JunB expression leads to up-regulation of CD48, MICA/B, and SLAMF7 in ALK+ ALCL cell lines.

## Figure 4.5

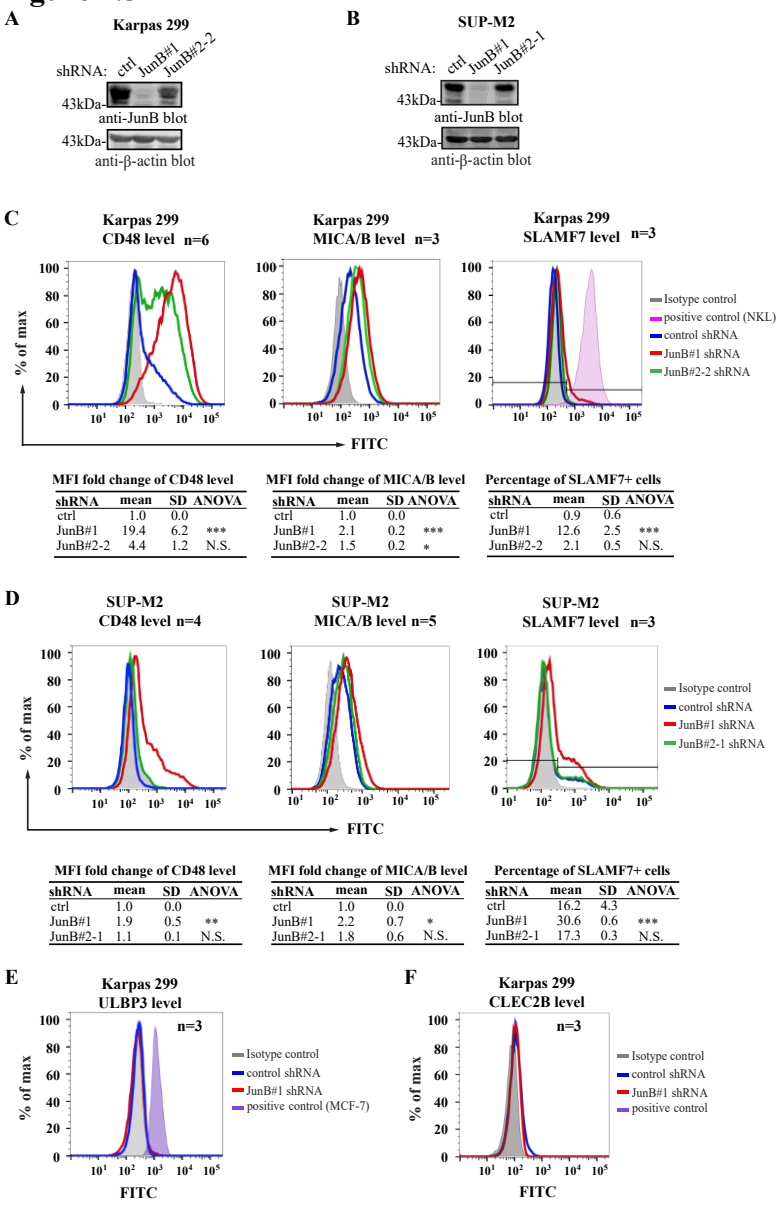


**Figure 4.5 - JunB knock-down resulted in increased surface expression of NK ligands on ALK+ ALCL cells**

**A-B.** Western blots showing JunB knock-down in JunB#1 shRNA and JunB #2-1 shRNA-expressing Karpas 299 cells **(A)** and SUP-M2 cells **(B)**. **C-D.** Representative flow plots and tables showing the expression of CD48, MICA/B, and SLAMF7 in Karpas 299 cells (**C**) or SUP-M2 cells (**D**) expressing JunB shRNAs or control shRNA. **E-F.** Representative flow plots showing the expression of ULBP3 and CLEC2B in Karpas 299 cells expressing JunB shRNAs or control shRNA. The tables represent three to six independent experiments. p values represent ANOVA test with TUKEY *post-hoc* test by comparing control and c-Jun/JunB shRNA–expressing cells. * $p<0.05$, ** $p<0.01$, *** $p<0.001$, N.S. not significant. Molecular mass markers (in kDa) are indicated to the left of western blots. Fold changes represent the changes in median of fluorescence intensity obtained from flow cytometry.

### 4.2.6 Inhibition of histone deacetylation results in up-regulation of CD48, MICA/B and SLAMF7

Next, we investigated the potential mechanism for the up-regulation of NK ligands in JunB shRNA-expressing cells. One possibility is through inhibition of histone deacetylation. Histone deacetylases (HDAC) are enzymes that remove the acetyl functional group from histone proteins, thus the chromatin will become wrapped tightly together and cannot be reached by transcription factors or RNA polymerase [281]. As a result, the transcription of the genes will be repressed [281]. Because CD48 was demonstrated to by repressed through HDACs in AML [282], I hypothesized that the NK ligands were possibly repressed through similar epigenetic mechanisms in ALK+ ALCL cells. To test this hypothesis, I examined whether the NK ligands were increased in ALK+ ALCL cells after HDAC inhibition. Karpas 299 and SUP-M2 cells were treated with increasing concentrations of MGCD0103 (**Figure 4.6A**), which inhibits Class I HDACs, namely HDAC1, HDAC2, and HDAC3 [283]. The surface levels of CD48, MICA/B, and SLAMF7 were measured by flow cytometry and determined to be increased in MGCD0103-treated Karpas 299 cells in a dose-dependent manner (**Figure 4.6A**). Similar results were observed in SUP-M2 cells; the surface levels of CD48, MICA/B, and SLAMF7 were increased after treatment with MGCD0103 (**Figure 4.6B**). In both Karpas 299 and SUP-M2 cells, the up-regulation of CD48 and MICA levels after drug treatment was considerable. SLAMF7 was only slightly up-regulated in Karpas 299 cells after treatment with MGCD0103; while it was moderately increased in SUP-M2 cells after MGCD0103 treatment. Thus, inhibition of histone deacetylation results in up-regulation of CD48, MICA and SLAMF7 in ALK+ ALCL cells.

## Figure 4.6

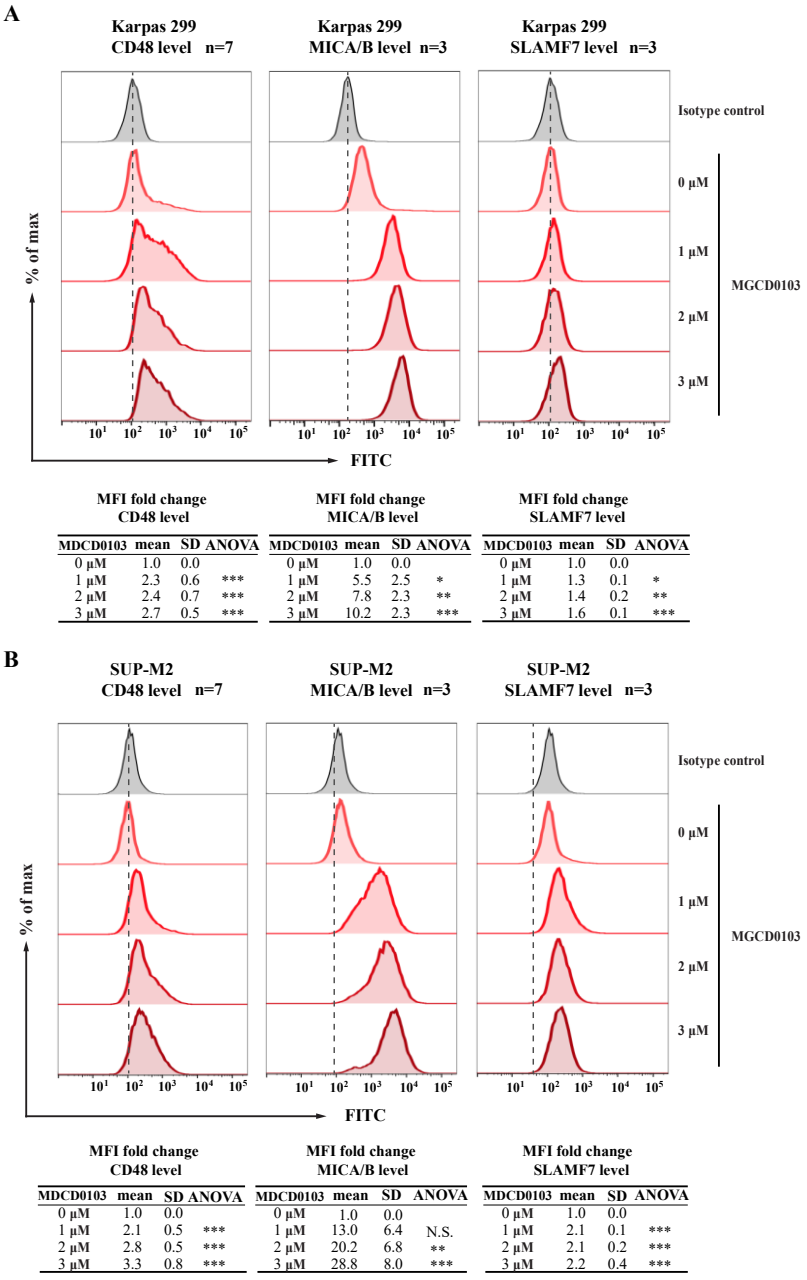


MFI fold change CD48 level

| MDCD0103 | mean | SD | ANOVA |
|---|---|---|---|
| 0 μM | 1.0 | 0.0 | |
| 1 μM | 2.3 | 0.6 | *** |
| 2 μM | 2.4 | 0.7 | *** |
| 3 μM | 2.7 | 0.5 | *** |

MFI fold change MICA/B level

| MDCD0103 | mean | SD | ANOVA |
|---|---|---|---|
| 0 μM | 1.0 | 0.0 | |
| 1 μM | 5.5 | 2.5 | * |
| 2 μM | 7.8 | 2.3 | ** |
| 3 μM | 10.2 | 2.3 | *** |

MFI fold change SLAMF7 level

| MDCD0103 | mean | SD | ANOVA |
|---|---|---|---|
| 0 μM | 1.0 | 0.0 | |
| 1 μM | 1.3 | 0.1 | * |
| 2 μM | 1.4 | 0.2 | ** |
| 3 μM | 1.6 | 0.1 | *** |

MFI fold change CD48 level

| MDCD0103 | mean | SD | ANOVA |
|---|---|---|---|
| 0 μM | 1.0 | 0.0 | |
| 1 μM | 2.1 | 0.5 | *** |
| 2 μM | 2.8 | 0.5 | *** |
| 3 μM | 3.3 | 0.8 | *** |

MFI fold change MICA/B level

| MDCD0103 | mean | SD | ANOVA |
|---|---|---|---|
| 0 μM | 1.0 | 0.0 | |
| 1 μM | 13.0 | 6.4 | N.S. |
| 2 μM | 20.2 | 6.8 | ** |
| 3 μM | 28.8 | 8.0 | *** |

MFI fold change SLAMF7 level

| MDCD0103 | mean | SD | ANOVA |
|---|---|---|---|
| 0 μM | 1.0 | 0.0 | |
| 1 μM | 2.1 | 0.1 | *** |
| 2 μM | 2.1 | 0.2 | *** |
| 3 μM | 2.2 | 0.4 | *** |

**Figure 4.6 - Inhibition of histone deacetylation results in up-regulation of CD48, MICA and SLAMF7**

**A-B.** Representative histograms and summary tables showing the levels and fold changes of CD48, MICA/B, and SLAMF7 in Karpas 299 cells **(A)** and SUP-M2 cells (**B**) after HDAC inhibitor MGCD0103 treatment for 24 hours or 48 hours respectively at increasing MGCD0103 concentrations. Representative histograms and summary tables represent three independent experiments. p values represent ANOVA test with TUKEY *post-hoc* test comparing control and c-Jun/JunB shRNA–expressing cells. * $p<0.05$, ** $p<0.01$, *** $p<0.001$, N.S. not significant. Fold changes represent the changes in median of fluorescence intensity obtained from flow cytometry.

### 4.2.7 Inhibition of DNA methylation results in up-regulation of CD48, MICA/B and SLAMF7

In ALK+ ALCL, NPM-ALK signalling regulates the expression of DNA methyltransferase 1 (DNMT1) [45, 284], and several studies have shown genes are silenced through DNA promoter methylation in ALK+ ALCL [285-287]. Therefore, I further tested whether DNA methylation also participated in the repression of the NK ligands in ALK+ ALCL. Specifically, I treated the cells with the DNMT inhibitor, 5-aza-2'-deoxycytidine (DAC) [284], and then measured the levels of the NK ligands by flow cytometry. 96 hours post DAC treatment, CD48, MICA/B, and SLAMF7 were statistically significantly increased in Karpas 299 cells (**Figure 4.7A**), although the increase of CD48 and SLAMF7 was very slight, and the increase of MICA/B was moderate. Similar results were observed in SUP-M2 cells (**Figure 4.7B**), but the increases in CD48, MICA/B, and SLAMF7 were more impressive than the changes observed in Karpas 299 cells. Thus, the repression of ligands for NK activating receptors in ALK+ ALCL could be also through DNA methylation of the promoters of these genes.

## Figure 4.7

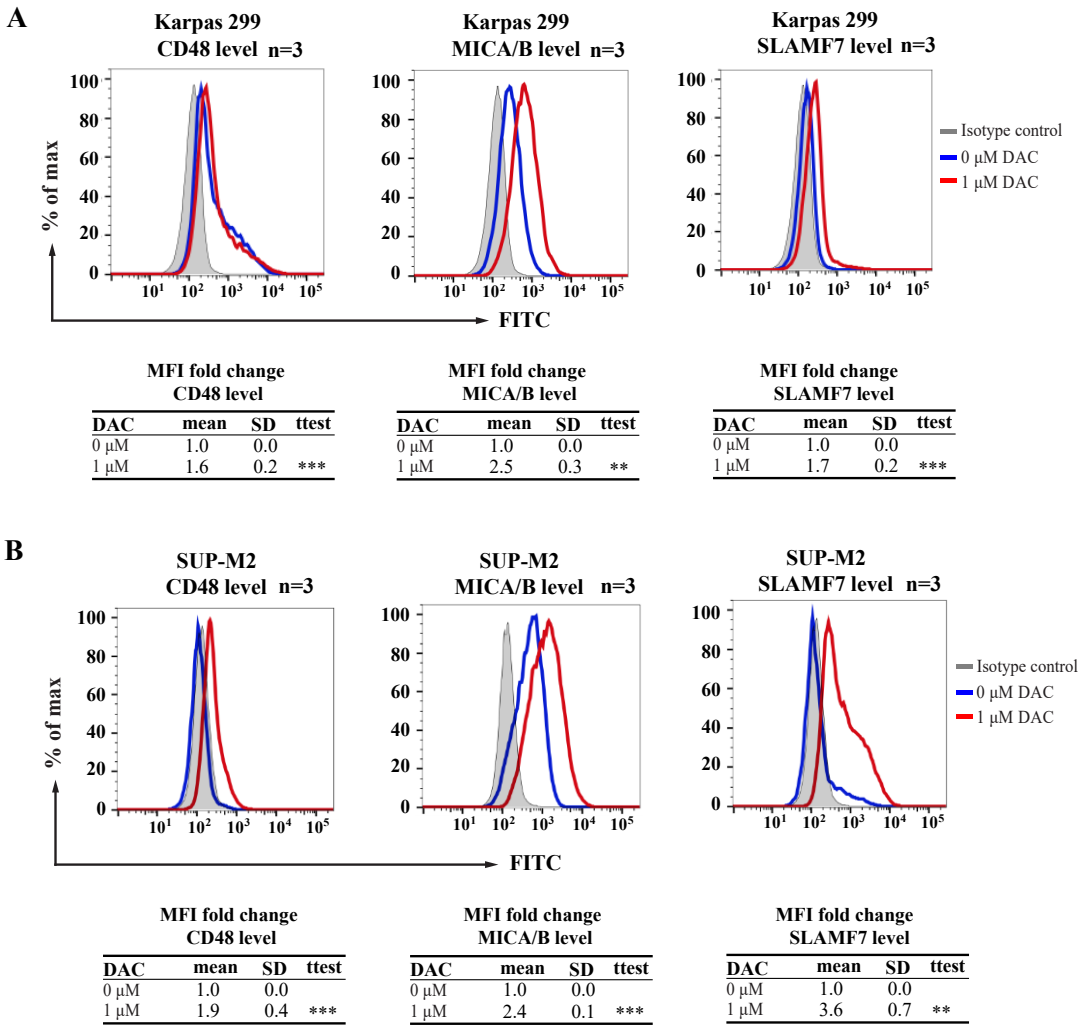


**Figure 4.7 - Inhibition of DNA methylation resulted in up-regulation of CD48, MICA/B and SLAMF7**

**A-B.** Representative histograms and summary tables showing the levels and fold changes of CD48, MICA/B, and SLAMF7 in Karpas 299 cells (**A**) and SUP-M2 cells (**B**) after DNMT inhibitor, DAC, treatment for 96 hours at the indicated concentration. Representative histograms and summary tables represent three independent experiments. p values were obtained by performing independent two-tailed t tests comparing control and c-Jun/JunB shRNA–expressing cells. * $p<0.05$, ** $p<0.01$, *** $p<0.001$, N.S. not significant. Fold changes represent the changes in median of fluorescence intensity obtained from flow cytometry.

### 4.2.8 NPM-ALK inhibition results in increased expression of CD48, but not MICA/B or SLAMF7

NPM-ALK activates downstream signalling in ALK+ ALCL, including the expression and activation of JunB [54, 136, 225], so I further evaluated the role of NPM-ALK in the regulation of the NK ligands by treating ALK+ ALCL cells with the ALK inhibitor, Crizotinib [24, 36, 288]. After treatment with Crizotinib for 72 hours, CD48 surface expression was determined to be greatly increased in Karpas 299 cells (**Figure 4.8A**), but it was only moderately increased in Crizotinib-treated SUP-M2 cells (**Figure 4.8B**). MICA/B was slightly decreased both in Karpas 299 cells and SUP-M2 cells after Crizotinib treatment (**Figures 4.8A and B**), and the change in SUP-M2 cells was more impressive than in Karpas 299 cells. Flow cytometry plots show that SLAMF7 did not change significantly in Karpas 299 cells, but slightly decreased in SUP-M2 cells after being treated with Crizotinib. Thus, NPM-ALK signalling appears to participate in the inhibition of CD48 expression in Karpas 299 and SUP-M2 cells, but it does not appear to have much effect on the expression of SLAMF7. NPM-ALK signalling also regulates the MICA/B expression in SUP-M2 cells but not in Karpas 299 cells.

## Figure 4.8

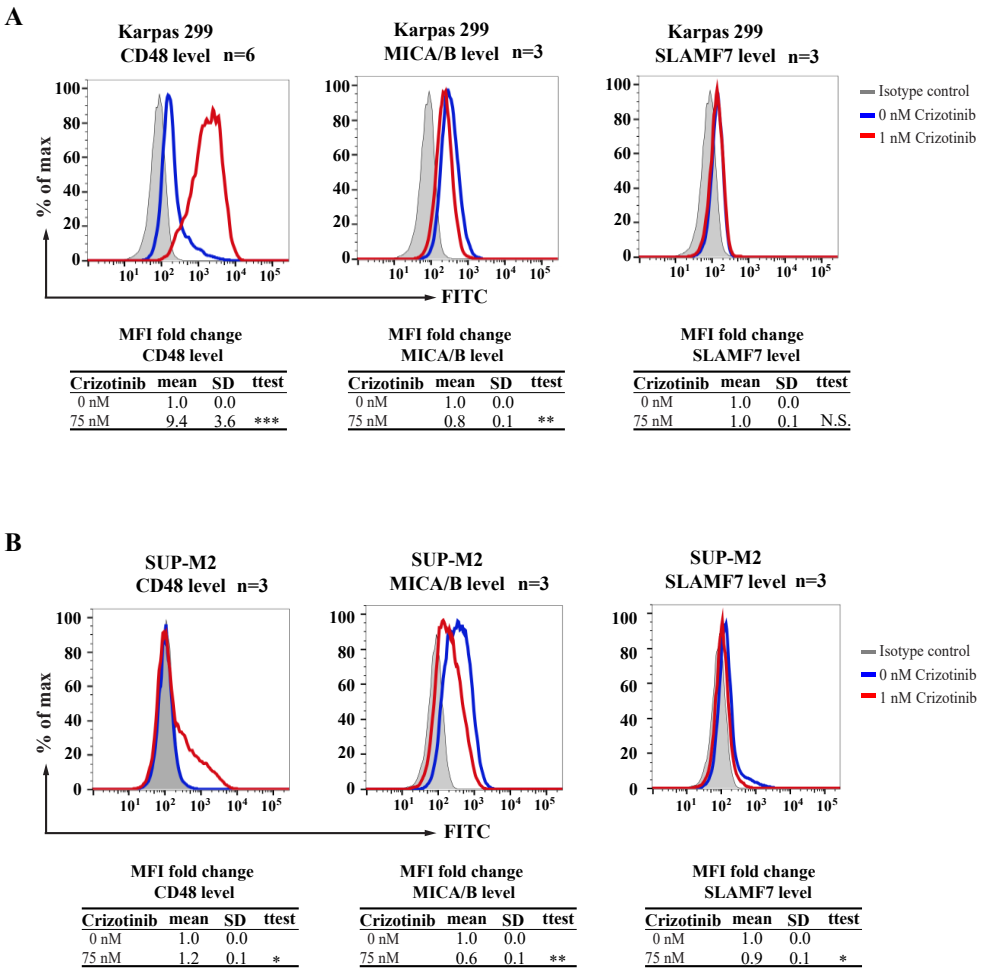


**Figure 4.8 – NPM-ALK inhibition increased the expression of CD48, but not MICA/B or SLAMF7**

**A-B.** Representative histograms and summary tables showing the levels and fold changes of CD48, MICA/B, and SLAMF7 in Karpas 299 cells (**A**) and SUP-M2 cells (**B**) after ALK inhibitor, Crizotinib, treatment for 72 hours at indicated concentration. Representative histograms and summary tables represent three or six independent experiments. p values were obtained by performing independent two-tailed t tests comparing control and c-Jun/JunB shRNA–expressing cells. * $p<0.05$, ** $p<0.01$, *** $p<0.001$, N.S. not significant. Fold changes represent the changes in median of fluorescence intensity obtained from flow cytometry.

### 4.2.9 JunB knock-down does not result in significant changes of DNMT-1, HDAC1/2/3 in Karpas 299 and SUP-M2 cells

I further checked whether JunB knock-down resulted in the decreased levels of DNMT-1 and HDAC1/2/3, since inhibition of DNMT-1 and HDAC1/2/3 results in increased levels of CD48, MICA/B and SLAMF7. Only DNMT-1 was down-regulated at the mRNA level in SUP-M2 cells (**Figure 4.9A**). Then, I further checked DNMT-1 and HDAC1/2/3 protein levels in JunB knock-down cells. As shown in **Figures 4.9B and C,** DNMT-1 was modestly decreased in JunB shRNA-expressing Karpas 299 and SUP-M2 cells; HDAC1/2/3 levels were similar in Karpas 299 and SUP-M2 cells expressing JunB shRNAs or control shRNA cells. Thus, JunB knock-down resulted in slight changes in expression of DNMT-1, but no significant changes of HDAC1/2/3 in Karpas 299 and SUP-M2 cells.

**Figure 4.9**

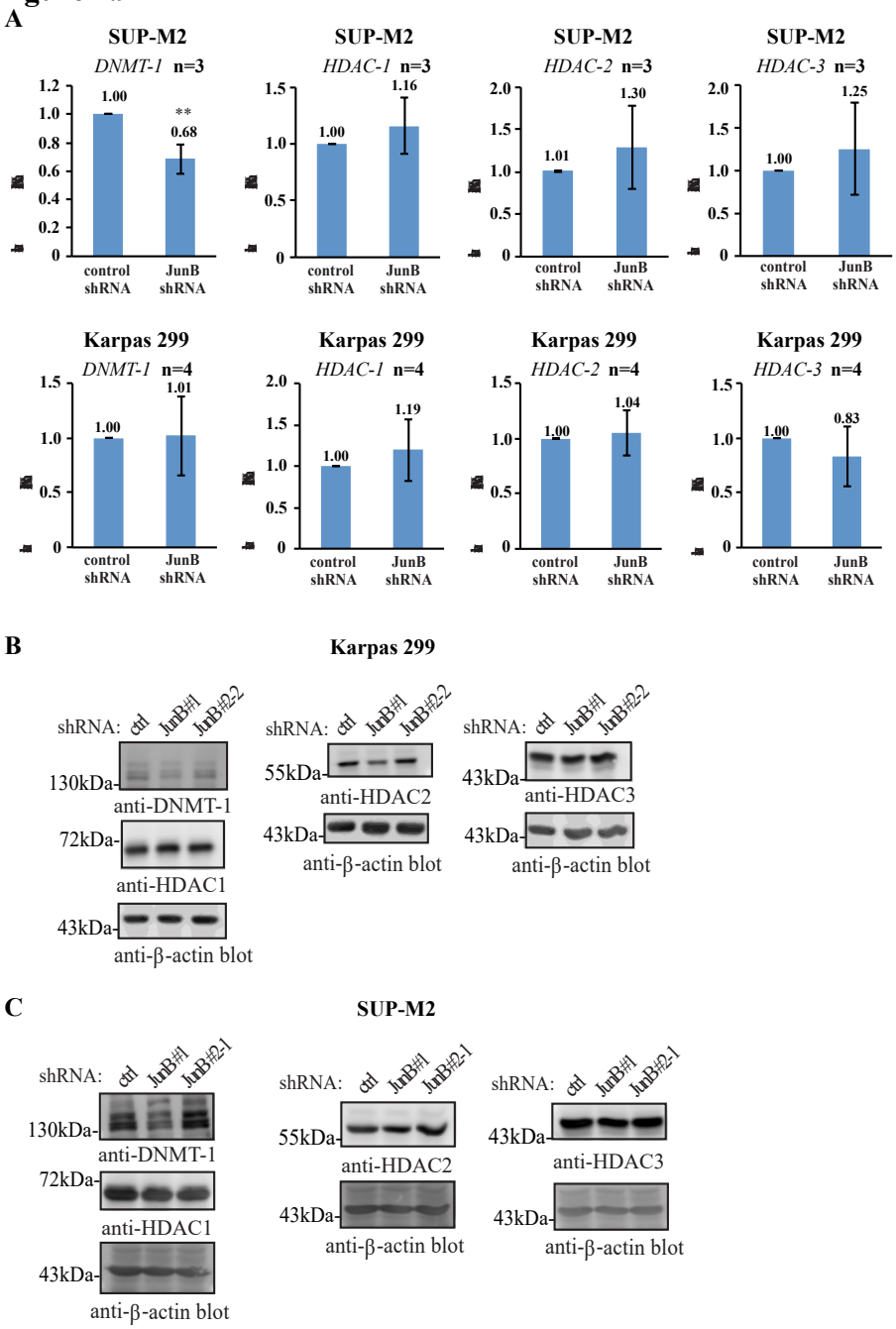


**Figure 4.9 - JunB knock-down results in slight changes of DNMT-1, and no significant changes of HDAC1/2/3 in Karpas 299 and SUP-M2 cells**

**A.** qRT-PCR examining the levels of indicated genes in JunB and control shRNA-expressing SUP-M2 and Karpas 299 cells. The results represent the average and standard deviation of three/four independent experiments. p values represent independent, two-tailed t tests.* $p<0.05$, ** $p<0.01$, *** $p<0.001$. **B-C.** Western blots showing the expression of indicated proteins in JunB shRNA-expressing Karpas 299 cells (**B**) and SUP-M2 cells (**C**) expressing cells. Molecular mass markers (in kDa) are indicated to the left of western blots. The western blots were done on more than three sets of samples.

### 4.2.10 Karpas 299 cells with reduced JunB expression, but not SUP-M2 cells, are more sensitive to NK-92 cell-mediated killing

CD48 is a ligand for the activating receptor, 2B4 (CD244) that is expressed on NK cells and serves as signal for NK-mediated killing [274, 289, 290]. Our results suggest that signalling events mediated by NPM-ALK (**Figure 4.8**) and JunB (**Figure 4.5C**) in ALK+ ALCL cell lines reduce CD48 expression, and that this reduced expression may partly be due to epigenetic silencing (**Figures 4.6** and **4.7**). Elias and colleagues reported similar observations in acute myeloid leukemia (AML) where the oncogenic fusions proteins, PML-RARA and AML1-ETO, repressed CD48 via epigenetic mechanisms [282]. Moreover, this group showed that NK cells were better able to kill AML cells when these oncogenic fusion proteins were inhibited and this killing was CD48 dependent [282]. Therefore, I examined whether the increased expression of CD48 observed in our JunB knock-down cell lines, made these cells more susceptible to NK-mediated killing. I used NK cell lines NK-92 [291], NKL [292] and YTS [293] as killers to incubate with Karpas 299 cells expressing either JunB or control shRNA, and then measured the cell lysis of the target cells. I found that JunB knock-down Karpas 299 cells were more sensitive to NK-92 cell-mediated killing than control shRNA-expressing cells (**Figure 4.10A**). Neither NKL nor YTS could kill the Karpas 299 cells expressing JunB shRNA or control shRNA (**Figures 4.9B and C**); I included the 221 cell lines as a positive control for the killing assay [294]. Importantly, the JunB knock-down cells Karpas 299 cells were not intrinsically more sensitive to apoptosis. Treatment of Karpas 299 cells with the apoptosis-inducing drugs, STS (staurosporine) or Doxo (doxorubicin), demonstrated that the JunB knock-down cells were actually less sensitive to killing by these drugs than cells

expressing control shRNA (**Figures 4.10E** and **F**). Among the two drugs, doxorubicin is a standard agent used in combination chemotherapies used to treat ALK+ ALCL in the clinic [295]. To further examine whether this increased killing of JunB shRNA-expressing cells by NK-92 cells is cell line specific, I performed killing assays on SUP-M2 cells expressing JunB shRNA. However, I did not observe a similar phenotype in SUP-M2 cells as in Karpas 299 cells. Instead, the JunB shRNA-expressing SUP-M2 cells were less susceptible to NK-92 cells mediated killing (**Figure 4.10D**). Thus, while stable JunB knock-down does not appear to increase the sensitivity of cells to chemotherapeutic drugs, it does result in them being more sensitive to NK-92 cell-mediated killing.

**Figure 4.10**

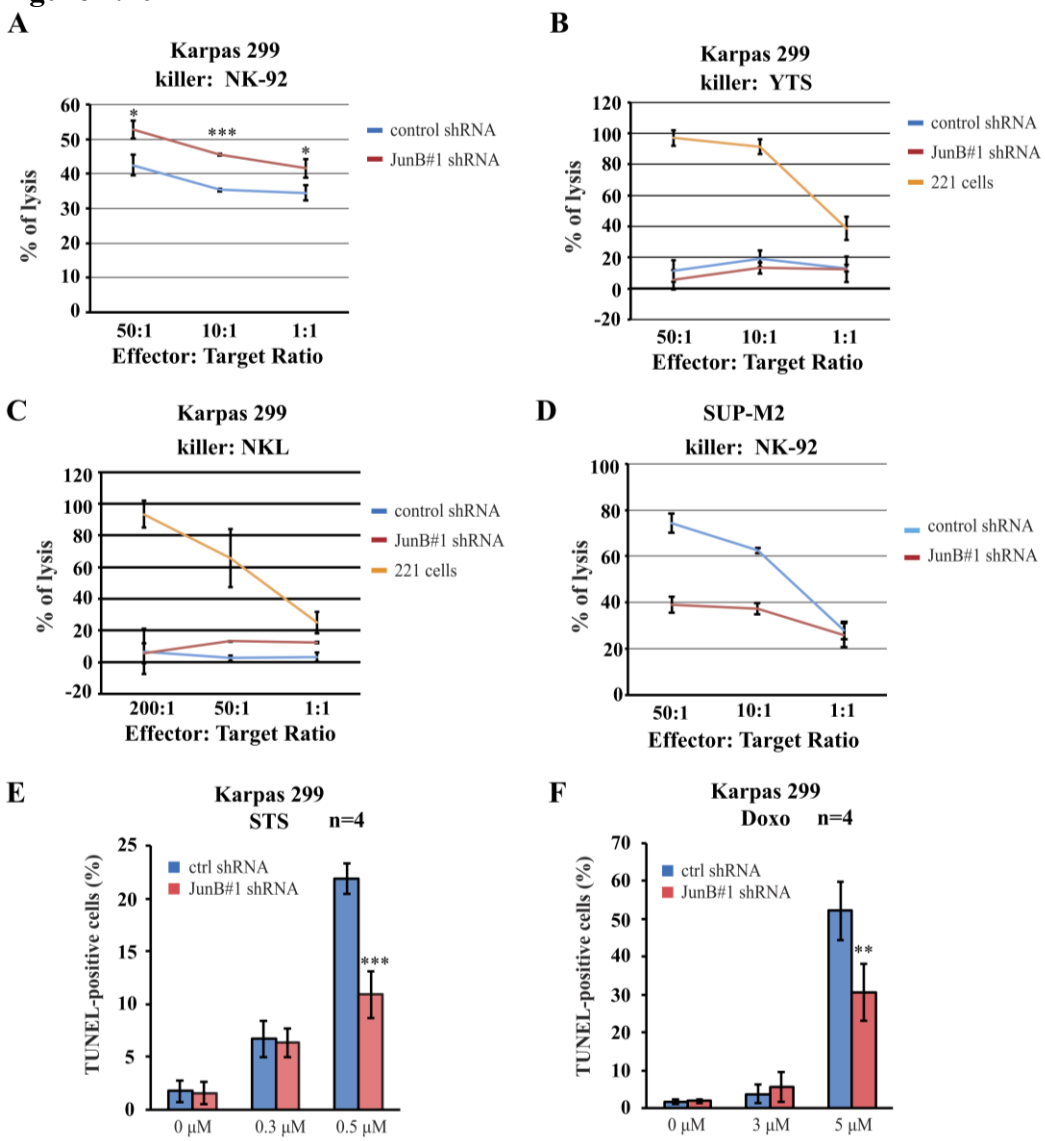


**Figure 4.10 - Karpas 299 cells with reduced JunB expression are more sensitive to NK-92 cell-mediated killing**

**A.** Graph showing a representative killing assay out of four, examining the percentage of cells killed by NK-92 cells at 50:1, 10:1, and 1:1 effector to target ratios. **B-C**. Graph showing a representative killing assay out of three, examining the percentage of cells killed by YTS (**B**) or NKL (**C**) cells at different effector to target ratios. **D.** Graph showing a representative killing assay out of three, examining the percentage of cells killed by NK-92 cells at 50:1, 10:1, and 1:1 effector to target ratios. The graphs represent the average and standard deviation from triplicates from one experiment. **E-F.** Bar graphs showing the percentage TUNEL-positive (apoptotic) cells after STS (**D**) and Doxo (**E**) treatment for 6 hours and 12 hours respectively. The results represent the mean and standard deviation of four independent experiments. p values were obtained by performing independent two-tailed t tests comparing control and JunB shRNA–expressing cells. * $p<0.05$, ** $p<0.01$, *** $p<0.001$, N.S. not significant.

### 4.2.11 The increased killing in JunB shRNA-expressing Karpas 299 cells is inhibited by blocking MICA/B, but not CD48

To examine what ligand-receptor interaction is mediating the killing of Karpas 299 cells expressing JunB shRNA, I first examined the CD48-2B4 interaction as CD48 expression was increased the greatest in JunB knock-down Karpas 299 cells (**Figure 4.5**). I found that CD48 and 2B4 were both expressed in JunB shRNA-expressing Karpas 299 cells and NK-92 cells (**Figure 4.11A**), so adding anti-CD48 or anti-2B4 antibodies into the killing assay could trigger antibody-dependent cell-mediated cytotoxicity (ADCC) [296], which could interfere with our examination. To circumvent this issue, CD48 was expressed on Karpas 299 cells with lentiviral particles containing either a CD48 cDNA or empty virus. Flow cytometry plots indicate that CD48 surface expression in CD48-overexpressing cells was comparable to, albeit a bit lower, than in JunB knock-down cells (**Figure 4.11B**). Killing assays showed no significant increase in NK-92 mediated killing when CD48 was over-expressed in Karpas 299 cells (**Figure 4.11C**), arguing that the CD48-2B4 interaction was not sufficient to induce the increased killing that is associated with JunB knock-down (see **Figure 4.10A**). I then further examined whether the interaction of MICA/B and NKG2D was important for the killing by adding anti-NKG2D antibody into the killing system. Decreased killing of JunB shRNA-expressing cells was observed with the addition of anti-NKG2D antibodies compared to the addition of isotype control antibodies (**Figure 4.11D**). The results demonstrated that the increased killing of JunB knock-down cells was inhibited when MICA/B and NKG2D interaction was blocked.

Taken together, JunB knock-down Karpas 299 cells were killed by NK-92 cells more easily, and the increased killing was possibly through MICA/B NKG2D interaction.

**Figure 4.11**

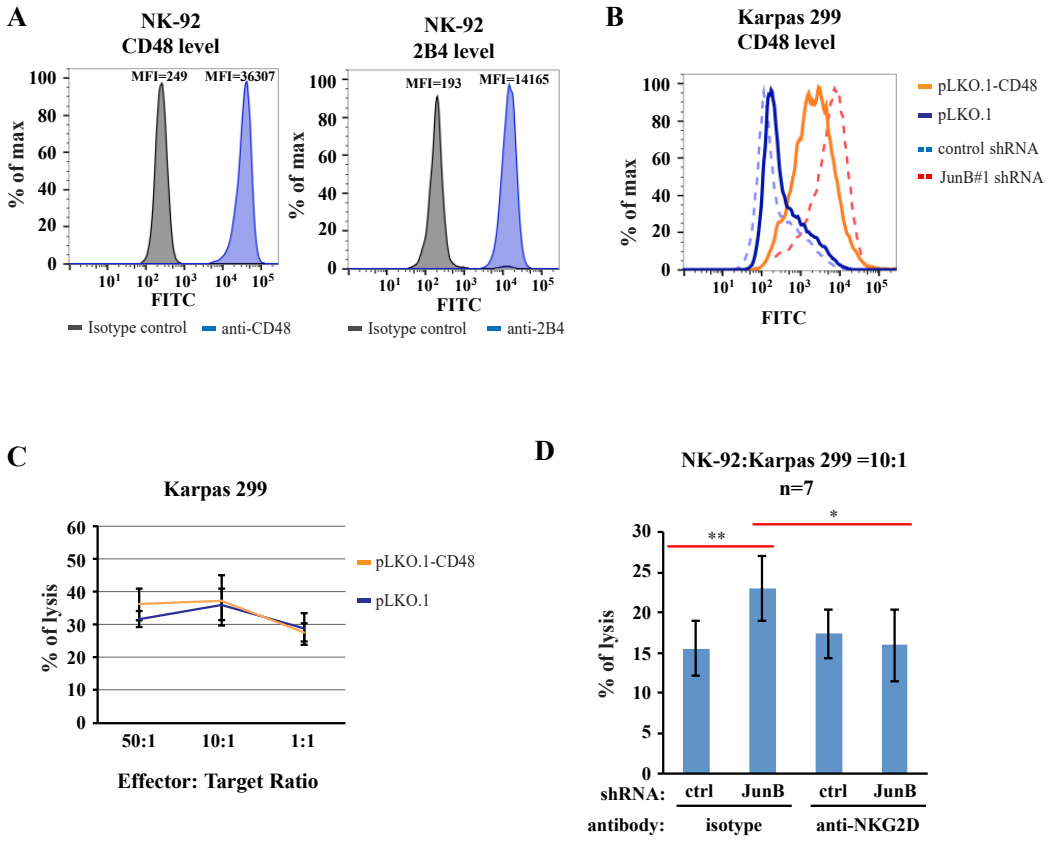


**Figure 4.11 - The increased killing of JunB shRNA-expressing Karpas 299 cells by NK-92 cells was blocked when anti-NKG2D antibodies were added**

**A.** Flow cytometry histograms showing CD48 and 2B4 levels on the indicated cells. **B.** Histograms showing the expression level of CD48 in CD48-overexpressing or empty virus-infected Karpas 299 cells, as well as JunB#1 shRNA or control shRNA-expressing Karpas 299 cells. **C.** Graph showing a representative killing assay out of four, examining killing of CD48-overexpressing or empty virus-infected Karpas 299 cells by NK-92 cells at 50:1, 10:1, and 1:1 effector and target ratios. The graph represents the average and standard deviation of triplicate measurements from one experiment. **D.** Bar graph showing the percentage of killing by NK-92 with isotype control antibodies or anti-NKG2D antibodies in the killing system. p values represent ANOVA test with TUKEY *post-hoc* test. * $p<0.05$, ** $p<0.01$, *** $p<0.001$. MFI is the median of fluorescence.

### 4.2.12 The increased killing of JunB shRNA-expressing Karpas 299 cells was not observed with primary NK cells.

I also examined whether primary NK cells would kill Karpas 299 cells expressing JunB shRNA better than control shRNA-expressing cells, or Karpas 299 cells over-expressing CD48 expression better than control cells. Primary NK cells were separated from a healthy donor and used in killing assays. However, I did not observe a consistent trend in the three independent experiments (**Figure 4.11A**). I also checked the expression of NK cell receptors on the primary NK cells. 2B4, CD48, and NKG2D were all present in the primary NK cells. (**Figure 4.11B**). The levels of 2B4 and NKG2D on primary NK cells were comparable to those on the NK-92 cells, but much higher than their levels on Karpas 299 cells expressing JunB shRNA. Thus, it is unlikely the different killing observed with NK-92 cells and primary NK cells is due to the lack of the activating receptors on the surface of the primary NK cells. Therefore, I did not see any evidence of increased killing of JunB knock-down cells with the primary NK cells, nor did I observe any consistent increase in killing in the CD48 over-expressing cells.

**Figure 4.12**

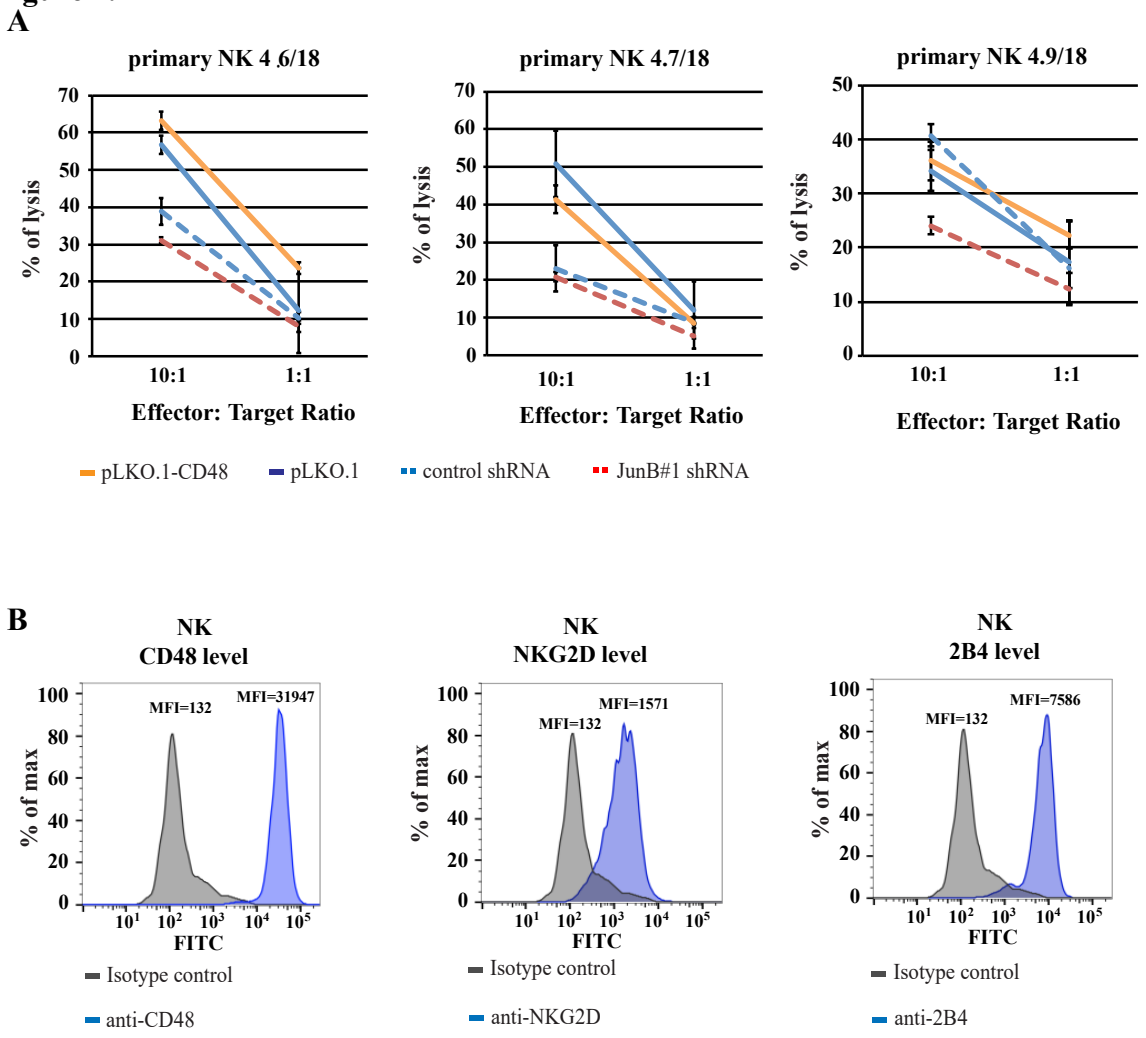


**Figure 4.12 - The increased killing of JunB shRNA-expressing Karpas 299 cells was not observed with the primary NK cells**

**A**. Graphs showing the killing assays, examining the percentage of Karpas 299 cells killed by primary NK cells at 10:1 and 1:1 effector and target ratios. 4.6/18, 4.7/18, 4.9/18 are the dates of experiments. Error bars are the standard deviation of the triplicate readings from one independent experiment. **B.** Flow cytometry histograms showing the CD48, NKG2D and 2B4 levels on indicated primary human NK cells used in **A**. MFI is the median of fluorescence.

## 4.3 Discussion

In Chapter 4, I performed microarray experiments in order to gain a comprehensive understanding of the function of the JunB transcription factor in the pathobiology of ALK+ ALCL. Of the more than 600 genes whose transcription was altered in JunB shRNA–expressing cells, the up-regulation of ligands associated with NK cell-mediated killing caught my attention (**Figure 4.3C**), in particular CD48 and MICA/B (**Figures 4.3C** and **4.5**).

I further demonstrated that signals through NPM-ALK are critical for the down-regulation of some of these genes (**Figure 4.8**) and that this repression may be partially mediated by epigenetic silencing (**Figures 4.6** and **4.7**). Moreover, we show that while JunB shRNA-expressing Karpas 299 cells were less sensitive to apoptosis-inducing drugs (**Figures 4.10E and F**), these cells were more sensitive to NK-92 cell-mediated killing (**Figure 4.10A**) and this killing was blocked by antibodies against NKG2D on NK-92 cells (**Figure 4.11D**). However, the increased killing of JunB knock-down cells was not observed in SUP-M2 cells when NK-92 cells were used as killers (**Figure 4.9D**). The increased killing of JunB shRNA-expressing Karpas 299 cells was not observed when the primary NK cells were used as killers (**Figure 4.12A**). Taken together, this report suggests that JunB may contribute to the down-regulation of ligands for some NK activation receptors possibly through epigenetic mechanisms. Moreover, my data suggest that JunB may play a role in immune evasion in ALK+ ALCL, but a more thorough investigation needs to be done.

Our microarray results identified many dysregulated genes in the JunB knock-down cells, and this included genes that have been previously identified as JunB targets.

These include *GzB* [270] and *Annexin A1* [297], which were identified by quantitative proteomics to be either down- or up-regulated respectively, in Karpas 299 cells transfected with JunB siRNA. These genes were found to be similarly altered in our microarray studies (**Figures 4.2A and C**). However, some previously described JunB targets were not identified in our microarray experiments. We did not see a significant change in PDGFR-β expression in JunB knock-down cells, perhaps because c-Jun and JunB both regulate PDGFR-β transcription in ALK+ ALCL [229]. *CD30* has been argued to be regulated by JunB, because electrophoretic mobility assay supershifting experiments showed that only anti-JunB antibody, was able to supershift complexes containing a probe with AP-1 site in the *CD30* promoter. Moreover, siRNA mediated JunB knock-down reduced the luciferase activity of luciferase reporter construct containing *CD30* promoter [54]. However, we have evidence from chromatin immunoprecipitation-sequencing (ChIP-seq) experiments (see Chapter 5) that c-Jun can also bind to an AP-1 site in the *CD30* promoter which might explain why we found that JunB knock-down was not sufficient to reduce CD30 expression. The AP-1 site identified in Chapter 5 is different from the one described in the Watanabe, *et al* paper. Moreover, JunB and c-Jun likely regulate some transcriptional targets together in this lymphoma, which is supported by our observation that many of the genes altered in the JunB knock-down cells were similarly changed in c-Jun knock-down cells, but much less so (**Figure 4.2**).

KEGG analysis revealed many functional categories and genes in other categories like “cytokine-cytokine interaction”, “p53 signalling pathway” and “pathways in cancer” can also play important roles in the biology of ALK+ALCL. For example, CXCL12,

suggested to be up-regulated in ALK+ ALCL through JunB based on the microarray, could promote the formation of immunosuppression environment in lymphomas [298, 299]. ITK was down-regulated in JunB shRNA-expressing Karpas 299 cells based on microarray and it has been indicated to be expressed in peripheral T cell lymphomas [300] and the inhibition ITK could reduce the viability and migration of these tumour cell lines [301]. Wnt family member 7B (WNT-7B) which is also down-regulated in JunB knock-down Karpas 299 cells based on microarray, is a positive regulator of Wnt-β-catenin pathway, and inhibition of WNT-7B by micro-RNA could repress the development of oral squamous cell carcinoma and glioblastoma [302, 303]. Future studies looking into these genes would help us further understand the role of JunB in ALK+ ALCL. Here in Chapter 4, I focused on the genes in the category of "natural killer cell mediated cytotoxicity", because these genes exhibited some of the greatest fold-change and this category was the most statistically significant. This group included the up-regulation of receptors usually expressed on NK cells (**Figure 4.3D**), signalling molecules used by these receptors (**Figure 4.3E**), as well as the ligands recognized by NK cell receptors (**Figure 4.3C**). Among them, CD48 and MICA/B were up-regulated in both Karpas 299 and SUP-M2 cells when JunB was knocked down, although the change of MICA/B is not as impressive as CD48 (**Figures 4.4 and 4.5**).

For the genes that were verified to change at the mRNA level by qRT-PCR, not all of them are changed at the protein level or their change was very subtle compared to what was observed at mRNA level. For example, surface levels of ULBP3 and CLEC2B were not changed when JunB was knocked down, even though they were verified to change at mRNA level by qRT-PCR. SLAMF7 was only up-regulated with a small tail at

the protein level in JunB knocked down cells, although it was dramatically increased at the mRNA level. The difference could be due to that the basal level of SLAMF7 was low in Karpas 299 cells (based on Cancer Cell Line Encyclopedia CCLE data base), thus a slight increase of SLAMF7 in JunB knock-down (a small tail in the histograms in **Figures 4.5C and D**) may result in a large fold-change in microarray and qRT-PCR experiments (**Figures 4.3C and 4.4**). Another possible explanation could be due to the post-translational mechanisms: SLAMF7 may be secreted out of the cells or trapped within the cytoplasm instead of being expressed on the cell surface.

The down-regulation of CD48 and MICA/B in tumour cells has been suggested to be through epigenetic mechanisms, specifically through DNA methylation and histone deacetylation [282, 304, 305]. I demonstrated that DNMTs and HDACs participate in the repression of CD48 and MICA/B in ALK+ ALCL cell lines as well (**Figures 4.6 and 4.7**), but the changes after DNMT and HDAC inhibition was not same as what observed in JunB knock-downs. In the DNMT and HDAC inhibition experiments, I found the overall changes of the ligands in both cells lines with DAC were less profound compared to those after HDAC inhibition. One possible explanation is that the two processes are related: the histone acetylation is necessary for the DNA to be transcribed [306, 307]. That is HDAC inhibition (inhibition of deacetylation) is necessary for the expression to be expressed, so DAC inhibition (inhibition of methylation) alone may not be sufficient to induce the expression of the genes if the histone is still deacetylated. To address the question, it would be necessary to test whether the promoters of the genes are methylated or/and actelycated in the future. Specifically, the methylation status of the promoters could be measured by bisulfite converted DNA amplification [308, 309]; the acetylation

status could be evaluated by ChIP assay with anti-histone acetylation markers antibodies[310, 311].

ChIP-seq data (performed in Chapter 5) showed that DNMT-1, HDAC1 and HDAC2 were bound by c-Jun and JunB at the promoter region (-/+ 1 kb from TSS), suggesting JunB and c-Jun may together regulate the expression of DNMT-1 and HDAC1/2 and thus to down-regulate the NK ligands. The ChIP-seq data related to the DNMTs and HDACs is listed in **Appendix 4**. However, JunB knock-down alone did not result in the changes HDAC 1/2/3 in Karpas 299 and SUP-M2 cells at the protein level, although it resulted in modest change in DNMT-1 (**Figure 4.9**). Thus the up-regulation of CD48, MICA/B and SLAMF7 in JunB knock-down was not likely due to the changed expression HDAC 1/2/3, but may be partially due to the decreased expression of DNMT-1. Other mechanism may also involve in the up-regulation of these ligands in JunB knock-down ALK+ ALCL cells, as DNMT or HDAC inhibition did not mimic the up-regulation of CD48, MICA/B and SLAMF7 in JunB knock-down cells. It is possible other HDACs also participate in the repression of CD48, MICA/B and SLAMF7, as the HDAC inhibitor, MGCD0103, that I used inhibited HDAC 1/2/3. Inhibiting other HDACs with other inhibitors or decrease the levels of other HDACs with siRNA would help address this point better.

Although CD48 was increased after Crizotinib treatment, I did not observe much change in MICA/B and SLAMF7 after NPM-ALK inhibition (**Figure 4.8**). Because NPM-ALK regulates many other signalling pathways [128, 312-314], other molecules changed after NPM-ALK inhibition could repress the up-regulation of these genes resulting from reduced JunB levels. It is also possible that the genes may not be

accessible to the transcription factors, or the essential transcription factors for the expression of genes are absent after NPM-ALK inhibition.

CD48 has been shown to be inhibited by oncogenic signalling in AML, in order to facilitate the immune-evasion of tumour cells [282]. Although CD48 was highly expressed in Karpas 299 cells expressing JunB shRNA, NK-92-mediated killing was not likely mediated through a CD48 and 2B4 interaction, because the overexpression of CD48 did not induce increased killing of Karpas 299 cells by NK-92 cells (**Figure 4.11B**). It could be the case that the killing was just not mediated by CD48-2B4 interaction. It is also possible that CD48 and 2B4 on the NK-92 cells may interact with each other, thus the function of 2B4 receptor might be "locked" by the endogenous CD48 on the same killer cells [315]. Further investigation is still needed to clearly address the question.

MICA/B belong to the family of MHC class I–related chain genes and are expressed in a variety of malignant cells and virally infected cells, and the NK cells would kill the transformed or infected cells [304, 316]. High surface MICA/B level has been associated with better survival of patient in various tumours [317-319]; and low levels of MICA/B was associated with worse overall survival [320], because of the immune evasion of the transformed or infected cells. I demonstrated that inhibition of MICA/B could be a potential immune evasion strategy in ALK+ ALCL, as the increased killing in JunB shRNA-expressing Karpas 299 cells was inhibited when MICA/B and NKG2D interaction was blocked (**Figure 4.11D**). Although the increase in MICA/B expression was not as dramatic as for CD48, these modest changes have been shown to increase killing in other studies [321], where MICA was expressed at low level and

killing could be blocked by anti-NKG2D antibody or anti-MICA antibody. To address the question of whether MICA/B is sufficient to induce killing of Karpas 299 cells, future experiments where MICA/B is over-expressed in Karpas 299 cells as what I did for CD48 and examine whether the MICA/B over-expressing cells are killed by the cell will be killer by NK-92 cells. Furthermore, I could knock-down MICA/B in JunB shRNA-expressing cells, and check whether the increased killing of JunB knock-down cells is inhibited when MICA/B is reduced. On the other hand, MICA/B could be induced by stress stimulation [322, 323], thus it is possible MICA/B are up-regulated as a response to the reduction of JunB, which could be a stress to cells.

The increased killing was not observed in JunB shRNA-expressing SUP-M2 cells (**Figure 4.10D**). Since the microarray data was only performed in Karpas 299 cells, no direct information was available for whether other ligands for the activating/inhibitory receptors changed when JunB was knocked down in SUP-M2 cells. Thus we do not have enough information on whether other ligands and receptor interaction would affect the killing of the SUP-M2 cells by NK-92 cells. It is possible that other ligands for inhibitory receptors were also changed in SUP-M2 expressing JunB shRNA, thus no increased killing was observed in SUP-M2 cells when JunB was knocked-down, even though MICA/B was increased.

For the killing assays, I chose NK-92 cells as the killer because NK-92 cells do not express inhibitory receptors KIRs (killer-cell immunoglobulin-like receptor) on the surface [291], which made the killing system easier to interpret and manage. I have tried other NK cell lines, YTS and NKL, for the killing assay, but I did not observe any killing of the Karpas 299 cells (**Figures 4.10B and C**), possibly due to the fact that they express

some inhibitory receptors on the cell surface [324, 325] or different NK cells intrinsically have different effects on cells [324].

I also tried primary NK cells for the killing assays to see if non-transformed NK cells would kill the Karpas 299 cells expressing JunB shRNA. However, I did not observe consistent results for the killing assays (**Figure 4.12A**). It would be worthwhile if primary NK cell from more donors were used for killing assays in the future [326, 327]. In the NK-92 cell line, the ligands for NK inhibitory receptors are absent thus they could kill the target cells better [291]. In primary NK cells, multiple activating or inhibitory receptors could be expressed on the cell surface and may generate different outcomes for the killing assays.

In this chapter, I showed that JunB significantly contributed to shaping the expression profile of ALK+ ALCL. The microarray experiments revealed many genes with altered expression, which participated in several cellular pathways related to tumour pathology. In particular, I found JunB could repress ligands for NK activating receptors, possibly through epigenetic mechanism, and may play a role in immune evasion of ALK+ ALCL.

# Chapter 5: Identifying JunB /c-Jun binding sites by chromatin immunoprecipitation (ChIP) sequencing

The majority of experiments were performed by Zuoqiao Wu. Parts of this Chapter were written with Dr. Ingham as part of a manuscript in preparation. The western blots for FAM129B levels in panel lysates and Crizotinib treated cells were performed by Farynna Loubich Facundo and Mary Nicoll, under my supervision.

## 5.1 Introduction

In Chapter 4, I performed microarray experiments comparing the expression profiles of JunB shRNA-expressing and control shRNA-expressing Karpas 299 cells. I identified genes that are potentially regulated by JunB, and studied whether and how they may contribute to the pathobiology of this disease. However, the microarray experiments cannot provide information about whether those genes are direct transcriptional targets of JunB, or whether JunB binds the promoters of these genes or not. Thus, the genes identified through microarray could be either direct targets of JunB or targets of other pathways that are regulated by JunB. I postulate that the latter scenario is true for many of the genes identified in the microarray experiments, because JunB commonly functions as an activator of transcription [328] and there were many genes identified to be up-regulated when JunB was knocked down. In addition, the possible redundancy between AP-1 proteins in ALK+ ALCL also makes it difficult to identify the targets of JunB by microarray in JunB single knock-down cells. Other AP-1 proteins, like c-Jun and BATF3, may also promote genes that are regulated by JunB, so the difference in expression may be too subtle to be observed when only JunB was reduced. Thus, to identify potential direct targets of JunB and c-Jun, and gain an understanding of the redundancy between JunB and c-Jun transcription factors, I wanted to perform chromatin immunoprecipitation (ChIP) sequencing that would provide me with information about where the two AP-1 transcription factors bind in the genome. By comparing the regions that JunB and c-Jun bind to, I would know what genes are associated with JunB/c-Jun intervals at putative promoters and could further study whether they are regulated transcriptionally by JunB/c-

Jun. In addition, I could investigate whether they are potential targets of JunB/c-Jun and play a role in the pathobiology of ALK+ALCL.

## 5.2 Results

### 5.2.1 Identification of JunB and c-Jun binding sites in Karpas 299 cells by ChIP-sequencing

To identify JunB and c-Jun binding sites in ALK+ ALCL, ChIP-seq was performed on exponentially growing Karpas 299 cells using JunB or c-Jun specific antibodies. As indicated in **Figure 5.1A,** cells were fixed and cross-linked, DNA was sheared into small fragments, the fragments associated with JunB/c-Jun were immunoprecipitated and then sequenced. The sequences of the immunoprecipitated fragments were mapped onto the genome; peaks were identified as the regions with enriched overlapping sequences (**Figure 5.1A**). The peaks are called intervals. Sometimes intervals overlap together, and the regions covering the overlapping intervals or the non-overlapping intervals are both called active regions. Thus, the number of active regions would be a bit smaller than the number of intervals. Specifically, we identified 40,419 intervals (40,369 active regions) for JunB and 13,725 intervals (13,083 active regions) for c-Jun **(Figure 5.1B)**. About 10% of the intervals were located +/- 500 bp from transcription start sites (TSS) which may be in promoter regions of genes, and about 50% of the intervals were located in introns. Fifty-nine percent (7,669) of the c-Jun active regions were in common with JunB **(Figure 5.1C)** illustrating the significant overlap in binding sites recognized by these transcription factors. The majority of intervals (74% for JunB and 83% for c-Jun) were located within 10 kb of known genes, and many of these intervals were found within potential promoter regions (-7.5 kb/+1.5 kb from TSS) (**Figure 5.1B**). Moreover, ~80% of the c-Jun/JunB

intervals within these putative promoter regions were also associated within 200 bp of the known CpG islands (the GC content is greater than 50%), which is an indicator of promoter region as [329, 330]. (**Figure 5.1B**). An examination of the sequence of the top 1000 c-Jun or JunB intervals with highest peak intensities revealed a consensus sequence that conforms to the well-known AP-1 binding TRE motif (**Figure 5.1F**).

An examination of genes associated with JunB/c-Jun intervals revealed that 6,070 genes were located within 10 kb of 1 or more c-Jun intervals, whereas 14,531 genes were similarly associated with JunB intervals **(Figure 5.1D)**. The majority of these genes had at least one interval within putative promoter regions (-7.5 kb/+1.5 kb from TSS), and many were also associated with CpG islands **(Figure 5.1D)**. Strikingly, 97% of genes within 10 kb of c-Jun intervals were also associated with JunB intervals; albeit these were not always the same interval(s) **(Figure. 5.1E)**. Taken together, these data demonstrate that c-Jun and JunB binding sites are prevalent in the genome of Karpas 299 cells, and that many of these binding sites are located within putative promoter regions. Moreover, our results reveal that c-Jun and JunB share a significant number of binding sites, and the majority of genes associated with c-Jun intervals are also associated with JunB intervals.

**Figure 5.1**

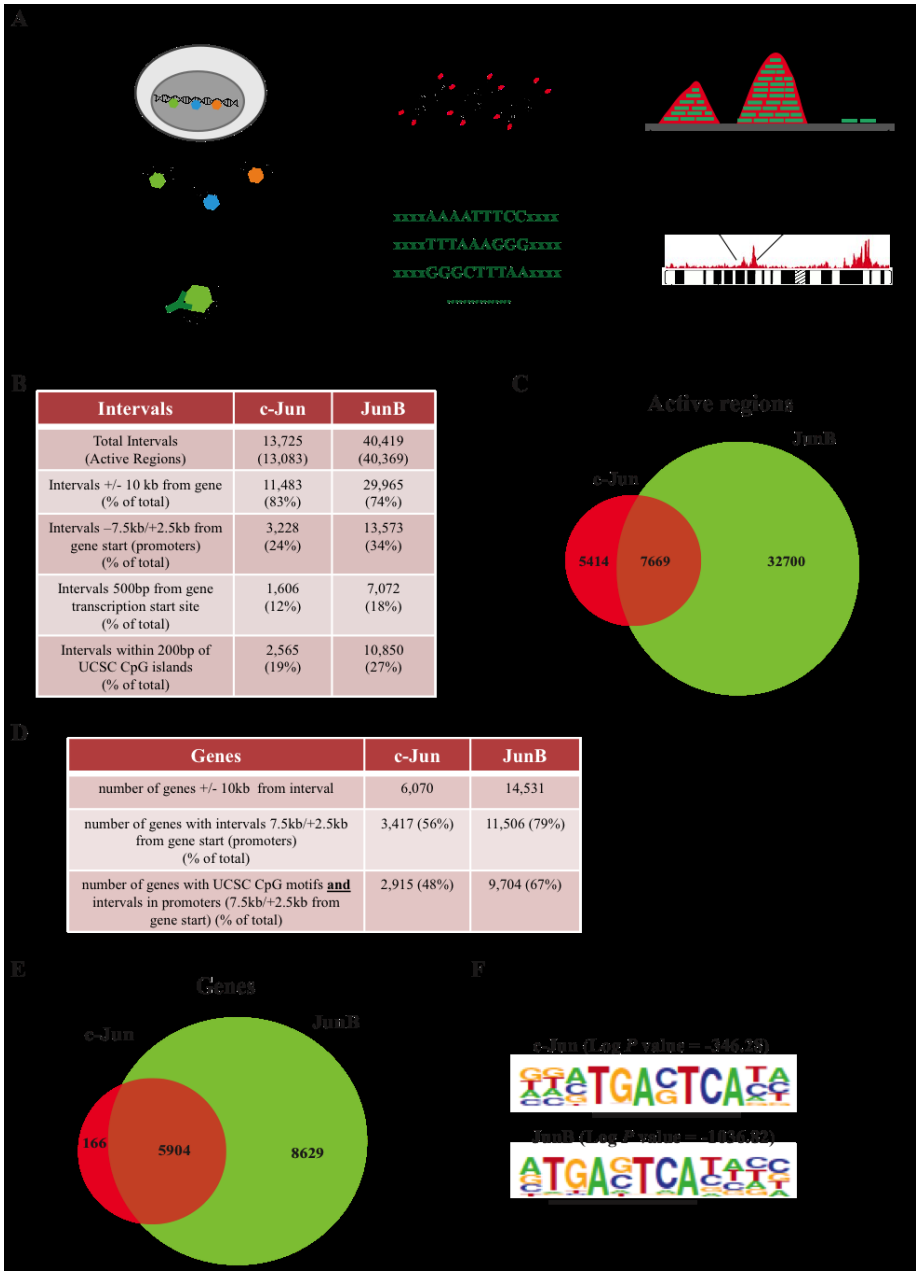


| Intervals | c-Jun | JunB |
|---|---|---|
| Total Intervals (Active Regions) | 13,725 (13,083) | 40,419 (40,369) |
| Intervals +/- 10 kb from gene (% of total) | 11,483 (83%) | 29,965 (74%) |
| Intervals –7.5kb/+2.5kb from gene start (promoters) (% of total) | 3,228 (24%) | 13,573 (34%) |
| Intervals 500bp from gene transcription start site (% of total) | 1,606 (12%) | 7,072 (18%) |
| Intervals within 200bp of UCSC CpG islands (% of total) | 2,565 (19%) | 10,850 (27%) |

| Genes | c-Jun | JunB |
|---|---|---|
| number of genes +/- 10kb from interval | 6,070 | 14,531 |
| number of genes with intervals 7.5kb/+2.5kb from gene start (promoters) (% of total) | 3,417 (56%) | 11,506 (79%) |
| number of genes with UCSC CpG motifs **and** intervals in promoters (7.5kb/+2.5kb from gene start) (% of total) | 2,915 (48%) | 9,704 (67%) |

**Figure 5.1 - Identification of JunB and c-Jun binding sites by ChIP-seq**
**A.** Schematic diagram illustrating the process of ChIP-seq. **B.** Table showing the numbers of identified intervals for JunB or c-Jun in the genome of Karpas 299 cells. **C.** Venn diagram showing the numbers of intervals associated with JunB only, c-Jun only, or both JunB and c-Jun. **D.** Table showing the number of genes associated with the indicated JunB or c-Jun intervals. **E.** Venn diagram showing the number of genes associated with JunB only, c-Jun only, or both JunB and c-Jun. **F.** Consensus AP-1 sites were enriched in the top 1000 JunB/c-Jun intervals with highest peak intensities.

### 5.2.2 Comparison and characterization of prominent JunB and c-Jun active regions

Given the prevalence of AP-1 binding sites in the genome and the important role these proteins play in many cell types, we were not surprised by the number of c-Jun and JunB binding sites identified. We therefore focused on the most prominent c-Jun and JunB active regions, as measured by peak intensity value, to gain insight into whether these sites were shared by these transcription factors. We found that slightly less than half of the top 1,000 (and ties) active regions were shared by these two transcription factors **(Figure 5.2A)**, but that this decreased to 25% when the top 100 (and ties) active regions were examined (**Figure 5.2B**). We also examined whether the prominent active regions for one transcription factor were also active regions for the other transcription factor. **Figures 5.2C and D** show that ~75% of the top 1,000 c-Jun active regions also had a JunB active region, whereas greater than 90% of the top 1,000 JunB active regions also had a c-Jun active region. This overlap was even more impressive when the top 100 active regions for each transcription factor were examined **(Figures 5.2C and D)**. Taken together, these results demonstrate that c-Jun and JunB share some prominent active regions, but many are not in common. Moreover, our findings show that the majority of prominent active regions associated with one transcription factor are also active regions for the other, especially in the case of c-Jun.

We also investigated where the most prominent c-Jun/JunB active regions were located in relation to TSS. Of the top 1,000 c-Jun active regions, greater than 32% were within 1 kb of a TSS of 1 or more genes, whereas only 22% of the top 1,000 JunB active regions were +/- 1 kb from a TSS **(Figure 5.2E)**. This difference was even more pronounced when the top 100 active regions were examined. We found that 62% of the

top 100 c-Jun active regions were within 1 kb of a TSS **(Figure 5.2F)**. In contrast, only 17% of the top 100 JunB active regions were found at that distance from a TSS **(Figure 5.2F)**. More of the prominent JunB active regions were either located within 10 kb of known genes **(Figures 5.2E and F)**, or as observed in the top 100 JunB active regions, >10 kb away from TSS **(Figure 5.2F)**. Thus, the majority of the prominent c-Jun binding sites are located within putative promoter regions, whereas the majority of the prominent JunB binding sites are distant from TSS.

**Figure 5.2**

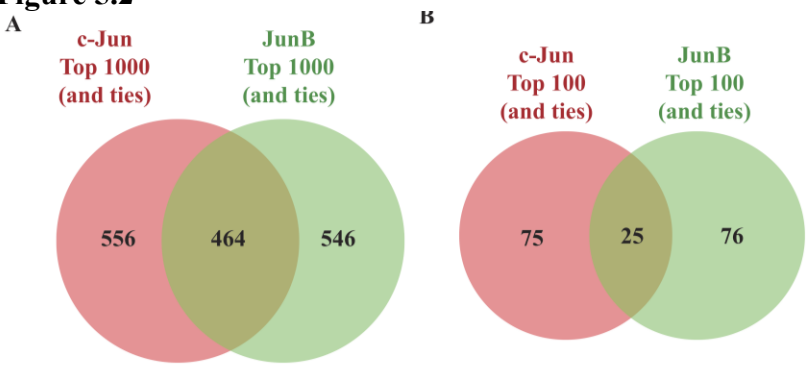


C

| | corresponding JunB active region (%) |
|---|---|
| **c-Jun Top 1000** | 761/1020 (74.6%) |
| **c-Jun Top 100** | 87/100 (87%) |

D

| | corresponding c-Jun active region (%) |
|---|---|
| **JunB Top 1000** | 938/1010 (92.8%) |
| **JunB Top 100** | 101/101 (100%) |

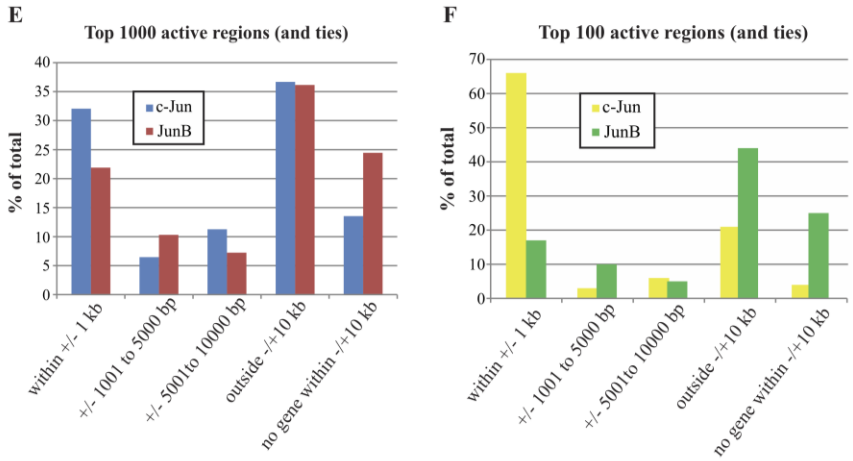


**Figure 5.2 - Comparison and characterization of prominent JunB and c-Jun active regions**

**A-B.** Venn diagrams showing the comparison of top 1000 **(A)** and top 100 **(B)** active regions of JunB and c-Jun with highest peak intensities**. C.** Table showing the number and percentage of top1000/100 c-Jun active regions that are also JunB active regions. **D.** Table showing the number and percentage of top1000/100 JunB active regions that are also c-Jun active regions. **E-F.** Bar graphs showing the locations of the JunB and c-Jun active regions with top 1000 (**E**) or top 100 (**F**) peak intensities in relation to transcription start site.

### 5.2.3 Active regions are found near previously described JunB/c-Jun targets in ALK+ ALCL

We next turned our focus to the examination of specific genes associated with c-Jun/JunB active regions. We identified intervals associated with several genes previously suggested to be direct transcriptional targets of AP-1 family proteins in ALK+ ALCL **(Table 5.1)**. In some cases, such as *Granzyme B* (*GzB*), the active region identified overlapped with AP-1 sites previously characterized by Electrophoretic mobility shift assay (EMSA) and luciferase reporter studies (**Table 5.1 and Figure 5.3A**) [231]. In contrast, we identified no interval encompassing the AP-1 site in the *TNFRSF8* (*CD30*) microsatellite sequence previous argued by Watanabe and colleagues to bind JunB and promote *CD30* transcription **(Table 5.1 and Figure 5.3B)** [54]. However, we did identify multiple c-Jun and JunB intervals associated with the gene. In particular, a prominent JunB interval ~6000 bp upstream from the TSS of *CD30* contained a consensus TRE motif and it was partially overlapped with a c-Jun interval (**Table 5.1 and Figure 5.3B**). I also identified a JunB interval in the *PDGFR-β* promoter that was previously identified as a c-Jun and JunB binding site **(Table 5.1 and Figure 5.3C)** [229]. We also explored whether c-Jun and JunB binding sites identified in other CD30-positive lymphomas were also present in Karpas 299 cells. An enhancer region containing two AP-1 sites in the first intron of the *PD-L1* (*CD274*) has previously been shown to promote PD-L1 expression in classical Hodgkin lymphoma [331], and we found a JunB, but not c-Jun, interval corresponding to this site **(Table 5.1 and Figure 5.3D** indicated by the middle red box**)**. Another two intervals associated with JunB and c-Jun were also identified in the promoter and third intron, and consensus TRE site were present in the two intervals **(Table 5.1 and Figure**

**5.3D** indicated by the left and right red boxes**)**. Thus, our results confirm that c-Jun and JunB binding sites are present in the promoters of the genes that c-Jun and JunB have been argued to directly regulate in CD30-positive lymphomas.

**Table 5.1 – AP-1 sites identified in previous described JunB/c-Jun targets genes**

Table summarizes the AP-1 sites identified from the ChIP-seq and from literature for the target genes.

| Genes | ChIP-seq | | | Literature | |
|---|---|---|---|---|---|
| | **bound by** | **intensity** | **location** | **bound by** | **assays** |
| **GzB** | JunB/ c-Jun | 52/24 | promoter | JunB | EMSA/luciferase assay [231] |
| **CD30** | JunB/ c-Jun | 34/102 | promoter | JunB | EMSA/luciferase assay [54] |
| **PDGFR-β** | JunB | 34 | intron | JunB/ c-Jun | ChIP/EMSA/lucif-erase assay [229] |
| **PD-L1** | JunB | 20/31/42 | promoter/promote r/intron | JunB/ c-Jun | ChIP/luciferase assay (in cHL/enhancer) [331] |

**Figure 5.3**

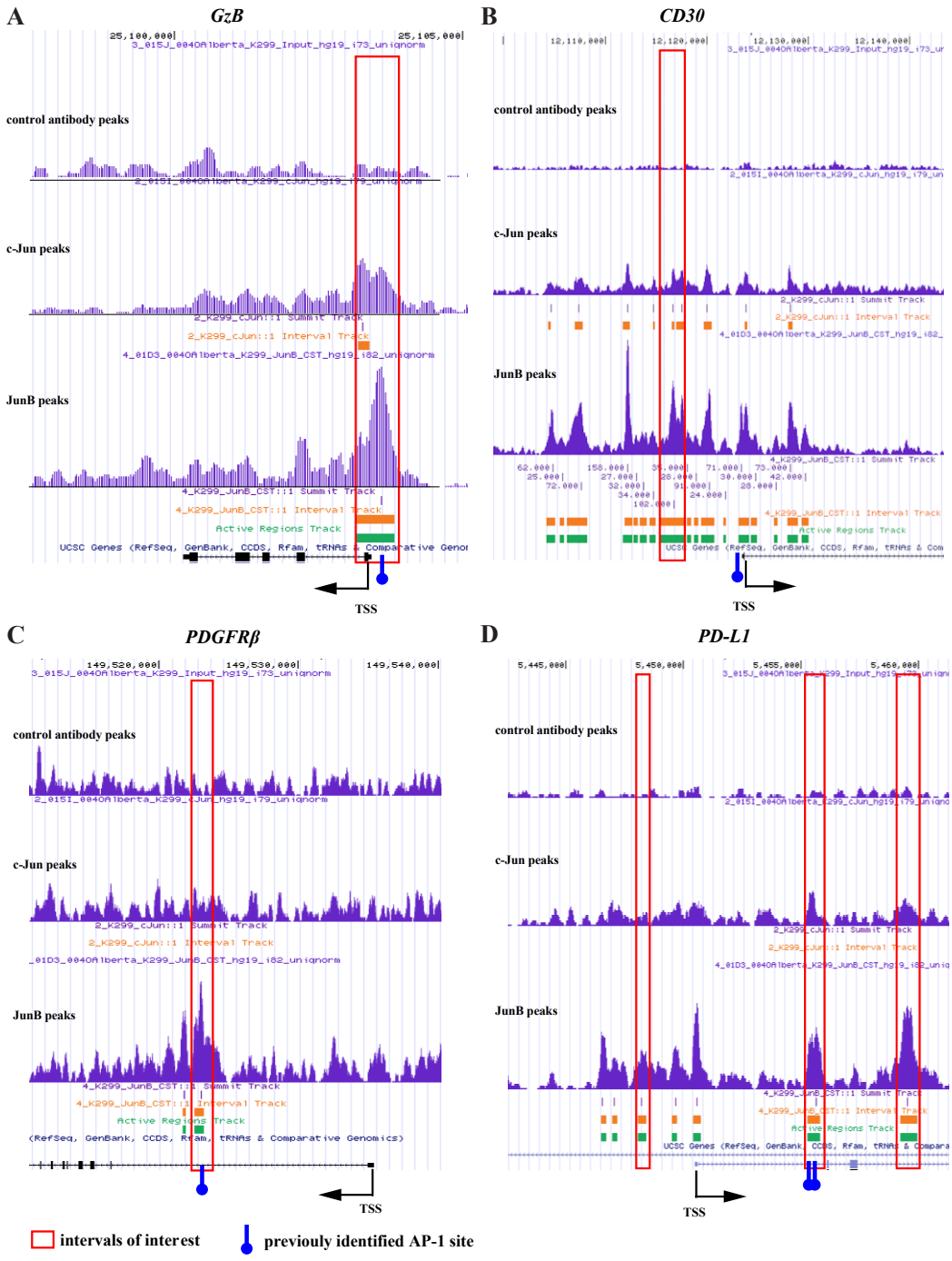


**Figure 5.3 – Active regions associated with previously previous identified targets of JunB and/or c-Jun**

**A-D.** Screen shots showing the active regions, intervals, and peak sizes for the targets. The screen shots are from UCSC gene browser with our ChIP-seq tracks. The red boxes indicate the mentioned intervals in the **Section 5.2.3** and **Table 5.1**.The numbers at the top of each panel indicate the location and scale of the genes in the chromosome.

### 5.2.4 Comparison of genes associated with active regions with microarray results

To examine how many genes identified in the microarray experiments performed in Chapter 2 were associated with JunB or c-Jun intervals, I compared the list of genes with a cut-off of 1.5 from the microarray experiments to the list of genes with JunB or c-Jun intervals from ChIP-seq. Among the 1,855 genes identified by microarray, 745 (~40%) were associated with JunB intervals within +/- 10 kb from the gene, 713 (~38%) were associated with both JunB and c-Jun intervals within +/- 10 kb from the gene, and 6 (~0.3%) were associated with c-Jun intervals within +/- 10 kb from the gene **(Figure 5.4A)**. Thus, about 80% of the genes identified in the microarray experiments with a fold change greater than 1.5 are associated with either JunB or c-Jun intervals within +/- 10 kb. Then I looked at the up-regulated and down-regulated genes from the microarray experiments separately and examined whether those genes associated with by JunB or c-Jun intervals were within putative promoter regions, which I considered to be +/- 1 kb from the TSS. Of the 588 down-regulated genes, 235 (~40%) were associated with JunB intervals, 67 (~11%) were associated with both JunB and c-Jun intervals, and 3 were associated with c-Jun intervals.

Amongst the 1,267 up-regulated genes that are potential indirect targets of JunB, 477 (~37%) genes were associated with JunB intervals, 181 (~14%) genes were associated with JunB and c-Jun intervals, and 7 were associated with c-Jun intervals within +/- 1 kb from the TSS (**Figure 5.4B**). The percentage of genes associated with JunB intervals alone of c-Jun intervals alone did not change much when I focused on intervals within +/- 1 kb from the TSS compared to intervals within +/- 10 kb from the

gene. However, the genes associated with both JunB and c-Jun intervals within +/- 1 kb from the TSS were decreased to ~10-15% of the genes.

I also included some examples of the genes identified as down-regulated in the microarray array studies that were associated with JunB and/or c-Jun intervals within +/- 1 kb from the TSS in **Figure 5.4C**. Moreover, I confirmed *Transducin (beta)-like 1X-linked (TBL1X)* and *POU domain class 2-associating factor 1* (*POU2AF1)* were also down-regulated in JunB knock-down cells by qRT-PCR (**Figure 5.4D**).

**Figure 5.4**

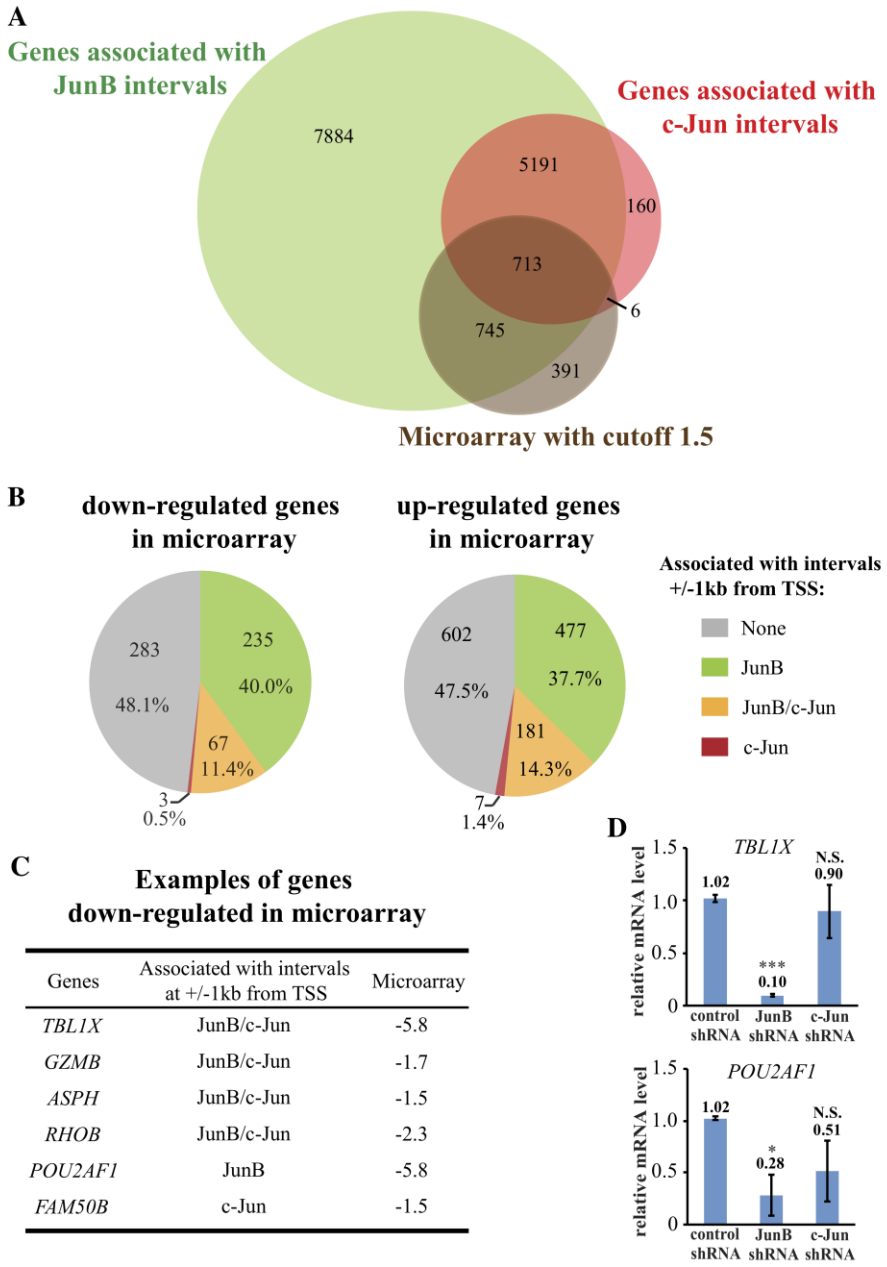


| Genes | Associated with intervals at +/-1kb from TSS | Microarray |
|---|---|---|
| *TBL1X* | JunB/c-Jun | -5.8 |
| *GZMB* | JunB/c-Jun | -1.7 |
| *ASPH* | JunB/c-Jun | -1.5 |
| *RHOB* | JunB/c-Jun | -2.3 |
| *POU2AF1* | JunB | -5.8 |
| *FAM50B* | c-Jun | -1.5 |

**Figure 5.4 – Comparing ChIP-seq results to microarray data from Chapter 2**

**A.** Venn diagram showing comparison of JunB-regulated genes genes identified in microarray experiments and genes associated with JunB or/and c-Jun intervals. **B.** Pie charts show the percentages of down-regulated genes (left) and up-regulated genes (right) associated JunB/c-Jun intervals. **C.** Selected examples from **B.** (left). **D.** qRT-PCR examining the mRNA levels of the indicated genes in JunB or c-Jun shRNA-expressing Karpas 299 cells. The results represent the average and standard deviation of three (*POU2AF1*) or four (*TBL1X*) independent experiments. p values represent ANOVA test with TUKEY *post-hoc* test comparing the JunB/c-Jun shRNA-expressing cells to control shRNA-expressing cells.* $p<0.05$, ** $p<0.01$, *** $p<0.001$.

### 5.2.5 Comparison of genes associated with active regions with genes that distinguish ALK+ ALCL from activated T cells

To study whether c-Jun or JunB intervals were associated with genes that characterize ALK+ ALCL, I compared the ChIP-seq data to published microarray data from GEO database (GSE14879) [332]. Among the genes sets they collected, I specifically compared the mRNA expression profiles of ALK+ ALCL cell lines to those of activated T cells. ALK+ ALCL cell lines possess a unique expression profile of 9,304 genes that distinguish this lymphoma from activated T cells, which I termed "characteristic" genes [333]. About 40% of these genes were associated with JunB intervals within +/- 10 kb from the gene and ~35% of these genes were associated with both JunB and c-Jun intervals within +/- 10 kb from the gene, and less than 1% of the genes were associated with c-Jun intervals within +/- 10 kb form the gene (**Figure 5.5A**). I focused on the top 100 genes with greatest change within the list of characteristic genes and examined whether c-Jun or JunB bound to the putative promoter region (+/- 1 kb from the TTS) of these genes in Karpas 299 cells (**Figure 5.5B**). I found that 24 genes were associated with c-Jun and JunB intervals within +/- 1 kb from the TTS. 36 genes among the top 100 genes were associated with JunB intervals alone, and 3 genes were associated with c-Jun intervals alone. Therefore, 63 out of 100 genes are potentially regulated by c-Jun and/or JunB as they are bound by c-Jun and/or JunB at putative promoter regions. **Figure 5.5C** shows examples from each category from **Figure 5.5B.** Known targets of JunB in ALK+ ALCL, including GzB and CD30, appear up on the list. BATF3 and ATF-7 are also AP-1 transcription factors that could form dimers with JunB/c-Jun [48, 334], and they could be

potentially regulated by JunB/c-Jun in ALK+ ALCL, as suggested by ChIP-seq data (**Figure 5.5C**).

**Figure 5.5**

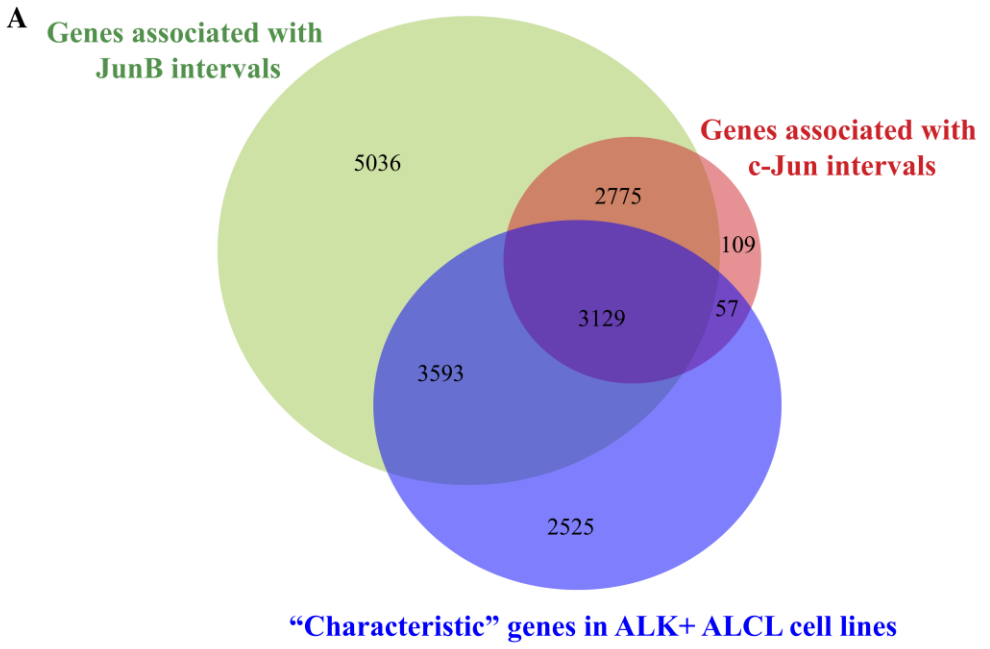


**B**

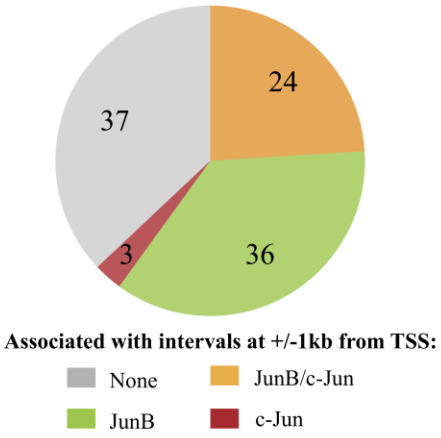


**C**

**Examples from top 100 charateristic genes in ALK+ ALCL**

| Genes | Associated with intervals at +/-1kb from TSS |
|---|---|
| *TIMP1* | JunB/c-Jun |
| *BATF3* | JunB/c-Jun |
| *CLU* | JunB/c-Jun |
| *GZMB* | JunB/c-Jun |
| *CD30* | JunB/c-Jun |
| *SERPINA1* | JunB |
| *VEGFA* | JunB |
| *CLEC4F* | JunB |
| *G0S2* | JunB |
| *ATF-7* | c-Jun |

**Figure 5.5 – Comparing ChIP-seq to published microarray data that identified "characteristic" genes of ALK+ ALCL from activated T cells**

**A.** Venn diagram showing the comparison between the "characteristic" genes identified in the published microarray (comparing ALK+ ALCL cell lines to activated T cells) and the genes associated with JunB or/and c-Jun intervals. **B.** Pie chart showing the percentage of the top 100 "characteristic" genes that were associated JunB or/and c-Jun intervals. **C.** Selected examples of genes associated with c-Jun and/or JunB intervals from **B.**

### 5.2.6 Gene ontogeny analysis of genes associated with c-Jun/JunB active regions

To gain an appreciation of putative cellular pathways regulated by c-Jun and JunB, we performed KEGG analysis on genes localized to active regions associated with c-Jun alone, JunB alone, or both c-Jun and JunB. Genes associated with JunB active regions within +/- 10 kb from the gene fell into 39 KEGG pathways, genes associated with both JunB and c-Jun intervals within +/- 10 kb from the gene fell into 94 KEGG pathways, and genes associated with c-Jun intervals within +/- 10 kb from the gene fell into 11 KEGG pathways (**Figure 5.6A**). The pathways were largely exclusive between the three categories of genes associated with c-Jun or JunB. Although more genes were associated with JunB intervals alone, they play not so different functions as only 38 pathways were identified from the KEGG annotation. On the other hand, the genes associated with both JunB and c-Jun intervals seem to play more diverse functions with 94 pathways identified from the KEGG annotation. **Figure 5.6B** shows that the top 5 pathways from each category are distinct (whole lists are included in **Appendix 5**). Of particular interest was the prevalence of cancer-related pathways associated with the c-Jun/JunB category and **Figure 5.6C** shows all the cancer-related pathways in this group. Thus, c-Jun and JunB likely both regulate many common genes associated with the cancer phenotype in this lymphoma.

**Figure 5.6**

**A**

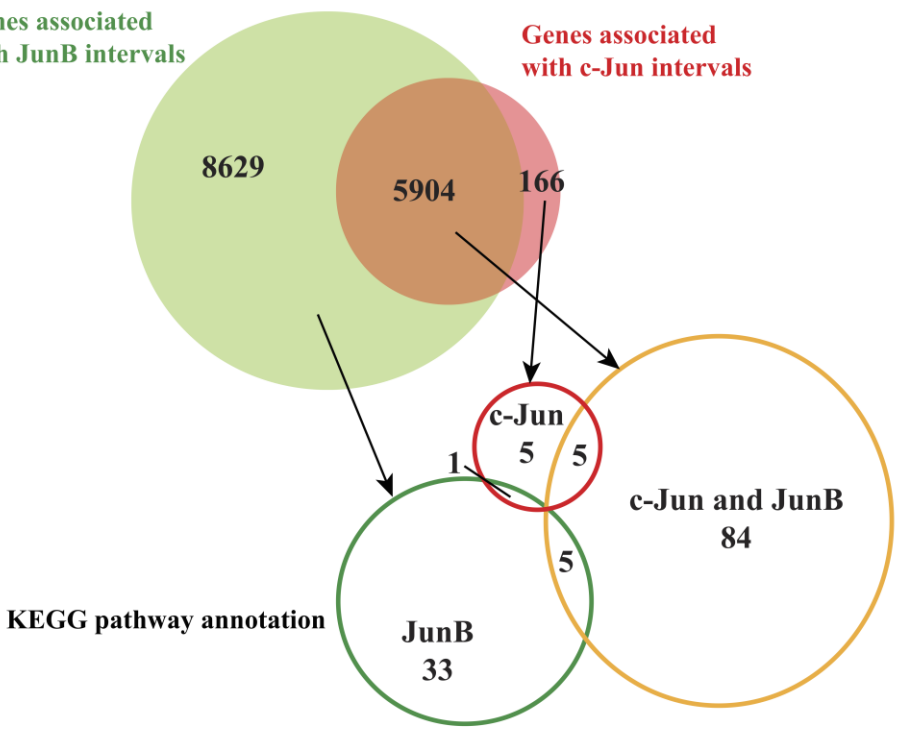


**B**

**Top 5 pathways**

| Genes associated with c-Jun intervals | Genes associated with JunB intervals | Genes associated with JunB/c-Jun intervals |
|---|---|---|
| Cell cycle | Metabolic pathways | Alcoholism |
| RNA transport | Ribosome | Viral Carcinogenesis |
| Cysteine and methionine metabolism | Lysosome | EBV infection |
| Basal transcription factors | Oxidative phosphorylation | Systemic Lupus Erythematosus |
| Proteoglycans in cancer | Biosynthesis of antibiotics | Pancreatic Cancer |

**C**

| Cancer related pathways in genes associated with JunB/c-Jun intervals | | |
|---|---|---|
| Viral carcinogenesis | Non-small cell lung cancer | Renal cell carcinoma |
| Pancreatic cancer | Small cell lung cancer | Central carbon metabolism in cancer |
| Chronic myeloid Leukemia | Glioma | Acute Myeloid Leukemia |
| Pathways in cancer | Bladder cancer | Choline metabolism in cancer |
| Prostate cancer | Colorectal cancer | Thyroid cancer |
| Renal cell carcinoma | Endometrial cancer | |

**Figure 5.6 – Annotation of the genes associated with JunB and/or c-Jun intervals**
**A.** Venn diagrams illustrating the KEGG pathways annotated from genes associated with JunB and/or c-Jun intervals. **B.** Tables showing the top 5 pathways from each category from **A**. **C.** Table showing the cancer-related pathways of genes associated with both JunB and c-Jun intervals.

### 5.2.7 Identification of FAM129B as a potential target of JunB/c-Jun in ALK+ ALCL

The ChIP-seq experiments revealed a number of AP-1 regulated genes that could be important in the pathobiology of ALK+ ALCL and which previously may have been missed in siRNA/shRNA knock-down studies of individual AP-1 family members. Therefore, we prepared a short-list of genes that: 1) had prominent c-Jun/JunB active regions within putative promoter regions (+/- 1 kb from TSS); 2) showed prominent expression in ALK+ ALCL cell lines relative to cell lines derived from other lymphomas ; and 3) which had not previously been studied in ALK+ ALCL, but would be predicted to be important in the pathobiology of this lymphoma.

Among the several genes identified based on the mentioned criteria (**Appendix 6**), we decided to follow-up on the gene of *FAM129B*. The structure of FAM129B protein is shown in **Figure 5.7A**. FAM129B is a pleckstrin homology domain-containing protein that was first identified as an Erk substrate, and it could be phosphorylated by Erk at four serine sites to mediate invasion in melanoma [335]. FAM129B has been shown to protect HeLa cells from apoptosis in response to a number of apoptotic stimuli [336]. Conversely in melanoma cells lines, FAM129B has also been shown to promote apoptosis induced by the stimulation of the Wnt3A-β-catenin pathway or inhibition of B-Raf pathway [337]. FAM129B also associates with and is a substrate of the EGFR receptor. The Y593 phosphorylated FAM129B was shown to interact with Ras, and prevent p120RasGAP from interacting with and turning off Ras [338]. In turn, the activated Ras leads to increased Erk activation and downstream activation of β-catenin and increased tumour cell metabolism and proliferation [338].

*FAM129B* had prominent c-Jun and JunB intervals within the promoter and an AP-1 site was identified from -158 bp to -152 bp relative to TSS (**Figure. 5.7B**). In addition, FAM129B levels were decreased when JunB was knocked down in SUP-M2 cells (**Figure 5.7C**), suggesting FAM129B could be regulated by JunB in SUP-M2 cells. Similar but modest change of FAM129B was observed in SUP-M2 cells expressing JunB2-2 shRNA, which results in weaker reduction in JunB. However, the JunB knock-down in Karpas 299 cells did not result in change of FAM129B (**Figure 5.7D**). Moreover, no research about the role of FAM129B in ALK+ ALCL had been done, so FAM129B would be a good candidate for further investigation.

**Figure 5.7**

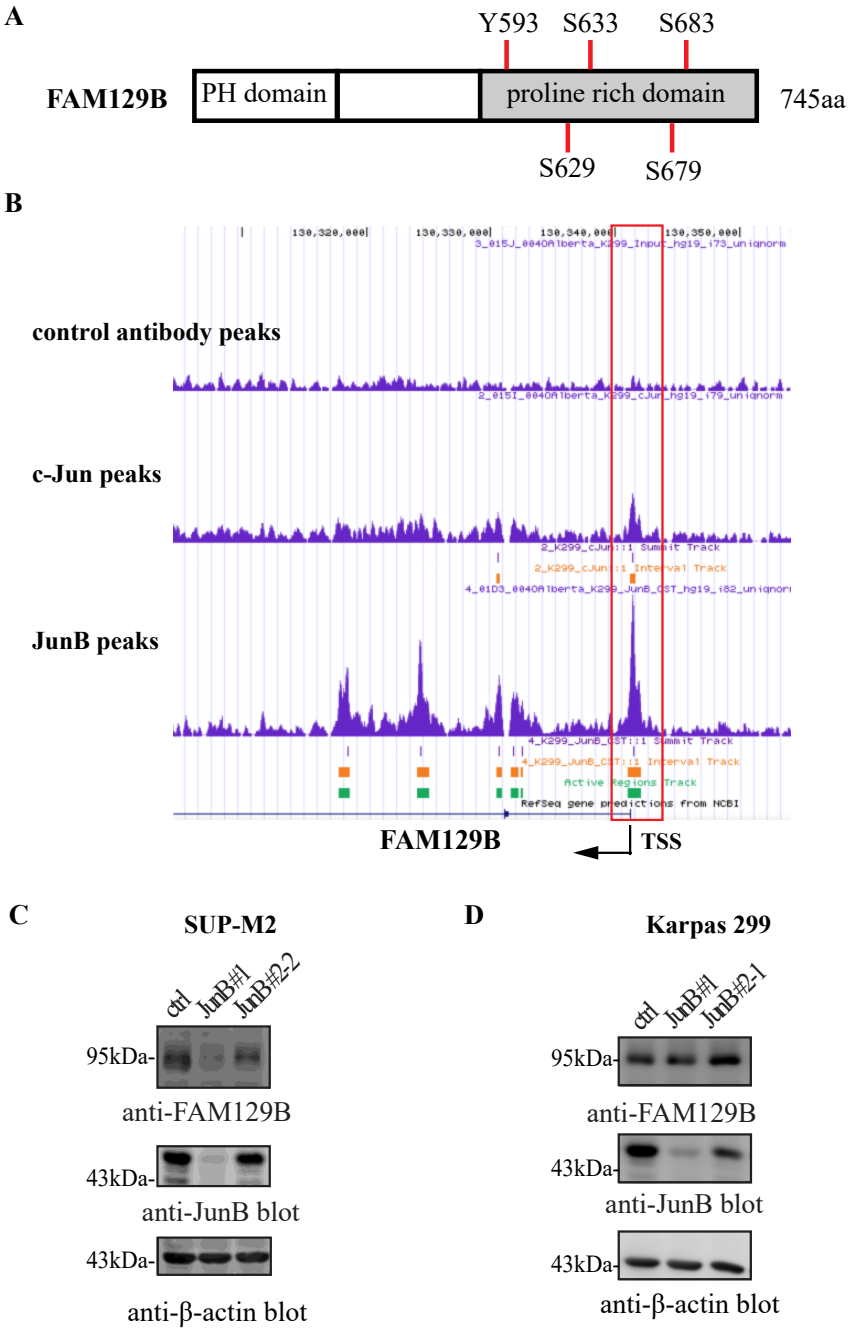


**Figure 5.7 – FAM129B is a potential transcription target of JunB and c-Jun in ALK+ ALCL.**

**A.** Structure of FAM129B. Tyrosine residue 593 is indicated as Y593 on the graph and it was shown be phosphorylated by EGFR. Four serine residues that could be phosphorylated by ERK are also indicated on the graph. **B.** Interval and peak sizes for the intervals found for FAM129B promoter. The intervals highlighted in the red box contain a consensus AP-1 site. **C-D.** Western blots showing the FAM129B levels when JunB was knocked down in SUP-M2 (**C**) and Karpas 299 cells (**D**). Molecular mass markers (in kDa) are indicated to the left of western blots. Check paper

### 5.2.8 FAM129B is highly expressed in ALK+ ALCL cell lines relative to other lymphomas

Given the fact *FAM129B* could be a putative transcriptional target of JunB and c-Jun in ALK+ ALCL, I wanted to examine whether FAM129B would be up-regulated in ALK+ ALCL as JunB and c-Jun are highly expressed or activated in ALK+ ALCL compared to other hematopoietic tumour cell lines. So I compared the expression of *FAM129B* mRNA in ALK+ ALCL to that of other types of lymphomas. Specifically, I went through the online database Cancer Cell Line Encyclopedia (CCLE) (Broad Institute, MA, US) to check the mRNA levels of *FAM129B* in a series of cell lines [339]. *FAM129B* is expressed highly in ALK+ ALCL cell lines compared to other types of lymphomas, and cHL cell lines have very different expression levels of *FAM129B* (**Figure 5.8A**). Then I further checked the expression of FAM129B protein levels in a collection ALK+ ALCL and other of B and T lymphoma/leukemia cell lines (**Figures 5.8 B, C and D**). Consistently, I observed expression of FAM129B in ALK+ ALCL cells, although there was a variation between the ALK+ ALCL cell lines. Specifically, SR and Karpas 299 had the highest protein levels of FAM129B, UCONN-L2 and SUDHL-1 possess intermediate levels of FAM129B, and SUP-M2 had the lowest level of FAM129B amongst the ALK+ ALCL cell lines (**Figure 5.8B**). The expression of FAM129B in classic Hodgkin lymphoma cell lines varied a bit, but similar to what was observed at mRNA level. HD-MYZ possessed very high levels of FAM129B, L-540 had some FAM129B expressed, but L-428 and KM-H2 cell hardly express any FAM129B protein (**Figure 5.8C**). HeLa cells have the highest level of FAM129B at protein level, which was consistent with mRNA level. The Burkitt B cell lymphoma cell lines (Ramos, BJAB, DG-75) had very

little FAM129B; Jurkat cells, a T cell leukemia cell line, also expressed very low levels of FAM129B (**Figure 5.8D**). Taken together, ALK+ ALCL cells express relatively high levels of FAM129B at both mRNA and protein levels compared to other lymphoma/leukemia lines examined.

**Figure 5.8**

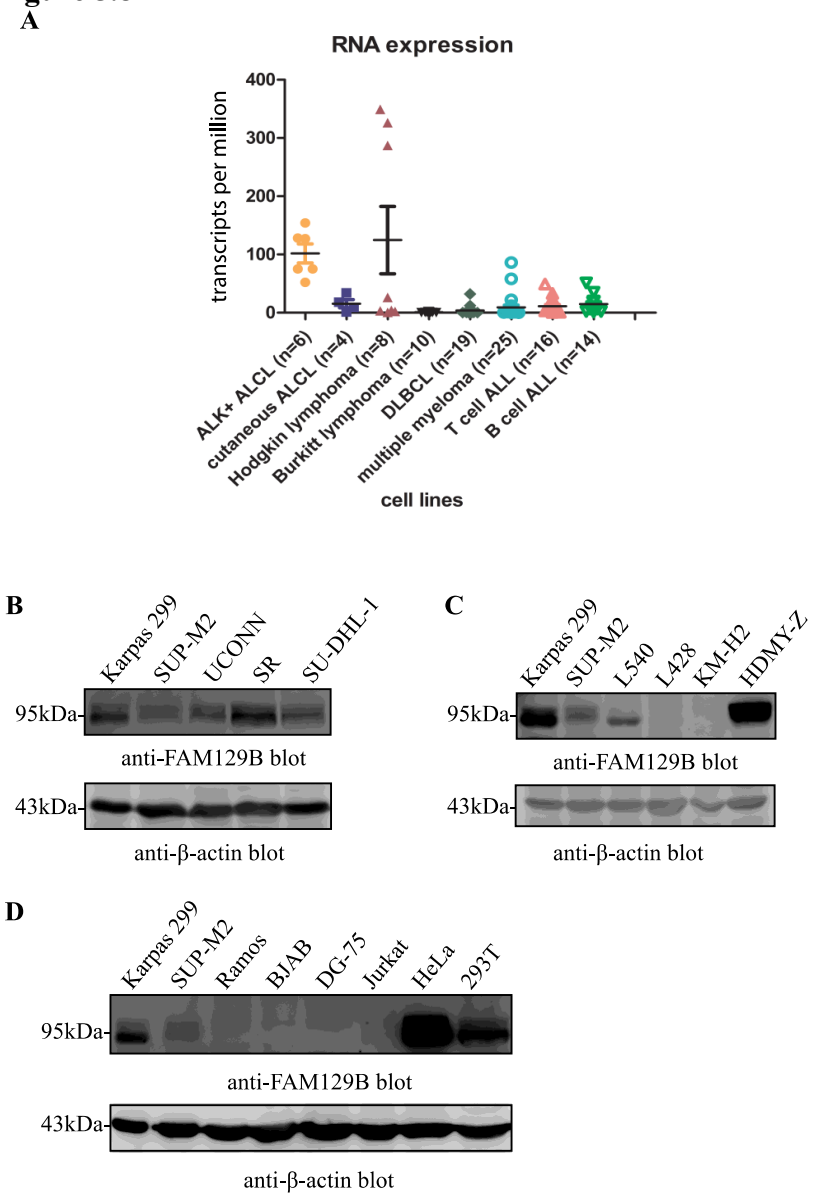


**Figure 5.8 – FAM129B is highly expressed in ALK+ ALCL cell lines compared to other lymphoma/leukemia cell lines**

**A.** Bar graph showing the mRNA level of FAM129B in different cell lines based on CCLE database. Transcripts Per Million is a normalization method for RNA-seq: it means for every 1,000,000 RNA molecules in the RNA-seq sample, how many are from this gene/transcript. Each dot represents the expression of FAM129B in one cell line, and the line indicates the mean expression level of FAM129B in the same type of cell lines. **B-D.** Western blots showing the level of FAM129B in ALK+ ALCL cell lines (**B**), classic Hodgkin lymphoma cell lines (**D**), Burkitt's lymphoma cell lines, a T cell leukemia cell line, and non-hematopoietic cell lines (**E**). Molecular mass markers (in kDa) are indicated to the left of western blots.

### 5.2.9 Stable knock-down of FAM129B in ALK+ ALCL cell lines resulted an increased percentage of cells in $G_0/G_1$ phase cells and decreased numbers of cells in S phase

To examine whether FAM129B plays a role in ALK+ ALCL pathobiology, I reduced the level of FAM129B in ALK+ ALCL cell lines with lentiviral particles containing FAM129B shRNAs. I generated the FAM129B knock-down in four commonly used ALK+ ALCL cell lines, namely Karpas 299, SUP-M2, UCONN-L2 and SR. As shown in **Figure 5.9,** FAM129B levels were significantly decreased in all the ALK+ ALCL cell lines, and this knock-down was observed with two distinct FAM129B shRNAs. FAM129B has been suggested to promote the proliferation of glioblastoma cells and contribute to the tumourgensis of the glioblastoma in nude mice [338]. Therefore, I wanted to examine whether the knock-down of FAM129B would lead to slower proliferation of ALK+ALCL cells. I performed BrdU-7AAD doubling staining to analyze the cell cycle distribution, and found that FAM129B knock-down resulted in a decreased percentage of cells in S phase, and increased percentage of cells in $G_0/G_1$ phase in Karpas 299, SUP-M2 and SR cells (**Figures 5.10 A, B, and C**). Similar trends were observed in UCONN-L2 cells, but the changes did not reach statistical significance when the data was combined from four independent experiments (**Figure 5.10D**). The same phenotype was observed with two distinct shRNAs for FAM129B, suggesting the changes were caused by the loss of FAM129B instead of the shRNAs targeting other genes. The changes of $G_2$/M phase were subtle in all the four ALK+ ALCL cells, albeit the percentage of $G_2$/M cells was decreased in FAM129B shRNA-expressing SUP-M2 cells (**Figure 5.10B**). Moreover, the changes observed in SUP-M2 cells were more

impressive when FAM129B was knocked down, with ~20% decrease in the percentage of cells in S phase and ~60% increase in $G_0$/G1 phase compared to control shRNA-expressing cells. The differences observed in SR and Karpas cells were similar when FAM129B was reduced, with ~20% decrease in the percentage off cells in S phase and ~25% increase in the percentage of cells in $G_0/G_1$ phase compared to control shRNA-expressing cells. Collectively, the results demonstrate that FAM129B knock-down results in slower proliferation in ALK+ ALCL cells, with increased percentage of cells in $G_0/G_1$ phase and decreased percentage of cells in S phase.

**Figure 5.9**

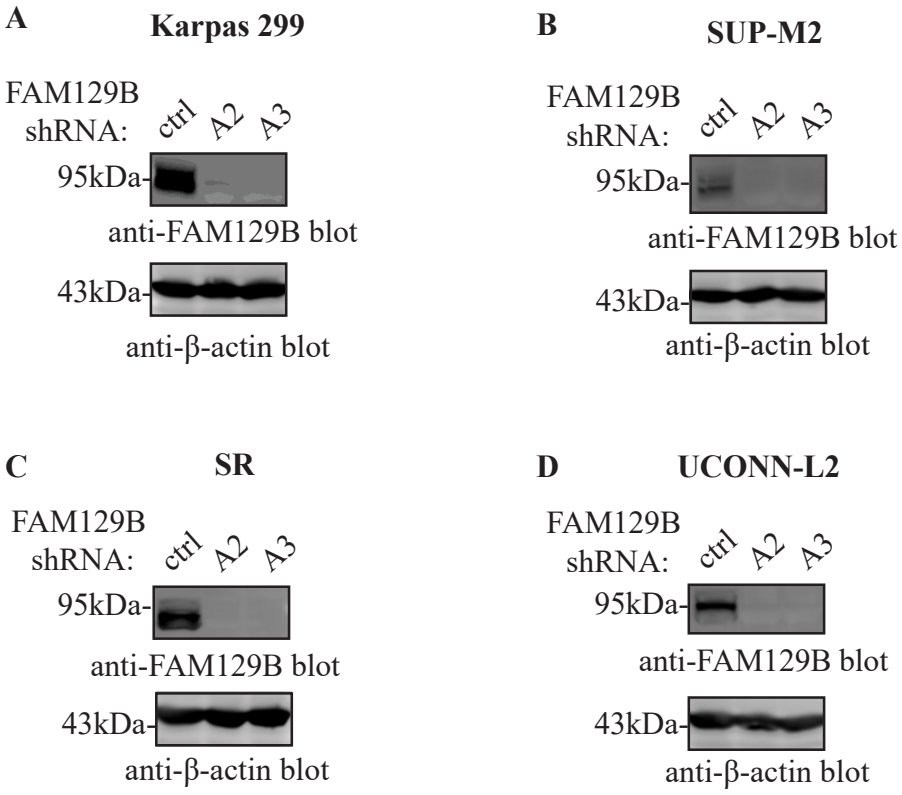


**Figure 5.9 – shRNA-mediated knock-down FAM129B in ALK+ ALCL cell lines.**

**A-D.** Western blots showing the levels of FAM129B in Karpas 299 (**A**), SUP-M2 (**B**), SR (**C**) and UCONN-L2 (**D**) cells expressing FAM129B shRNA or control shRNA. Molecular mass markers (in kDa) are indicated to the left of western blots.

## Figure 5.10

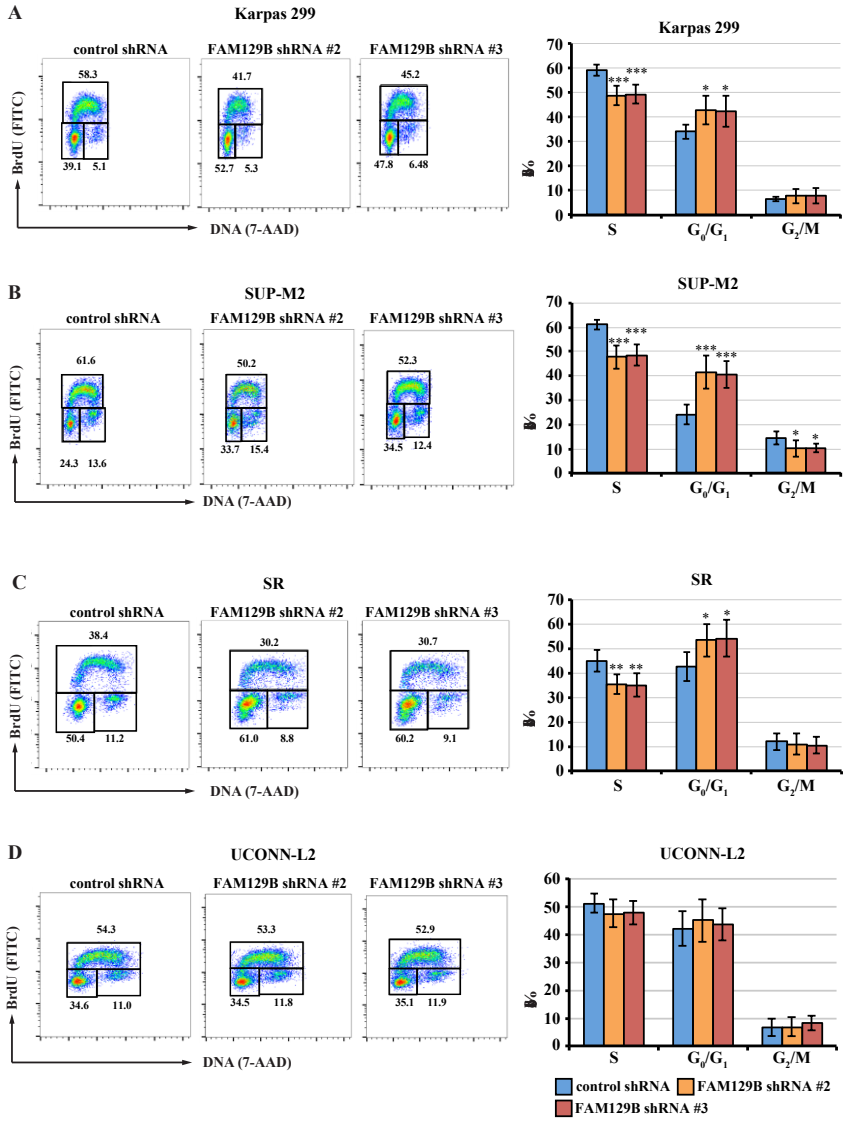


**Figure 5.10 - Stable knock-down of FAM129B in ALK+ ALCL cell lines results in increased percentage of cells in $G_0/G_1$ phase cells and decreased percentage of cells in S phase.**

**A-D.** Graphs showing the cell cycle distribution analysis and summaries for Karpas 299 (**A**), SUP-M2 (**B**), SR (**C**) and UCONN-L2 (**D**) cells expressing FAM129B shRNA or control shRNA. Results represent the average and standard deviation of seven independent experiments from two infections for **A and C**, six independent experiments from three infections for **B** and four independent experiments from three infections for **D**. p values represent ANOVA test with TUKEY *post-hoc* test. * $p<0.05$, ** $p<0.01$, *** $p<0.001$. The raw data is same from that in **Figure 5.11**, and sub-$G_0/G_1$ populations were removed.

### 5.2.10 Stable knock-down of FAM129B in ALK+ ALCL cell lines results in increased percentage of cells in sub-$G_0/G_1$ population

When I performed the cell cycle analysis on FAM129B knock-down cells, I noticed a significant build-up of sub-$G_0/G_1$ cells when FAM129B was reduced especially in SUP-M2 cells (**Figure 5.11B**). Sub-$G_0/G_1$ cells are a group cells undergoing cell death, possibility through apoptosis or necrosis and the DNA fragmentation/degradation process results in reduced DNA contents [340, 341]. Thus, cell cycle analysis with DNA content staining and BrdU staining could be a simple way to detect apoptosis/necrosis and cell cycle simultaneously [342, 343]. An increased percentage of sub-$G_0$ cells was observed in all four cell lines when FAM129B was knocked-down, although there was a variation in the basal level of sub-$G_0/G_1$ cells in these cell lines. The changes were most impressive in SUP-M2 cells, with about 30% of cells in sub-$G_0$ phase when FAM129B was reduced (**Figure 5.11B).** FAM129B knock-down in Karpas 299, SR and UCONN-L2 cells resulted in ~6%, 15% and 10% of the cells in sub-$G_0/G_1$ phase, respectively (**Figures 5.11A, C and D**). Despite the absolute percentage of sub-$G_0/G_1$ cells varied among the cell lines, the fold changes were similar in different cell lines when comparing control shRNA-expressing cells to FAM129B shRNA-expressing cells. The BrdU and 7AAD double-staining experiments were performed between Day 7 to Day 12 post-infection, when stable knock-down was established and the antibiotics selection process was finished. Therefore, FAM129B knock-down results in increased percentages of cells in sub $G_0/G_1$ phase in ALK+ALCL cells, which may indicate a population of apoptotic cells.

**Figure 5.11**

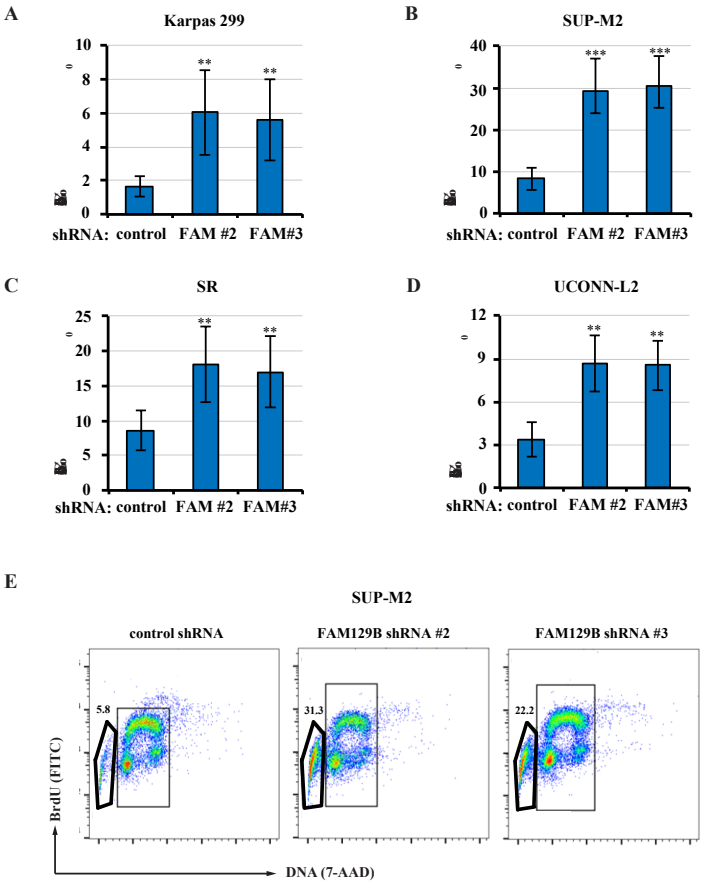


**Figure 5.11 - Stable knock-down of FAM129B in ALK+ ALCL cell lines resulted in increased percentage of cells in sub-$G_0/G_1$ population**

**A-D.** Graphs showing summaries for the percentage of cell in sub-$G_0/G_1$ phase for Karpas 299 (**A**), SUP-M2 (**B**), SR (**C**) and UCONN-L2 (**D**) cells expressing FAM129B shRNA or control shRNA. Results represent the average and standard deviation of seven independent experiments from three infections for **A, C** and, and six independent experiments from three infections for **B,** and four independent experiments from two infections for **D**. **E**. Graphs showing the sub-$G_0/G_1$ population in the bold gate from one representative experiment in SUP-M2 cells. p values represent ANOVA test with TUKEY *post-hoc* test.* $p<0.05$, ** $p<0.01$, *** $p<0.001$. The raw data is same from that in **Figure 5.10**, and sub-$G_0/G_1$ populations were included.

### 5.2.11 Inhibition of NPM-ALK resulted in increased electrophoretic mobility of FAM129B in ALK+ ALCL

Given the fact that FAM129B could be phosphorylated by EGFR at the Tyrosine593 residue to activate the Ras/Erk pathway and ALK and EGFR are both transmembrane receptor tyrosine kinases [338], I predicted that FAM129B could be phosphorylated by NPM-ALK in ALK+ ALCL. However, the anti-FAM129B antibody did not work well for immunoprecipitation and I could not determine whether FAM129B was phosphorylated by NPM-ALK or not. I treated the cells with ALK inhibitor, Crizotinib, and checked whether the electrophoretic mobility of FAM129B changed, as the change of molecular weights may indicate the phosphorylation status of the protein. I observed the higher molecular bands of FAM129B gradually went away and the lower molecular bands of FAM129B accumulated overtime when Karpas 299 cells were treated with Crizotinib (**Figure 5.12A**). The western blots were performed by the summer project student Farynna Loubich Facundo. Thus, I clearly demonstrated inhibition of NPM-ALK resulted in decreased electrophoretic mobility of FAM129B in ALK+ ALCL, possibly due to the deceased phosphorylation of FAM129B.

### 5.2.12 Expression of NPM-ALK in HEK-293 cells resulted in decreased electrophoretic mobility of FAM129B

I would further evaluate the role of NPM-ALK in regulating the electrophoretic mobility of FAM129B, which may due to the phosphorylation of FAM129B. In HEK-293 cells with NPM-ALK expression under the control of Tet-on system, NPM-ALK would be

expressed when doxycycline was added into the cell culture [233]. I observed the FAM129B bands of higher molecular weight gradually built up while the bands with lower molecular weight decreased, when NPM-ALK expression was induced by doxycycline (**Figure 5.12B**). The expression of NPM-ALK was successful based on the anti-ALK blots. The experiments were performed by two summer project students Farynna Loubich Facundo and Mary Nicoll. Taken together, the ectopic expression of NPM-ALK resulted in increased electrophoretic mobility of FAM129B in HEK-293 cells, which could be due to phosphorylation of FAM129B.

**Figure 5.12**

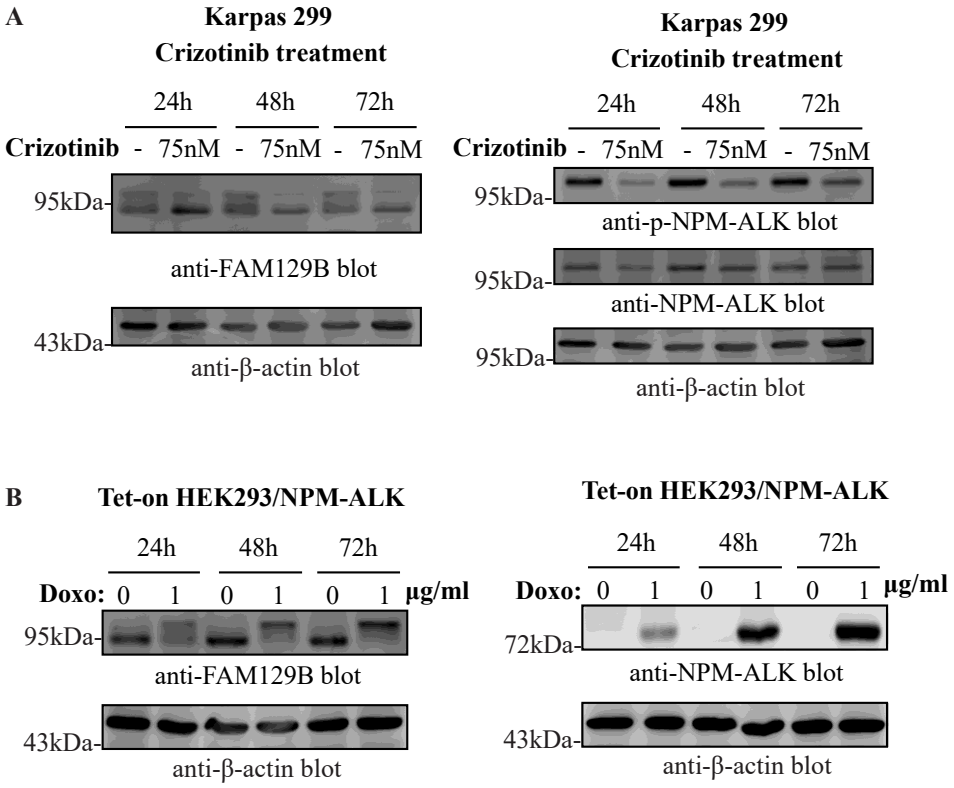


**Figure 5.12 –NPM-ALK inhibition or expression resulted in increased or decreased electrophoretic mobility of FAM129B, respectively**

**A.** Western blots showing the levels and electrophoretic mobility of FAM129B in Karpas 299 cells when treated with Crizotinib. **B.** Western blots showing the levels of FAM129B in HEK-293 containing pTRE-TIGHT/NPM-ALK under the control of doxycycline. The two panels in and B are blots for the same samples but run on different gels. Molecular mass markers (in kDa) are indicated to the left of western blots.

## 5.13 Discussion

In this Chapter, ChIP-seq was performed with anti-JunB and anti-cJun antibodies and identified genes that could be potential direct targets of the JunB or c-Jun transcription factors. The ChIP-seq and initial data analysis were done at Active Motif. I found large numbers of genes were associated with JunB or/and c-Jun intervals (**Figure 5.1**), which is consistent with the fact that AP-1 sites are abundant in the genome. More genes were associated with JunB or both JunB and c-Jun, and only a small number of genes were associated with c-Jun only (**Figure 5.1)**, suggesting JunB and c-Jun could regulate some common genes, but JunB may regulate many more genes than c-Jun does.

About half of the genes identified in the Chapter 2 microarray experiments were associated with JunB and/or c-Jun intervals at the putative promoter regions (+/- 1000 bp from TSS) (**Figure 5.4**). More than half of the characteristic genes of ALK+ ALCL that distinguish this lymphoma from activated T cells were associated with JunB and/or c-Jun intervals; ~60% of the top 100 characteristic genes are associated with JunB and/or c-Jun intervals at the promoter regions (+/- 1000 bp from TSS) (**Figure 5.5)**. Thus, the comparison of ChIP-seq data to microarray data in JunB knock-down Karpas 299 cells, and the comparison of ChIP-seq data to the published microarray data identifying the characteristic genes of ALK+ ALCL cell lines both suggested that JunB and c-Jun contribute to the expression profile of the ALK+ALCL cells.

Among the genes associated with JunB and/or c-Jun at the promoter regions (+/- 1000 bp from TSS), more genes were associated with JunB alone than genes associated with JunB and c-Jun together, and only a very small number of genes were associated

with c-Jun only (**Figures 5.4B and 5.5B**). This suggests JunB possibly contributes more to the gene expression than c-Jun does in ALK+ ALCL.

Annotation of the genes indicates that those genes are functionally distinct among the three groups and cancer related categories were mostly associated with intervals common to JunB and c-Jun (**Figure 5.6**). In addition, the genes associated with both JunB and c-Jun may not be identified by microarray. Thus, we focused on the genes associated with JunB and c-Jun intervals, and found one of the candidates, FAM129B, which was associated with both JunB and c-Jun intervals at the promoter region (-158 to -152 bp from TSS) with high intensities (**Figure 5.7**). FAM129B was highly expressed in ALK+ ALCL (**Figure 5.8**) and contributed to cell cycle progression, although the extent of the growth defect varied amongst the ALK+ ALCL cell lines (**Figure 5.10**). FAM129B may also contribute to the survival of the ALK+ ALCL cells, as increased percentages of sub-$G_0/G_1$ cells were observed when FAM129B was reduced (**Figure 5.11**). In addition, the electrophoretic mobility of FAM129B was dependent on ALK activity, suggesting NPM-ALK may regulate the phosphorylation of FAM129B (**Figure 5.12**). Moreover, recently Farynna and Mary demonstrated that HA-FAM129B was tyrosine phosphorylated when NPM-ALK was co-transfected in HEK-293 cells, however NPM-ALK was not directly associated with HA-FAM129B (personal communication; Farynna Loubich Facundo, Mary Nicoll). The electrophoretic mobility was decreased when Karpas 299 cells were treated with Erk inhibitor U0126, suggesting Erk could potentially promote the phosphorylation of FAM129B as well (personal communication: Mary Nicoll). Thus, FAM129B could be a potential transcriptional target of both JunB and c-Jun. FAM129B could contribute to the pathobiology of ALK+ALCL and also

could be potentially regulated through NPM-ALK and its down-stream pathways in ALK+ ALCL.

The growth defects were significant in three ALK+ALCL cell lines when FAM129B was reduced; the phenotype was observed in UCONN-L2 as well, but did not reach statistical significance. This variation of the phenotypes in ALK+ ALCL cell lines has been observed in Dr. Ingham's lab as well as other labs. For example, in Chapter 3 JunB knock-down did not result in significant growth defect in UCONN-L2 cells, which was different from other two ALK+ ALCL cell lines expressing JunB shRNA. In Chapter 4, the changes of the ligands for NK receptors in JunB knock-down cells were different among different cell lines. In addition, other member from Dr. Ingham's lab also observed that the percentages of apoptosis were quite different among the GzB shRNA-expressing ALK+ ALCL cell lines when treated with the same apoptosis inducing drugs [270]. Thus, there is heterogeneity within the ALK+ ALCL cell lines from different patients and they may respond differently to the same stimulation.

FAM129B also has been implicated in regulating apoptosis in response to apoptosis inducing molecules including TNF-α, WNT3A, or Raf inhibitor PLX4720, although it has different outcomes in different cell types [336, 337]. The observed increase in sub-$G_0$ cells in FAM129B knock-down cells suggests that FAM129B may inhibit the spontaneous apoptosis in ALK+ ALCL cells. However, sub-$G_0/G_1$ cells may also be due to cells undergoing necrosis, a more accurate assay such as TUNEL or Annexin-V staining would be needed to distinguish between apoptosis and necrosis will be performed in the future [244, 344].

Another important question that needs to be addressed is whether the AP-1 site in the *FAM129B* promoter is important for transcription of the gene. One way to answer this question would be cloning the *FAM129B* promoter region into the pGL-2 luciferase plasmid and then I would also generate a construct with a mutant AP-1 site. I would then transfect the wild type and mutant constructs into ALK+ ALCL cell lines and measure luciferase activity. If the AP-1 site is important for the transcription of the *FAM129B* gene, I should observe luciferase activity in the wild type construct transfected cells, and lower luciferase activity in the mutant construct transfected cells. I worked on cloning these constructs for about 3 months; however, it did not work out. I had a commercial service generated these constructs and I will perform these experiments in the future.

In all, I demonstrated that JunB and c-Jun bind to many sites in the genome in ALK+ ALCL cells. Many binding sites of c-Jun are bound by JunB. In addition, JunB appears to regulate many genes that c-Jun does not. Tumour-related pathways are enriched in the genes regulated by both JunB and c-Jun in ALK+ ALCL. Moreover, a novel potential transcriptional target of JunB and c-Jun was shown to promote proliferation and may inhibit spontaneous apoptosis of ALK+ ALCL cells.

# Chapter 6: Overall Discussion

The data shown in **Figure 6.3** and **Figure 6.4** are from the paper "The c-Jun and JunB transcription factors facilitate the transit of classical Hodgkin lymphoma tumour cells through $G_1$" in *Scientific Reports.* This manuscript was written by myself, JingXi (Cathy) Zhang, and Dr. Ingham.

## 6.1 Summary of the results

In my thesis I examined the role of the JunB and c-Jun transcription factors and identified the genes regulated directly and indirectly by JunB/c-Jun and sites bound by JunB/c-Jun in the genome of ALK+ ALCL. In Chapter 3, I examined the role of JunB and c-Jun in cell growth by stably knocking down the two AP-1 transcription factors with shRNA-containing lentiviral particles. I found knock-down of JunB, but not knock-down of c-Jun, resulted in slower proliferation of the cells with increased percentage of cells in $G_0/G_1$ phase and decreased percentage of cells in S phase. Consistently, the knock-down of JunB also resulted in the up-regulation of the CDK inhibitor $p27^{Kip1}$. Thus, JunB, but not c-Jun, promotes cell proliferation by promoting the cell cycle progression through $G_0/G_1$ phase in most of the ALK+ ALCL cell lines examined.

After examining the role of JunB and c-Jun in cell proliferation, I further examined how JunB contributes to the expression profile of the ALK+ ACL cell line, Karpas 299 in Chapter 4 by microarray. In microarray performed on JunB knock-down cells, I identified about 700 genes with fold change of expression greater than 2, and about 80% of them were up-regulated in JunB knock-down cells. KEGG annotation of the gene list identified a group of genes related to "NK-mediated cytotoxicity" and other groups related to tumour pathobiology. Further study revealed that the expression of several ligands for NK activating receptors (CD48, MICA/B) were up-regulated in JunB knock-down cells, and possibly regulated indirectly through epigenetic mechanisms. In addition, JunB knock-down Karpas 299 cells were more susceptible to NK-92 mediated killing possibly through the interaction between NKG2D (on NK-92 cells) and MICA/B

(on Karpas 299 cells expressing JunB shRNA). The results suggested the JunB could protect ALK+ ALCL cells from NK-92 mediated killing. However, SUP-M2 cells with reduced JunB expression were less susceptible to NK-92 mediated killing compared to control cells; no consistent trends were observed when primary NK cells were used to kill the Karpas 299 cells expressing JunB shRNA or control cells. Thus, the role of JunB in immune evasion was not consistent between ALK+ ALCL cell lines and further investigation is needed to address the function of JunB in ALK+ ALCL tumour immune evasion.

The microarray results provided us with information about how JunB and c-Jun contributed to the mRNA expression profile of the ALK+ ALCL cell line, Karpas 299. However, no information was gained about whether the promoters of the genes were bound by these AP-1 proteins and not all of the genes identified by microarray would likely be direct transcriptional targets of JunB.

In Chapter 5, I performed ChIP-seq with anti-JunB or anti-c-Jun antibodies to identify the potential direct transcription targets of JunB and/or c-Jun. A large number of genes (14,762) were identified to be associated with JunB and/or c-Jun intervals and previously identified genes transcriptional regulated by JunB were also shown to be associated with JunB intervals in the ChIP-seq. About 60% of the genes identified were associated with JunB intervals only within +/- 10 kb from the gene, about 40% of them were associated with both JunB intervals and c-Jun intervals within +/- 10 kb from the gene, and only 1% of the genes were associated with c-Jun intervals only within +/- 10 kb from the gene. In addition, 97% of the genes associated with c-Jun intervals within +/- 10 kb from the gene were also associated with JunB intervals within +/- 10 kb from the

gene, but only 40% the genes associated with JunB intervals within +/- 10 kb from the gene were also associated with c-Jun intervals within +/- 10 kb from the gene. KEGG annotation analysis revealed that several cancer-related categories were found in the genes associated with both JunB and c-Jun intervals, suggesting this group of genes may play important roles in the pathobiology of ALK+ ALCL. Further study focused on one gene called *FAM129B*, whose putative promoter was associated with both JunB and c-Jun intervals with high intensities and expression levels were higher in ALK+ ALCL cell lines compared to other hematopoietic lymphoma cell lines. Stable knock-down of FAM129B in ALK+ ALCL cell lines resulted in reduced proliferation with increased percentage of cells in $G_0/G_1$ phase and fewer cells in S phase. I also observed an increased percentage of sub-$G_0/G_1$ cells in FAM129B shRNA-expressing ALK+ ALCL cell lines, indicating potential increase in cell death in FAM129B stable knock-down cells. In addition, the electrophoretic mobility of FAM129B was decreased when ALK activity was inhibited, suggesting FAM129B phosphorylation may be dependent on NPM-ALK. Thus ChIP-seq identified a gene that is associated with JunB and c-Jun intervals in the putative promoter region, suggesting FAM129B could be a potential direct transcriptional target of JunB and c-Jun. In addition, my results showed that FAM129B plays a role in the pathobiology of ALK+ ALCL.

**Figure 6.1**

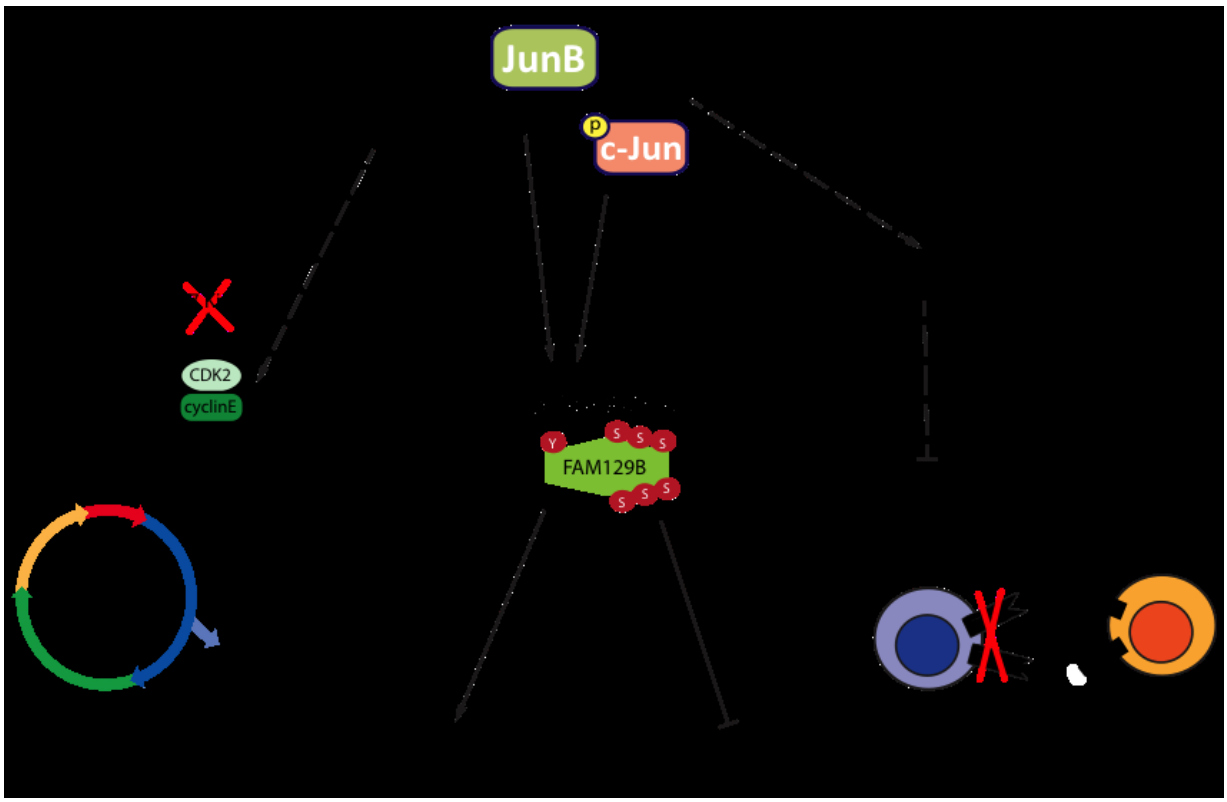


**Figure 6.1 - Summary model for JunB/c-Jun functions identified in the thesis**

Schematic diagram showing the summary model for the thesis. JunB promotes the cell proliferation by promoting cells transit through $G_0/G_1$ phase via directly or indirectly down-regulating $p27^{Kip1}$ and up-regulating CDK2 (Chapter 3); JunB also down-regulates some ligands for NK activating receptors possibly through epigenetic mechanisms to protect the cells from immune surveillance. (Chapter 4); JunB and c-Jun together potentially regulate the transcription of FAM129B, which also promotes the proliferation and may inhibit apoptosis of the ALK+ ALCL cells (Chapter 5).

### 6.2 JunB and c-Jun have overlapping functions in ALK+ ALCL

The model I proposed for how JunB and c-Jun regulate genes in ALK+ ALCL is illustrated in **Figure 6.2.** Specifically, I proposed JunB and c-Jun can regulate many genes together, and JunB could itself also regulate many genes. But c-Jun only regulates a very small number of genes in ALK+ ALCL by itself. Therefore, JunB could compensate or partially compensate for the loss of c-Jun in most of the cases, however c-Jun could not compensate for the loss of JunB in ALK+ ALCL. I will talk about how I came to the model in the following paragraphs.

JunB and c-Jun has been demonstrated to have redundancy in tumourigenesis in the mouse model where the expression of NPM-ALK is under the control of CD4 promoter [229]. Only when JunB and c-Jun were both deleted in the CD4-NPM-ALK transgenic mice, the mice would survive longer with slower proliferation of tumour cells, increased apoptosis of tumour cells, less blood vessels formed in tumour tissue and no dissemination of the disease [229]. The authors did not look at the roles that JunB and c-Jun individually play on cell proliferation, apoptosis, dissemination and vessel formation. Thus, it is possible that JunB and c-Jun regulate different aspects of the tumourigenesis and only when both of them were deleted that all the effects collectively resulted in better survival of the mice. It is also possible JunB and c-Jun regulate genes involving some aspects of pathobiology together; only when JunB and c-Jun were knocked down together, the expression of the genes regulating the tumour pathobiology would be changed. The latter scenario possibly is the case, as reasoned below. First of all, KEGG annotation of the ChIP-seq results (**Figure 5.6)** showed that JunB itself could regulate many genes that are important for cellular processes, and c-Jun itself could regulate a very small number

of genes. Therefore knock-out of JunB alone would generate some defect of the tumour biology in the CD4/NPM-ALK transgenic mice, if the former scenario was correct. However, it was clearly not the case in the transgenic mice as JunB knock-out had no effect on tumour pathogenesis, thus the former scenario was not likely correct. Secondly, in the microarray experiments, no statistically significant changed genes were identified in c-Jun knock-down cells compared to control shRNA-expressing cells after p-value correction, which was a personal observation. Because I performed microarray on JunB knock-down and c-Jun knock-down Karpas 299 cells simultaneously, it was unlikely the case that the microarray itself was a failure. It was possible that no genes changed at all, or the number of genes changed was quite small, or the changes of the expression of genes were quite subtle in c-Jun knock-down cells. As a result, c-Jun knock-down did not result in any statistically significantly changed genes, and it suggested that JunB or other AP-1 proteins may compensate for the loss of c-Jun for the genes that they potentially regulate together.

There are four possible scenarios for how genes are regulated by JunB and c-Jun together (**Figure 6.2**). In **Scenario A**, JunB controls the regulation of the genes dominantly: JunB knock-down results in the reduction of the genes, but c-Jun knock-down does not. That is JunB could compensate for the loss of c- Jun but c-Jun could not compensate the loss of JunB for the regulation of these genes (like TBLX1 **Figure 5.4D).** In **Scenario B**, either JunB or c-Jun is sufficient to promote the transcription of the genes: JunB or c-Jun knock-down results in no reduction in the transcription of the genes. Only when JunB and c-Jun are both knocked-down, would there be differences in the levels of the genes. FAM129B in Karpas 299 cells could be an example of genes in **Scenario B,**

although further investigation is still needed to examine whether FAM129B is regulated transcriptionally by JunB/c-Jun. These genes would not be identified in microarray but would associate with JunB and c-Jun intervals from ChIP-seq result. Double knock-down of JunB and c-Jun would better evaluate the role of JunB and c-Jun in regulating the genes in **Scenario B**. I have tried double knock-down of JunB and c-Jun in the early stage of my thesis project, however I experienced technical difficulties in maintaining efficient reduction in JunB and c-Jun expression simultaneously. The double knock-down was generated by infecting the cells with JunB shRNA-containing lentiviral particle (G418-resistant) and c-Jun shRNA-containing lentiviral particles (puromycin-resistant) subsequently, and the selection process was long and may result in restoration problems. Future work trying to put JunB shRNA and c-Jun shRNA in the same vector could improve the efficacy of the double knock-down.

In **Scenario C**, both JunB and c-Jun contribute to the transcription of the genes: either JunB knock-down or c-Jun knock-down would result in a modest reduction in the levels of the genes and double knock-down of JunB and c-Jun result in dramatic decrease levels of the genes. PDGFR-β is an example for **Scenario C** as JunB or c-Jun knock-out in the transgenic mice resulted in decreased expression of it, and both JunB and c-Jun deletion resulted in more dramatic decrease of PDGFR-β [229]. In **Scenario D,** c-Jun contributes more to the transcription of genes, which is the opposite of **Scenario A**. That is knock-down of c-Jun would result in the reduction of the expression of the genes, while knock-down of JunB would have no effect on the expression of the genes. Given that microarray in c-Jun knock-down identified no significant changed, it is possible that this scenario is not happening, or changes of genes in c-Jun knock-down cells were quite

subtle that they did not reach significance. It is also possible the number of the genes in this scenario is very small that I could find an example for it.

To put things together, in Chapter 3 and 4, when JunB was knocked-down, genes in **Group 1** would be decreased, and **Scenarios A and C** in **Group 2** would be decreased as well. The downstream molecules of some of the genes with decreased expression would also change and thus I observed many changed genes in microarray. On the other hand, when c-Jun was knocked-down, genes in **Group 2 Scenario C** would change, and genes in **Group 3** would change as well. But possibly due to the small number of genes and modest changes, no significantly changed genes in microarray were identified. In terms of the growth defect observed in JunB knock-down cells, genes in **Group 1** or **Group 2 Scenario A** or the downstream genes regulated by some of them would regulate proliferation related genes and account for the decreased proliferation in JunB shRNA-expressing cells. The genes in **Group 2 Scenario C** and **Group 3,** and the downstream genes of some of them may regulate other aspects of cellular processes instead of proliferation, thus no growth defect was observed in c-Jun knock-down cells.

To sum up, my results supports the model that JunB and c-Jun regulate some genes together in ALK+ ALCL. JunB itself could also regulate some genes, and c-Jun regulates only a small number of genes by itself in ALK+ ALCL.

**Figure 6.2**

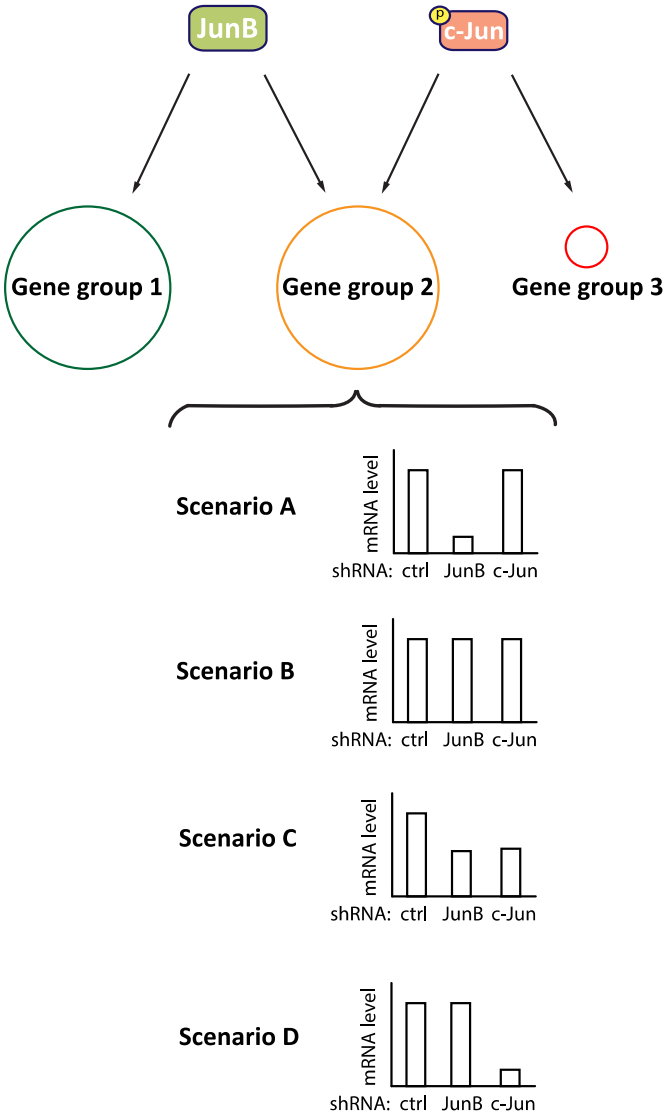


**Figure 6.2 - Proposed models for how JunB and c-Jun regulate genes in ALK+ ALCL.**

Schematic figure showing the potential model for how JunB and c-Jun regulate genes in ALK+ ALCL. Genes in Group 1 are regulated by JunB alone; genes in Group 3 are regulated by c-Jun alone. Genes in Group 2 are regulated by JunB and c-Jun together. For the genes in Group 2, several scenarios could happen regarding whether JunB or c-Jun dominates the regulation of the genes. In scenario A, JunB is necessary for expression of genes and JunB could compensate the loss of c-Jun. In scenario B, JunB and c-Jun compensate for the loss of each other. In scenario C, both JunB and c-Jun are necessary for the expression of genes, and they cannot compensate for the loss of each other. In scenario D, c-Jun is necessary for expression of genes, and c-Jun could compensate for the loss of JunB. Details are included in the main text **Section 6.2**.

### 6.3 Relative levels of JunB and c-Jun in ALK+ ALCL cells

One possible explanation for the different roles of JunB and c-Jun in ALK+ ALCL could be the different levels of JunB and c-Jun in ALK+ ALCL. The expression levels of JunB in ALK+ ALCL cell lines that we examined are roughly the same, so are the expression levels of c-Jun in ALK+ ALCL (**Figure 6.4C**). However, the expression levels of JunB are higher than the expression levels of c-Jun in ALK+ ALCL, as indicated in the paper from Staber *et al.*[136], where the mRNA levels of JunB were higher compared to other AP-1 proteins, namely c-Jun, JunD, c-Fos, Fra1, Fra2, and ATF2 in Karpas 299 and SR cells. Moreover, the mRNA levels of JunB were more highly up-regulated compared to c-Jun when NPM-ALK was expressed in TonBaf.1 cells [136]. The evidence suggests that JunB level is much higher than c-Jun, which may be a reason why JunB plays more important roles in ALK+ ALCL.

No direct information is available about the relative protein levels of these AP-1 proteins in ALK+ ALCL. Thus, quantitative mass spectrometry would help me determine the amount of AP-1 proteins in the ALK+ ALCL cell lines and would help elucidate the reason for the different roles of AP-1 proteins in ALK+ ALCL in the future.

### 6.4 JunB and c-Jun partners in ALK+ ALCL

The different partners of JunB and c-Jun may also explain why the genes could be regulated by JunB and c-Jun differently, especially for the genes in **Group 2 scenario B and C**. JunB and c-Jun demonstrate several amino acid differences in the DNA binding domain and dimerization motif [345], thus it is possible that the small differences in

sequence may impact other transcription factors that interact with JunB/c-Jun to AP-1, and further affect the function of JunB and c-Jun in ALK+ ALCL.

In ALK+ ALCL, JunB and c-Jun can dimerize with BATF proteins, which only contain the leucine zippier motif for dimerization but no transactivation domain. BATF and BATF-3 are highly expressed in ALK+ ALCL and can form dimers with JunB [48]. Moreover, knock-out of BATF/BATF3 impaired the proliferation ALK+ ALCL cell lines, suggesting BATF/BATF3 and JunB may together regulate important genes in ALK+ ALCL. Thus BATF/BATF3 could account for the difference of JunB and c-Jun in ALK+ ALCL as JunB could dimerize with them but c-Jun may not. Although BATF/BATF3 association with c-Jun in ALK+ ALCL has yet to be shown, it was reported that JunB and c-Jun could form dimers with BATF in mouse fibroblasts [160, 346]. Thus, it is not likely the different capability for JunB and c-Jun to form dimers with BATF that accounts for the different roles of JunB and c-Jun in ALK+ ALCL.

In ALK+ ALCL cell lines, Karpas 299 and SUP-M2, the mRNA levels of FRA1, FRA2 and ATF2 were comparable to the mRNA levels of c-Jun [136]. Fra-1 was also up-regulated to the similar levels as c-Jun at mRNA levels in the NPM-ALK expressing-TonBaf.1 cells [136]. It was reported that Jun family members could dimerize with Fos family members [160, 347, 348], and specifically JunB could form dimer with c-Fos and FRA2 in ALK + ALCL [349]. It is possible JunB and c-Jun could form dimers with FRA1, FRA2 and ATF2 to regulate the gene differently due to the different affinities and preferences for the AP-1 sites in ALK+ ALCL [350]. Therefore, future studies identifying the partners for JunB or c-Jun would help us understand the different role of JunB and c-Jun in ALK+ ALCL. Immunoprecipitation with anti-JunB/c-Jun antibody and

then examining whether the other AP-1 proteins are immunoprecipitated by western blotting would provide us with information about the partners of JunB and c-Jun.

### 6.6 ChIP-seq, Microarray, Mass spectrometry

When the Ingham lab examined the function of JunB by omics studies, mass-spectrometry was initially performed to compare the protein levels between JunB siRNA transfected cells and control siRNA transfected cells. However, the fold change of protein levels was modest and the number of the proteins identified with changed levels was small. This may be due to the fact that the transient knock-down of JunB may not be sufficient to induce changes and the short time window of siRNA mediated knock-down may make it hard to catch the differences at the protein level. Thus, microarray experiments were performed on stable knock-down cells to compare the mRNA expression profiles of JunB shRNA and control shRNA-expressing cells. More genes with changed expression were identified and the fold changes were more impressive. The microarray provided us with more information about how JunB contributes to the mRNA expression profiles of ALK+ ALCL so that the targets of JunB could be identified. However, not all of genes identified are likely regulated directly by JunB and redundancies between JunB and c-Jun may make it difficult to identify the genes that are regulated transcriptionally by JunB and c-Jun together. Therefore, to further identify the direct targets of JunB and/or c-Jun, ChIP-seq was performed with anti-JunB and anti-c-Jun antibodies, which would provide direct information on the binding sites of the AP-1 proteins in the genome. A large number of the genes were found to be associated with JunB and/or c-Jun intervals and we identified a potential JunB and c-Jun transcriptional

target (FAM129B) that is highly expressed in ALK+ ALCL and contributes to the pathobiology of this disease. More candidates were also identified as JunB and c-Jun transcriptional targets, and further work to characterize the candidate genes would help us understand the role of JunB and c-Jun in the pathobiology of ALK+ ALCL.

### 6.7 Comparing JunB and c-Jun function in ALK+ ALCL with another CD30+ lymphoma, classic Hodgkin lymphoma

In this thesis, JunB and c-Jun function were evaluated in ALK+ ALCL, where the two transcription factors are highly expressed and/or activated. In ALK+ ALCL, JunB but not c-Jun promotes the cell cycle progression through $G_0/G_1$ phase, and JunB may contribute more to the regulation of the genes that are important to the pathobiology of ALK+ ALCL. JunB and c-Jun are also highly expressed and activated in a related CD30+ disease classic Hodgkin lymphoma (cHL), and we wanted to know whether JunB and c-Jun play similar roles in cHL as in ALK+ ALCL. We found both JunB and c-Jun contribute to the proliferation of the tumour cells in cHL by facilitating the cell cycle progression through $G_0/G_1$ phase, and JunB and c-Jun down-regulating $p21^{Cip1}$ in cHL. This work in cHL was performed by Ms. Zhang, a former MSc. student from the Ingham lab and published in *Scientific Reports* titled "The c-Jun and JunB transcription factors facilitate the transit of classical Hodgkin lymphoma tumour cells through G1" [243]. The levels of JunB and c-Jun in cHL are relatively similar to the levels of JunB and c-Jun in ALK+ ALCL, but the two AP-1 transcription factors have different roles in the two related lymphomas [243]. This may be due to the partners of JunB and c-Jun are different in the two lymphomas. Or the cellular origin could account for the difference, as the

healthy counterpart for cHL is B cell, while for ALK+ ALCL is T cell. Most likely, the genes regulated by JunB and c-Jun are different in cHL compared to ALK+ ALCL. Thus, future work to study the direct targets of JunB and c-Jun in cHL would help us further elucidate the role of JunB and c-Jun in CD30+ lymphomas.

### 6.8 Significance of the thesis

In this thesis, I first characterized the roles of JunB and c-Jun with stable shRNA mediated knock-down that resulted in significant reduction of these two AP-1 proteins. I found JunB knock-down resulted in growth defect which consistent with what was observed by other groups with siRNA transfection. I also clearly demonstrated that c-Jun had no effect on cell growth, providing another piece of solid evidence to solve the discrepancies in this field. Secondly, I took advantage of the greater knock-down that shRNA afforded to perform microarray experiments to globally identify genes regulated by JunB in ALK+ ALCL. Among all the potential pathways that JunB may regulate, my results suggest that JunB may play a role in immune evasion in the pathobiology of ALK+ ALCL. Thirdly, our ChIP-sequencing was the first to comprehensively determine the binding sites of JunB and c-Jun in ALK+ ALCL, and examine how many binding sites are overlapping between JunB and c-Jun and how many are unique to each transcription factor. ChIP-seq enabled me to identify the targets of AP-1 proteins that may have been missed by "omics" studies on cells where one AP-1 protein was knocked-down; one example is FAM129B. Collectively, my thesis has provided a much more comprehensive understanding on how these two AP-1 proteins contribute to multiple aspects of pathobiology in ALK+ ALCL.

# References

1. Stein, H., et al., *The expression of the Hodgkin's disease associated antigen Ki-1 in reactive and neoplastic lymphoid tissue: evidence that Reed-Sternberg cells and histiocytic malignancies are derived from activated lymphoid cells.* Blood, 1985. **66**(4): p. 848-58.
2. Bonzheim, I., et al., *ALK-positive anaplastic large cell lymphoma: an evolving story.* Front Biosci (Schol Ed), 2015. **7**: p. 248-59.
3. Sabattini, E., et al., *WHO classification of tumours of haematopoietic and lymphoid tissues in 2008: an overview.* Pathologica, 2010. **102**(3): p. 83-7.
4. Benharroch, D., et al., *ALK-positive lymphoma: a single disease with a broad spectrum of morphology.* Blood, 1998. **91**(6): p. 2076-84.
5. Swerdlow, S.H., et al., *The 2016 revision of the World Health Organization classification of lymphoid neoplasms.* Blood, 2016. **127**(20): p. 2375-90.
6. Leonard, J.P., P. Martin, and G.J. Roboz, *Practical Implications of the 2016 Revision of the World Health Organization Classification of Lymphoid and Myeloid Neoplasms and Acute Leukemia.* J Clin Oncol, 2017. **35**(23): p. 2708-2715.
7. Campo, E., et al., *The 2008 WHO classification of lymphoid neoplasms and beyond: evolving concepts and practical applications.* Blood, 2011. **117**(19): p. 5019-32.
8. Pearson, J.D., et al., *NPM-ALK: The Prototypic Member of a Family of Oncogenic Fusion Tyrosine Kinases.* J Signal Transduct, 2012. **2012**: p. 123253.
9. *A clinical evaluation of the International Lymphoma Study Group classification of non-Hodgkin's lymphoma. The Non-Hodgkin's Lymphoma Classification Project.* Blood, 1997. **89**(11): p. 3909-18.
10. Stein, H., et al., *CD30(+) anaplastic large cell lymphoma: a review of its histopathologic, genetic, and clinical features.* Blood, 2000. **96**(12): p. 3681-95.
11. Mora, J., et al., *Large cell non-Hodgkin lymphoma of childhood: Analysis of 78 consecutive patients enrolled in 2 consecutive protocols at the Memorial Sloan-Kettering Cancer Center.* Cancer, 2000. **88**(1): p. 186-97.
12. Ferreri, A.J., et al., *Anaplastic large cell lymphoma, ALK-positive.* Crit Rev Oncol Hematol, 2012. **83**(2): p. 293-302.
13. Savage, K.J., et al., *ALK- anaplastic large-cell lymphoma is clinically and immunophenotypically different from both ALK+ ALCL and peripheral T-cell lymphoma, not otherwise specified: report from the International Peripheral T-Cell Lymphoma Project.* Blood, 2008. **111**(12): p. 5496-504.
14. Falini, B., et al., *ALK+ lymphoma: clinico-pathological findings and outcome.* Blood, 1999. **93**(8): p. 2697-706.
15. Le Deley, M.C., et al., *Prognostic factors in childhood anaplastic large cell lymphoma: results of a large European intergroup study.* Blood, 2008. **111**(3): p. 1560-6.
16. Falini, B., et al., *Lymphomas expressing ALK fusion protein(s) other than NPM-ALK.* Blood, 1999. **94**(10): p. 3509-15.
17. Willemze, R., et al., *WHO-EORTC classification for cutaneous lymphomas.* Blood, 2005. **105**(10): p. 3768-85.

18. Armitage, J.O., J.M. Vose, and D.D. Weisenburger, *Towards understanding the peripheral T-cell lymphomas.* Ann Oncol, 2004. **15**(10): p. 1447-9.
19. Brugieres, L., et al., *Relapses of childhood anaplastic large-cell lymphoma: treatment results in a series of 41 children--a report from the French Society of Pediatric Oncology.* Ann Oncol, 2000. **11**(1): p. 53-8.
20. Mori, T., et al., *Recurrent childhood anaplastic large cell lymphoma: a retrospective analysis of registered cases in Japan.* Br J Haematol, 2006. **132**(5): p. 594-7.
21. Woessmann, W., et al., *Relapsed or refractory anaplastic large-cell lymphoma in children and adolescents after Berlin-Frankfurt-Muenster (BFM)-type first-line therapy: a BFM-group study.* J Clin Oncol, 2011. **29**(22): p. 3065-71.
22. Zinzani, P.L., et al., *Clinical implications of serum levels of soluble CD30 in 70 adult anaplastic large-cell lymphoma patients.* J Clin Oncol, 1998. **16**(4): p. 1532-7.
23. Brugieres, L., et al., *CD30(+) anaplastic large-cell lymphoma in children: analysis of 82 patients enrolled in two consecutive studies of the French Society of Pediatric Oncology.* Blood, 1998. **92**(10): p. 3591-8.
24. Foyil, K.V. and N.L. Bartlett, *Brentuximab vedotin and crizotinib in anaplastic large-cell lymphoma.* Cancer J, 2012. **18**(5): p. 450-6.
25. Gross, T.G., et al., *Hematopoietic stem cell transplantation for refractory or recurrent non-Hodgkin lymphoma in children and adolescents.* Biol Blood Marrow Transplant, 2010. **16**(2): p. 223-30.
26. Woessmann, W., et al., *Allogeneic haematopoietic stem cell transplantation in relapsed or refractory anaplastic large cell lymphoma of children and adolescents--a Berlin-Frankfurt-Munster group report.* Br J Haematol, 2006. **133**(2): p. 176-82.
27. Brugieres, L., et al., *Single-drug vinblastine as salvage treatment for refractory or relapsed anaplastic large-cell lymphoma: a report from the French Society of Pediatric Oncology.* J Clin Oncol, 2009. **27**(30): p. 5056-61.
28. Lowe, E.J. and T.G. Gross, *Anaplastic large cell lymphoma in children and adolescents.* Pediatr Hematol Oncol, 2013. **30**(6): p. 509-19.
29. de Claro, R.A., et al., *U.S. Food and Drug Administration approval summary: brentuximab vedotin for the treatment of relapsed Hodgkin lymphoma or relapsed systemic anaplastic large-cell lymphoma.* Clin Cancer Res, 2012. **18**(21): p. 5845-9.
30. Fanale, M.A., et al., *A phase I weekly dosing study of brentuximab vedotin in patients with relapsed/refractory CD30-positive hematologic malignancies.* Clin Cancer Res, 2012. **18**(1): p. 248-55.
31. Younes, A., et al., *Brentuximab vedotin (SGN-35) for relapsed CD30-positive lymphomas.* N Engl J Med, 2010. **363**(19): p. 1812-21.
32. Rothe, A., et al., *Brentuximab vedotin for relapsed or refractory CD30+ hematologic malignancies: the German Hodgkin Study Group experience.* Blood, 2012. **120**(7): p. 1470-2.
33. Pro, B., et al., *Brentuximab vedotin (SGN-35) in patients with relapsed or refractory systemic anaplastic large-cell lymphoma: results of a phase II study.* J Clin Oncol, 2012. **30**(18): p. 2190-6.

34. Forero-Torres, A., et al., *A Phase II study of SGN-30 (anti-CD30 mAb) in Hodgkin lymphoma or systemic anaplastic large cell lymphoma.* Br J Haematol, 2009. **146**(2): p. 171-9.
35. Bagcchi, S., *First-line crizotinib shows promise in patients with NSCLC.* Lancet Respir Med, 2015. **3**(1): p. 17.
36. Gambacorti-Passerini, C., C. Messa, and E.M. Pogliani, *Crizotinib in anaplastic large-cell lymphoma.* N Engl J Med, 2011. **364**(8): p. 775-6.
37. Gambacorti Passerini, C., et al., *Crizotinib in advanced, chemoresistant anaplastic lymphoma kinase-positive lymphoma patients.* J Natl Cancer Inst, 2014. **106**(2): p. djt378.
38. Cleary, J.M., et al., *Crizotinib as salvage and maintenance with allogeneic stem cell transplantation for refractory anaplastic large cell lymphoma.* J Natl Compr Canc Netw, 2014. **12**(3): p. 323-6; quiz 326.
39. Foss, H.D., et al., *Anaplastic large-cell lymphomas of T-cell and null-cell phenotype express cytotoxic molecules.* Blood, 1996. **88**(10): p. 4005-11.
40. Malcolm, T.I., et al., *Anaplastic large cell lymphoma arises in thymocytes and requires transient TCR expression for thymic egress.* Nat Commun, 2016. **7**: p. 10087.
41. Bonzheim, I., et al., *Anaplastic large cell lymphomas lack the expression of T-cell receptor molecules or molecules of proximal T-cell receptor signaling.* Blood, 2004. **104**(10): p. 3358-60.
42. Kanzler, H., et al., *Hodgkin and Reed-Sternberg-like cells in B-cell chronic lymphocytic leukemia represent the outgrowth of single germinal-center B-cell-derived clones: potential precursors of Hodgkin and Reed-Sternberg cells in Hodgkin's disease.* Blood, 2000. **95**(3): p. 1023-31.
43. Stein, H., et al., *Down-regulation of BOB.1/OBF.1 and Oct2 in classical Hodgkin disease but not in lymphocyte predominant Hodgkin disease correlates with immunoglobulin transcription.* Blood, 2001. **97**(2): p. 496-501.
44. Pai, S.Y., et al., *Critical roles for transcription factor GATA-3 in thymocyte development.* Immunity, 2003. **19**(6): p. 863-75.
45. Ambrogio, C., et al., *NPM-ALK oncogenic tyrosine kinase controls T-cell identity by transcriptional regulation and epigenetic silencing in lymphoma cells.* Cancer Res, 2009. **69**(22): p. 8611-9.
46. Turner, S.D., et al., *Anaplastic large cell lymphoma in paediatric and young adult patients.* Br J Haematol, 2016. **173**(4): p. 560-72.
47. Felgar, R.E., et al., *The expression of TIA-1+ cytolytic-type granules and other cytolytic lymphocyte-associated markers in CD30+ anaplastic large cell lymphomas (ALCL): correlation with morphology, immunophenotype, ultrastructure, and clinical features.* Hum Pathol, 1999. **30**(2): p. 228-36.
48. Schleussner, N., et al., *The AP-1-BATF and -BATF3 module is essential for growth, survival and TH17/ILC3 skewing of anaplastic large cell lymphoma.* Leukemia, 2018.
49. Chiarle, R., et al., *NPM-ALK transgenic mice spontaneously develop T-cell lymphomas and plasma cell tumors.* Blood, 2003. **101**(5): p. 1919-27.

50. Moti, N., et al., *Anaplastic large cell lymphoma-propagating cells are detectable by side population analysis and possess an expression profile reflective of a primitive origin.* Oncogene, 2015. **34**(14): p. 1843-52.
51. Muta, H. and E.R. Podack, *CD30: from basic research to cancer therapy.* Immunol Res, 2013. **57**(1-3): p. 151-8.
52. Hu, S., et al., *CD30 expression defines a novel subgroup of diffuse large B-cell lymphoma with favorable prognosis and distinct gene expression signature: a report from the International DLBCL Rituximab-CHOP Consortium Program Study.* Blood, 2013. **121**(14): p. 2715-24.
53. Hsu, F.Y., et al., *The expression of CD30 in anaplastic large cell lymphoma is regulated by nucleophosmin-anaplastic lymphoma kinase-mediated JunB level in a cell type-specific manner.* Cancer Res, 2006. **66**(18): p. 9002-8.
54. Watanabe, M., et al., *JunB induced by constitutive CD30-extracellular signal-regulated kinase 1/2 mitogen-activated protein kinase signaling activates the CD30 promoter in anaplastic large cell lymphoma and reed-sternberg cells of Hodgkin lymphoma.* Cancer Res, 2005. **65**(17): p. 7628-34.
55. Hsu, P.L. and S.M. Hsu, *Autocrine growth regulation of CD30 ligand in CD30-expressing Reed-Sternberg cells: distinction between Hodgkin's disease and anaplastic large cell lymphoma.* Lab Invest, 2000. **80**(7): p. 1111-9.
56. Horie, R., et al., *Ligand-independent signaling by overexpressed CD30 drives NF-kappaB activation in Hodgkin-Reed-Sternberg cells.* Oncogene, 2002. **21**(16): p. 2493-503.
57. Horie, R., et al., *The NPM-ALK oncoprotein abrogates CD30 signaling and constitutive NF-kappaB activation in anaplastic large cell lymphoma.* Cancer Cell, 2004. **5**(4): p. 353-64.
58. Al-Shamkhani, A., *The role of CD30 in the pathogenesis of haematopoietic malignancies.* Curr Opin Pharmacol, 2004. **4**(4): p. 355-9.
59. Horie, R., M. Higashihara, and T. Watanabe, *Hodgkin's lymphoma and CD30 signal transduction.* Int J Hematol, 2003. **77**(1): p. 37-47.
60. Watanabe, M., et al., *Ets-1 activates overexpression of JunB and CD30 in Hodgkin's lymphoma and anaplastic large-cell lymphoma.* Am J Pathol, 2012. **180**(2): p. 831-8.
61. Atsaves, V., et al., *The oncogenic JUNB/CD30 axis contributes to cell cycle deregulation in ALK+ anaplastic large cell lymphoma.* Br J Haematol, 2014. **167**(4): p. 514-23.
62. Wendtner, C.M., et al., *CD30 ligand signal transduction involves activation of a tyrosine kinase and of mitogen-activated protein kinase in a Hodgkin's lymphoma cell line.* Cancer Res, 1995. **55**(18): p. 4157-61.
63. Morris, S.W., et al., *Fusion of a kinase gene, ALK, to a nucleolar protein gene, NPM, in non-Hodgkin's lymphoma.* Science, 1994. **263**(5151): p. 1281-4.
64. Shiota, M., et al., *Hyperphosphorylation of a novel 80 kDa protein-tyrosine kinase similar to Ltk in a human Ki-1 lymphoma cell line, AMS3.* Oncogene, 1994. **9**(6): p. 1567-74.
65. Sugawara, E., et al., *Identification of anaplastic lymphoma kinase fusions in renal cancer: large-scale immunohistochemical screening by the intercalated antibody-enhanced polymer method.* Cancer, 2012. **118**(18): p. 4427-36.

66. Holla, V.R., et al., *ALK: a tyrosine kinase target for cancer therapy.* Cold Spring Harb Mol Case Stud, 2017. **3**(1): p. a001115.
67. Arber, D.A., L.H. Sun, and L.M. Weiss, *Detection of the t(2;5)(p23;q35) chromosomal translocation in large B-cell lymphomas other than anaplastic large cell lymphoma.* Hum Pathol, 1996. **27**(6): p. 590-4.
68. Tort, F., et al., *Molecular characterization of a new ALK translocation involving moesin (MSN-ALK) in anaplastic large cell lymphoma.* Lab Invest, 2001. **81**(3): p. 419-26.
69. Cools, J., et al., *Identification of novel fusion partners of ALK, the anaplastic lymphoma kinase, in anaplastic large-cell lymphoma and inflammatory myofibroblastic tumor.* Genes Chromosomes Cancer, 2002. **34**(4): p. 354-62.
70. Lamant, L., et al., *Non-muscle myosin heavy chain (MYH9): a new partner fused to ALK in anaplastic large cell lymphoma.* Genes Chromosomes Cancer, 2003. **37**(4): p. 427-32.
71. Lamant, L., et al., *A new fusion gene TPM3-ALK in anaplastic large cell lymphoma created by a (1;2)(q25;p23) translocation.* Blood, 1999. **93**(9): p. 3088-95.
72. Siebert, R., et al., *Complex variant translocation t(1;2) with TPM3-ALK fusion due to cryptic ALK gene rearrangement in anaplastic large-cell lymphoma.* Blood, 1999. **94**(10): p. 3614-7.
73. Lawrence, B., et al., *TPM3-ALK and TPM4-ALK oncogenes in inflammatory myofibroblastic tumors.* Am J Pathol, 2000. **157**(2): p. 377-84.
74. Meech, S.J., et al., *Unusual childhood extramedullary hematologic malignancy with natural killer cell properties that contains tropomyosin 4--anaplastic lymphoma kinase gene fusion.* Blood, 2001. **98**(4): p. 1209-16.
75. Jazii, F.R., et al., *Identification of squamous cell carcinoma associated proteins by proteomics and loss of beta tropomyosin expression in esophageal cancer.* World J Gastroenterol, 2006. **12**(44): p. 7104-12.
76. Du, X.L., et al., *Proteomic profiling of proteins dysregulted in Chinese esophageal squamous cell carcinoma.* J Mol Med (Berl), 2007. **85**(8): p. 863-75.
77. Hernandez, L., et al., *TRK-fused gene (TFG) is a new partner of ALK in anaplastic large cell lymphoma producing two structurally different TFG-ALK translocations.* Blood, 1999. **94**(9): p. 3265-8.
78. Rikova, K., et al., *Global survey of phosphotyrosine signaling identifies oncogenic kinases in lung cancer.* Cell, 2007. **131**(6): p. 1190-203.
79. Trinei, M., et al., *A new variant anaplastic lymphoma kinase (ALK)-fusion protein (ATIC-ALK) in a case of ALK-positive anaplastic large cell lymphoma.* Cancer Res, 2000. **60**(4): p. 793-8.
80. Ma, Z., et al., *Inv(2)(p23q35) in anaplastic large-cell lymphoma induces constitutive anaplastic lymphoma kinase (ALK) tyrosine kinase activation by fusion to ATIC, an enzyme involved in purine nucleotide biosynthesis.* Blood, 2000. **95**(6): p. 2144-9.
81. Colleoni, G.W., et al., *ATIC-ALK: A novel variant ALK gene fusion in anaplastic large cell lymphoma resulting from the recurrent cryptic chromosomal inversion, inv(2)(p23q35).* Am J Pathol, 2000. **156**(3): p. 781-9.

82. Debiec-Rychter, M., et al., *ALK-ATIC fusion in urinary bladder inflammatory myofibroblastic tumor.* Genes Chromosomes Cancer, 2003. **38**(2): p. 187-90.
83. Touriol, C., et al., *Further demonstration of the diversity of chromosomal changes involving 2p23 in ALK-positive lymphoma: 2 cases expressing ALK kinase fused to CLTCL (clathrin chain polypeptide-like).* Blood, 2000. **95**(10): p. 3204-7.
84. Bridge, J.A., et al., *Fusion of the ALK gene to the clathrin heavy chain gene, CLTC, in inflammatory myofibroblastic tumor.* Am J Pathol, 2001. **159**(2): p. 411-5.
85. De Paepe, P., et al., *ALK activation by the CLTC-ALK fusion is a recurrent event in large B-cell lymphoma.* Blood, 2003. **102**(7): p. 2638-41.
86. Gascoyne, R.D., et al., *ALK-positive diffuse large B-cell lymphoma is associated with Clathrin-ALK rearrangements: report of 6 cases.* Blood, 2003. **102**(7): p. 2568-73.
87. Ma, Z., et al., *Fusion of ALK to the Ran-binding protein 2 (RANBP2) gene in inflammatory myofibroblastic tumor.* Genes Chromosomes Cancer, 2003. **37**(1): p. 98-105.
88. Panagopoulos, I., et al., *Fusion of the SEC31L1 and ALK genes in an inflammatory myofibroblastic tumor.* Int J Cancer, 2006. **118**(5): p. 1181-6.
89. Van Roosbroeck, K., et al., *ALK-positive large B-cell lymphomas with cryptic SEC31A-ALK and NPM1-ALK fusions.* Haematologica, 2010. **95**(3): p. 509-13.
90. Bedwell, C., et al., *Cytogenetically complex SEC31A-ALK fusions are recurrent in ALK-positive large B-cell lymphomas.* Haematologica, 2011. **96**(2): p. 343-6.
91. Takeuchi, K., et al., *Pulmonary inflammatory myofibroblastic tumor expressing a novel fusion, PPFIBP1-ALK: reappraisal of anti-ALK immunohistochemistry as a tool for novel ALK fusion identification.* Clin Cancer Res, 2011. **17**(10): p. 3341-8.
92. Takeuchi, K., et al., *Identification of a novel fusion, SQSTM1-ALK, in ALK-positive large B-cell lymphoma.* Haematologica, 2011. **96**(3): p. 464-7.
93. Soda, M., et al., *Identification of the transforming EML4-ALK fusion gene in non-small-cell lung cancer.* Nature, 2007. **448**(7153): p. 561-6.
94. Lin, E., et al., *Exon array profiling detects EML4-ALK fusion in breast, colorectal, and non-small cell lung cancers.* Mol Cancer Res, 2009. **7**(9): p. 1466-76.
95. Takeuchi, K., et al., *KIF5B-ALK, a novel fusion oncokinase identified by an immunohistochemistry-based diagnostic system for ALK-positive lung cancer.* Clin Cancer Res, 2009. **15**(9): p. 3143-9.
96. Togashi, Y., et al., *KLC1-ALK: a novel fusion in lung cancer identified using a formalin-fixed paraffin-embedded tissue only.* PLoS One, 2012. **7**(2): p. e31323.
97. Lipson, D., et al., *Identification of new ALK and RET gene fusions from colorectal and lung cancer biopsies.* Nat Med, 2012. **18**(3): p. 382-4.
98. Debelenko, L.V., et al., *Renal cell carcinoma with novel VCL-ALK fusion: new representative of ALK-associated tumor spectrum.* Mod Pathol, 2011. **24**(3): p. 430-42.

99. Marino-Enriquez, A., et al., *ALK rearrangement in sickle cell trait-associated renal medullary carcinoma.* Genes Chromosomes Cancer, 2011. **50**(3): p. 146-53.
100. Iwahara, T., et al., *Molecular characterization of ALK, a receptor tyrosine kinase expressed specifically in the nervous system.* Oncogene, 1997. **14**(4): p. 439-49.
101. Morris, S.W., et al., *ALK, the chromosome 2 gene locus altered by the t(2;5) in non-Hodgkin's lymphoma, encodes a novel neural receptor tyrosine kinase that is highly related to leukocyte tyrosine kinase (LTK).* Oncogene, 1997. **14**(18): p. 2175-88.
102. Fadeev, A., et al., *ALKALs are in vivo ligands for ALK family receptor tyrosine kinases in the neural crest and derived cells.* Proc Natl Acad Sci U S A, 2018. **115**(4): p. E630-E638.
103. Mo, E.S., et al., *Alk and Ltk ligands are essential for iridophore development in zebrafish mediated by the receptor tyrosine kinase Ltk.* Proc Natl Acad Sci U S A, 2017. **114**(45): p. 12027-12032.
104. Reshetnyak, A.V., et al., *Augmentor alpha and beta (FAM150) are ligands of the receptor tyrosine kinases ALK and LTK: Hierarchy and specificity of ligand-receptor interactions.* Proc Natl Acad Sci U S A, 2015. **112**(52): p. 15862-7.
105. Palmer, R.H., et al., *Anaplastic lymphoma kinase: signalling in development and disease.* Biochem J, 2009. **420**(3): p. 345-61.
106. Bilsland, J.G., et al., *Behavioral and neurochemical alterations in mice deficient in anaplastic lymphoma kinase suggest therapeutic potential for psychiatric indications.* Neuropsychopharmacology, 2008. **33**(3): p. 685-700.
107. Weiss, J.B., et al., *Anaplastic lymphoma kinase and leukocyte tyrosine kinase: functions and genetic interactions in learning, memory and adult neurogenesis.* Pharmacol Biochem Behav, 2012. **100**(3): p. 566-74.
108. Lasek, A.W., et al., *An evolutionary conserved role for anaplastic lymphoma kinase in behavioral responses to ethanol.* PLoS One, 2011. **6**(7): p. e22636.
109. Mi, R., W. Chen, and A. Hoke, *Pleiotrophin is a neurotrophic factor for spinal motor neurons.* Proc Natl Acad Sci U S A, 2007. **104**(11): p. 4664-9.
110. Amin, H.M. and R. Lai, *Pathobiology of ALK+ anaplastic large-cell lymphoma.* Blood, 2007. **110**(7): p. 2259-67.
111. Bischof, D., et al., *Role of the nucleophosmin (NPM) portion of the non-Hodgkin's lymphoma-associated NPM-anaplastic lymphoma kinase fusion protein in oncogenesis.* Mol Cell Biol, 1997. **17**(4): p. 2312-25.
112. Tort, F., et al., *Heterogeneity of genomic breakpoints in MSN-ALK translocations in anaplastic large cell lymphoma.* Hum Pathol, 2004. **35**(8): p. 1038-41.
113. Bai, R.Y., et al., *Nucleophosmin-anaplastic lymphoma kinase of large-cell anaplastic lymphoma is a constitutively active tyrosine kinase that utilizes phospholipase C-gamma to mediate its mitogenicity.* Mol Cell Biol, 1998. **18**(12): p. 6951-61.
114. Turner, S.D., et al., *Vav-promoter regulated oncogenic fusion protein NPM-ALK in transgenic mice causes B-cell lymphomas with hyperactive Jun kinase.* Oncogene, 2003. **22**(49): p. 7750-61.

115. Turner, S.D., et al., *CD2 promoter regulated nucleophosmin-anaplastic lymphoma kinase in transgenic mice causes B lymphoid malignancy.* Anticancer Res, 2006. **26**(5A): p. 3275-9.
116. Miething, C., et al., *The oncogenic fusion protein nucleophosmin-anaplastic lymphoma kinase (NPM-ALK) induces two distinct malignant phenotypes in a murine retroviral transplantation model.* Oncogene, 2003. **22**(30): p. 4642-7.
117. Lange, K., et al., *Overexpression of NPM-ALK induces different types of malignant lymphomas in IL-9 transgenic mice.* Oncogene, 2003. **22**(4): p. 517-27.
118. Kuefer, M.U., et al., *Retrovirus-mediated gene transfer of NPM-ALK causes lymphoid malignancy in mice.* Blood, 1997. **90**(8): p. 2901-10.
119. Johnston, P.A. and J.R. Grandis, *STAT3 signaling: anticancer strategies and challenges.* Mol Interv, 2011. **11**(1): p. 18-26.
120. Zamo, A., et al., *Anaplastic lymphoma kinase (ALK) activates Stat3 and protects hematopoietic cells from cell death.* Oncogene, 2002. **21**(7): p. 1038-47.
121. Amin, H.M., et al., *Inhibition of JAK3 induces apoptosis and decreases anaplastic lymphoma kinase activity in anaplastic large cell lymphoma.* Oncogene, 2003. **22**(35): p. 5399-407.
122. Marzec, M., et al., *Inhibition of ALK enzymatic activity in T-cell lymphoma cells induces apoptosis and suppresses proliferation and STAT3 phosphorylation independently of Jak3.* Lab Invest, 2005. **85**(12): p. 1544-54.
123. Zhang, Q., et al., *Multilevel dysregulation of STAT3 activation in anaplastic lymphoma kinase-positive T/null-cell lymphoma.* J Immunol, 2002. **168**(1): p. 466-74.
124. Khoury, J.D., et al., *Differential expression and clinical significance of tyrosine-phosphorylated STAT3 in ALK+ and ALK- anaplastic large cell lymphoma.* Clin Cancer Res, 2003. **9**(10 Pt 1): p. 3692-9.
125. Chiarle, R., et al., *Stat3 is required for ALK-mediated lymphomagenesis and provides a possible therapeutic target.* Nat Med, 2005. **11**(6): p. 623-9.
126. Amin, H.M., et al., *Selective inhibition of STAT3 induces apoptosis and G(1) cell cycle arrest in ALK-positive anaplastic large cell lymphoma.* Oncogene, 2004. **23**(32): p. 5426-34.
127. Piva, R., et al., *Gene expression profiling uncovers molecular classifiers for the recognition of anaplastic large-cell lymphoma within peripheral T-cell neoplasms.* J Clin Oncol, 2010. **28**(9): p. 1583-90.
128. Zhang, Q., et al., *Oncogenic tyrosine kinase NPM-ALK induces expression of the growth-promoting receptor ICOS.* Blood, 2011. **118**(11): p. 3062-71.
129. Anastasov, N., et al., *C/EBPbeta expression in ALK-positive anaplastic large cell lymphomas is required for cell proliferation and is induced by the STAT3 signaling pathway.* Haematologica, 2010. **95**(5): p. 760-7.
130. Coluccia, A.M., et al., *Bcl-XL down-regulation suppresses the tumorigenic potential of NPM/ALK in vitro and in vivo.* Blood, 2004. **103**(7): p. 2787-94.
131. Piva, R., et al., *Functional validation of the anaplastic lymphoma kinase signature identifies CEBPB and BCL2A1 as critical target genes.* J Clin Invest, 2006. **116**(12): p. 3171-82.

132. Prutsch, N., et al., *Dependency on the TYK2/STAT1/MCL1 axis in anaplastic large cell lymphoma.* Leukemia, 2018.
133. Bai, R.Y., et al., *Nucleophosmin-anaplastic lymphoma kinase associated with anaplastic large-cell lymphoma activates the phosphatidylinositol 3-kinase/Akt antiapoptotic signaling pathway.* Blood, 2000. **96**(13): p. 4319-27.
134. Slupianek, A., et al., *Role of phosphatidylinositol 3-kinase-Akt pathway in nucleophosmin/anaplastic lymphoma kinase-mediated lymphomagenesis.* Cancer Res, 2001. **61**(5): p. 2194-9.
135. Gu, T.L., et al., *NPM-ALK fusion kinase of anaplastic large-cell lymphoma regulates survival and proliferative signaling through modulation of FOXO3a.* Blood, 2004. **103**(12): p. 4622-9.
136. Staber, P.B., et al., *The oncoprotein NPM-ALK of anaplastic large-cell lymphoma induces JUNB transcription via ERK1/2 and JunB translation via mTOR signaling.* Blood, 2007. **110**(9): p. 3374-83.
137. Rassidakis, G.Z., et al., *Rapamycin sensitizes tumor cells to chemotherapy-induced apoptosis and induces cell cycle arrest in ALK+ anaplastic large cell lymphoma.* Cancer Research, 2005. **65**(9 Supplement): p. 106-107.
138. Fujimoto, J., et al., *Characterization of the transforming activity of p80, a hyperphosphorylated protein in a Ki-1 lymphoma cell line with chromosomal translocation t(2;5).* Proc Natl Acad Sci U S A, 1996. **93**(9): p. 4181-6.
139. Pulford, K., S.W. Morris, and F. Turturro, *Anaplastic lymphoma kinase proteins in growth control and cancer.* J Cell Physiol, 2004. **199**(3): p. 330-58.
140. Marzec, M., et al., *Oncogenic tyrosine kinase NPM/ALK induces activation of the rapamycin-sensitive mTOR signaling pathway.* Oncogene, 2007. **26**(38): p. 5606-14.
141. Vega, F., et al., *Activation of mammalian target of rapamycin signaling pathway contributes to tumor cell survival in anaplastic lymphoma kinase-positive anaplastic large cell lymphoma.* Cancer Res, 2006. **66**(13): p. 6589-97.
142. Leventaki, V., et al., *NPM-ALK oncogenic kinase promotes cell-cycle progression through activation of JNK/cJun signaling in anaplastic large-cell lymphoma.* Blood, 2007. **110**(5): p. 1621-30.
143. Ambrogio, C., et al., *p130Cas mediates the transforming properties of the anaplastic lymphoma kinase.* Blood, 2005. **106**(12): p. 3907-16.
144. Voena, C., et al., *The tyrosine phosphatase Shp2 interacts with NPM-ALK and regulates anaplastic lymphoma cell growth and migration.* Cancer Res, 2007. **67**(9): p. 4278-86.
145. Armstrong, F., et al., *Differential effects of X-ALK fusion proteins on proliferation, transformation, and invasion properties of NIH3T3 cells.* Oncogene, 2004. **23**(36): p. 6071-82.
146. Cussac, D., et al., *Nucleophosmin-anaplastic lymphoma kinase of anaplastic large-cell lymphoma recruits, activates, and uses pp60c-src to mediate its mitogenicity.* Blood, 2004. **103**(4): p. 1464-71.
147. Colomba, A., et al., *Activation of Rac1 and the exchange factor Vav3 are involved in NPM-ALK signaling in anaplastic large cell lymphomas.* Oncogene, 2008. **27**(19): p. 2728-36.

148. Curran, T., et al., *FBJ murine osteosarcoma virus: identification and molecular cloning of biologically active proviral DNA.* J Virol, 1982. **44**(2): p. 674-82.
149. Curran, T. and N.M. Teich, *Candidate product of the FBJ murine osteosarcoma virus oncogene: characterization of a 55,000-dalton phosphoprotein.* J Virol, 1982. **42**(1): p. 114-22.
150. Lee, W., et al., *Activation of transcription by two factors that bind promoter and enhancer sequences of the human metallothionein gene and SV40.* Nature, 1987. **325**(6102): p. 368-72.
151. Lee, W., P. Mitchell, and R. Tjian, *Purified transcription factor AP-1 interacts with TPA-inducible enhancer elements.* Cell, 1987. **49**(6): p. 741-52.
152. Maki, Y., et al., *Avian sarcoma virus 17 carries the jun oncogene.* Proc Natl Acad Sci U S A, 1987. **84**(9): p. 2848-52.
153. Vogt, P.K., T.J. Bos, and R.F. Doolittle, *Homology between the DNA-binding domain of the GCN4 regulatory protein of yeast and the carboxyl-terminal region of a protein coded for by the oncogene jun.* Proc Natl Acad Sci U S A, 1987. **84**(10): p. 3316-9.
154. Bohmann, D., et al., *Human proto-oncogene c-jun encodes a DNA binding protein with structural and functional properties of transcription factor AP-1.* Science, 1987. **238**(4832): p. 1386-92.
155. Angel, P., et al., *Oncogene jun encodes a sequence-specific trans-activator similar to AP-1.* Nature, 1988. **332**(6160): p. 166-71.
156. Chiu, R., et al., *The c-Fos protein interacts with c-Jun/AP-1 to stimulate transcription of AP-1 responsive genes.* Cell, 1988. **54**(4): p. 541-52.
157. Rauscher, F.J., 3rd, et al., *Fos and Jun bind cooperatively to the AP-1 site: reconstitution in vitro.* Genes Dev, 1988. **2**(12B): p. 1687-99.
158. Eychene, A., N. Rocques, and C. Pouponnot, *A new MAFia in cancer.* Nat Rev Cancer, 2008. **8**(9): p. 683-93.
159. Shaulian, E., *AP-1--The Jun proteins: Oncogenes or tumor suppressors in disguise?* Cell Signal, 2010. **22**(6): p. 894-9.
160. Chinenov, Y. and T.K. Kerppola, *Close encounters of many kinds: Fos-Jun interactions that mediate transcription regulatory specificity.* Oncogene, 2001. **20**(19): p. 2438-52.
161. Hess, J., P. Angel, and M. Schorpp-Kistner, *AP-1 subunits: quarrel and harmony among siblings.* J Cell Sci, 2004. **117**(Pt 25): p. 5965-73.
162. Kataoka, K., M. Noda, and M. Nishizawa, *Maf nuclear oncoprotein recognizes sequences related to an AP-1 site and forms heterodimers with both Fos and Jun.* Mol Cell Biol, 1994. **14**(1): p. 700-12.
163. Kerppola, T.K. and T. Curran, *A conserved region adjacent to the basic domain is required for recognition of an extended DNA binding site by Maf/Nrl family proteins.* Oncogene, 1994. **9**(11): p. 3149-58.
164. Garces de Los Fayos Alonso, I., et al., *The Role of Activator Protein-1 (AP-1) Family Members in CD30-Positive Lymphomas.* Cancers (Basel), 2018. **10**(4).
165. Wagner, E.F. and R. Eferl, *Fos/AP-1 proteins in bone and the immune system.* Immunol Rev, 2005. **208**: p. 126-40.
166. Jochum, W., E. Passegue, and E.F. Wagner, *AP-1 in mouse development and tumorigenesis.* Oncogene, 2001. **20**(19): p. 2401-12.

167. Hilberg, F., et al., *c-jun is essential for normal mouse development and hepatogenesis.* Nature, 1993. **365**(6442): p. 179-81.
168. Johnson, R.S., et al., *A null mutation at the c-jun locus causes embryonic lethality and retarded cell growth in culture.* Genes Dev, 1993. **7**(7B): p. 1309-17.
169. Schorpp-Kistner, M., et al., *JunB is essential for mammalian placentation.* EMBO J, 1999. **18**(4): p. 934-48.
170. Eferl, R., et al., *Functions of c-Jun in liver and heart development.* J Cell Biol, 1999. **145**(5): p. 1049-61.
171. Chen, J., et al., *Generation of normal T and B lymphocytes by c-jun deficient embryonic stem cells.* Immunity, 1994. **1**(1): p. 65-72.
172. Behrens, A., et al., *Jun N-terminal kinase 2 modulates thymocyte apoptosis and T cell activation through c-Jun and nuclear factor of activated T cell (NF-AT).* Proc Natl Acad Sci U S A, 2001. **98**(4): p. 1769-74.
173. Passegue, E., et al., *Chronic myeloid leukemia with increased granulocyte progenitors in mice lacking junB expression in the myeloid lineage.* Cell, 2001. **104**(1): p. 21-32.
174. Li, B., et al., *Regulation of IL-4 expression by the transcription factor JunB during T helper cell differentiation.* EMBO J, 1999. **18**(2): p. 420-32.
175. Schreiber, M., et al., *Control of cell cycle progression by c-Jun is p53 dependent.* Genes Dev, 1999. **13**(5): p. 607-19.
176. Bakiri, L., et al., *Cell cycle-dependent variations in c-Jun and JunB phosphorylation: a role in the control of cyclin D1 expression.* EMBO J, 2000. **19**(9): p. 2056-68.
177. Wisdom, R., R.S. Johnson, and C. Moore, *c-Jun regulates cell cycle progression and apoptosis by distinct mechanisms.* EMBO J, 1999. **18**(1): p. 188-97.
178. Passegue, E. and E.F. Wagner, *JunB suppresses cell proliferation by transcriptional activation of p16(INK4a) expression.* EMBO J, 2000. **19**(12): p. 2969-79.
179. Papoudou-Bai, A., et al., *The expression levels of JunB, JunD and p-c-Jun are positively correlated with tumor cell proliferation in diffuse large B-cell lymphomas.* Leuk Lymphoma, 2016. **57**(1): p. 143-50.
180. Eckhoff, K., et al., *The prognostic significance of Jun transcription factors in ovarian cancer.* J Cancer Res Clin Oncol, 2013. **139**(10): p. 1673-80.
181. Xia, Y., et al., *Differential regulation of c-Jun protein plays an instrumental role in chemoresistance of cancer cells.* J Biol Chem, 2013. **288**(27): p. 19321-9.
182. Saez, E., et al., *c-fos is required for malignant progression of skin tumors.* Cell, 1995. **82**(5): p. 721-32.
183. Zenz, R., et al., *c-Jun regulates eyelid closure and skin tumor development through EGFR signaling.* Dev Cell, 2003. **4**(6): p. 879-89.
184. Ivanov, V.N., et al., *Cooperation between STAT3 and c-jun suppresses Fas transcription.* Mol Cell, 2001. **7**(3): p. 517-28.
185. Eferl, R., et al., *Liver tumor development. c-Jun antagonizes the proapoptotic activity of p53.* Cell, 2003. **112**(2): p. 181-92.

186. Mariani, O., et al., *JUN oncogene amplification and overexpression block adipocytic differentiation in highly aggressive sarcomas.* Cancer Cell, 2007. **11**(4): p. 361-74.
187. Nateri, A.S., B. Spencer-Dene, and A. Behrens, *Interaction of phosphorylated c-Jun with TCF4 regulates intestinal cancer development.* Nature, 2005. **437**(7056): p. 281-5.
188. Gan, X.Q., et al., *Nuclear Dvl, c-Jun, beta-catenin, and TCF form a complex leading to stabilization of beta-catenin-TCF interaction.* J Cell Biol, 2008. **180**(6): p. 1087-100.
189. Sancho, R., et al., *JNK signalling modulates intestinal homeostasis and tumourigenesis in mice.* EMBO J, 2009. **28**(13): p. 1843-54.
190. Toualbi, K., et al., *Physical and functional cooperation between AP-1 and beta-catenin for the regulation of TCF-dependent genes.* Oncogene, 2007. **26**(24): p. 3492-502.
191. Hanahan, D. and R.A. Weinberg, *Hallmarks of cancer: the next generation.* Cell, 2011. **144**(5): p. 646-74.
192. Marques, N., et al., *Regulation of protein translation and c-Jun expression by prostate tumor overexpressed 1.* Oncogene, 2014. **33**(9): p. 1124-34.
193. Lin, Z.Y., et al., *MicroRNA-30d promotes angiogenesis and tumor growth via MYPT1/c-JUN/VEGFA pathway and predicts aggressive outcome in prostate cancer.* Mol Cancer, 2017. **16**(1): p. 48.
194. Vleugel, M.M., et al., *c-Jun activation is associated with proliferation and angiogenesis in invasive breast cancer.* Hum Pathol, 2006. **37**(6): p. 668-74.
195. Zhao, C., et al., *Genome-wide profiling of AP-1-regulated transcription provides insights into the invasiveness of triple-negative breast cancer.* Cancer Res, 2014. **74**(14): p. 3983-94.
196. Comijn, J., et al., *The two-handed E box binding zinc finger protein SIP1 downregulates E-cadherin and induces invasion.* Mol Cell, 2001. **7**(6): p. 1267-78.
197. Gokulnath, M., et al., *Transforming growth factor-beta1 regulation of ATF-3, c-Jun and JunB proteins for activation of matrix metalloproteinase-13 gene in human breast cancer cells.* Int J Biol Macromol, 2017. **94**(Pt A): p. 370-377.
198. Blonska, M., et al., *Jun-regulated genes promote interaction of diffuse large B-cell lymphoma with the microenvironment.* Blood, 2015. **125**(6): p. 981-91.
199. Luo, A., et al., *Differentiation-associated genes regulated by c-Jun and decreased in the progression of esophageal squamous cell carcinoma.* PLoS One, 2014. **9**(5): p. e96610.
200. Kharman-Biz, A., et al., *Expression of activator protein-1 (AP-1) family members in breast cancer.* BMC Cancer, 2013. **13**: p. 441.
201. Sreeramaneni, R., et al., *Ras-Raf-Arf signaling critically depends on the Dmp1 transcription factor.* Mol Cell Biol, 2005. **25**(1): p. 220-32.
202. Eferl, R. and E.F. Wagner, *AP-1: a double-edged sword in tumorigenesis.* Nat Rev Cancer, 2003. **3**(11): p. 859-68.
203. Andrecht, S., et al., *Cell cycle promoting activity of JunB through cyclin A activation.* J Biol Chem, 2002. **277**(39): p. 35961-8.

204. Gurzov, E.N., et al., *JunB Inhibits ER Stress and Apoptosis in Pancreatic Beta Cells.* PLoS One, 2008. **3**(8): p. e3030.
205. Winter, C., et al., *JunB and Bcl-2 overexpression results in protection against cell death of nigral neurons following axotomy.* Brain Res Mol Brain Res, 2002. **104**(2): p. 194-202.
206. Kovary, K. and R. Bravo, *The jun and fos protein families are both required for cell cycle progression in fibroblasts.* Mol Cell Biol, 1991. **11**(9): p. 4466-72.
207. Bossy-Wetzel, E., D.D. Newmeyer, and D.R. Green, *Mitochondrial cytochrome c release in apoptosis occurs upstream of DEVD-specific caspase activation and independently of mitochondrial transmembrane depolarization.* EMBO J, 1998. **17**(1): p. 37-49.
208. Passegue, E., et al., *JunB can substitute for Jun in mouse development and cell proliferation.* Nat Genet, 2002. **30**(2): p. 158-66.
209. Mathas, S., et al., *Aberrantly expressed c-Jun and JunB are a hallmark of Hodgkin lymphoma cells, stimulate proliferation and synergize with NF-kappa B.* EMBO J, 2002. **21**(15): p. 4104-13.
210. Devary, Y., et al., *Rapid and preferential activation of the c-jun gene during the mammalian UV response.* Mol Cell Biol, 1991. **11**(5): p. 2804-11.
211. Mao, X., et al., *BCL2 and JUNB abnormalities in primary cutaneous lymphomas.* Br J Dermatol, 2004. **151**(3): p. 546-56.
212. Mao, X., et al., *Amplification and overexpression of JUNB is associated with primary cutaneous T-cell lymphomas.* Blood, 2003. **101**(4): p. 1513-9.
213. Troen, G., et al., *Constitutive expression of the AP-1 transcription factors c-jun, junD, junB, and c-fos and the marginal zone B-cell transcription factor Notch2 in splenic marginal zone lymphoma.* J Mol Diagn, 2004. **6**(4): p. 297-307.
214. Fan, F., et al., *The AP-1 transcription factor JunB is essential for multiple myeloma cell proliferation and drug resistance in the bone marrow microenvironment.* Leukemia, 2017. **31**(7): p. 1570-1581.
215. Sundqvist, A., et al., *JUNB governs a feed-forward network of TGFbeta signaling that aggravates breast cancer invasion.* Nucleic Acids Res, 2018. **46**(3): p. 1180-1195.
216. Hicks, M., et al., *JUNB promotes the survival of Flavopiridol treated human breast cancer cells.* Biochem Biophys Res Commun, 2014. **450**(1): p. 19-24.
217. Lian, S., et al., *PDK1 induces JunB, EMT, cell migration and invasion in human gallbladder cancer.* Oncotarget, 2015. **6**(30): p. 29076-86.
218. Yogev, O., et al., *Jun proteins are starvation-regulated inhibitors of autophagy.* Cancer Res, 2010. **70**(6): p. 2318-27.
219. Thomsen, M.K., et al., *Loss of JUNB/AP-1 promotes invasive prostate cancer.* Cell Death Differ, 2015. **22**(4): p. 574-82.
220. Schorpp, M., et al., *The human ubiquitin C promoter directs high ubiquitous expression of transgenes in mice.* Nucleic Acids Res, 1996. **24**(9): p. 1787-8.
221. Szremska, A.P., et al., *JunB inhibits proliferation and transformation in B-lymphoid cells.* Blood, 2003. **102**(12): p. 4159-65.
222. Yang, M.Y., et al., *JunB gene expression is inactivated by methylation in chronic myeloid leukemia.* Blood, 2003. **101**(8): p. 3205-11.

223. Steidl, U., et al., *Essential role of Jun family transcription factors in PU.1 knockdown-induced leukemic stem cells.* Nat Genet, 2006. **38**(11): p. 1269-77.
224. Fan, S.J., et al., *miRNA-149* promotes cell proliferation and suppresses apoptosis by mediating JunB in T-cell acute lymphoblastic leukemia.* Leuk Res, 2016. **41**: p. 62-70.
225. Perez-Benavente, B., et al., *GSK3-SCF(FBXW7) targets JunB for degradation in G2 to preserve chromatid cohesion before anaphase.* Oncogene, 2013. **32**(17): p. 2189-99.
226. Smeal, T., et al., *Oncogenic and transcriptional cooperation with Ha-Ras requires phosphorylation of c-Jun on serines 63 and 73.* Nature, 1991. **354**(6353): p. 494-6.
227. Tsai, L.N., et al., *Extracellular signals regulate rapid coactivator recruitment at AP-1 sites by altered phosphorylation of both CREB binding protein and c-jun.* Mol Cell Biol, 2008. **28**(13): p. 4240-50.
228. Lollies, A., et al., *An oncogenic axis of STAT-mediated BATF3 upregulation causing MYC activity in classical Hodgkin lymphoma and anaplastic large cell lymphoma.* Leukemia, 2017.
229. Laimer, D., et al., *PDGFR blockade is a rational and effective therapy for NPM-ALK-driven lymphomas.* Nat Med, 2012. **18**(11): p. 1699-704.
230. Pearson, J.D., et al., *The heat shock protein-90 co-chaperone, Cyclophilin 40, promotes ALK-positive, anaplastic large cell lymphoma viability and its expression is regulated by the NPM-ALK oncoprotein.* BMC Cancer, 2012. **12**: p. 229.
231. Pearson, J.D., et al., *NPM-ALK and the JunB transcription factor regulate the expression of cytotoxic molecules in ALK-positive, anaplastic large cell lymphoma.* Int J Clin Exp Pathol, 2011. **4**(2): p. 124-33.
232. Atsaves, V., et al., *Constitutive control of AKT1 gene expression by JUNB/CJUN in ALK+ anaplastic large-cell lymphoma: a novel crosstalk mechanism.* Leukemia, 2015. **29**(11): p. 2162-72.
233. Young, L.C., et al., *Fusion tyrosine kinase NPM-ALK Deregulates MSH2 and suppresses DNA mismatch repair function novel insights into a potent oncoprotein.* Am J Pathol, 2011. **179**(1): p. 411-21.
234. Livak, K.J. and T.D. Schmittgen, *Analysis of relative gene expression data using real-time quantitative PCR and the 2(T)(-Delta Delta C) method.* Methods, 2001. **25**(4): p. 402-408.
235. Kim, J.H., et al., *High cleavage efficiency of a 2A peptide derived from porcine teschovirus-1 in human cell lines, zebrafish and mice.* PLoS One, 2011. **6**(4): p. e18556.
236. Korzynska, A., Zychowicz, M., *A Method of Estimation of the Cell Doubling Time on Basis of the Cell Culture Monitoring Data.* Biocybernetics and Biomedical Engineering, 2008. **28**(75-82).
237. Solovei, I., Schermelleh, L., Albeiz, H., Cremer, T. , *Detection of Cell Cycle Stages in situ in Growing Cell Populations.*, in *Cell biology : a laboratory handbook* J.E. Celis, Editor. 2006, Elsevier Academic: Boston. p. p. 293.
238. Somanchi, S.S., et al., *A Novel Method for Assessment of Natural Killer Cell Cytotoxicity Using Image Cytometry.* PLoS One, 2015. **10**(10): p. e0141074.

239. Zhang, Y., et al., *Model-based analysis of ChIP-Seq (MACS).* Genome Biol, 2008. **9**(9): p. R137.
240. Zang, C., et al., *A clustering approach for identification of enriched domains from histone modification ChIP-Seq data.* Bioinformatics, 2009. **25**(15): p. 1952-8.
241. Heinz, S., et al., *Simple combinations of lineage-determining transcription factors prime cis-regulatory elements required for macrophage and B cell identities.* Mol Cell, 2010. **38**(4): p. 576-89.
242. Huang da, W., B.T. Sherman, and R.A. Lempicki, *Systematic and integrative analysis of large gene lists using DAVID bioinformatics resources.* Nat Protoc, 2009. **4**(1): p. 44-57.
243. Zhang, J., et al., *The c-Jun and JunB transcription factors facilitate the transit of classical Hodgkin lymphoma tumour cells through G1.* Scientific Reports, 2018. **8**(1): p. 16019.
244. Kyrylkova, K., et al., *Detection of apoptosis by TUNEL assay.* Methods Mol Biol, 2012. **887**: p. 41-7.
245. Yousefi, M., et al., *Msi RNA-binding proteins control reserve intestinal stem cell quiescence.* J Cell Biol, 2016. **215**(3): p. 401-413.
246. Eddaoudi, A., S.L. Canning, and I. Kato, *Flow Cytometric Detection of G0 in Live Cells by Hoechst 33342 and Pyronin Y Staining.* Methods Mol Biol, 2018. **1686**: p. 49-57.
247. Kapuscinski, J., *DAPI: a DNA-specific fluorescent probe.* Biotech Histochem, 1995. **70**(5): p. 220-33.
248. Lopez, F., et al., *Modalities of synthesis of Ki67 antigen during the stimulation of lymphocytes.* Cytometry, 1991. **12**(1): p. 42-9.
249. Scholzen, T. and J. Gerdes, *The Ki-67 protein: from the known and the unknown.* J Cell Physiol, 2000. **182**(3): p. 311-22.
250. Chu, I.M., L. Hengst, and J.M. Slingerland, *The Cdk inhibitor p27 in human cancer: prognostic potential and relevance to anticancer therapy.* Nat Rev Cancer, 2008. **8**(4): p. 253-67.
251. le Sage, C., R. Nagel, and R. Agami, *Diverse ways to control p27Kip1 function: miRNAs come into play.* Cell Cycle, 2007. **6**(22): p. 2742-9.
252. Galardi, S., et al., *miR-221 and miR-222 expression affects the proliferation potential of human prostate carcinoma cell lines by targeting p27Kip1.* J Biol Chem, 2007. **282**(32): p. 23716-24.
253. Volinia, S., et al., *A microRNA expression signature of human solid tumors defines cancer gene targets.* Proc Natl Acad Sci U S A, 2006. **103**(7): p. 2257-61.
254. Visone, R., et al., *MicroRNAs (miR)-221 and miR-222, both overexpressed in human thyroid papillary carcinomas, regulate p27Kip1 protein levels and cell cycle.* Endocr Relat Cancer, 2007. **14**(3): p. 791-8.
255. Calin, G.A., et al., *A MicroRNA signature associated with prognosis and progression in chronic lymphocytic leukemia.* N Engl J Med, 2005. **353**(17): p. 1793-801.
256. Nakayama, K.I. and K. Nakayama, *Ubiquitin ligases: cell-cycle control and cancer.* Nat Rev Cancer, 2006. **6**(5): p. 369-81.

257. Bloom, J. and M. Pagano, *Deregulated degradation of the cdk inhibitor p27 and malignant transformation.* Semin Cancer Biol, 2003. **13**(1): p. 41-7.
258. Moller, M.B., et al., *Clinical significance of cyclin-dependent kinase inhibitor p27Kip1 expression and proliferation in non-Hodgkin's lymphoma: independent prognostic value of p27Kip1.* Br J Haematol, 1999. **105**(3): p. 730-6.
259. Andreu, E.J., et al., *BCR-ABL induces the expression of Skp2 through the PI3K pathway to promote p27Kip1 degradation and proliferation of chronic myelogenous leukemia cells.* Cancer Res, 2005. **65**(8): p. 3264-72.
260. Turturro, F. and P. Seth, *Prolonged adenovirus-mediated expression of p27(Kip1) unveils unexpected effects of this protein on the phenotype of SUDHL-1 cells derived from t(2;5)-anaplastic large cell lymphoma.* Leuk Res, 2003. **27**(4): p. 329-35.
261. Turturro, F., et al., *Effects of adenovirus-mediated expression of p27Kip1, p21Waf1 and p16INK4A in cell lines derived from t(2;5) anaplastic large cell lymphoma and Hodgkin's disease.* Leuk Lymphoma, 2002. **43**(6): p. 1323-8.
262. Turturro, F., et al., *Biochemical differences between SUDHL-1 and KARPAS 299 cells derived from t(2;5)-positive anaplastic large cell lymphoma are responsible for the different sensitivity to the antiproliferative effect of p27(Kip1).* Oncogene, 2001. **20**(33): p. 4466-75.
263. Morisaki, H., et al., *Cell cycle-dependent phosphorylation of p27 cyclin-dependent kinase (Cdk) inhibitor by cyclin E/Cdk2.* Biochem Biophys Res Commun, 1997. **240**(2): p. 386-90.
264. Perez-Roger, I., et al., *Myc activation of cyclin E/Cdk2 kinase involves induction of cyclin E gene transcription and inhibition of p27(Kip1) binding to newly formed complexes.* Oncogene, 1997. **14**(20): p. 2373-81.
265. Deng, X., et al., *The cyclin-dependent kinase inhibitor p27Kip1 is stabilized in G(0) by Mirk/dyrk1B kinase.* J Biol Chem, 2004. **279**(21): p. 22498-504.
266. Besson, A., et al., *A pathway in quiescent cells that controls p27Kip1 stability, subcellular localization, and tumor suppression.* Genes Dev, 2006. **20**(1): p. 47-64.
267. Cassimere, E.K., C. Mauvais, and C. Denicourt, *p27Kip1 Is Required to Mediate a G1 Cell Cycle Arrest Downstream of ATM following Genotoxic Stress.* PLoS One, 2016. **11**(9): p. e0162806.
268. Myers, T.K., S.E. Andreuzza, and D.S. Franklin, *p18INK4c and p27KIP1 are required for cell cycle arrest of differentiated myotubes.* Exp Cell Res, 2004. **300**(2): p. 365-78.
269. Slupianek, A. and T. Skorski, *NPM/ALK downregulates p27Kip1 in a PI-3K-dependent manner.* Exp Hematol, 2004. **32**(12): p. 1265-71.
270. Pearson;, J.D., et al., *Granzyme B sensitizes ALK+ ALCL cell lines to apoptosis-inducing drugs*, in *BMC Cancer*2013.
271. Bartlett, N.L., et al., *A phase 1 multidose study of SGN-30 immunotherapy in patients with refractory or recurrent CD30+ hematologic malignancies.* Blood, 2008. **111**(4): p. 1848-54.

272. Ansell, S.M., et al., *Phase I/II study of an anti-CD30 monoclonal antibody (MDX-060) in Hodgkin's lymphoma and anaplastic large-cell lymphoma.* J Clin Oncol, 2007. **25**(19): p. 2764-9.
273. Lieberman, J., *The ABCs of granule-mediated cytotoxicity: new weapons in the arsenal.* Nat Rev Immunol, 2003. **3**(5): p. 361-70.
274. Assarsson, E., et al., *2B4/CD48-mediated regulation of lymphocyte activation and function.* Journal of Immunology, 2005. **175**(4): p. 2045-2049.
275. Hosen, N., et al., *CD48 as a novel molecular target for antibody therapy in multiple myeloma.* British Journal of Haematology, 2012. **156**(2): p. 213-224.
276. Veillette, A. and H.J. Guo, *CS1, a SLAM family receptor involved in immune regulation, is a therapeutic target in multiple myeloma.* Critical Reviews in Oncology Hematology, 2013. **88**(1): p. 168-177.
277. Steinle, A., et al., *Interactions of human NKG2D with its ligands MICA, MICB, and homologs of the mouse RAE-1 protein family.* Immunogenetics, 2001. **53**(4): p. 279-87.
278. Klimosch, S.N., et al., *Genetically coupled receptor-ligand pair NKp80-AICL enables autonomous control of human NK cell responses.* Blood, 2013. **122**(14): p. 2380-9.
279. Le Borgne, M. and A.S. Shaw, *SAP signaling: a dual mechanism of action.* Immunity, 2012. **36**(6): p. 899-901.
280. Chen, J., et al., *SLAMF7 is critical for phagocytosis of haematopoietic tumour cells via Mac-1 integrin.* Nature, 2017. **544**(7651): p. 493-497.
281. Seto, E. and M. Yoshida, *Erasers of histone acetylation: the histone deacetylase enzymes.* Cold Spring Harb Perspect Biol, 2014. **6**(4): p. a018713.
282. Elias, S., et al., *Immune evasion by oncogenic proteins of acute myeloid leukemia.* Blood, 2014. **123**(10): p. 1535-43.
283. Fournel, M., et al., *MGCD0103, a novel isotype-selective histone deacetylase inhibitor, has broad spectrum antitumor activity in vitro and in vivo.* Mol Cancer Ther, 2008. **7**(4): p. 759-68.
284. Hassler, M.R., et al., *Antineoplastic activity of the DNA methyltransferase inhibitor 5-aza-2'-deoxycytidine in anaplastic large cell lymphoma.* Biochimie, 2012. **94**(11): p. 2297-307.
285. Hassler, M.R., et al., *Insights into the Pathogenesis of Anaplastic Large-Cell Lymphoma through Genome-wide DNA Methylation Profiling.* Cell Rep, 2016. **17**(2): p. 596-608.
286. Hoareau-Aveilla, C. and F. Meggetto, *Crosstalk between microRNA and DNA Methylation Offers Potential Biomarkers and Targeted Therapies in ALK-Positive Lymphomas.* Cancers (Basel), 2017. **9**(8).
287. Schiefer, A.I., et al., *The role of AP-1 and epigenetics in ALCL.* Front Biosci (Schol Ed), 2015. **7**: p. 226-35.
288. Mosse, Y.P., et al., *Safety and activity of crizotinib for paediatric patients with refractory solid tumours or anaplastic large-cell lymphoma: a Children's Oncology Group phase 1 consortium study.* Lancet Oncol, 2013. **14**(6): p. 472-80.

289. Thorley-Lawson, D.A., et al., *Epstein-Barr virus superinduces a new human B cell differentiation antigen (B-LAST 1) expressed on transformed lymphoblasts.* Cell, 1982. **30**(2): p. 415-25.
290. Yokoyama, S., et al., *Expression of the Blast-1 activation/adhesion molecule and its identification as CD48.* J Immunol, 1991. **146**(7): p. 2192-200.
291. Maki, G., et al., *Factors regulating the cytotoxic activity of the human natural killer cell line, NK-92.* J Hematother Stem Cell Res, 2001. **10**(3): p. 369-83.
292. Robertson, M.J., et al., *Characterization of a cell line, NKL, derived from an aggressive human natural killer cell leukemia.* Exp Hematol, 1996. **24**(3): p. 406-15.
293. Chuang, S.S., et al., *2B4 stimulation of YT cells induces natural killer cell cytolytic function and invasiveness.* Immunology, 2000. **100**(3): p. 378-83.
294. Bhat, R. and C. Watzl, *Serial killing of tumor cells by human natural killer cells--enhancement by therapeutic antibodies.* PLoS One, 2007. **2**(3): p. e326.
295. Hudson, S., et al., *Crizotinib induces apoptosis and gene expression changes in ALK+ anaplastic large cell lymphoma cell lines; brentuximab synergizes and doxorubicin antagonizes.* Pediatr Blood Cancer, 2018: p. e27094.
296. Wang, W., et al., *NK Cell-Mediated Antibody-Dependent Cellular Cytotoxicity in Cancer Immunotherapy.* Front Immunol, 2015. **6**: p. 368.
297. Pearson, J.D., *Understanding the function of the JunB transcription factor in anaplastic lymphoma kinase-positive, anaplastic large cell lymphoma*, in *Medical Microbiology and Immunology*2013, University of Alberta: Edmonton, Alberta,Canada.
298. Durr, C., et al., *CXCL12 mediates immunosuppression in the lymphoma microenvironment after allogeneic transplantation of hematopoietic cells.* Cancer Res, 2010. **70**(24): p. 10170-81.
299. Pandey, S., et al., *IL-4/CXCL12 loop is a key regulator of lymphoid stroma function in follicular lymphoma.* Blood, 2017. **129**(18): p. 2507-2518.
300. Agostinelli, C., et al., *Intracellular TCR-signaling pathway: novel markers for lymphoma diagnosis and potential therapeutic targets.* Am J Surg Pathol, 2014. **38**(10): p. 1349-59.
301. Mamand, S., et al., *Comparison of interleukin-2-inducible kinase (ITK) inhibitors and potential for combination therapies for T-cell lymphoma.* Sci Rep, 2018. **8**(1): p. 14216.
302. Zhang, C., et al., *Combination with TMZ and miR-505 inhibits the development of glioblastoma by regulating the WNT7B/Wnt/beta-catenin signaling pathway.* Gene, 2018. **672**: p. 172-179.
303. Shiah, S.G., et al., *Downregulated miR329 and miR410 promote the proliferation and invasion of oral squamous cell carcinoma by targeting Wnt-7b.* Cancer Res, 2014. **74**(24): p. 7560-72.
304. Kato, N., et al., *Regulation of the expression of MHC class I-related chain A, B (MICA, MICB) via chromatin remodeling and its impact on the susceptibility of leukemic cells to the cytotoxicity of NKG2D-expressing cells.* Leukemia, 2007. **21**(10): p. 2103-8.

305. Suarez-Alvarez, B., et al., *Epigenetic mechanisms regulate MHC and antigen processing molecules in human embryonic and induced pluripotent stem cells.* PLoS One, 2010. **5**(4): p. e10192.
306. Chistiakov, D.A., et al., *Epigenetically Active Drugs Inhibiting DNA Methylation and Histone Deacetylation.* Curr Pharm Des, 2017. **23**(8): p. 1167-1174.
307. Zahnow, C.A., et al., *Inhibitors of DNA Methylation, Histone Deacetylation, and Histone Demethylation: A Perfect Combination for Cancer Therapy.* Adv Cancer Res, 2016. **130**: p. 55-111.
308. Liu, B. and C. Pilarsky, *Analysis of DNA Hypermethylation in Pancreatic Cancer Using Methylation-Specific PCR and Bisulfite Sequencing.* Methods Mol Biol, 2018. **1856**: p. 269-282.
309. Tejedor, J.R., et al., *Epigenome-wide analysis reveals specific DNA hypermethylation of T cells during human hematopoietic differentiation.* Epigenomics, 2018. **10**(7): p. 903-923.
310. Jayani, R.S., P.L. Ramanujam, and S. Galande, *Studying histone modifications and their genomic functions by employing chromatin immunoprecipitation and immunoblotting.* Methods Cell Biol, 2010. **98**: p. 35-56.
311. Chatterjee, C. and T.W. Muir, *Chemical approaches for studying histone modifications.* J Biol Chem, 2010. **285**(15): p. 11045-50.
312. Turner, S.D., et al., *The NPM-ALK tyrosine kinase mimics TCR signalling pathways, inducing NFAT and AP-1 by RAS-dependent mechanisms.* Cell Signal, 2007. **19**(4): p. 740-7.
313. Buetti-Dinh, A., T. O'Hare, and R. Friedman, *Sensitivity Analysis of the NPM-ALK Signalling Network Reveals Important Pathways for Anaplastic Large Cell Lymphoma Combination Therapy.* PLoS One, 2016. **11**(9): p. e0163011.
314. Hubinger, G., et al., *The tyrosine kinase NPM-ALK, associated with anaplastic large cell lymphoma, binds the intracellular domain of the surface receptor CD30 but is not activated by CD30 stimulation.* Exp Hematol, 1999. **27**(12): p. 1796-805.
315. Claus, M., S. Wingert, and C. Watzl, *Modulation of natural killer cell functions by interactions between 2B4 and CD48 in cis and in trans.* Open Biol, 2016. **6**(5).
316. Suresh, P.K., *Membrane-bound versus soluble major histocompatibility complex Class I-related chain A and major histocompatibility complex Class I-related chain B differential expression: Mechanisms of tumor eradication versus evasion and current drug development strategies.* J Cancer Res Ther, 2016. **12**(4): p. 1224-1233.
317. Weiss-Steider, B., et al., *Expression of MICA, MICB and NKG2D in human leukemic myelomonocytic and cervical cancer cells.* J Exp Clin Cancer Res, 2011. **30**: p. 37.
318. Li, K., et al., *Clinical significance of the NKG2D ligands, MICA/B and ULBP2 in ovarian cancer: high expression of ULBP2 is an indicator of poor prognosis.* Cancer Immunol Immunother, 2009. **58**(5): p. 641-52.
319. Ribeiro, C.H., et al., *Clinical significance of tumor expression of major histocompatibility complex class I-related chains A and B (MICA/B) in gastric cancer patients.* Oncol Rep, 2016. **35**(3): p. 1309-17.

320. Zhao, Y., et al., *Prognostic value of MICA/B in cancers: a systematic review and meta-analysis.* Oncotarget, 2017. **8**(56): p. 96384-96395.
321. Verneris, M.R., et al., *Role of NKG2D signaling in the cytotoxicity of activated and expanded CD8+ T cells.* Blood, 2004. **103**(8): p. 3065-72.
322. Xu, X., G. Rao, and Y. Li, *Xanthine oxidoreductase is required for genotoxic stress-induced NKG2D ligand expression and gemcitabine-mediated antitumor activity.* Oncotarget, 2016. **7**(37): p. 59220-59235.
323. Streltsova, M.A., et al., *Ethanol-dependent expression of the NKG2D ligands MICA/B in human cell lines and leukocytes.* Biochem Cell Biol, 2017. **95**(2): p. 280-288.
324. Cheng, M., et al., *Natural killer cell lines in tumor immunotherapy.* Front Med, 2012. **6**(1): p. 56-66.
325. Klingemann, H., L. Boissel, and F. Toneguzzo, *Natural Killer Cells for Immunotherapy - Advantages of the NK-92 Cell Line over Blood NK Cells.* Front Immunol, 2016. **7**: p. 91.
326. Imai, C., S. Iwamoto, and D. Campana, *Genetic modification of primary natural killer cells overcomes inhibitory signals and induces specific killing of leukemic cells.* Blood, 2005. **106**(1): p. 376-83.
327. Angelo, L.S., et al., *Practical NK cell phenotyping and variability in healthy adults.* Immunol Res, 2015. **62**(3): p. 341-56.
328. Mechta-Grigoriou, F., D. Gerald, and M. Yaniv, *The mammalian Jun proteins: redundancy and specificity.* Oncogene, 2001. **20**(19): p. 2378-89.
329. Saxonov, S., P. Berg, and D.L. Brutlag, *A genome-wide analysis of CpG dinucleotides in the human genome distinguishes two distinct classes of promoters.* Proc Natl Acad Sci U S A, 2006. **103**(5): p. 1412-7.
330. Deaton, A.M. and A. Bird, *CpG islands and the regulation of transcription.* Genes Dev, 2011. **25**(10): p. 1010-22.
331. Green, M.R., et al., *Constitutive AP-1 activity and EBV infection induce PD-L1 in Hodgkin lymphomas and posttransplant lymphoproliferative disorders: implications for targeted therapy.* Clin Cancer Res, 2012. **18**(6): p. 1611-8.
332. Eckerle, S., et al., *Gene expression profiling of isolated tumour cells from anaplastic large cell lymphomas: insights into its cellular origin, pathogenesis and relation to Hodgkin lymphoma.* Leukemia, 2009. **23**(11): p. 2129-38.
333. Crescenzo, R., et al., *Convergent mutations and kinase fusions lead to oncogenic STAT3 activation in anaplastic large cell lymphoma.* Cancer Cell, 2015. **27**(4): p. 516-32.
334. Juilland, M., et al., *CARMA1- and MyD88-dependent activation of Jun/ATF-type AP-1 complexes is a hallmark of ABC diffuse large B-cell lymphomas.* Blood, 2016. **127**(14): p. 1780-9.
335. Old, W.M., et al., *Functional proteomics identifies targets of phosphorylation by B-Raf signaling in melanoma.* Mol Cell, 2009. **34**(1): p. 115-31.
336. Chen, S., H.G. Evans, and D.R. Evans, *FAM129B/MINERVA, a novel adherens junction-associated protein, suppresses apoptosis in HeLa cells.* J Biol Chem, 2011. **286**(12): p. 10201-9.
337. Conrad, W., et al., *FAM129B is a novel regulator of Wnt/beta-catenin signal transduction in melanoma cells.* F1000Res, 2013. **2**: p. 134.

338. Ji, H., et al., *EGFR phosphorylates FAM129B to promote Ras activation.* Proc Natl Acad Sci U S A, 2016. **113**(3): p. 644-9.
339. Pavel, A.B. and K.S. Korolev, *Genetic load makes cancer cells more sensitive to common drugs: evidence from Cancer Cell Line Encyclopedia.* Sci Rep, 2017. **7**(1): p. 1938.
340. Kajstura, M., et al., *Discontinuous fragmentation of nuclear DNA during apoptosis revealed by discrete "sub-G1" peaks on DNA content histograms.* Cytometry A, 2007. **71**(3): p. 125-31.
341. Majno, G. and I. Joris, *Apoptosis, oncosis, and necrosis. An overview of cell death.* Am J Pathol, 1995. **146**(1): p. 3-15.
342. Babes, R.M., et al., *Simple discrimination of sub-cycling cells by propidium iodide flow cytometric assay in Jurkat cell samples with extensive DNA fragmentation.* Cell Cycle, 2018. **17**(6): p. 766-779.
343. Darzynkiewicz, Z., et al., *Cytometry in cell necrobiology: analysis of apoptosis and accidental cell death (necrosis).* Cytometry, 1997. **27**(1): p. 1-20.
344. Rieger, A.M., et al., *Modified annexin V/propidium iodide apoptosis assay for accurate assessment of cell death.* J Vis Exp, 2011(50).
345. Deng, T. and M. Karin, *JunB differs from c-Jun in its DNA-binding and dimerization domains, and represses c-Jun by formation of inactive heterodimers.* Genes Dev, 1993. **7**(3): p. 479-90.
346. Echlin, D.R., et al., *B-ATF functions as a negative regulator of AP-1 mediated transcription and blocks cellular transformation by Ras and Fos.* Oncogene, 2000. **19**(14): p. 1752-63.
347. Halazonetis, T.D., et al., *c-Jun dimerizes with itself and with c-Fos, forming complexes of different DNA binding affinities.* Cell, 1988. **55**(5): p. 917-24.
348. O'Shea, E.K., R. Rutkowski, and P.S. Kim, *Mechanism of specificity in the Fos-Jun oncoprotein heterodimer.* Cell, 1992. **68**(4): p. 699-708.
349. Jason K. H. Lee, J.D.P., Brandon E. Maser and Robert J. Ingham, *Cleavage of the JunB Transcription Factor by Caspases Generates a Carboxyl-terminal Fragment That Inhibits Activator Protein-1 Transcriptional Activity.* J Biol Chem, 2013. **288**.
350. Bakiri, L., et al., *Promoter specificity and biological activity of tethered AP-1 dimers.* Mol Cell Biol, 2002. **22**(13): p. 4952-64.
351. O'Sullivan, C. and K.K. Dev, *The structure and function of the S1P1 receptor.* Trends Pharmacol Sci, 2013. **34**(7): p. 401-12.
352. Kojima, Y., et al., *CD47-blocking antibodies restore phagocytosis and prevent atherosclerosis.* Nature, 2016. **536**(7614): p. 86-90.
353. Barreyro, L., et al., *Overexpression of IL-1 receptor accessory protein in stem and progenitor cells and outcome correlation in AML and MDS.* Blood, 2012. **120**(6): p. 1290-8.
354. Wu, J.X., et al., *Rap2a is a novel target gene of p53 and regulates cancer cell migration and invasion.* Cell Signal, 2015. **27**(6): p. 1198-207.
355. Yue, Y., et al., *Nucks1 synergizes with Trp53 to promote radiation lymphomagenesis in mice.* Oncotarget, 2016. **7**(38): p. 61874-61889.

356. Cheong, J.Y., et al., *Identification of NUCKS1 as a putative oncogene and immunodiagnostic marker of hepatocellular carcinoma.* Gene, 2016. **584**(1): p. 47-53.

# Appendixes

**Appendix 1. JunB or c-Jun knock-down did not affect cell cycle distribution in UCONN-L2 cells**

Representative BrdU/7-AAD plots for cell cycle analysis in JunB shRNA, c-Jun shRNA or control shRNA-expressing UCONN-L2 cells from two independent experiments in two infections.

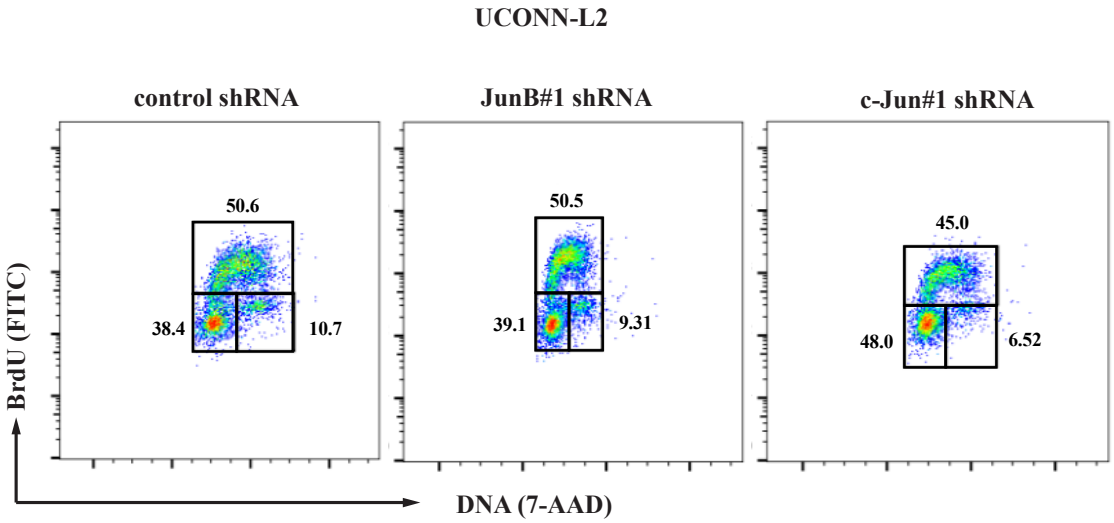

**Appendix 2. Microarray KEGG pathway annotation analysis**

KEGG Pathways annotation analysis for genes identified from microarray in JunB knock-down Karpas 299 cells are listed below, as mentioned in **Section 4.2.3**. "Category" indicates the pathways identified through KEGG annotation analysis; "Count" indicates the number of genes identified in corresponding category; "%" indicates the percentage of the genes identified from each category in the whole gene list in JunB knock-down cells (fold change ≥2); "P-value" indicates the significance of the correlation between the pathway and genes identified from microarray in JunB knock-down cells (fold change ≥2).

| Category | Count | % | P-Value |
|---|---|---|---|
| Natural killer cell mediated cytotoxicity | 21 | 3.3 | 1.70E-07 |
| FoxO signaling pathway | 19 | 3 | 1.40E-05 |
| Cytokine-cytokine receptor interaction | 25 | 3.9 | 4.10E-05 |
| Alcoholism | 20 | 3.2 | 1.80E-04 |
| p53 signaling pathway | 11 | 1.7 | 4.90E-04 |
| Pathways in cancer | 32 | 5.1 | 6.10E-04 |
| Proteoglycans in cancer | 19 | 3 | 2.10E-03 |
| Systemic lupus erythematosus | 14 | 2.2 | 4.60E-03 |
| Neurotrophin signaling pathway | 13 | 2.1 | 5.00E-03 |
| Chemokine signaling pathway | 17 | 2.7 | 5.80E-03 |
| MAPK signaling pathway | 21 | 3.3 | 6.00E-03 |
| Focal adhesion | 18 | 2.8 | 6.70E-03 |
| Cell adhesion molecules (CAMs) | 14 | 2.2 | 7.40E-03 |
| Leukocyte transendothelial migration | 12 | 1.9 | 1.20E-02 |
| Chagas disease (American trypanosomiasis) | 11 | 1.7 | 1.30E-02 |
| Pertussis | 9 | 1.4 | 1.40E-02 |
| TNF signaling pathway | 11 | 1.7 | 1.50E-02 |
| Influenza A | 15 | 2.4 | 1.60E-02 |
| Measles | 12 | 1.9 | 2.60E-02 |
| Wnt signaling pathway | 12 | 1.9 | 3.30E-02 |
| Rheumatoid arthritis | 9 | 1.4 | 3.40E-02 |
| Apoptosis | 7 | 1.1 | 4.80E-02 |
| African trypanosomiasis | 5 | 0.8 | 5.00E-02 |
| Glycosaminoglycan biosynthesis - chondroitin sulfate / dermatan sulfate | 4 | 0.6 | 5.10E-02 |
| Inflammatory bowel disease (IBD) | 7 | 1.1 | 5.40E-02 |
| Malaria | 6 | 0.9 | 5.70E-02 |

| | | | |
|---|---|---|---|
| PI3K-Akt signaling pathway | 22 | 3.5 | 6.30E-02 |
| T cell receptor signaling pathway | 9 | 1.4 | 7.20E-02 |
| Complement and coagulation cascades | 7 | 1.1 | 7.30E-02 |
| cAMP signaling pathway | 14 | 2.2 | 8.10E-02 |
| Prolactin signaling pathway | 7 | 1.1 | 8.20E-02 |
| Basal cell carcinoma | 6 | 0.9 | 8.40E-02 |
| GnRH signaling pathway | 8 | 1.3 | 9.30E-02 |
| Viral carcinogenesis | 14 | 2.2 | 9.80E-02 |

**Appendix 3. Genes in top 10 KEGG categories**

Genes from top 10 KEGG categories (**Appendix 2**) are listed below, as mentioned in **Section 4.2.3.**

**Natural killer cell mediated cytotoxicity**

| |
|---|
| CD48 molecule(CD48) |
| FYN proto-oncogene, Src family tyrosine kinase(FYN) |
| Fas cell surface death receptor(FAS) |
| Fas ligand(FASLG) |
| KLRC4-KLRK1 readthrough(KLRC4-KLRK1) |
| SH2 domain containing 1A(SH2D1A) |
| SH2 domain containing 1B(SH2D1B) |
| SHC adaptor protein 4(SHC4) |
| SOS Ras/Rho guanine nucleotide exchange factor 2(SOS2) |
| TNF receptor superfamily member 10a(TNFRSF10A) |
| UL16 binding protein 3(ULBP3) |
| hematopoietic cell signal transducer(HCST) |
| integrin subunit beta 2(ITGB2) |
| intercellular adhesion molecule 1(ICAM1) |
| interferon gamma receptor 2 (interferon gamma transducer 1)(IFNGR2) |
| killer cell immunoglobulin like receptor, two Ig domains and long cytoplasmic tail 2(KIR2DL2) |
| lymphocyte cytosolic protein 2(LCP2) |
| nuclear factor of activated T-cells 2(NFATC2) |
| protein kinase C alpha(PRKCA) |
| tumor necrosis factor superfamily member 10(TNFSF10) |
| vav guanine nucleotide exchange factor 3(VAV3) |

**FoxO signaling pathway**

| |
|---|
| C8orf44-SGK3 readthrough(C8orf44-SGK3) |
| F-box protein 32(FBXO32) |
| Fas ligand(FASLG) |
| GABA type A receptor associated protein like 1(GABARAPL1) |
| SOS Ras/Rho guanine nucleotide exchange factor 2(SOS2) |
| cyclin D2(CCND2) |
| cyclin G2(CCNG2) |
| cyclin dependent kinase inhibitor 2B(CDKN2B) |
| forkhead box O3(FOXO3) |

| |
|---|
| growth arrest and DNA damage inducible alpha(GADD45A) |
| growth arrest and DNA damage inducible gamma(GADD45G) |
| insulin like growth factor 1 receptor(IGF1R) |
| insulin receptor substrate 1(IRS1) |
| interleukin 7 receptor(IL7R) |
| nemo like kinase(NLK) |
| protein kinase AMP-activated non-catalytic subunit gamma 2(PRKAG2) |
| serum/glucocorticoid regulated kinase 1(SGK1) |
| transforming growth factor beta receptor 2(TGFBR2) |
| tumor necrosis factor superfamily member 10(TNFSF10) |

**Cytokine-cytokine receptor interaction**

| |
|---|
| C-C motif chemokine ligand 20(CCL20) |
| C-C motif chemokine ligand 3(CCL3) |
| C-C motif chemokine receptor 1(CCR1) |
| C-C motif chemokine receptor 5 (gene/pseudogene)(CCR5) |
| C-X-C motif chemokine ligand 10(CXCL10) |
| C-X-C motif chemokine ligand 11(CXCL11) |
| C-X-C motif chemokine ligand 12(CXCL12) |
| C-X-C motif chemokine ligand 13(CXCL13) |
| Fas cell surface death receptor(FAS) |
| Fas ligand(FASLG) |
| TNF receptor superfamily member 19(TNFRSF19) |
| TNF receptor superfamily member 21(TNFRSF21) |
| hepatocyte growth factor(HGF) |
| interferon gamma receptor 2 (interferon gamma transducer 1)(IFNGR2) |
| interleukin 17 receptor A(IL17RA) |
| interleukin 18 receptor 1(IL18R1) |
| interleukin 18 receptor accessory protein(IL18RAP) |
| interleukin 22 receptor subunit alpha 2(IL22RA2) |
| interleukin 22(IL22) |
| interleukin 23 subunit alpha(IL23A) |
| interleukin 7 receptor(IL7R) |
| transforming growth factor beta receptor 2(TGFBR2) |
| tumor necrosis factor superfamily member 10(TNFSF10) |
| tumor necrosis factor superfamily member 4(TNFSF4) |
| tumor necrosis factor superfamily member 9(TNFSF9) |

**Alcoholism**

| |
|---|
| G protein subunit gamma 2(GNG2) |
| G protein subunit gamma 4(GNG4) |
| SHC adaptor protein 4(SHC4) |

| |
|---|
| SOS Ras/Rho guanine nucleotide exchange factor 2(SOS2) |
| brain derived neurotrophic factor(BDNF) |
| cAMP responsive element binding protein 3 like 2(CREB3L2) |
| dopa decarboxylase(DDC) |
| histone cluster 1 H2A family member b(HIST1H2AB) |
| histone cluster 1 H2A family member c(HIST1H2AC) |
| histone cluster 1 H2A family member d(HIST1H2AD) |
| histone cluster 1 H2A family member g(HIST1H2AG) |
| histone cluster 1 H2B family member c(HIST1H2BC) |
| histone cluster 1 H2B family member d(HIST1H2BD) |
| histone cluster 1 H2B family member j(HIST1H2BJ) |
| histone cluster 1 H2B family member k(HIST1H2BK) |
| histone cluster 1 H3 family member a(HIST1H3A) |
| histone cluster 1 H4 family member a(HIST1H4A) |
| histone cluster 2 H2A family member a3(HIST2H2AA3) |
| histone cluster 2 H2B family member e(HIST2H2BE) |
| neurotrophic receptor tyrosine kinase 2(NTRK2) |

**p53 signaling pathway**

| |
|---|
| CD82 molecule(CD82) |
| EI24, autophagy associated transmembrane protein(EI24) |
| Fas cell surface death receptor(FAS) |
| cyclin D2(CCND2) |
| cyclin G2(CCNG2) |
| cyclin dependent kinase 6(CDK6) |
| growth arrest and DNA damage inducible alpha(GADD45A) |
| growth arrest and DNA damage inducible gamma(GADD45G) |
| insulin like growth factor binding protein 3(IGFBP3) |
| sestrin 2(SESN2) |
| thrombospondin 1(THBS1) |

**Pathways in cancer**

| |
|---|
| C-X-C motif chemokine ligand 12(CXCL12) |
| Fas cell surface death receptor(FAS) |
| Fas ligand(FASLG) |
| Fos proto-oncogene, AP-1 transcription factor subunit(FOS) |
| G protein subunit alpha 11(GNA11) |
| G protein subunit alpha q(GNAQ) |
| G protein subunit gamma 2(GNG2) |
| G protein subunit gamma 4(GNG4) |
| GLI family zinc finger 3(GLI3) |
| Jun proto-oncogene, AP-1 transcription factor subunit(JUN) |

| |
|---|
| RAS guanyl releasing protein 2(RASGRP2) |
| Rho guanine nucleotide exchange factor 12(ARHGEF12) |
| SOS Ras/Rho guanine nucleotide exchange factor 2(SOS2) |
| Wnt family member 11(WNT11) |
| Wnt family member 5B(WNT5B) |
| Wnt family member 7B(WNT7B) |
| baculoviral IAP repeat containing 3(BIRC3) |
| coagulation factor II thrombin receptor(F2R) |
| cyclin dependent kinase 6(CDK6) |
| cyclin dependent kinase inhibitor 2B(CDKN2B) |
| death associated protein kinase 1(DAPK1) |
| frizzled class receptor 3(FZD3) |
| hepatocyte growth factor(HGF) |
| insulin like growth factor 1 receptor(IGF1R) |
| integrin subunit alpha 6(ITGA6) |
| neurotrophic receptor tyrosine kinase 1(NTRK1) |
| patched 1(PTCH1) |
| prostaglandin E receptor 3(PTGER3) |
| protein kinase C alpha(PRKCA) |
| ret proto-oncogene(RET) |
| transforming growth factor alpha(TGFA) |
| transforming growth factor beta receptor 2(TGFBR2) |

**Proteoglycans in cancer**

| |
|---|
| Fas cell surface death receptor(FAS) |
| Fas ligand(FASLG) |
| Rho guanine nucleotide exchange factor 12(ARHGEF12) |
| SOS Ras/Rho guanine nucleotide exchange factor 2(SOS2) |
| Wnt family member 11(WNT11) |
| Wnt family member 5B(WNT5B) |
| Wnt family member 7B(WNT7B) |
| frizzled class receptor 3(FZD3) |
| glypican 3(GPC3) |
| heparin binding EGF like growth factor(HBEGF) |
| hepatocyte growth factor(HGF) |
| insulin like growth factor 1 receptor(IGF1R) |
| integrin subunit alpha 5(ITGA5) |
| patched 1(PTCH1) |
| plasminogen activator, urokinase receptor(PLAUR) |
| protein kinase C alpha(PRKCA) |
| syndecan 4(SDC4) |

| |
|---|
| thrombospondin 1(THBS1) |
| twist family bHLH transcription factor 1(TWIST1) |

**Systemic lupus erythematosus**

| |
|---|
| actinin alpha 1(ACTN1) |
| complement C1r(C1R) |
| histone cluster 1 H2A family member b(HIST1H2AB) |
| histone cluster 1 H2A family member c(HIST1H2AC) |
| histone cluster 1 H2A family member d(HIST1H2AD) |
| histone cluster 1 H2A family member g(HIST1H2AG) |
| histone cluster 1 H2B family member c(HIST1H2BC) |
| histone cluster 1 H2B family member d(HIST1H2BD) |
| histone cluster 1 H2B family member j(HIST1H2BJ) |
| histone cluster 1 H2B family member k(HIST1H2BK) |
| histone cluster 1 H3 family member a(HIST1H3A) |
| histone cluster 1 H4 family member a(HIST1H4A) |
| histone cluster 2 H2A family member a3(HIST2H2AA3) |
| histone cluster 2 H2B family member e(HIST2H2BE) |

**Neurotrophin signaling pathway**

| |
|---|
| Fas ligand(FASLG) |
| Jun proto-oncogene, AP-1 transcription factor subunit(JUN) |
| MAGE family member D1(MAGED1) |
| Rho GDP dissociation inhibitor beta(ARHGDIB) |
| SHC adaptor protein 4(SHC4) |
| SOS Ras/Rho guanine nucleotide exchange factor 2(SOS2) |
| brain derived neurotrophic factor(BDNF) |
| forkhead box O3(FOXO3) |
| insulin receptor substrate 1(IRS1) |
| interleukin 1 receptor associated kinase 2(IRAK2) |
| mitogen-activated protein kinase kinase kinase 1(MAP3K1) |
| neurotrophic receptor tyrosine kinase 1(NTRK1) |
| neurotrophic receptor tyrosine kinase 2(NTRK2) |

**Chemokine signaling pathway**

| |
|---|
| C-C motif chemokine ligand 20(CCL20) |
| C-C motif chemokine ligand 3(CCL3) |
| C-C motif chemokine receptor 1(CCR1) |
| C-C motif chemokine receptor 5 (gene/pseudogene)(CCR5) |
| C-X-C motif chemokine ligand 10(CXCL10) |
| C-X-C motif chemokine ligand 11(CXCL11) |
| C-X-C motif chemokine ligand 12(CXCL12) |
| C-X-C motif chemokine ligand 13(CXCL13) |
| G protein subunit gamma 2(GNG2) |
| G protein subunit gamma 4(GNG4) |
| G protein-coupled receptor kinase 5(GRK5) |
| IL2 inducible T-cell kinase(ITK) |
| RAS guanyl releasing protein 2(RASGRP2) |
| SHC adaptor protein 4(SHC4) |
| SOS Ras/Rho guanine nucleotide exchange factor 2(SOS2) |
| forkhead box O3(FOXO3) |
| vav guanine nucleotide exchange factor 3(VAV3) |

**Appendix 4. DNMTs and HDACs information from ChIP-seq**

Some of the DNMTs and HDACs are associated with JunB or c-Jun as indicated in the ChIP-seq data. The information is listed below: "Intervals" indicates the JunB/c-Jun-associated intervals identified from ChIP-seq; "Intervals Dists to Start" indicates the distance from the interval to the transcription start site (TSS) of the corresponding genes.

| Gene Name | Intervals | Interval Dists to Start |
|---|---|---|
| HDAC2 | 2_K299_cJun::1::11252, 4_K299_JunB_CST::1::32900 | -89, -249 |
| HDAC4 | 2_K299_cJun::1::7927, 4_K299_JunB_CST::1::21953, 4_K299_JunB_CST::1::21954, 2_K299_cJun::1::7928, 2_K299_cJun::1::7929, 2_K299_cJun::1::7930, 2_K299_cJun::1::7931, 2_K299_cJun::1::7932, 2_K299_cJun::1::7933, 2_K299_cJun::1::7934, 4_K299_JunB_CST::1::21955, 4_K299_JunB_CST::1::21956, 4_K299_JunB_CST::1::21957, 4_K299_JunB_CST::1::21958, 4_K299_JunB_CST::1::21959, 4_K299_JunB_CST::1::21960, 4_K299_JunB_CST::1::21961, 4_K299_JunB_CST::1::21962, 4_K299_JunB_CST::1::21963, 4_K299_JunB_CST::1::21964, 4_K299_JunB_CST::1::21965, 4_K299_JunB_CST::1::21966, 4_K299_JunB_CST::1::21967, 4_K299_JunB_CST::1::21968, 4_K299_JunB_CST::1::21969, 4_K299_JunB_CST::1::21970, 4_K299_JunB_CST::1::21971, 4_K299_JunB_CST::1::21972, 4_K299_JunB_CST::1::21973, 4_K299_JunB_CST::1::21974, 4_K299_JunB_CST::1::21975, 4_K299_JunB_CST::1::21976, 4_K299_JunB_CST::1::21977, 4_K299_JunB_CST::1::21978, 4_K299_JunB_CST::1::21979, 4_K299_JunB_CST::1::21980, 4_K299_JunB_CST::1::21981, 4_K299_JunB_CST::1::21982, | 344627, 344707, 331123, 184147, 133715, 126259, 125651, 120531, 95752, 979, 303955, 302595, 282323, 281219, 256787, 184131, 143283, 142547, 140819, 137203, 135987, 135251, 134803, 133907, 132723, 132339, 130835, 125619, 120531, 115603, 115048, 113939, 106739, 95747, 94451, |

| | | |
|---|---|---|
| | 4_K299_JunB_CST::1::21983,<br>4_K299_JunB_CST::1::21984,<br>4_K299_JunB_CST::1::21985,<br>4_K299_JunB_CST::1::21986,<br>4_K299_JunB_CST::1::21987,<br>4_K299_JunB_CST::1::21988,<br>4_K299_JunB_CST::1::21989,<br>4_K299_JunB_CST::1::21990,<br>4_K299_JunB_CST::1::21991 | 85459, 73811,<br>73155, 36691,<br>35091, 30899,<br>30355, 29971,<br>25107, 19955,<br>1032, -621 |
| HDAC1 | 2_K299_cJun::1::371, 2_K299_cJun::1::372,<br>4_K299_JunB_CST::1::772 | -236, 148, 148 |
| HDAC7 | 2_K299_cJun::1::2741, 4_K299_JunB_CST::1::7527,<br>4_K299_JunB_CST::1::7528,<br>4_K299_JunB_CST::1::7529 | 1411, 7011,<br>675, -413 |
| HDAC9 | 2_K299_cJun::1::11544, 2_K299_cJun::1::11545,<br>2_K299_cJun::1::11546, 2_K299_cJun::1::11547,<br>4_K299_JunB_CST::1::34021,<br>4_K299_JunB_CST::1::34022,<br>4_K299_JunB_CST::1::34023,<br>4_K299_JunB_CST::1::34024,<br>4_K299_JunB_CST::1::34025,<br>4_K299_JunB_CST::1::34026,<br>4_K299_JunB_CST::1::34027,<br>4_K299_JunB_CST::1::34028,<br>4_K299_JunB_CST::1::34029,<br>4_K299_JunB_CST::1::34030,<br>4_K299_JunB_CST::1::34031,<br>4_K299_JunB_CST::1::34032,<br>4_K299_JunB_CST::1::34033,<br>4_K299_JunB_CST::1::34034,<br>4_K299_JunB_CST::1::34035 | 76599,<br>153399,<br>365943,<br>399735, 247,<br>13495, 14007,<br>42956, 76535,<br>116855,<br>142935,<br>143415,<br>150711,<br>153879,<br>274759,<br>349207,<br>365911,<br>399863,<br>482519 |
| HDAC3 | 2_K299_cJun::1::10451, 4_K299_JunB_CST::1::30320,<br>4_K299_JunB_CST::1::30321,<br>4_K299_JunB_CST::1::30322,<br>4_K299_JunB_CST::1::30323 | 17671, 18375,<br>17735, 2503, -<br>1081 |
| HDAC8 | 4_K299_JunB_CST::1::40117,<br>4_K299_JunB_CST::1::40118 | 224153,<br>223769 |
| HDAC6 | 4_K299_JunB_CST::1::40031 | -679 |
| HDAC10 | 4_K299_JunB_CST::1::24438,<br>4_K299_JunB_CST::1::24439,<br>4_K299_JunB_CST::1::24440 | 6378, 394, -<br>630 |
| HDAC5 | 4_K299_JunB_CST::1::15114,<br>4_K299_JunB_CST::1::15115,<br>4_K299_JunB_CST::1::15116 | 52630, 36886,<br>-282 |
| DNMT1 | 2_K299_cJun::1::6437, 2_K299_cJun::1::6438,<br>2_K299_cJun::1::6439, 2_K299_cJun::1::6440, | 56411, 55483,<br>54107, 52955, |

| | | |
|---|---|---|
| | 2_K299_cJun::1::6441, 2_K299_cJun::1::6442, 2_K299_cJun::1::6443, 2_K299_cJun::1::6444, 2_K299_cJun::1::6445, 2_K299_cJun::1::6446, 2_K299_cJun::1::6447, 2_K299_cJun::1::6448, 2_K299_cJun::1::6449, 2_K299_cJun::1::6450, 2_K299_cJun::1::6451, 2_K299_cJun::1::6452, 2_K299_cJun::1::6453, 2_K299_cJun::1::6454, 2_K299_cJun::1::6455, 2_K299_cJun::1::6456, 2_K299_cJun::1::6457, 2_K299_cJun::1::6458, 4_K299_JunB_CST::1::17412, 4_K299_JunB_CST::1::17413 | 51323, 50443, 49931, 48683, 46171, 45499, 44699, 42395, 40475, 39611, 36379, 35723, 34939, 33979, 32667, 27323, 19323, 43, 5371, 699 |
| DNMT3A | 2_K299_cJun::1::6879, 4_K299_JunB_CST::1::18828, 4_K299_JunB_CST::1::18829, 4_K299_JunB_CST::1::18830 | 40883, 115571, 40883, 27891 |
| DNMT3B | 4_K299_JunB_CST::1::22479 | -9423 |

## Appendix 5. ChIP-seq data KEGG pathway annotation analysis

KEGG pathways annotation analysis for genes identified from ChIP-seq data is listed below, as mentioned in **Section 5.2.6**. The genes identified from ChIP-seq are divided intro three groups: Genes that are associated with both JunB and c-Jun intervals, genes that are associated with JunB only, and genes that are associated with c-Jun only. KEGG pathway annotation analysis was performed in the three groups individually as shown below.

"Term" indicates the pathways identified through KEGG annotation analysis; "Count" indicates the number of genes identified in corresponding category; "%" indicates the percentage of the genes identified from each category in the whole gene list; "P-value" indicates the significance of the correlation between the pathway and genes identified from ChIP-seq.

**Genes associated with both JunB and c-Jun intervals**

| Category | Term | RT | Genes | Count | % | P-Value |
|---|---|---|---|---|---|---|
| KEGG_PATHWAY | Alcoholism | RT | | 94 | 1.9 | 2.5E-12 |
| KEGG_PATHWAY | Viral carcinogenesis | RT | | 96 | 1.9 | 9.9E-9 |
| KEGG_PATHWAY | Epstein-Barr virus infection | RT | | 89 | 1.8 | 3.6E-8 |
| KEGG_PATHWAY | Systemic lupus erythematosus | RT | | 66 | 1.3 | 2.8E-7 |
| KEGG_PATHWAY | Pancreatic cancer | RT | | 38 | 0.8 | 8.2E-7 |
| KEGG_PATHWAY | Ubiquitin mediated proteolysis | RT | | 65 | 1.3 | 1.8E-6 |
| KEGG_PATHWAY | Chronic myeloid leukemia | RT | | 40 | 0.8 | 2.3E-6 |
| KEGG_PATHWAY | Cell cycle | RT | | 59 | 1.2 | 5.3E-6 |
| KEGG_PATHWAY | Pathways in cancer | RT | | 150 | 3.0 | 6.8E-6 |
| KEGG_PATHWAY | Prostate cancer | RT | | 45 | 0.9 | 8.7E-6 |
| KEGG_PATHWAY | Transcriptional misregulation in cancer | RT | | 74 | 1.5 | 9.7E-6 |
| KEGG_PATHWAY | Non-small cell lung cancer | RT | | 32 | 0.6 | 1.4E-5 |
| KEGG_PATHWAY | Oocyte meiosis | RT | | 52 | 1.0 | 1.9E-5 |
| KEGG_PATHWAY | Circadian rhythm | RT | | 21 | 0.4 | 2.3E-5 |
| KEGG_PATHWAY | HIF-1 signaling pathway | RT | | 47 | 0.9 | 4.4E-5 |
| KEGG_PATHWAY | Small cell lung cancer | RT | | 42 | 0.8 | 5.2E-5 |
| KEGG_PATHWAY | Glioma | RT | | 34 | 0.7 | 7.8E-5 |
| KEGG_PATHWAY | Endocytosis | RT | | 100 | 2.0 | 1.4E-4 |
| KEGG_PATHWAY | Apoptosis | RT | | 32 | 0.6 | 1.8E-4 |
| KEGG_PATHWAY | HTLV-I infection | RT | | 98 | 2.0 | 2.9E-4 |
| KEGG_PATHWAY | Thyroid hormone signaling pathway | RT | | 50 | 1.0 | 3.7E-4 |
| KEGG_PATHWAY | Neurotrophin signaling pathway | RT | | 52 | 1.0 | 4.0E-4 |
| KEGG_PATHWAY | Bladder cancer | RT | | 23 | 0.5 | 4.5E-4 |
| KEGG_PATHWAY | Colorectal cancer | RT | | 31 | 0.6 | 4.8E-4 |
| KEGG_PATHWAY | Fc gamma R-mediated phagocytosis | RT | | 39 | 0.8 | 5.0E-4 |
| KEGG_PATHWAY | Spliceosome | RT | | 56 | 1.1 | 5.4E-4 |
| KEGG_PATHWAY | Hepatitis B | RT | | 60 | 1.2 | 5.7E-4 |
| KEGG_PATHWAY | Focal adhesion | RT | | 80 | 1.6 | 6.7E-4 |
| KEGG_PATHWAY | Insulin signaling pathway | RT | | 57 | 1.1 | 8.4E-4 |
| KEGG_PATHWAY | T cell receptor signaling pathway | RT | | 45 | 0.9 | 8.5E-4 |
| KEGG_PATHWAY | Toxoplasmosis | RT | | 50 | 1.0 | 9.6E-4 |
| KEGG_PATHWAY | Endometrial cancer | RT | | 26 | 0.5 | 1.6E-3 |
| KEGG_PATHWAY | MAPK signaling pathway | RT | | 94 | 1.9 | 1.6E-3 |
| KEGG_PATHWAY | RNA degradation | RT | | 35 | 0.7 | 1.6E-3 |
| KEGG_PATHWAY | Long-term potentiation | RT | | 31 | 0.6 | 1.7E-3 |
| KEGG_PATHWAY | FoxO signaling pathway | RT | | 54 | 1.1 | 2.3E-3 |
| KEGG_PATHWAY | Progesterone-mediated oocyte maturation | RT | | 38 | 0.8 | 2.3E-3 |
| KEGG_PATHWAY | Renal cell carcinoma | RT | | 30 | 0.6 | 2.9E-3 |
| KEGG_PATHWAY | RNA transport | RT | | 66 | 1.3 | 2.9E-3 |
| KEGG_PATHWAY | mRNA surveillance pathway | RT | | 39 | 0.8 | 3.0E-3 |
| KEGG_PATHWAY | Adherens junction | RT | | 32 | 0.6 | 3.2E-3 |

| | | | | | |
|---|---|---|---|---|---|
| KEGG_PATHWAY | B cell receptor signaling pathway | RT | 31 | 0.6 | 3.9E-3 |
| KEGG_PATHWAY | Dopaminergic synapse | RT | 51 | 1.0 | 4.0E-3 |
| KEGG_PATHWAY | Proteasome | RT | 22 | 0.4 | 4.0E-3 |
| KEGG_PATHWAY | mTOR signaling pathway | RT | 27 | 0.5 | 4.3E-3 |
| KEGG_PATHWAY | Bacterial invasion of epithelial cells | RT | 34 | 0.7 | 4.3E-3 |
| KEGG_PATHWAY | VEGF signaling pathway | RT | 28 | 0.6 | 4.5E-3 |
| KEGG_PATHWAY | Sphingolipid signaling pathway | RT | 48 | 1.0 | 4.9E-3 |
| KEGG_PATHWAY | Protein processing in endoplasmic reticulum | RT | 64 | 1.3 | 4.9E-3 |
| KEGG_PATHWAY | Cholinergic synapse | RT | 45 | 0.9 | 4.9E-3 |
| KEGG_PATHWAY | Hepatitis C | RT | 52 | 1.0 | 5.7E-3 |
| KEGG_PATHWAY | TNF signaling pathway | RT | 43 | 0.9 | 5.9E-3 |
| KEGG_PATHWAY | Prolactin signaling pathway | RT | 31 | 0.6 | 6.5E-3 |
| KEGG_PATHWAY | Regulation of actin cytoskeleton | RT | 76 | 1.5 | 8.9E-3 |
| KEGG_PATHWAY | Central carbon metabolism in cancer | RT | 28 | 0.6 | 9.8E-3 |
| KEGG_PATHWAY | Shigellosis | RT | 28 | 0.6 | 9.8E-3 |
| KEGG_PATHWAY | Leukocyte transendothelial migration | RT | 46 | 0.9 | 1.0E-2 |
| KEGG_PATHWAY | Tight junction | RT | 52 | 1.0 | 1.1E-2 |
| KEGG_PATHWAY | Osteoclast differentiation | RT | 50 | 1.0 | 1.1E-2 |
| KEGG_PATHWAY | Wnt signaling pathway | RT | 52 | 1.0 | 1.3E-2 |
| KEGG_PATHWAY | Oxytocin signaling pathway | RT | 58 | 1.2 | 1.5E-2 |
| KEGG_PATHWAY | Glucagon signaling pathway | RT | 39 | 0.8 | 1.5E-2 |
| KEGG_PATHWAY | Estrogen signaling pathway | RT | 39 | 0.8 | 1.5E-2 |
| KEGG_PATHWAY | Measles | RT | 50 | 1.0 | 1.5E-2 |
| KEGG_PATHWAY | Amphetamine addiction | RT | 28 | 0.6 | 1.6E-2 |
| KEGG_PATHWAY | ErbB signaling pathway | RT | 35 | 0.7 | 1.6E-2 |
| KEGG_PATHWAY | Proteoglycans in cancer | RT | 71 | 1.4 | 1.6E-2 |
| KEGG_PATHWAY | Phosphatidylinositol signaling system | RT | 38 | 0.8 | 2.2E-2 |
| KEGG_PATHWAY | Amyotrophic lateral sclerosis (ALS) | RT | 22 | 0.4 | 2.2E-2 |
| KEGG_PATHWAY | Influenza A | RT | 62 | 1.2 | 2.3E-2 |
| KEGG_PATHWAY | Acute myeloid leukemia | RT | 24 | 0.5 | 2.3E-2 |
| KEGG_PATHWAY | Insulin resistance | RT | 41 | 0.8 | 2.4E-2 |
| KEGG_PATHWAY | Rap1 signaling pathway | RT | 73 | 1.5 | 2.5E-2 |
| KEGG_PATHWAY | PI3K-Akt signaling pathway | RT | 114 | 2.3 | 2.5E-2 |
| KEGG_PATHWAY | Notch signaling pathway | RT | 21 | 0.4 | 2.8E-2 |
| KEGG_PATHWAY | AMPK signaling pathway | RT | 45 | 0.9 | 3.0E-2 |
| KEGG_PATHWAY | Platelet activation | RT | 47 | 0.9 | 3.8E-2 |
| KEGG_PATHWAY | Adrenergic signaling in cardiomyocytes | RT | 52 | 1.0 | 3.8E-2 |
| KEGG_PATHWAY | Melanoma | RT | 28 | 0.6 | 4.1E-2 |
| KEGG_PATHWAY | Hypertrophic cardiomyopathy (HCM) | RT | 30 | 0.6 | 4.8E-2 |
| KEGG_PATHWAY | Dorso-ventral axis formation | RT | 13 | 0.3 | 4.9E-2 |
| KEGG_PATHWAY | Pathogenic Escherichia coli infection | RT | 21 | 0.4 | 5.4E-2 |
| KEGG_PATHWAY | Choline metabolism in cancer | RT | 37 | 0.7 | 5.5E-2 |
| KEGG_PATHWAY | p53 signaling pathway | RT | 26 | 0.5 | 6.0E-2 |
| KEGG_PATHWAY | Lysosome | RT | 43 | 0.9 | 6.1E-2 |
| KEGG_PATHWAY | Hippo signaling pathway | RT | 52 | 1.0 | 6.6E-2 |
| KEGG_PATHWAY | Aldosterone synthesis and secretion | RT | 30 | 0.6 | 7.5E-2 |
| KEGG_PATHWAY | Huntington's disease | RT | 64 | 1.3 | 7.7E-2 |

| | | | | | |
|---|---|---|---|---|---|
| KEGG_PATHWAY | Chemokine signaling pathway | RT | 62 | 1.2 | 8.1E-2 |
| KEGG_PATHWAY | Ras signaling pathway | RT | 74 | 1.5 | 8.2E-2 |
| KEGG_PATHWAY | Thyroid cancer | RT | 13 | 0.3 | 8.3E-2 |
| KEGG_PATHWAY | Herpes simplex infection | RT | 61 | 1.2 | 8.4E-2 |
| KEGG_PATHWAY | Tuberculosis | RT | 59 | 1.2 | 8.8E-2 |
| KEGG_PATHWAY | Amino sugar and nucleotide sugar metabolism | RT | 19 | 0.4 | 9.6E-2 |

**Genes associated with JunB intervals alone**

| Category | Term | RT | Genes | Count | % | P-Value |
|---|---|---|---|---|---|---|
| KEGG_PATHWAY | Metabolic pathways | RT | 510 | 7.1 | 2.9E-7 |
| KEGG_PATHWAY | Ribosome | RT | 72 | 1.0 | 2.9E-5 |
| KEGG_PATHWAY | Lysosome | RT | 62 | 0.9 | 3.7E-4 |
| KEGG_PATHWAY | Oxidative phosphorylation | RT | 67 | 0.9 | 3.8E-4 |
| KEGG_PATHWAY | Biosynthesis of antibiotics | RT | 99 | 1.4 | 4.9E-4 |
| KEGG_PATHWAY | Purine metabolism | RT | 83 | 1.2 | 1.0E-3 |
| KEGG_PATHWAY | Valine, leucine and isoleucine degradation | RT | 28 | 0.4 | 1.4E-3 |
| KEGG_PATHWAY | Citrate cycle (TCA cycle) | RT | 20 | 0.3 | 1.5E-3 |
| KEGG_PATHWAY | Non-alcoholic fatty liver disease (NAFLD) | RT | 71 | 1.0 | 2.7E-3 |
| KEGG_PATHWAY | Carbon metabolism | RT | 55 | 0.8 | 3.6E-3 |
| KEGG_PATHWAY | Endocytosis | RT | 112 | 1.6 | 4.7E-3 |
| KEGG_PATHWAY | Peroxisome | RT | 42 | 0.6 | 5.1E-3 |
| KEGG_PATHWAY | Pyrimidine metabolism | RT | 50 | 0.7 | 7.6E-3 |
| KEGG_PATHWAY | Huntington's disease | RT | 85 | 1.2 | 7.8E-3 |
| KEGG_PATHWAY | Parkinson's disease | RT | 65 | 0.9 | 8.7E-3 |
| KEGG_PATHWAY | DNA replication | RT | 21 | 0.3 | 9.6E-3 |
| KEGG_PATHWAY | Epithelial cell signaling in Helicobacter pylori infection | RT | 34 | 0.5 | 1.2E-2 |
| KEGG_PATHWAY | 2-Oxocarboxylic acid metabolism | RT | 12 | 0.2 | 1.2E-2 |

| | | | | | |
|---|---|---|---|---|---|
| KEGG_PATHWAY | Alzheimer's disease | RT | 74 | 1.0 | 1.5E-2 |
| KEGG_PATHWAY | Phagosome | RT | 68 | 1.0 | 1.6E-2 |
| KEGG_PATHWAY | Protein processing in endoplasmic reticulum | RT | 74 | 1.0 | 1.7E-2 |
| KEGG_PATHWAY | SNARE interactions in vesicular transport | RT | 19 | 0.3 | 2.5E-2 |
| KEGG_PATHWAY | Synaptic vesicle cycle | RT | 31 | 0.4 | 2.7E-2 |
| KEGG_PATHWAY | Protein export | RT | 14 | 0.2 | 2.9E-2 |
| KEGG_PATHWAY | Synaptic vesicle cycle | RT | 31 | 0.4 | 2.7E-2 |
| KEGG_PATHWAY | Protein export | RT | 14 | 0.2 | 2.9E-2 |
| KEGG_PATHWAY | N-Glycan biosynthesis | RT | 25 | 0.4 | 3.2E-2 |
| KEGG_PATHWAY | Propanoate metabolism | RT | 16 | 0.2 | 3.5E-2 |
| KEGG_PATHWAY | Base excision repair | RT | 18 | 0.3 | 3.9E-2 |
| KEGG_PATHWAY | Terpenoid backbone biosynthesis | RT | 13 | 0.2 | 4.9E-2 |
| KEGG_PATHWAY | Mineral absorption | RT | 23 | 0.3 | 5.2E-2 |
| KEGG_PATHWAY | Collecting duct acid secretion | RT | 15 | 0.2 | 5.5E-2 |
| KEGG_PATHWAY | Glyoxylate and dicarboxylate metabolism | RT | 15 | 0.2 | 5.5E-2 |
| KEGG_PATHWAY | RNA polymerase | RT | 17 | 0.2 | 6.0E-2 |
| KEGG_PATHWAY | Mismatch repair | RT | 13 | 0.2 | 7.0E-2 |
| KEGG_PATHWAY | Renal cell carcinoma | RT | 30 | 0.4 | 7.2E-2 |
| KEGG_PATHWAY | Pyruvate metabolism | RT | 20 | 0.3 | 7.2E-2 |
| KEGG_PATHWAY | Inositol phosphate metabolism | RT | 32 | 0.4 | 8.5E-2 |
| KEGG_PATHWAY | beta-Alanine metabolism | RT | 16 | 0.2 | 8.9E-2 |
| KEGG_PATHWAY | Biosynthesis of amino acids | RT | 33 | 0.5 | 9.1E-2 |
| KEGG_PATHWAY | Synthesis and degradation of ketone bodies | RT | 7 | 0.1 | 9.7E-2 |

**Genes associated with c-Jun intervals alone**

| Category | Term | RT | Genes | Count | % | P-Value |
|---|---|---|---|---|---|---|
| KEGG_PATHWAY | Cell cycle | RT | | 5 | 3.6 | 6.5E-3 |
| KEGG_PATHWAY | RNA transport | RT | | 5 | 3.6 | 2.0E-2 |
| KEGG_PATHWAY | Cysteine and methionine metabolism | RT | | 3 | 2.2 | 2.2E-2 |
| KEGG_PATHWAY | Basal transcription factors | RT | | 3 | 2.2 | 3.0E-2 |
| KEGG_PATHWAY | Proteoglycans in cancer | RT | | 5 | 3.6 | 3.2E-2 |
| KEGG_PATHWAY | Sulfur metabolism | RT | | 2 | 1.5 | 5.9E-2 |
| KEGG_PATHWAY | Sulfur relay system | RT | | 2 | 1.5 | 5.9E-2 |
| KEGG_PATHWAY | Hippo signaling pathway | RT | | 4 | 2.9 | 6.3E-2 |
| KEGG_PATHWAY | Inositol phosphate metabolism | RT | | 3 | 2.2 | 6.9E-2 |
| KEGG_PATHWAY | TGF-beta signaling pathway | RT | | 3 | 2.2 | 9.2E-2 |
| KEGG_PATHWAY | Progesterone-mediated oocyte maturation | RT | | 3 | 2.2 | 9.8E-2 |

**Appendix 6. Top 5 candidates from ChIP-seq short-listed for future investigation**

The top 5 candidates are listed for future investigation, as mentioned in **Section 5.2.7**. "Expression level" indicates the expression level of the corresponding gene in ALK+ ALCL cell lines compared to other hematopoietic cell lines; "JunB KD microarray" indicates the fold change of the corresponding gene in the microarray performed in JunB knock-down Karpas 299 cells; "Biological functions" indicates the roles that the corresponding genes play, reported from the literatures.

| Gene | Expression level | JunB KD microarray | Biological functions |
|---|---|---|---|
| ***FAM129B*** | High | - | Promote proliferation/ inhibit apoptosis [336-338] |
| ***SIPR1*** | High | - | Promote proliferation and migration/ inhibit apoptosis [351] |
| ***CD47*** | Intermediate | 1.28 | "Don't eat me" signal for macrophages/ promote migration [352] |
| ***IL1RAP*** | Intermediate | 1.96 | Promote cell growth [353] |
| ***RAP2A*** | High, overall similar | - | p53 target/ promote and inhibit migration [354] |
| ***NUCKS1*** | High, overall similar | -1.32 | Synergize with Trp53 in lymphomagensis / oncogene in hepatocellular carcinoma [355, 356] |